FACILITY FORM 602
N68-19007 (ACCESSION NUMBER)
256 (PAGES)
CR-72273 (NASA CR OR TMX OR AD NUMBER)
1 (THRU)
(CODE)
03 (CATEGORY)

NASA-CR-72273

3000 HOUR TEST - TWO STAGE POTASSIUM TURBINE

FINAL REPORT

PRICE $ _____
PRICE(S) $ _____
Hard copy (HC) 3.00
Microfiche (MF) .65
July 65

EDITED BY E. SCHNETZER

JULY, 1967

prepared for
NATIONAL AERONAUTICS AND SPACE ADMINISTRATION
CONTRACT NAS 5-1143

SPACE POWER AND PROPULSION SECTION
MISSILE AND SPACE DIVISION
GENERAL ELECTRIC
CINCINNATI, OHIO 45215

NOTICE

This report was prepared as an account of Government sponsored work. Neither the United States, nor the National Aeronautics and Space Administration (NASA), nor any person acting on behalf of NASA:

A.) Makes any warranty or representation, expressed or implied, with respect to the accuracy, completeness, or usefulness of the information contained in this report, or that the use of any information, apparatus, method, or process disclosed in this report may not infringe privately owned rights; or

B.) Assumes any liabilities with respect to the use of, or for damages resulting from the use of any information, apparatus, method or process disclosed in this report.

As used above, "person acting on behalf of NASA" includes any employee or contractor of NASA, or employee of such contractor, to the extent that such employee or contractor of NASA, or employee of such contractor prepares, disseminates, or provides access to, any information pursuant to his employment or contract with NASA, or his employment with such contractor.

Requests for copies of this report should be referred to:

National Aeronautics & Space Administration
21000 Brookpark Road
Cleveland, Ohio 44135
Attn: Contracting Officer
Space Power Systems Procurement Section
MS 500-309

3000 HOUR TEST-
TWO STAGE POTASSIUM TURBINE

FINAL REPORT

Edited By
E. Schnetzer, Manager
Development Engineering

NATIONAL AERONAUTICS AND SPACE ADMINISTRATION

Contract NAS 5-1143

Technical Management
NASA - Lewis Research Center
Advanced Rankine Systems Branch
Joseph P. Joyce, Technical Manager

SPACE POWER AND PROPULSION SECTION
MISSILE AND SPACE DIVISION
GENERAL ELECTRIC COMPANY
CINCINNATI, OHIO 45215

ACKNOWLEDGEMENT

The following contributed to the writing of this report:

S. E. Eckard, Manager, Test Project

R. W. Fink, Engineer, Turbine Design & Evaluation

W. F. Lemond, Engineer, Turbomachinery Development

H. E. Nichols, Manager, Turbomachinery Components

R. J. Rossbach, Manager, Fluid and Thermodynamics

W. F. Zimmerman, Manager, Material Applications

TABLE OF CONTENTS

		Page No.
I.	SUMMARY	1
II.	INTRODUCTION	3
III.	TEST PREPARATIONS	9
	A. Test Assembly	9
	1. Design Modifications	9
	a. Modification of Instrumentation	9
	b. Exclusion of Oil From Outer Diameter of Pivoted-Pad Bearing	10
	c. Increase of Flow Area in Turbine Exhaust Region	11
	d. Redesign of the Copper Labyrinth Seals on the Bearing Housing	11
	e. Addition of a Disk Brake to Turbine Rotor	11
	2. Stator Assembly	12
	3. Rotor Assembly	13
	4. Final Assembly and Turbine Installation	13
	B. Metallurgical Specimens	14
	1. Turbine Rotor Blades	15
	2. Erosion Inserts	15
	3. Refractory Alloy Ring Specimens	16
	4. Tensile Test Specimens	16
	C. Instrumentation and Calibration	17
	D. Facility Preparation	17

TABLE OF CONTENTS (Continued)

		Page No.
IV.	TESTING	23
	A. Mechanical Checkout Test	23
	B. Parasitic Torque Calibration Test	26
	C. Endurance Test	27
	1. Test Conditions	27
	2. Chronology	27
	3. Key Events	28
	a. Initiation of Test	28
	b. Actuation of Disk Brake	28
	c. Water Brake Vibrations	30
	d. Repair of Throttle Valve	34
	e. Water Brake Bearing Failure	35
	f. Completion of Test	35
	4. General Observations During Testing	36
V.	TEST RESULTS	39
	A. Mechanical Data	39
	1. Turbine Disassembly and Visual Inspection	39
	2. Stator Inspection	40
	3. Rotor Inspection	41
	4. Bearing Housing Inspection	44
	B. Metallurgical Evaluation	45
	1. Turbine Rotor Blades	45
	a. Macrophotographs	45
	b. Rotor Blade Weight Change	49

TABLE OF CONTENTS (Continued)

		Page No.
	c. Tensile Strength Tests	50
	d. Microexamination of U-700 Alloy Rotor Blades	53
	e. Microexamination of Refractory Alloy Rotor Blades	59
	2. Environmental Cleanliness	60
	a. Refractory-Alloy Contamination Specimens	61
	b. Potassium Purity	62
	c. Absence of Rotor Blade Corrosion	64
	3. Erosion Inserts	65
	4. Rotor Blade Clips	68
	5. Honeycomb Tip Shrouds	69
	6. Erosion Discussion	69
	C. Performance	71
	1. Validity of Measurements	71
	2. History	72
VI.	CONCLUSIONS	75
	REFERENCES	77

I. SUMMARY

After successfully completing 2000 hours test of a two-stage turbine with inlet potassium vapor at 1500°F and vapor quality at 99 percent, an additional 3000 hours test was completed at the same test conditions which included a second stage inlet vapor quality calculated to be 96.7 percent. The objective of both tests was to determine the resistance of rotor-blade refractory materials to liquid impact erosion and/or corrosion. These data are needed in the design of vapor turbines for use in Rankine-cycle space electric power generators.

The conclusions from a detailed mechanical inspection, a thorough metallurgical evaluation and performance surveillance during testing are as follows:

1. The turbine experienced no damage affecting its safety and reliability.
2. The facility demonstrated its potentiality of supporting a long-duration endurance test especially by its characteristic of reducing the already low potassium purity level as testing progresses.
3. Only minor evidences of erosion and/or corrosion were observed on the turbine superalloy and refractory-metal parts.
4. No deterioration in turbine performance was noted.

PRECEDING PAGE BLANK NOT FILMED.

II. INTRODUCTION

On space missions in which the required power for life support, electronic devices, and/or electrical propulsion exceeds one or two hundreds of kilowatts, serious consideration is being given by NASA to the use of nuclear-fueled, Rankine-cycle, powerplants using potassium vapor as the working fluid. Since operation of the turbine at least partially in the wet region is mandatory, it is necessary to establish the severity of the turbine rotor-blade erosion problem which is expected based upon the constant experience with erosion in the central-station steam turbine industry. The General Electric Company designed, fabricated and endurance tested a two-stage potassium vapor turbine under NASA, Lewis Research Center Contract NAS 5-1143. The fluid dynamic design, mechanical design, materials support and facility design aspects of this program are described in references 1, 2, 3, and 4, respectively.

The two-stage turbine 2000-hour endurance test was conducted at an inlet temperature and vapor quality of 1500°F and above 99 percent, respectively. The inlet quality and tip speed of the second stage was calculated to be 96.7 percent and 770 fps, respectively. The exit temperature of the turbine was 1240°F, which resulted in operating at the design total-to-static pressure ratio of 3.47. The rotative speed was 18,250 rpm for the test.

The 2000-hour endurance test was completed with but one interruption. At 254 hours into the test the routine calibration of a speed measuring inadvertently triggered the overspeed trip, stopping the turbine. No deterioration of the

bearings or seals occurred during the 2000 hours of testing. Visual inspection after the test revealed no evidence of damage affecting the reliability of the turbine.

The all-welded method of assembling the turbine from its components and of installing the turbine in the facility proved highly reliable and resistant to potassium vapor leakage.

Columbium-base alloys were not used for turbine blades since it had been earlier determined that these alloys were contaminated and surface embrittled by oxygen and nitrogen when exposed in the turbine facility even when the oxygen content in liquid potassium in the condenser was as low as 10 ppm.

Low oxygen content in the potassium may logically appear not to be a potential source of contamination; however, the large amount of potassium in the facility (3000 lbs), the high recirculation rate of the potassium (7200 lbs/hr), and the fact that the highly gettering columbium base alloys represent only a small surface area competing for the available oxygen supply, all tend to support the likelihood of columbium alloy contamination in a stainless steel system. If the system had been completely composed of columbium base alloys in a proper vacuum environment, the large gettering area of the facility relative to the available oxygen supply would most likely not result in any significant contamination of the columbium alloys.

While the molybdenum-base alloys were insignificantly affected by contamination in the facility, the columbium alloys were excellent indicators

of such contamination because of their gettering ability. Refractory-alloy contamination specimens of columbium alloys (and of molybdenum alloys) were placed in the potassium-vapor stream forward of and aft of the turbine. In general, contamination of these specimens was greater ahead of the turbine and less behind the turbine; weight losses of specimens were greater behind the turbine where the quality was less and where the surface contamination may have been corroded away by larger quantities of liquid.

Analysis of the above refractory alloy contamination specimens also served to indicate the relative cleanliness of the system. Weight loss and contamination impurity levels in those specimens indicated the initial startup period of turbine operation, including the first 254 hours of testing, provided an environment considerably less clean than the remaining 1746 hours of testing.

Highly localized rotor-blade corrosion was observed at the concave leading edge and at the convex trailing edge. This corrosion appeared to be the result of liquid metal accumulating on the surface of the airfoils in areas of flow separation or local turbulence. Its depth was less than 3-4 mils in the worst instances and was not considered detrimental to further turbine operation. It was believed that this corrosion occurred in the very early stages of turbine operation as the result of surface contamination on the walls of the facility and turbine hardware which could not be flushed with potassium (and thereby cleaned) prior to turbine operation. This hypothesis is supported by two observations. First, the potassium in the condenser remained at 5-12 ppm oxygen during the 2000-hour test except for an initial high oxygen analysis

of 69 ppm noted after two hours of potassium vapor testing. Second, the contamination of the refractory alloy inserts was much more severe in the first 254 hours of test as compared to the remaining 1746 hours of test.

The blades and other operating hardware showed no evidence of mechanical damage by impact erosion. The only observed evidences of impact erosion occurred on the stationary erosion inserts of U-700 alloy installed immediately behind the tips of the second-stage blades. A small cluster of holes about 2-3 mils in diameter and 7-10 mils deep was noted at a location where impacting droplets were likely to strike. Small cracks along the surface of these holes indicated the mechanical nature of this erosion. Refractory molybdenum-base alloys of TZM and TZC were not thus affected.

Minor instances of metal transfer were noted. A metal film on the front face of the first-stage turbine wheel was 2 mils thick at the hub and less than 1 mil thick at the rim. Other surface effects were noted on turbine blades where a 0.5-mil metal film formed on the first-stage blades and a 0.2-mil film formed on the second-stage blades.

After the 2000-hour test, some sigma phase was noted in highly stressed areas of the first-stage-blade dovetails where the temperature was sufficiently high for it to form. The U-700 blade materials exhibited significant decreases in room temperature ductility after turbine test but retained adequate ductility for further testing. The TZC tensile bars exposed to turbine exhaust conditions likewise revealed a decrease in low temperature ductility; the high temperature ductility of such test specimens still remained adequate for additional test operation.

While many minor effects were noted in the behavior of materials during the 2000-hour test, none of them were of sufficient significance to cause concern for the safety or reliable operation of the turbine for an additional 3000 hours.

From turbine performance data obtained with a digital data acquisition system at four-hour intervals, no deterioration of performance was observed. This is as is to be expected since no significant damage was done to the turbine blading, bearings or seals.

In view of the lack of any significant deterioration of the turbine due to the exposure to potassium vapor for 2000 hours, it was decided to endurance test the two-stage turbine for an additional 3000 hours. The objectives of this test were to ascertain what changes, if any, the rotor blades, erosion inserts, the turbine in general, and the turbine performance would undergo in 3000 additional hours.

In this report the test preparations undergone by the two-stage turbine and the 3000 KWt turbine test facility are discussed. The metallurgical specimens and performance instrumentation used are described. The important events in all aspects of test are delineated. Finally, the test results of a mechanical, metallurgical and performance nature are fully discussed.

PRECEDING PAGE BLANK NOT FILMED.

III. TEST PREPARATIONS

A. TEST ASSEMBLY

A detailed description of the individual turbine parts, their functions and the design considerations of each is given in Reference 2. The major assembly drawing of the turbine is shown in Figure 1, and an exploded view of its individual parts is shown in Figure 2. Figure 3 shows the overall arrangement drawing of the turbine and its load train, the latter comprising a water brake and steam turbine in tandem supported by two respective strain-gage torque meters. The majority of components used in the build-up for the 3000-hour test were the same as those employed in the previous 2000-hour test, with the result that many of the turbine parts presented herein show the effects of testing for a total of 5000 hours in potassium vapor. Table I shows a list of the components used in the build-up, and their status regarding previous usage.

1. Design Modifications

Prior to assembling the turbine for running, a number of minor design modifications were made to improve its overall reliability, as a result of experience gained in the previous 2000-hour test [2] as follows:

a. Modification of Instrumentation

The turbine instrumentation for the 3000-hour endurance test is as shown in Figure 4 and as described in detail in Table II.

Most of the instrumentation was the same as it was for the 2000-hour endurance test described in Reference 1. One of the changes was the addition

of an efflux system differential pressure sensor in the bullet nose to permit a vapor flow rate measurement in addition to that of the electromagnetic flowmeter. An efflux system stagnation tube was also provided at station 7 to measure exit total pressure. These efflux system measurements were made only at certain times, usually once each day. Another instrumentation modification was the change of three thermocouples, one each at stations 1, 7 and 8, from chromel-alumel to platinum-platinum 10 percent rhodium. It was believed that the platinum thermocouples would be less likely to drift over a 3000-hour period.

Before installing it for test, all turbine pressure measurement tubing and thermocouple wells and thermocouples were replaced to obtain maximum initial mechanical integrity. All other instrumentation remained the same.

b. Exclusion of Oil From Outer Diameter of Pivoted Pad Bearing

Upon disassembly of the turbine following the 2000-hour test, it was discovered that the clearance space between the pad bearing outer socket ring and the bearing housing into which it fits was filled with a carbonized material, resulting from oil which had entered the cavity and had then been "coked" from the heat of the bearing housing in that region. Figure 5 shows the modification which was subsequently made to prevent oil from entering this cavity. It involves sealing of the cavity with o-ring seals and purging it with pressurized argon, thereby preventing the entering of any oil and/or purging it from the region, should it enter.

c. Increase of Flow Area in Turbine Exhaust Region

To increase the flow area in the exhaust region of the turbine and prevent premature choking, eighteen of the twenty-six vanes in the outlet guide vane assembly were removed by cutting and grinding, resulting in an increase of the flow area of 8.05 percent.

d. Redesign of the Copper Labyrinth Seals on the Bearing Housing

Because of the difficulties of obtaining a reliable plating of copper on the outer labyrinth seals of the forward region of the bearing housing (due to its geometry), the procedure of plating directly on the bearing housing was replaced by that of inserting, and seal-welding in place, a prepared ring already containing the necessary copper surface. This change was one of improved fabrication but no change in basic turbine design.

e. Addition of a Disk Brake to Turbine Rotor

The disk brake was added to the turbine as an additional safety device to minimize the possibility of accidental overspeed during the 3000-hour test. In the unlikely event of water supply failure to the water brake, the disk brake would be automatically actuated to stop the turbine. The disk brake basic configuration is shown in Figure 6. It consists of a 7.7-inch diameter disk, made of U-700, and mounted on the splined coupling at the aft end of the turbine rotor. It can be seen that the disk has a widened hub section, made necessary by its stress distribution at 25,000 rpm. Torque is delivered to the rotor by two integral lugs at the disk hub which fit into closely mating slots on the coupling. The braking load is simultaneously applied to both sides of

the disk by a pair of 1 1/2-inch diameter loader pucks, of an organic resin impregnated with metal particles (designated as Goodyear BL56 Compound), and no net thrust load is applied to the disk. To increase wear life and reliability, two pairs of loader puck assemblies were used.

2. Stator Assembly

On the turbine stationary parts, all components from the 2000-hour test were reused with the exception of the nozzle diaphragms. These were replaced because of damage and wear which had occurred prior to the 2000-hour endurance testing. In preparing the turbine components for reuse, rework was performed to resize all critical rabbeting diameters on the inlet duct, casings, and the exhaust scroll, since all of them had undergone some thermal distortion during the previous high-temperature testing. Rabbet surfaces were replaced by press-fitting and tack-welding rings onto existing rabbets and then remachining them. Figures 7 through 13 show the inlet duct, casings, honeycomb tip seals, nozzle diaphragms, and exhaust scroll prior to subassembly of the parts for the 3000-hour test. Figure 10 is a photograph of the reworked outlet guide vane assembly following removal of the eighteen struts, as previously discussed.

Figure 14 shows the inlet duct subassembly with the first stage nozzle diaphragm and honeycomb tip seal installed. Figure 15 shows the top and bottom halves of the turbine casing subassembly, comprising the casings, second stage nozzle diaphragms, honeycomb tip seals, and outlet guide vane assembly. Figure 16 shows a view into the aft end of the clamped-together casings, which shows the installation of the twelve erosion inserts of various materials

downstream of the second stage nozzle diaphragm (also shown in the drawing of Figure 1).

The bearing housing is shown in Figure 17. In this photograph, the hydrodynamic seal has been welded to the forward end, and the expansion heat shield has been installed. The heat shield covers the many flow tubes extending to and from the bearing and seal region and protects them from the heat of condensing potassium vapor during operation (see Figure 1). The internal components of the bearing housing assembly in the forward (pivoted pad) bearing region are shown in the exploded view of Figure 18, and the aft thrust bearing subassembly which is attached to the rear of the bearing housing is shown in Figure 19.

3. Rotor Assembly

On the turbine rotor (as indicated in Table I) new turbine wheels were used because of material life limitation on the first stage wheel. Also, some of the blades on both stages were replaced to support the metallurgical investigation discussed in Section V.B. of this report. All other rotor components were the same as those used in the 2000-hour test. Figure 20 shows the assembled turbine rotor, including the disk brake on the aft end of the shaft.

4. Final Assembly and Turbine Installation

The initial step in the final assembly consisted of inserting the bearing housing into the scroll central bore and welding the aft conical flange (Figure 1). The shaft was then inserted from the forward end, protruding through the aft end of the bearing housing as shown in Figure 21. The individual

components shown in Figure 18 were then inserted, and the internal instrumentation to monitor turbine vibrations, shaft orbital motion, bearing temperatures, and pressures was installed (according to the instrumentation drawing of Figure 4). The ball-bearing housing assembly (Figure 19) was then mounted.

The assembly of the turbine casings and rotor wheels were then performed as shown in Figure 22. The rotor-to-stator clearances which had previously been calculated and predicted from individual parts dimensions and stack-up were verified by actual measurements at this point in assembly. The predicted clearances between rotor and stator (obtained from individual parts measurement) are tabulated in Figure 23. The welding of the casing flanges was done in the sequence and manner discussed in Reference 2.

Figure 24 shows the complete turbine mounted in the test facility with all flanges welded and instrumentation hooked-up. Figure 25 is an aft view prior to mounting of the shaft rear parts, and Figure 26 shows the region following the addition of the glove box dished head and the turbine coupling and disk brake. Figure 27 is an aft quarter view of the installed turbine including its power train (Figure 3) and prepared for running. Figure 28 is a forward quarter view of the same installation.

B. METALLURGICAL SPECIMENS

While all of the turbine components were potentially metallurgical specimens available for post-test evaluation, certain components and added test specimens were of particular note. These included (1) turbine blades in the first and second stages, (2) stationary erosion inserts installed immediately

behind the second-stage blade tips, (3) refractory alloy ring specimens installed in the vapor stream ahead of, and behind, the turbine, and (4) tensile test specimens installed in a similar manner ahead of, and behind, the turbine.

1. Turbine Rotor Blades

The rotor blades of the two-stage turbine are fastened to the disks in each stage by dovetail connections, making it possible to expose blades of several materials to the same environment for the duration of an endurance test. For the 3000-hour test, 54 of the 62 U-700 alloy first-stage blades, 45 of the 52 U-700 alloy second-stage blades, two of the four TZM alloy blades and the four TZC alloy blades used in the 2000-hour test were installed.

U-700 blades - Seven new blades were installed at the start of the 3000-hour test.

U-700 blades - Forty-five blades which were used in the previous 2000-hour test were continued on test for 5,000 hours total.

TZM blades - Two of the four blades from the 2000-hour test were replaced by new blades at the start of the 3000-hour test.

TZM blades - Two blades which were used in the previous 2000-hour test were continued on test for 5000 total hours.

2. Erosion Inserts

Erosion inserts of the type shown in Figure 29 were installed immediately behind the second-stage blades; they were attached to the turbine

shroud ring in such a manner that liquid droplets, leaving the trailing edge blade tips, impacted upon the inserts at a velocity of about 770 ft./sec.. The following materials were thus tested in the 3000-hour test:

U-700 - Two specimens from the 2000-hour test were exposed for an additional 3000 hours for a total of 5000 hours of erosion testing.

U-700 - Three new erosion inserts were tested for 3000 hours.

TZM & TZC - Two each stress relieved TZM and TZC specimens from the 2000-hour test were exposed for an additional 3000 hours for a total of 5000 hours of erosion testing.

AS-30 - Three new stress relieved specimens of this columbium-base alloy were installed for the 3000-hour test.

3. Refractory Alloy Ring Specimens

For purposes of determining the effect of the potassium vapor environment on the contamination of refractory alloys during the test, one stainless steel probe containing six refractory alloy ring specimens, 1/2-inch OD x 1/4-inch ID x 3/8-inch high, was installed in the potassium vapor upstream of the turbine, and another was installed similarly, downstream of the turbine. Each probe contained two each TZC and TZM molybdenum alloy ring specimens and two each F48 columbium alloy ring specimens and the probes are shown in Figure 30.

4. Tensile Test Specimens

For the purpose of determining the effects of the environment on the properties of the TZM and TZC alloys, four 1 1/2-inch long tensile specimens

of each alloy were installed in the vapor stream in perforated stainless steel cylindrical cages. The TZM specimens were installed ahead of the turbine, and the TZC specimens were installed downstream of the turbine. After completion of the 3000-hour turbine test, tensile tests were performed on these at room temperature and at elevated temperatures for comparison with similar test data prior to turbine testing.

C. INSTRUMENTATION AND CALIBRATION

Shown in Figure 4 is a drawing which indicates the location of instrumentation used to monitor turbine performance during the 3000-hour endurance test. The instrumentation is also listed in Tables II and III.

In preliminary testing in 1964 and early 1965 it was found that flexible connections between the test facility and the water brake and/or the steam turbine could cause erratic torque readings. These errors were virtually eliminated by careful alignment of the flexible connections. Therefore, a rotating torque meter calibration was performed prior to endurance testing to assure that the flexible connections were properly aligned.

D. FACILITY PREPARATION

Before starting the 3000-hour potassium turbine endurance test, a number of modifications were made to the facility. These modifications were made to improve the reliability of the facility as well as to simplify control of the facility by increased automation.

Greater reliability was achieved by installing redundant systems and/or components, and by replacing what was considered to be unreliable. For example, a secondary lube pump was installed for the water brake and steam turbine. The control circuit for this pump was designed so that the pump would automatically start if the discharge pressure from the primary lube pump for the steam turbine and water brake dropped too low. Parallel oil filters and appropriate valving were installed in the water brake and steam turbine lube oil system. This permitted the isolation and cleaning of a dirty oil filter without disturbing the oil flow rate to the water brake and steam turbine. Additional micro air filters were installed in the air supply line to critical pneumatic controllers and instrumentation. This insured a continuous supply of clean instrument air to these components. A standby transformer was installed in the main EM pump electrical control circuit. This provided an auxiliary source of power to keep the EM pump in operation in the event of failure of the primary power circuit. (The primary circuit did fail during the 3000-hour endurance test. The standby transformer maintained the facility in operation while repairs were being made.) A larger size, better positioned, overflow drain between the slinger seal loop head tank and dump tank was installed. The overflow drain line automatically maintained a constant potassium liquid level in the head tank as long as the slinger seal loop accumulated potassium. (Accumulation of potassium was the result of potassium vapor condensing in the area of the turbine slinger seal.) Three corrugated metal hoses, which previously contained liquid potassium at pressure and temperature up to 120 psig and 850°F, respectively, were replaced by rigid pipe. Flexibility of the liquid metal loop was maintained by appropriate expansion bends.

The following automatic features were incorporated into the facility to simplify its control and to reduce required operating manpower. An automatic controller was installed to sense and maintain the boiler discharge temperature at the required 1500°F. The required temperature was generally held within ± 5°F. Automatic controllers were installed to maintain constant lube oil flow to the pad bearing and ball bearing regardless of turbine speed, lube oil temperature, or lube oil supply pressure. An automatic controller was installed to maintain constant argon pressure at the inlet to the turbine argon labyrinth seal regardless of turbine speed, argon temperature, or argon supply pressure. (During the 2000-hour endurance test, argon pressure and oil flow to the bearing required constant attention. During the 3000-hour endurance test these parameters, being regulated by automatic controllers, required only occasional checking.) A system was installed to automatically maintain a constant pre-set pressure at the steam turbine inlet. As a result, the power produced by the steam turbine, under idling conditions, was constant. The automatic control system for maintaining condenser pressure was improved so that changes in ambient temperature would not noticeably influence condenser pressure (turbine exit pressure).

Several additions were made to the facility to warn the test personnel of impending danger or deviation from the required operating conditions. It was necessary to maintain the water temperature, discharging from the water brake, above 185°F but less than 195°F for optimum water brake stability. An audible alarm was installed to warn the operating personnel when the water temperature deviated from the above limits. An audible alarm was installed

to sound if the turbine speed deviated from the required set point by as little as $\pm$ 100 rpm. An overspeed safety system was installed which automatically flooded the water brake when the turbine speed exceeded the required setting. Generally the trip point was 2,000 to 3,000 rpm higher than the set point. When the turbine speed decreased below the set point the water brake flooding valve would close. An argon purge system was installed to exclude lube oil from beneath the turbine pad bearing ring during testing. During testing the bearing housing temperature in the vicinity of the pad bearing retainer ring was in the order of 550°F. This high temperature caused the oil in the area to deteriorate to a hard carbon deposit, thus closing the thermal expansion gap between the bearing housing and retainer ring. During the 2000-hour test, carbon deposits under the bearing ring was a direct cause of the bearing seizure on turbine cool-down. There was no indication of bearing seizure during cool-down following the completion of the 3000-hour endurance test, and there was no carbon deposit found beneath the pad bearing ring after the 3000-hour test.

All critical components of the test facility which might have suffered damage during the 2000-hour endurance test were inspected. For example, the outside diameter of all boiler tubes were measured to obtain an indication of loss of tube wall due to oxidation. Also several of the boiler tubes were radiographed to detect the loss of tube wall due to combined oxidation and corrosion by potassium. Individual tubes were radiographed one foot from the bottom, the mid point and one foot from the top. An unused boiler tube was inspected in a similar manner to serve as a "standard". Comparing the boiler

tubes with the "standard" indicated a net loss of tube wall in the order of five mils. In the design of the boiler 60 mils was provided for corrosion and 60 mils was provided for oxidation of the tube wall.

Critical welded joints in the boiler, condenser and loop piping were inspected in various ways. Some were radiographed and some were dye-penetrant inspected. Damage to welded joints was not found any place in the facility.

All thermocouples on the boiler tube bundle were replaced since the sheath of many of these thermocouples was excessively oxidized after completion of the 2000-hour test. (Only 3 out of 40 thermocouples actually failed during the 2000-hour endurance test.) Immersion thermocouples at the boiler discharge, turbine inlet and outlet were replaced. All thermocouples on the condenser tube bundle were also replaced.

Routine maintenance was performed on all facility equipment such as motors, blowers, valves, pneumatic actuators and controllers, etc. All instrumentation such as Taylor Company pressure gauges, pressure transducers, critical thermocouples, etc. were calibrated.

During shutdown after completion of the 2000-hour test the eight-inch vapor valve did not close as smoothly as it should. Galling of the lower stem bearing was evident. During the 2000-hour test the valve contained a Stellite-12 bearing supporting the valve stem which was hard-faced with Stellite-6. The Stellite-12 bearing was replaced by a bearing made of high purity aluminum oxide. (On completion of the 3000-hour test, valve action was quite smooth.)

On April 5, 1966 the test turbine was returned to the test cell for installation and for continuance of testing.

IV. TESTING

A. MECHANICAL CHECKOUT TEST

Upon completion of turbine installation in the test facility, the turbine starting and loading equipment was installed without the Koppers Company coupling between the water brake and test turbine. During the installation of the water brake and steam turbine, great care was taken to insure that good alignment of these components with respect to each other was assured. For example, necessary measurements and adjustments were made so that the water brake and steam turbine shafts were aligned within 1.0 mil with respect to each other.

Hose connections to the water brake and steam turbine were routed and supported in a manner to minimize torsional reaction at the water brake and steam turbine Bytrex Company torque meters. Also the water brake and steam turbine were weight counterbalanced to essentially eliminate all bending moment otherwise imposed on the torque meters.

After lube oil, cooling water and seal air were established to the water brake and steam turbine, steam was slowly admitted to the steam turbine at sufficient pressure to produce rotation of the water brake and steam turbine up to 20,000 rpm. Vibration amplitudes of the water brake and steam turbine were measured at all rpm's by continuously recording these parameters, along with speed on Sanborn recorders. Typically the steam turbine vibrational amplitudes have been less than 0.2 mil vertically and horizontally. Water brake vibrational amplitudes have been in the order of 0.7 to 1.0 mil vertically

and 0.4 to 0.6 mil horizontally. The water brake has exhibited a critical speed at about 16,800 to 17,000 rpm at which the vibrational amplitudes have been in the order of 2.0 mil and 1.0 mil on the vertical and horizontal, respectively. (These have been higher with poor balance of the water brake rotor.)

While the steam turbine and water brake are rotating without the test turbine engaged, steam turbine torque should be equal to water brake torque. However, if the steam inlet line to the steam turbine is not precisely aligned with the horizontal axis of the steam turbine, an erroneous steam turbine torque is introduced by the radial component of the steam pressure reacting on turbine casing from the steam inlet line. Therefore, the steam inlet line was shifted until the water brake indicated torque agreed with the steam turbine torque within three inch pounds. The above torque comparison test was generally carried out over a torque range of 0 to 120 inch pounds and over a speed range of 0 to 16,000 rpm. When the speed was reduced to zero both torque meters were required to indicate zero torque within three inch pounds. In the past some adjustments to hoses and tubing such as oil and air lines have been required to minimize this influence on zero shift. Also adjustments to the electronic zero have been required. Upon completion of all adjustments the steam turbine and water brake are accelerated to about 16,000 rpm at 120 inch pound torque level and back to zero speed and torque three times to insure repeatability of zero torque indication and to insure repeatability of torque comparison within $\pm$ 3 inch pounds.

Both torque meters are calibrated at zero speed with dead weights of known mass suspended on a lever arm of known length. This calibration was

conducted with the water brake and steam turbine mounted in place and with all service connections to these components installed. Weights were applied in increments to produce a maximum torque approximating the value expected during actual potassium turbine testing. The torque meters were calibrated for increasing and decreasing torque.

After the water brake and steam turbine were checked out, the Koppers Company shaft coupling was installed between the potassium turbine and the water brake. Following the establishment of lube oil flows, sealing argon, etc. and after the test turbine casing was heated to about 500°F, the test turbine was accelerated to about 19,000 rpm with the steam turbine. Vibration of all components, test turbine, water brake and steam turbine were monitored. Vibrational amplitudes of the water brake and steam turbine were as indicated above. The test turbine generally exhibited a maximum indication occurred at about 15,000 rpm.

During this test, bearing temperatures, lube oil supply pressure, and lube oil flow rates were monitored to verify acceptable bearing performance. Also argon flow rate and pressure differential across the test turbine labyrinth seal were monitored to determine the characteristics of the turbine argon labyrinth seal.

Upon completion of the above preliminary tests and after the results of these tests were determined to be within acceptable limits, the facility was made ready for potassium vapor testing. Just prior to the generation of potassium vapor by the facility boiler, the test turbine was again rotated

with the steam turbine at various speeds. This phase of testing was designed to permit the measurement of parasitic torque of the test turbine. This test is discussed in detail below.

B. PARASITIC TORQUE CALIBRATION TEST

As during previous testing, performance data were to be based upon the work done by the turbine blading. As a result, the work required to overcome bearing and seal friction had to be determined by means of a parasitic torque test prior to endurance testing. Because slightly different values of parasitic torque as a function of rotative speed were obtained for each previous build-up, the parasitic torque test was repeated prior to each startup of the 3000-hour endurance test and after the shutdown at the completion of the test.

The parasitic torque is the difference between the steam turbine and water brake torque meter values when the test turbine shaft is driven by the steam turbine. Constant speed tests were run at three or more levels of argon pressure in the facility and parasitic torque was plotted as a function of argon density. If the test data is extrapolated to zero density, the windage torque on the test turbine blades is zero and the remaining torque is the bearing and seal parasitic torque at the rotative speeds used.

The results of the various parasitic torque tests are shown in Figure 31 as a function of rotative speed and argon density in the turbine, and in Figure 32 as a function of rotative speed at zero density. The results of the five tests were represented by the equation $Q_{pt} = 0.005\ N$ with an accuracy of about $\pm$ 3 inch pounds, where Q_{pt} is parasitic torque in inch pounds, and N is rotative speed in rpm.

C. ENDURANCE TEST

1. Test Conditions

The test conditions for the 3000-hour test were to be the same as for the 2000-hour endurance test; that is, inlet temperature of 1500°F, turbine exit temperature of 1240°F, and rotative speed of 18,250 rpm. The exit temperature was chosen to set a turbine total-to-static pressure of 3.47. During the first portion of the endurance test the rotative speed was varied in an attempt to operate at a minimum vibration condition. As a result, a major portion of the first 600 hours of the test was run at about 18,800 rpm. The test conditions for the remainder of the 3000-hour test were accordingly changed so that the rotative speed was set at 18,800 rpm. Based on an inlet vapor quality of 99 percent, the estimated vapor quality at the inlet to the second stage was 96.7 percent.

2. Chronology

The 3000-hour endurance test of the two-stage potassium vapor turbine was initiated on April 18, 1966, following completion of the parasitic torque test. The turbine operated continuously until May 13, 1966, for a total of 600 hours. At that time it was necessary to interrupt the test because of excessive water brake vibrations. The endurance test was restarted again on May 31, 1966, and an additional 214 hours, for a total of 814, was completed on June 9, 1966. The test was again interrupted at that time to repair a potassium leak in the main throttle valve. Testing resumed on June 11, 1966 and 1361 additional hours were accumulated until August 7, 1966. At this point, a total of 2175 hours, testing was again interrupted due to a water

brake bearing failure. After repair of the water brake, testing was resumed on August 16, 1966. The remaining 825 hours of the endurance test were then completed on September 19, 1966.

3. Key Events

The following is a chronological description of the 3000-hour endurance test, with a discussion of all pertinent incidents affecting performance or requiring mechanical modifications to either the turbine power train or test facility components.

a. Initiation of Test

The first vapor operation occurred at 1455 hours on April 18, 1966 at a boiler temperature of 1200°F. The turbine start-up was typical (Reference 2) wherein the speed of the turbine is controlled by varying the power from the auxiliary steam turbine while the potassium vapor temperature increases to its design point (1500°F), and the water brake is brought on the line as turbine power increases. Speed was maintained in this manner until at 1800 hours (April 18, 1966), when endurance test conditions were reached, and the turbine speed was set on automatic control.

b. Actuation of Disk Brake

Typically, the start-up and shutdown periods are the most critical, as observed during the previous 2000-hour testing (Reference 2), as indicated here by the following occurrence. At 1900 hours on April 18, a momentary period of low-power operation occurred as the result of sticking exhaust louvers on the potassium vapor condenser. Turbine speed was maintained

essentially at design-point level by reducing the power-absorbing capabilities of the water brake which in part, required operating it with a lower-than-normal water inventory. During this transient adjustment period, the brake momentarily unloaded with a consequent speed increase. A rapid-response water brake flooding device was actuated (manually) to prevent excessive overspeed. Before speed stability was restored, the water brake was flooded in this manner twice, and on the second occasion, the disk brake was actuated by an automatic overspeed trip (set for 21,000 rpm actuation). Within minutes, the louvers were freed, and normal operation was restored. A similar occurrence involving such actuation of the disk brake occurred the following day (April 19 at 1400 hours). The disk brake was not actuated again, but as was to be later observed and evaluated, damage had occurred to the brake disk during these two actuating periods.

Shown in Figure 33 are the speed and water brake torque characteristics of the turbine deceleration during the combined water brake flooding and disk brake employment on April 19, 1966. The initial turbine speed was 18,000 rpm and the torque was 600 in.-lbs. When the water brake unloaded, the speed increased to 21,000 rpm in one-half second. The water brake flooding device was actuated and became effective by the time the turbine had accelerated to a peak of 22,500 rpm. The disk brake was actuated and became effective by the time the water brake had decelerated the turbine to 20,000 rpm. The combined effect of the water and disk brakes caused the turbine to decelerate to 9,000 rpm in two seconds. At 9,000 rpm the disk brake released and the speed increased back to 14,000 rpm under restraint from the water brake. Within five minutes normal speed was regained.

c. Water Brake Vibrations

During the initial potassium vapor testing, it was observed that the water brake vibrations were running somewhat higher than normal (as observed on the 2000-hour test). At 19,000 rpm, the nominal amplitude of vibration was 2.5 mils (peak-to-peak) vertically and about 3.0 mils horizontally (see Figure 4 for location of vibration sensor.). Normally, these run about 0.5 to 1.0 mils. Within the speed range of interest, 19,040 rpm was found to be the speed at which the water brake vibration was minimum. It was also observed that the amplitude of these vibrations would suddenly increase or decrease about 1/2 mil from the nominal values given above. In an attempt to determine whether the potassium turbine might be contributing to the water brake vibrations, it was found that if the turbine oil sump pressure (in the bearing housing) were reduced (by venting argon), the frequency at which the above vibration excursions period was from 5 to 30 seconds, but with venting, the period varied from ten minutes to several hours. Although not conclusive, it has been suspected that the higher sump pressure (which resulted in a forward component of rotor thrust) helped reduce the aft thrust load on the turbine ball bearing sufficiently that when coupled with the high unbalance of the disk brake (discussed below), vibration excursions occurred in the turbine and were in part, felt in the water brake.

However, the turbine system continued to operate satisfactorily until about 500 hours of continuous running had been accumulated. Then in the one-hundred hour period between May 8 and May 13, 1966, the water brake forward vibrations increased from 2.5 mils (vertical) to 4.5 mils, and appeared to be

getting worse. At 600 hours accumulated testing time, the system was shut down to determine the cause of vibrations. The power train was removed intact from the aft end of the potassium turbine (Figure 3) and an inspection of the turbine coupling, the water brake, the disk brake, and the potassium turbine thrust bearings ensued with the following results:

It was immediately obvious on shutdown that the disk brake had been badly scored from the previously described brake actuations, as can be seen in Figure 34a. Subsequent dye penetrant checks showed that it had produced a severe crack pattern in the area swept by the brake loader pucks. It was removed from the turbine and was check-balanced, revealing that the disk had a 7.9 gram-inch unbalance. The two wear surfaces of the disk were ground to determine the depth of, and/or to remove the cracks from the surfaces, and to see if the surface refinishing would reduce or eliminate the unbalance condition. After removing 0.035 inches from each surface of the disk, the cracked condition was still visible, although much less severe, as shown in Figure 34b. Also, during the grinding, it was observed that the disk deviated 0.015 inches from being flat. Following the remachining of the surfaces, the disk unbalance remained at 3.5 gram-inches. It was concluded that the disk brake had been put out-of-balance as a result of uneven metal loss and warpage during the braking operation. Because the disk brake had used the available installation space (Figure 34a), no vibration sensors were at the aft end of the turbine to measure the resulting vibration. In addition, the vibration sensors on the bearing housing located midway axially between the ball bearings and the pad bearings (see Figure 4) gave no clear indication of the vibration problem, partly because

the source of vibration was very close to the massive dished head of the glove box upon which the turbine is mounted. This massive and rigid structure tends to subdue any vibrations in its vicinity.

An inspection of the balance condition of the water brake rotor revealed it to have an unbalance of 2.0 gram-inches on the forward (potassium turbine connecting) end. This was attributed to an inadequate fit between the splined coupling and the water brake rotor on the conical surface (Figure 3) which allowed the brake to be initially adequately balanced with its coupling, but not to be disassembled and then reassembled without losing this balance, when installed in the final test setup. A poor fit between the internal and external tapers of these shafts and splined couplings permitted a slight angular motion between the parts.

On the splined coupling, considerable wear was observed on the potassium turbine end. This is seen in Figure 35, where the internal spline which connects to the potassium turbine shaft can be seen to have badly worn teeth. The deposited material is apparently a mixture of tooth material and overheated lubricating grease. On the water brake end, no apparent deterioration of the similar coupling had occurred. It was seen immediately on disassembling the turbine drive train that the coupling had been running completely dry, although it had been originally adequately lubricated with a high-quality grease.* This condition obviously contributed to the severe wearing of the coupling.

---

* "Plastilube-Moly No. 3", manufactured by Warren Refining & Chemical Co., Cleveland, Ohio.

It is concluded that the loss of lubrication was primarily due to an excessive temperature for the lubricant. The high temperature resulted from heat being conducted into the coupling from the very last disk brake which had been actuated three times during turbine startup.

The turbine power train was reassembled with a new splined coupling assembly connecting the potassium turbine and water brake. Air cooling was applied to the coupling for the remainder of the test. The disk brake was not included in the reassembly. Although no deterioration was evident in the potassium turbine ball bearings, new ball bearings were installed for the subsequent testing. The splined coupling was balanced by first balancing each internal splined end separately, and then the central spool section was balanced by holding it in the splined sections on a special arbor. The water brake rotor was balanced first by itself, and then as an assembly with its splined end coupling. An unbalance of less than 0.1 gram-inch was achieved in each of the components. The fit between the water brake shaft and the splined-end coupling was improved by hand-lapping to ensure contact of the tapered joint. This proved effective in all following disassemblies and reassemblies, during which no change of balance was observed. During subsequent testing, water brake vibrations were less than 1/2 mil in amplitude at speeds up to 20,000 rpm, except for a critical speed at 17,500 rpm where its peak amplitude was about 1-1/2 mils.

During the time the above modifications were being made, a borescope inspection hole in the duct upstream of the turbine bullet nose was opened.

Inspection of the inlet region of the turbine (including the upstream face of the first stage nozzle diaphragm, bullet-nose, and the eight-inch vapor pipe) revealed no visible evidence of mass transfer or other damage or deterioration.

The turbine was back in operation on May 31, 1966 at the required endurance test conditions (as indicated in Table IV). Water brake vibrations were 0.7 to 0.9 mil, and steam turbine vibrations were 0.2 to 0.3 mils.

d. Repair of Throttle Valve

Turbine testing continued according to the conditions indicated in Table IV for two weeks, until June 9, 1966, when after having accumulated 813 hours of testing, a small wisp smoke was visually observed coming from the upper area of the eight-inch throttle valve body. Closer inspection revealed a definite indication of a small leak from within the valve assembly. Although the leak was hardly discernible, and presented no immediate hazard to either operations or safety, it was clearly necessary to interrupt the endurance test for further inspection and repairs.

The test shutdown occurred on June 9 and was orderly and without incident. The leak was found to be in the welded joint which seals the bellows to the top plate of the valve body assembly. This joint was repair-welded by the following day, and the facility was immediately restarted. Endurance test-point conditions were again established at 1330 hours on June 11, 1966.

e. Water Brake Bearing Failure

Testing continued as indicated in Table IV for eleven weeks until on August 7, when after accumulating 2176 hours of testing, the vibrations on the forward end of the water brake increased (in an 18 hour period) from 1.6 mils to over 5 mils as indicated in Figure 36. The turbine was shut down for inspection, with the following observations. The water brake front bearing and the shaft oil seals surrounding it were destroyed, as indicated in Figure 37. The rear bearing of the water brake was undamaged, but was replaced along the damaged bearing. The small splined coupling between the water brake and steam turbine (Figure 3) had been slightly damaged due to the misalignment of the shaft following the failure of the water brake bearing, and this splined coupling was replaced. The Koppers coupling between water brake and potassium turbine was in perfect condition, indicating no tooth wear or lubricant deterioration, and it was re-installed. During the down time, balancing of the water brake rotor and Koppers coupling were repeated. After eight days down time for repair, the turbine was back on potassium vapor at the required set point.

f. Completion of Test

As indicated in Table IV, the final 824 hours of the 3000-hour test were completed without incident and without any significant change in the operational characteristics of the turbine. As is typified in Figure 38, the speed remained within two percent of the set point. During this testing, the potassium turbine vibrations did not exceed three g's. The temperature patterns in the bearings were the same as measured in previous testing, and the labyrinth

seal pressures were constant, as shown in Figure 39. Water brake vibrations remained constant at amplitudes below 0.6 mils, peak-to-peak.

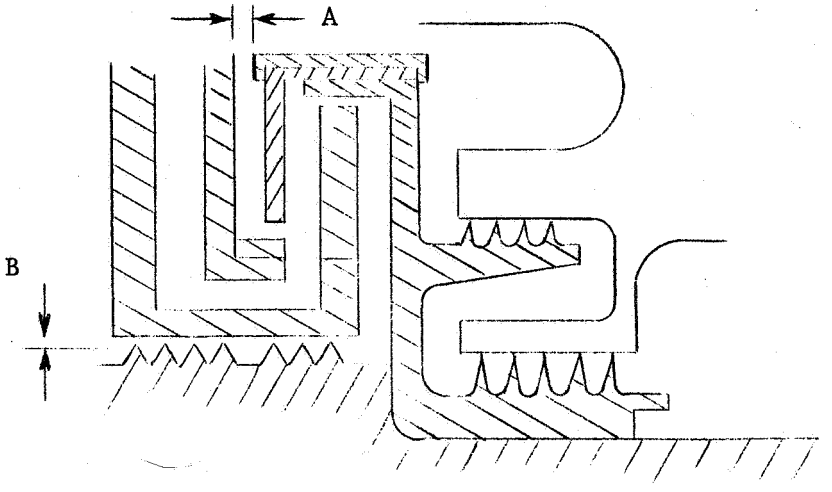
The 3000-hours of testing were completed at 2031 hours on September 19, 1966 and the turbine was shut down at this time. During the cooldown period, with decreasing vapor flow, expected speed excursions did occur as shown in Figure 40, as compared with typical speed control during endurance testing, and were controlled by water brake loading and the variation of steam turbine torque. At 2200 hours, the flow of potassium vapor had completely stopped, and rotation was maintained until final coóldown (twelve hours later) by driving the system with the steam turbine at a low speed (5,000 rpm).

4. General Observations During Testing

Throughout the testing period, it was observed that the pressure drop across the oil screw seal immediately forward of the pivoted-pad bearing (Figure 1) varied in a cyclic manner, corresponding to an apparent opening and closing of this seal. It was concluded that the seal was alternatively building up with oil which was carbonized by the environmental heat, with a resulting increase in effectiveness of the seal. Periodically it would open, reducing the seal effectiveness to design-point values.

Also, from the beginning of the 3000-hour test, the hydrodynamic seal appeared to be leaking seal liquid into the main vapor loop at a rate of about 1/4 gallon per hour. This differed from the observations made during the previous 2000-hour endurance test, during which the seal gained liquid at rates varying between 2 and 16 gallons per hour (presumed to be due to conden-

sation of vapor into the cooler seal liquid). Although originally suspected to be due to a weld crack on the seal-bearing housing attachment (later found to be completely intact upon turbine disassembly), the reason for seal liquid out-leakage was ultimately attributed to a seal flow restriction as shown below.



The seal used during this test had previously been repaired during manufacture by shrink-fitting a cap over the rotating housing when the housing outer wall had been machined too thin. This cap resulted in the restriction "A" which was 0.050 inches during this test, which is 0.030 inches less than before, and presumably resulted in an added restriction to the flow of 2.2 gpm of liquid potassium through the seal, sufficient that it caused the leakage through the clearance space (0.009 mil radial gap) at "B".

Also, during the shutdown at 600 hours of testing on May 13, 1966, it was observed that a minute leak in the bellows heat shield assembly of the bearing

housing had occurred. This allowed release of about 1/3 scfh of argon into the main facility. On startup of the system, the leak disappeared, and did not reappear until the last week of testing (in September 1966). This small leak caused no operational problems, since the argon extraction system was capable of continuously removing it from the condenser without difficulty.

V. TEST RESULTS

A. MECHANICAL DATA

No evidence of mechanical deterioration was observed throughout the 3000 hours of testing. Representative of the means used to monitor the mechanical operation during test are the conditions of the labyrinth seal which separates the oil and potassium, the proper functioning of which is extremely important. Plots of the pressure distribution across the various seal cavities (Figure 1) during operation are shown in Figure 39. Although the seal exhibited variations in pressure distribution from time to time, no degradation in sealing capacity was observed throughout the test.

1. Turbine Disassembly and Visual Inspection

On September 20, 1966, the turbine was removed from the test facility in typical fashion by cutting the welded flange at the forward end of the inlet duct and at the scroll outlet flange. Following the standard cleaning and deactivation of residual potassium, the casings were cut open, the rotor was removed, and the bearing assemblies were removed from the bearing housings. The immediate observation could be made that the turbine had endured the 3000-hour test without apparent physical deterioration as follows:

1. The stator aerodynamic components were completely intact and displayed no cracking or other mechanical or chemical deterioration.
2. The turbine rotor blades and blade retainer clips were completely intact and showed no mechanical or chemical deterioration.

3. The pivoted pad bearing was undamaged except for a single score mark on its surface.

4. The ball thrust bearings showed no evidence of spalling or of pending failure, and all bearing housing flow tubing was intact.

Presented in Table V are the major dimensional inspection records for key turbine components obtained during disassembly of the turbine following the 3000-hour endurance test. Key measurements before and after inspection are tabulated and the condition of the mating flange diameters and surfaces of the important static parts (inlet, duct, casing and scroll) are given in Figures 41 through 56. The distortions in these static components are due primarily to the high temperature operation in a closed loop where unknown forces are imposed on the turbine by the adjoining inlet and exhaust ducting.

2. Stator Inspection

Shown in Figure 47 are comparisons of the aft end of the inlet duct assembly containing the first stage nozzle diaphragm assembly and the rotor honeycomb tip seal before and after test. It can be seen that although experiencing the typical vane discoloration observed during the previous 2000-hour test, no mechanical deterioration structure or surface material loss to the fluid dynamic components was evident. The delicate trailing edges of the nozzle vanes were undamaged, and the honeycomb seal was intact. A similar view into the aft end of the turbine casings showing a comparison of the second stage nozzle exit region before and after the 3000-hour test is seen in Figure 48, with the same general conclusion that no mechanical deterioration occurred. The components were discolored as a result of testing, but were otherwise undamaged.

On the lower nozzle diaphragm at the 7 o'clock position it can be seen that the coloration is darker, which may indicate the presence of liquid at the bottom of the turbine.

Figures 49 and 50 show before and after comparisons of the split (but not yet disassembled) casings. Again, no damage to components and/or indication of blade tip rubs on the honeycomb seals is evident.

Figures 51 through 53 show the turbine fluid dynamic parts after further disassembly from the casings. Figure 51 shows forward and aft faces of the first stage nozzle diaphragm, with a closeup view of a segment of vanes shown in Figure 51c. Here, the discoloration pattern can be viewed and the braze joints are seen to be free from cracks or corrosive damage. Figure 52 shows similar forward and aft views of the second stage nozzle diaphragm with identical conclusions.

In Figure 53, the honeycomb tip seals can be seen to be intact and completely re-useable, although a faint track of impingement damage can be seen to be occurring in the 0.005-inch thick honeycomb stock of both stages. This occurs at the six-to-nine o'clock location looking forward, possibly attributable to the previously postulated presence of liquid along the bottom of the duct.

3. Rotor Inspection

Figure 54 shows the assembled turbine rotor before and after the 3000-hour test. It remained completely intact throughout the testing, with

the only major change being the typical coloration of the blades, especially the refractory metal blades. Most of the blades in both stages had also been run in the previous 2000-hour test, as discussed previously, thereby accumulating a total of 5000 hours operation in potassium vapor.

The unbalance of the turbine rotor before disassembly was determined on the balance machine as shown in Figure 55. The levels of rotor unbalance before and after the test are given in Table V and indicate that the forward (adjacent to wheels) bearing plane underwent approximately a 0.5 gram-inch increase in unbalance during the 3000-hour test, and the aft (adjacent to coupling) bearing plane was essentially unchanged.

Upon disassembly of the rotor a measurement of the tie-bolt residual tension revealed it to be 9300 lbs (which is 700 lbs less than the initial 10,000 lbs tension), thereby indicating an overall relaxation of seven percent. The before and after test measurement of the tie-bolt length indicates a 0.001 inch shortening due to testing (which appears illogical). This casts suspicion on the before-test measurement which, despite being performed under closely controlled conditions with accurate instruments, has to be discounted.

After removal of the tie-bolt, the wheels were separated at the curbic couplings by applying approximately 50 lbs axial load between the wheel faces. During running, the curvic coupling faces typically lock tightly together, presumably due to a minor degree of diffusion bonding. No physical measurement was made of the curvic coupling dimensions, although a visual inspection showed them to be unaffected by testing (see Figure 56). The wheel diameters

(both stages), measured at the blade tips, revealed an increase in diameter of 0.001 inches. This is the same as was measured following the 2000-hour test.

The general condition of the turbine rotor blades following the 3000-hour endurance test is given in Figures 57 through 59. In addition, the weights of the individual blades, before and after 3000 hours testing are presented in Table VI. In both stages, the blades were weighed prior to testing, and following testing were weighed twice, once after a superficial brush cleaning (to remove surface oxide and/or loose foreign material), and then again after a vapor blast* cleaning. It can be seen in Table VI that the U-700 stage two blades exhibited an average increase in weight of 0.013 percent. Correspondingly, the TZM blades (present only in stage two) revealed a weight loss of 0.035 percent and the TZC blades showed the same weight loss of 0.035 percent.

Figure 57 shows overall views of stage one and two wheels with some of the blades removed for dovetail inspection. The overall mechanical integrity of both stages was found to be good. Figures 58 and 59 show closer views of segments of blades in this assembly with corresponding indications of blade material and accumulated testing hours. Figure 60 shows the overall condition of the wheel dovetail connections of both stages. No evidence of fretting, galling, or corrosive deterioration on either blade or wheel dovetails was observed following the 3000-hour test.

*Light blast using slurry of water and Siliceous Earth #1250 NVB manufactured by Vapor Blast Manufacturing Company.

The central tie-bolt (U-700) and the shaft (A286) are shown in Figures 61 and 62, respectively. It can be seen that the static seals (a Bar-X seal on the tie-bolt and a chevron seal on the shaft, as shown in Figure 1) were both effective in preventing migration of potassium into the inner shaft bore, and the migration of oil forward under the hydrodynamic seal sleeve on the shaft, respectively. In Figure 61 the dark area forward of the seal location on the tie-bolt is an area of oxidized potassium, while the region immediately aft of the seal has remained totally clean. Similarly, the seal interface on the shaft can be seen in Figure 62.

4. Bearing Housing Inspection

The components in the bearing housing assembly are shown in Figures 63 through 66. Figure 63a shows the bearing housing immediately after removal from the scroll, before removal of the bellows expansion shield and hydrodynamic shield assembly. At its forward end, the hydrodynamic seal nickel inner diameter can be seen to have rubbed. Also, upon disassembly, it was discovered that the previously reported leak in the expansion heat shield cover was due to an electric arc-blown hole in the cylindrical section. This is presumed to have happened during assembly-welding prior to the test. However, the bellows section of this cover was found to be tight, thereby successfully undergoing 5000 hours of testing. The bearing housing, following removal of this bellows heat shield assembly and the hydrodynamic seal, is shown in Figure 63b. This disassembly revealed some rubbing of the labyrinth seals (as reported in Figures 41 through 46). These rubs resulted in a cold diametral clearance increase of 0.004 inches on both labyrinth seals, which occurred in the copper plating, with essentially no change in seal teeth diameter.

Figure 64 shows the hydrodynamic seal after separation from the bearing housing, and the removal of its potassium supply tubes. This component is structurally intact with dimensional changes recorded in Figures 41 through 46.

A photograph of the pivoted-pad bearing pads after test is shown in Figure 65. The only damage incurred to this component in 3000-hour testing was the slight scoring of the surfaces due to foreign material, and the opening of the diametral clearance of 0.0015 inches. The journal did not measurably change in dimension as indicated in Figures 41 through 46.

Figure 66 shows the ball bearing assembly, indicating the ball bearing contact surfaces to be completely free of any spalling or wear indications. This assembly showed slight wear grooves on the O.D. of the outer race, thereby indicating rotation of this race in its housing, although no associated loss in its functioning characteristics were observed.

B. METALLURGICAL EVALUATION

1. Turbine Rotor Blades

a. Macrophotographs

The appearances of the convex airfoil surfaces of U-700 first- and second-stage blades after the 3000-hour test are shown in Figure 67. Photographs are included, for comparison purposes, of the 2000-hour test blades. The 3000-hour blades entered the test as new blades; the 5000-hour blades had been subjected to both 2000-hour and 3000-hour tests. Note that in the 2000- and 3000-hour test blades there is little visible evidence of liquid metal

corrosion, and that the stain patterns indicate areas in which separation of flow occurred and liquid metal droplets may have accumulated.

The condition of the convex airfoil surfaces of molybdenum base TZM and TZC blades is shown in Figure 68. While corrosion traces along the convex leading edge appear more visible in the 5000-hour photos, the greater portion of this corrosion was in evidence after the 2000-hour test. A new TZM blade, installed in only the 3000-hour test, experienced only light corrosion traces in this area, whereas those blades tested for a total of 5000 hours (in both the 2000- and 3000-hour tests) had larger corrosion traces.

The lack of liquid metal impact damage on the convex leading edge of the first-stage blades is clearly indicated in Figure 69. A similar absence of impact erosion in second-stage U-700 and TZC blades is shown in Figure 70. Once again the corrosion traces on two TZC blades, tested for 2000 hours and, subsequently, for 3000 hours, are noted in areas away from expected impact erosion surfaces.

An examination of the appearance of the blade surfaces at a magnification of 10X is possible for convex mid-chord, concave leading edge, and convex trailing edge locations in Figures 71 through 75. Figure 71 shows the surfaces of U-700 first-stage and second-stage blades on the convex surface from the leading edge to the mid-chord position. These first-stage blades still show the mechanical impact damage done in earlier steam turbine testing in which solid particles impinged upon the blades; however, there is no evidence of liquid metal impact damage. The second-stage blade tested for 3000 hours had not been

previously tested in either potassium or steam; its relatively unaffected leading edge surface clearly indicates the absence of impact erosion.

The relative absence of concave leading edge corrosion during the 3000-hour test, is shown in Figure 72. In the first stage, the 3000-hour test blade was without evident surface corrosion whereas the blade tested for 5000 total hours still retained the leading edge corrosion which occurred in the 2000-hour portion of its test. While corrosion comparisons are not as striking in the second-stage blades, a comparison of the 2000-hour test blade and the 3000-hour test blade show the former to be much more affected.

The corrosion in the first 2000 hours and the lack of corrosion in the latter 3000 hours of testing is believed to be associated with two factors which changed between the 2000-hour and 2000-hour tests. First, a change was made in the inlet flow condition to the turbine rotor which apparently resulted in reduced stagnation particularly at the leading edge of the blades and second, the oxygen contamination in the loop was temporarily high only during the first startup. The first factor is discussed below; the second is treated in more detail under section V.B.2.

Shown in Figure 73 are the predicted inlet velocity vector diagrams for the 3000-hour endurance test. The angle of incidence on the first stage rotor blade increased from -18.4 to +4.2 degrees from the 2000- to the 3000-hour endurance test. This was due to the change in matching between the two stages which was caused by the use of the new stator-blade assembly.

Since a more positive angle of incidence results in a smaller tendency for local flow separation just downstream of the leading edge on the pressure surface, there would be less tendency for the collection of moisture in the 3000-hour test than in the 2000-hour test. This may have had a beneficial influence on the amount of corrosion observed near the leading edge of the first- and second-stage rotor blades. The apparent absence of subtle leading edge corrosion stains in the blade subjected to a total of 5000 hours testing may have resulted from a low level cleaning of the 2000-hour corrosion stain which may have occurred during the subsequent 3000-hour test.

Similarly, the trailing edge corrosion of U-700 blades noted in the 3000-hour test was negligible as compared to that observed in the 2000-hour test; Figure 74 illustrates this well and indicates the second-stage corrosion effects are, in general, less than those observed on the first stage, probably as the result of lower temperatures in the second stage.

A comparison of various airfoil surfaces in the second-stage TZC and U-700 blades tested for 5000 hours is shown in Figure 75. The greater corrosion in the TZC alloy would be expected in potassium temporarily contaminated with oxygen or in a multimetallic system in which the limited amount of refractory alloy would act to concentrate the effects of minor oxygen impurity levels over an extended test period.

Although the evidences of corrosion in the TZC molybdenum alloy are greater than in the U-700 alloy, they still do not represent a serious threat to the safety of the turbine. Furthermore, the more noticeable corrosion of

the TZC occurred during the 2000-hour test. Based upon other evidence, to be discussed below (see section V.B.2.), the gross corrosion, evidently, occurred during initial turbine startup of the 2000-hour test when oxygen impurity levels were higher than usual, and the corrosion did not progress significantly during the 3000-hour test.

b. Rotor Blade Weight Change

The blade weight changes after both the 2000-hour and 3000-hour tests are summarized in Table VII and shown in bar form in Figure 76 for comparative purposes. The weight changes are given in percentages of original weight and are compared in the as-steam-cleaned-and-brushed condition and after light vapor blasting to remove loose scale and stain. It should be noted that in comparison to the small changes in blade weight approximately 17,000 lbs of liquid flowed through the turbine each 1000 hours.

The previous blade history and prior surface condition had little influence on the weight losses in additional testing as indicated by a comparison of appropriate shaded and clear bar graphs comparing blades with and without previous potassium vapor test experience.

Weight losses, as the result of vapor blasting, were a good indication of the degree of surface stain and loose corrosion produce removed by this operation. Note that these vapor blast weight changes were more significant in blades from the 2000-hour test in which corrosion was more evident; the vapor blast weight changes were also more significant in the first-stage blades than in the second-stage blades of the 2000-hour test for the same reason. The

relative cleanliness of the 3000-hour test and the lesser corrosion experienced in 3000-hour blades is indicated by less severe total weight changes as well as by a lesser weight change after vapor blasting.

c. Tensile Strength Tests

The tensile strengths of blade materials after the 3000-hour test were determined on miniature tensile test specimens machined from the blades. A typical blade and tensile specimen is shown in Figure 77.

The results of room temperature tensile tests on U-700 blade materials after 3000-hour test exposure can be seen in Table VIII and are shown graphically for comparison with untested material in Figure 78. Note that while there were some reductions in tensile elongation, the mechanical properties were fairly well maintained in the U-700 taken from the second-stage blades; these blades operated at about 1240°F. In the first stage, which operated at a higher temperature (about 1407°F), the reduction in tensile elongation and reduction in area is progressive with increased test time; after 5000 hours of total testing, the tensile elongation was reduced to five percent from an initial 18-20 percent. As indicated in Table VIII, the high temperature ductility and strength properties were not significantly affected. The loss of room temperature ductility in the first-stage blades is believed to be due to the formation of sigma phase after long periods of testing; the presence of sigma phase was confirmed metallographically as indicated later in this report.

Miniature tensile bars were also machined from two TZC alloy, 5000-hour turbine blades in the same manner as those from the U-700 alloy blades; they

were tested at room temperature and at 250°F. The tensile results presented in Table IX indicate generally comparable strengths and ductilities compared with test specimens not exposed to the turbine test.

Bend specimens were made from the trailing edges of two TZC alloy, 5000-hour blades and were tested about a 2T radius with the convex surface in tension to determine the effects of surface deposits, etc. on bend ductility. The results, which are presented in Table X, indicate a brittle-to-ductile transition temperature between 125 and 250°F.

The marginal low temperature ductility of the TZC material in the turbine blades did not become worse during turbine test. In spite of the low ductility at room temperature to 250°F, a turbine preheat of approximately 700°F, which has been successfully used in the past tests, should continue to provide the required ductility for future safe restarts of the turbine after this amount of turbine testing.

In another type of experiment, decreases were demonstrated in the low temperature ductility of refractory alloy tensile specimens exposed to the turbine environment. Tensile test specimens were suspended in metal cages in the potassium vapor upstream and downstream of the turbine. After performance testing, these tensile specimens were tested at room temperature and at elevated temperature. The results are shown in Table XI, where data is also available for comparisons with similar materials not subject to exposure in the turbine facility.

The TZM tensile specimens exposed at a temperature of 1500°F ahead of the turbine for 3000 hours had a complete loss in room temperature ductility. However, there was scarcely any difference in the 1400°F tensile properties for these TZM specimens.

TZC tensile specimens had previously been tested downstream of the turbine for 1746 hours during the 2000-hour endurance test. The low temperature ductility of these TZC specimens was reduced some, but the change was not as severe as in the TZM alloy, which was located in a higher temperature region during endurance testing. On the other hand, TZC specimens tested downstream of the turbine for 3000 hours showed much more decided reductions in ductility and an increase in yield strength at 150°F and at 1400°F. The high temperature properties of TZC after this exposure were not adversely affected, as indicated by the 1400°F tensile test values. While it appears that the brittle-to-ductile transition temperatures of these molybdenum alloys have been raised, the availability of turbine preheat during turbine startup should avoid the consequences of this brittle characteristic during turbine testing.

AS-30 columbium alloy tensile specimens were also exposed for 3000 hours downstream of the turbine to determine the effects of the potassium vapor environment on their mechanical properties; it had earlier been decided not to install columbium alloy blades in the turbine because of their rapid surface contamination in the turbine facility. The tensile test specimens were embrittled by this exposure as indicated by their poor room temperature ductility; but the high temperature tensile characteristics remained relatively unchanged.

Both the gettering columbium-base alloy, AS-30, and the less active molybdenum-base alloy, TZM, were embrittled at room temperature by exposure to the turbine environment. This decrease in ductility was attributed to surface contamination of the specimens. The higher exposure temperature of the TZM may have been partially responsible for its increased sensitivity to embrittlement; nevertheless, the loss of room temperature ductility in the TZM alloy was a somewhat unexpected finding which points to the need for further evaluation of the effect of multimetallic turbine facility operation on refractory alloy properties. In a completely refractory alloy system, however, it is probable that this type of reaction and accompanying loss of low temperature ductility of the TZM alloy would not occur.

d. Microexamination of U-700 Alloy Rotor Blades

Since some new turbine blades were installed in both turbine stages for the 3000-hour endurance test, blades having 2000 hours, 3000 hours, and 5000 hours of endurance test times were available for evaluation and comparison at the end of testing. In these blades, as in those from the 2000-hour test, evidences were noted of surface alloy depletion, localized corrosion, thin deposits both of copper and of other metallic mass transfer elements, and the formation of the embrittling sigma phase.

Microscopic examination of turbine blades from 3000-hour endurance test did not reveal any structures of phases which had not previously been observed in the 2000-hour endurance test blades.

Alloy depletion of the surface material of the 3000-hour, U-700 alloy blades was observed to be of the same metallographic nature as that observed in the 2000-hour test blades; in those blades, electron microprobe techniques disclosed significant losses of nickel, cobalt, and chromium, and an increase in iron at the blade surfaces.

For test periods of 2000, 3000, or 5000 hours, the first-stage blades appeared to have less total surface affected by depletion than the second-stage blades, but the effects were deeper in the first-stage blades. Figure 79 is representative of the alloy depletion found to a depth of 1/4 to 1/2 mil on the convex surface of a first-stage, 5000-hour test blade.

A 0.1-mil thick, uniform depleted layer extended over the entire convex surface of the second-stage, 5000-hour blade airfoil; Figure 80 is typical of this thin layer. The depletion layer appeared to have poor integrity and adhesion to the underlying metal in most locations as evidenced by the presence of local eruptions and general spalling, which are seen in a locally severe case of alloy depletion in Figure 81.

Macroscopic corrosion of the U-700 alloy blades appeared to be much less for the 3000-hour, U-700 blades than that experienced in the 2000-hour test, particularly at the leading and trailing edges and at other places where aerodynamically influenced corrosion had occurred in the 2000-hour test. This is indicated by Figures 82 and 83 which show equivalent areas of the convex surfaces of a 2000-hour test blade and a 3000-hour test blade, respectively.

A cross section of a corrosion groove located on the convex surface approximately mid-chord of a 3000-hour, first-stage blade is presented in Figure 84. Note that the immediate area is essentially free of alloy depletion and the presence of surface deposits of diffusion zones. Grooves and channels of this kind are presumed to have been formed by the corrosive action of freshly condensed potassium being moved along the airfoil by the aerodynamic forces of the vapor stream. Corrosion grooves and channels were observed on practically all airfoil sections examined; occasionally a groove, which had formed during the 2000-hour test, had been filled to a smooth contour by metallic material transferred during the 3000-hour test. Those blades which had a total test time of 5000 hours reflected a combination of the aerodynamically influenced corrosion patterns from each of the separate turbine test conditions.

Microscopically, evidence of corrosive action on the intergranular carbide network was observed in the formation of a fissure in a first-stage, 5000-hour blade on the convex surface near the trailing edge. This fissure, which measures approximately 0.002-inch deep and is shown in Figure 85, appears to be covered over by a layer of depleted alloy, or else it existed in the blade at manufacture and was covered over with a layer of metallic transferred material during turbine operation. This was the only such fissure observed in all of the blade sections examined and would not appear to be detrimental to turbine blade integrity.

A bronze-colored deposit was observed on several of the 3000-hour test components at disassembly. Figure 86 shows the aft view of the second-stage

nozzle diaphragm where an extensive bronze-colored deposit was found. This was the largest metallic deposit which occurred during all of the turbine testing. Spectrographic analysis of this deposit showed that it contained a major amount of iron, minor amounts of nickel, chromium, copper, titanium, and zirconium, and trace amounts of less significant elements. The bronze color of the deposit may have been due either to its copper content or to bronze-colored suboxides of titanium. Bronze-colored deposits containing primarily titanium with trace amounts of copper were found on refractory alloy blades, as described below. These metallic deposits were, undoubtedly, picked up from the Type 316 stainless steel boiler and from the hot traps, carried to the turbine as solute in liquid metal droplets, and deposited there as the result of evaporation of the liquid potassium.

A copper-rich phase was observed in 3000-hour, U-700 turbine blades; it was similar to that observed in 2000-hour test blades, where it was identified as copper by electron microprobe examination. In the 3000-hour blades, this phase appeared not to be limited to any particular airfoil or dovetail location but was present wherever a metallic deposit had formed. The phase was more prevalent in the first-stage blades. In general, the depth of the phase was influenced by diffusion rates; the first-stage blades, which operated at the higher temperature, and those blades which were tested for longer times contained the copper to a greater depth. A typical example of this phase which occurred near the trailing edge on the convex surface of a first-stage, U-700, 5000-hour blade is shown in Figure 87. During the 5000 hours it has penetrated only 3/4 mil. Fissures through this phase to the underlying blade material are

shown in Figures 88 and 89 of a first-stage, U-700, 3000-hour blade. These fissures were not observed in thinner diffusion zones in 2000-hour test blades. Close examination of Figures 88 and 89 indicates that (1) the fissures were produced by corrosion between particles of the copper-rich phase and (2) they were not cracks.

The formation of the embrittling sigma phase was observed in the 3000-hour, U-700 alloy blades in the first stage only. The extent of sigma phase formation is known to have a direct time and temperature dependency; this is dramatically illustrated by the photomicrographs presented in Figure 90 in which sections of first- and second-stage blades tested for 2000, 3000, and 5000 hours are shown for comparison. The largest amount of sigma phase is apparent in the first-stage blades having the longer exposure times at the higher operating temperature. The presence of sigma phase effectively decreases the tensile ductility of tensile specimens extracted from tested blades as discussed above.

Since the procurement of the U-700 alloy for this turbine project, much effort has been expended in the aerospace industry to define the cause and to eliminate the formation of the embrittling sigma phase in superalloys. At present, the chemical analysis of many such alloys is controlled to prevent the formation of sigma phase. This is accomplished by a mathematical analysis*

* G.E. Spceification E50TF28, "Electron Vacancy Number Calculations".
See also: Woodyatt, L.R., Sim, C.T., and Beattie, H.J., Jr., "Prediction of Sigma Type Phase Occurrence from Compositions in Astenitic Superalloys", Trans. A.I.M.E., V236, April 1966, pp 519-26.

of the composition of the heat of material under study. The elements, in the amounts required to form the predominantly stable precipitated phases, are first identified; the composition of the residual matrix is then calculated, and it is used, in turn, to calculate the mean electron vacancy number of the matrix from the following equation:

$$\overline{N}_v = \sum_i^n = 1 \quad m_i(N_v)_i$$

where:

$\overline{N}_v$ = average electron vacancy number

m = the atomic fraction of a particular element

N_v = individual electron vacancy number of the particular element

n = number of elements in the matrix.

The electron vacancy numbers of a large number of alloys have been calculated. Sigma-free alloys have numbers less than 2.52 while those which form sigma phase have numbers greater than 2.52. Since the nominal value of the electron vacancy number for the matrix of U-700 alloy is close to 2.52, it is necessary to calculate the actual value based upon chemical analysis of the heat to determine whether or not the alloy is prone to formation of sigma phase. Current specifications for U-700 alloy in either cast or wrought form require that the average electron vacancy number be less than 2.32 in order to be resistant to the formation of sigma base over long periods of operation at elevated temperatures. Material currently used, and in which sigma phase formed, had an electron vacancy number of 2.502. In future potassium turbine work the use of U-700, at temperatures where sigma phase can form, will take advantage of alloys thus controlled.

e. Microexamination of Refractory Alloy Rotor Blades

A metallographic comparison was made of the relative degree of corrosion in the 2000-, 3000-, and 5000-hour test blades on the convex mid-chord section of the airfoil where aerodynamically influenced corrosion was observed. The 3000-hour test blade experienced only light surface corrosion and stains in this area; the blades exposed during the 2000-hour test (including those subsequently tested for an additional 3000 hours) exhibited actual corrosion grooves to depths of 2.5 to 4 mils. Figures 91 through 93 illustrate that the corrosion grooves observed in the 2000-hour test did not enlarge during the subsequent 3000-hour test. It should also be noted that the TZM blades installed new at the beginning of the 3000-hour test disclosed practically no distinct corrosion grooves along the tip, nor along either the concave leading edge or the convex trailing edge (as evidenced in Figures 72 and 74) nor on other surfaces as were observed on refractory alloy blades tested for 2000 hours. The TZM and TZC blades which accumulated 5000 hours testing time had, of course, retained the corrosion grooves and deposits which they had accumulated during the 2000-hour test.

As reported above, the U-700 blades from the 2000-hour test were shown to contain, by microprobe analysis, a copper-rich phase which was the result of copper deposits diffusing into the nickel-base alloy. The copper-colored deposits on the airfoil surfaces of refractory alloy blades from the 3000-hour test were presumed to be of the same nature. Spectrographic analysis indicated that these copper-colored deposits contained primarily titanium with only a trace amount of copper. The bronze, purple, and black surface stains observed

in metallographic examination are attributed to the various forms of titanium oxides. Because of the refractory nature of the molybdenum base alloys, no diffusion of these surface contaminants into the base metal was observed. Figure 94 of a TZM 5000-hour blade shows these sections in which copper-colored deposits can be seen.

A thin, uniform deposit of metallic material, less than 0.1-mil thick, was observed on the concave mid-chord surface of a 5000-hour TZM blade as shown in Figure 95. Note in Figure 96 that corrosion appears to have taken place through a similar metallic film, which was 0.1-mil thick, and into the base metal to a depth of 0.1 mil on the convex surface leading edge of a 3000-hour TZM test blade. These corrosion pits were not previously observed in 2000-hour test blades. They are probably cross sections of radial grooves generated by liquid potassium flowing on the blade subsequent to or during the time of the mass transfer of the metal film.

2. Environmental Cleanliness

The cleanliness of the potassium vapor and liquid droplet environment during turbine testing can have a direct effect on the corrosion characteristics of turbine materials. The slightly corroded appearance of the turbine blades from the 2000-hour test indicated that test environment was less clean than the environment during the 3000-hour test. This was confirmed by measurements of the contamination gettered by refractory alloy specimens inserted in the test facility and by intermittent analysis of the potassium in the condenser for oxygen and carbon content.

a. Refractory-alloy Contamination Specimens

In a manner similar to that of the 2000-hour test, refractory alloy specimens were installed in the facility during testing in front of and behind the turbine. These were inserted into the facility on Type 316 stainless steel probes as shown in Figure 30. Various refractory alloy ring specimens were inserted on the probes placed within the facility and later removed for analysis and/or replaced by new specimens during temporary shutdowns of the turbine test facility; these shutdowns occurred after 814 test hours and after 2175 test hours. Data covering the weight changes of these specimens and their C, O, N, and H analyses (taken within 0.030-inch of the exposed surface) are given in Tables XII through XV. The reference C, O, N, and H analyses for the refractory alloy specimens before test and their typical chemical compositions are given in Table XVI. For convenience in comparing the test results on these specimens exposed to the turbine facility environment, the data on changes in weight, carbon, oxygen, nitrogen and hydrogen content are shown graphically in Figure 97. The data are arranged to permit comparison of the effects of various test periods, of test locations, and of materials types. Data from the 2000-hour test are also shown graphically because of their importance for comparison purposes.

The contamination of refractory alloys in the 3000-hour test was very much less than that experienced in the 2000-hour test. This is evident from the very low changes in weight and in oxygen and nitrogen contents of the F-48 specimens in the 3000-hour test as compared to those of the 2000-hour test. The startup and the first 814 hours of the 3000-hour test appear to have

occurred in a relatively clean environment as indicated by low weight changes and low contamination levels in the refractory alloy specimens both upstream and downstream of the turbine. The latter portion of the 3000-hour test was also "clean" in its operation as evidenced by the lack of any significant changes in impurity levels from the anticipated trends.

b. Potassium Purity

Before, during, and after the 3000-hour endurance test, the potassium was sampled and analyzed using methods established by SPPS during the 2000-hour test. These are described in the Reference 3. The oxygen and carbon concentrations of the potassium for both the 2000-hour and the 3000-hour test are shown graphically in Figure 98.

Each time a high value for oxygen concentration was found during the 3000-hour test, the loop was resampled and reanalyzed immediately. It was always found that the sample for which the high value was found had been inadvertently contaminated except as indicated in the following paragraph. The analytical blank which is inherent in the technique has not been subtracted from the values shown; consequently, the actual oxygen concentration in the potassium is somewhat lower than indicated. This blank amounts to about seven micrograms, as reported in Reference 3. The oxygen content of the potassium during the 3000-hour test, thus, remained at the same low level as it did during most of the 2000-hour test.

The only time that high oxygen values were found to be significant was during the beginning of the 3000-hour test. It was anticipated that initial

high oxygen concentrations would drop to very low values during the first four hours. Once this did not occur, and it was reported to the operating personnel, a correlation was made with some other operational difficulties which led to the discovery of an air leak in the low pressure section of the loop. This was repaired with the result that the oxygen level subsequently dropped to the expected low values of less than 10 ppm.

The data for carbon indicates that this contaminant also remained at a very low concentration during the 3000-hour test. The sporadic higher values found for some samples have not been explained.

Some analyses for metallic impurities in potassium were performed. They were essentially the same as indicated for the 2000-hour test; that is, all metals determined were very close to, or below, the detection limits. For example, the data obtained for Sample 582 were: Ag < 1, Al < 1, Ba < 1, Be < 1, Ca = 1, Cb < 1, Co < 5, Cr < 1, Cu < 1, Fe < 1, Mg = 1, Mn < 1, Mo < 1, Na = 25, Ni < 5, Pb < 5, Si < 1, Sn < 5, Sr < 1, Ti < 5, V < 5, W < 50, and Zr < 5; reported as ppm in KCl.

The high purity of the potassium vapor flowing through the turbine indicated by the chemical analyses is substantiated by the low contamination levels observed for the refractory-alloy inserts which were exposed to the potassium.

The oxygen and water vapor concentrations of the argon used during the 3000-hour test were monitored continuously. The oxygen concentration remained between 1 and 1.5 molar ppm, and the water vapor concentration stayed between 0.4 and 0.7 molar ppm throughout the test.

c. Absence of Rotor Blade Corrosion

The slight corrosion of turbine blades in the 2000-hour test and the apparent absence of any significant corrosion during the 3000-hour test seem to be associated with (1) the impurity levels within the potassium vapor environment, and (2) the previously discussed fact that new nozzle diaphragms directed the vapor flow at closer to design flow angles. Several factors tend to support the first contention. First, the eight-inch diameter vapor line and throttle valve were removed and exposed to air immediately prior to the 2000-hour test. Although these components were carefully cleaned, it was not feasible to flush them with liquid potassium prior to operation of the turbine on potassium vapor. Secondly, the oxygen analysis of the potassium in the condenser indicated a high value of 69 ppm after two hours of the 2000-hour test as shown in Figure 98; the actual oxygen content in the potassium droplets passing the turbine may have been much higher as the turbine was started. The self-cleaning aspect of the turbine facility operation on potassium quickly reduced the oxygen impurity content in the potassium going to the condenser. The greater part of blade corrosion observed in the 2000-hour test may have occurred in this early startup period. Third, refractory alloy specimens subjected to the startup conditions of the 2000-hour test underwent contamination to an extent not witnessed in later exposures of much longer test time. Fourth, the installation of the test turbine in the facility for the 3000-hour test was accomplished without major exposure of the facility to air, and the facility remained in a relatively uncontaminated condition between the 2000- and 3000-hour test; consequently, the system was relatively clean at the start of the 3000-hour test. Fifth, the installation of the new first- and second-stage nozzles prior to

the 3000-hour test directed the vapor flow at the proper turbine entry angle and minimized the possibility of leading edge turbulence which was thought to have occurred in the 2000-hour test and to have been partially responsible for corrosion during the first endurance test.

It is believed that the 3000-hour test, with its minimal corrosion of superalloy and refractory alloy blades, is most representative of the typical turbine test experience which can be expected in the present type of turbine facility.

3. Erosion Inserts

Erosion inserts of the type shown in Figure 29 were installed behind the tip of the second stage rotor blades during the 3000-hour endurance test. The purpose of these inserts was to continue, beyond the previous 2000-hour test experience, the evaluation of various materials under the influence of impacting potassium droplets. These droplets came from the second-stage blade tips at turbine tip speeds of 770 ft/sec and at temperatures of about 1240°F. The twelve erosion inserts, consisting of U-700 alloy, TZM alloy, TZC alloy, and AS-30 alloy were arranged in the second-stage shroud as shown in Figure 99. Table XVII identifies the exposure times for various specimens.

Impacting liquid droplets from the blade trailing edge tips struck the specimens along the narrow face of the projecting tab of the insert near the 90° milled recess; Figure 100 shows the location of impact erosion pits in relation to the blade tip.

All of the erosion inserts were examined macroscopically at magnifications as high as 60X for evidence of erosion. Macrophotos of representative impact specimens from both the 2000- and 5000-hour endurance tests are presented for comparison in Figure 101. It was observed that: (1) additional erosion occurred on the 2000-hour U-700 alloy inserts, (2) only two of the three newly installed U-700 inserts were eroded, (3) no erosion occurred in the TZM, TZC, or AS-30 inserts after testing for periods up to 5000 hours, and (4) corrosion occurred in an unusual manner on the back side and the hidden forward surfaces of the AS-30 specimens.

As in the 2000-hour test inserts, the 3000-hour U-700 test inserts were coated with minor, non-uniform surface deposits and were discolored. Both were found to consist of corrosion products and mass-transported material similar to that observed on the test blades. This surface contamination was responsible for the increases in weight of U-700 specimens shown in Table XVIII. The presence of corrosion products and mass-transport material distorted the true weight changes of the specimens; it is significant to note that in spite of the erosion of the U-700 specimens, they show a weight gain, while the refractory alloys, which were not eroded, show a weight loss. This indicates that surface contamination and solution corrosion effects can mask the real weight changes brought about by metal loss due to impact erosion.

The U-700 alloy inserts were clearly the most affected; as in the 2000-hour test inserts, clusters of deep holes were radially apparent at approximately the same location as experienced in the 2000-hour test. These holes were

examined metallographically at several planes through the impacted area in an effort to distinguish between those holes which developed during the 2000-hour test and new holes developed during the additional 3000 hours of testing. The location of the polished surface with respect to that of the pattern of holes was continuously maintained as grinding proceeded through the cluster of holes. Figures 102 and 103 illustrate the microstructure at the surface of holes from the earlier 2000-hour test erosion insert. Figures 104 and 105 illustrate the nature of the holes which were formed during the 2000-hour test and which were subjected to further liquid droplet impact damage during the 3000-hour test. Figures 106 and 107 illustrate the microstructure at the surface of holes which were newly formed during the 3000-hour test. The diameter and depth of impact damage is similar in all cases. The most significant difference between the specimens of the different tests is the depth of the alloy depletion layer; the depleted layer became deeper with prolonged testing. This surface effect was, apparently, not a product of liquid impact as it was present on all exposed surfaces of the U-700 alloy inserts. Nevertheless, the depletion of surface alloying elements was undoubtedly produced by the presence of liquid potassium at the surface. In turn, the depletion of the surface may have rendered the surface more susceptible to impact erosion.

That the damage is similar to steam turbine erosion is indicated by its comparison with a macrophotograph of an eroded Stellite 6B erosion shield from a steam turbine as shown in Figure 108. A cross-section of this shield presented in Figure 109 shows an almost identical pattern of holes as observed in the U-700 alloy erosion specimens.

The refractory alloy specimens exhibited no impact erosion; however, some corrosion was noted in an AS-30 columbium alloy specimen as seen in Figure 110. A photomicrograph of a cross-section of one of the corrosion grooves is shown in Figure 111; its clean surfaces and absence of microcracks or subsurface contamination indicates the metal loss is corrosive in nature.

4. Rotor Blade Clips

Turbine blade retainer clips from both stages were found to have erosion pits on their advancing edges on the aft side of each wheel. Apparently, these clips were struck by liquid potassium droplets during some portion of the 3000-hour endurance test. The second-stage clips contained many more pits than the first-stage clips, probably because of the presence, in the second stage, of a greater quantity of condensed potassium. There was no apparent explanation for the fact that clip erosion occurred on the aft side of the first and second stages but not on the forward side of either.

The relative impact erosion which occurred on clips of the first and second stages is shown in Figures 112 and 113. Microscopic examination of these pits proved them to be similar in form to the pits observed in the erosion inserts, but the alloy depletion layer so apparent in the U-700 alloy erosion specimens is absent in the micrographs of the Rene' 41 blade clips seen in Figures 114 and 115. Furthermore, the characteristic microcracks associated with impact erosion are also absent in these blade clip micrographs.

5. Honeycomb Tip Shrouds

The turbine blade honeycomb tip shrouds of both stages sustained a minor distinguishable amount of erosion during the 3000-hour endurance test. Differences between the first- and second-stage honeycomb erosion were difficult to determine. In both stages, the erosion was greatest toward the aft portion of the honeycomb. At its worst, the depth of erosion was estimated at four times the thickness of the honeycomb material, or approximately 40 mils. Since this erosion occurred in a circumferential direction only, there were many cell walls oriented in a circumferential direction which were eroded very little. Rotor tip clearances affecting leakage in the axial direction were not increased; because of this, it is doubtful that the observed erosion adversely affected turbine performance.

Figures 116 and 117 show the impact area to be primarily those honeycomb components which had surfaces most nearly normal to the direction of the liquid droplets leaving the blade tips. A photomicrograph of our eroded honeycomb section is presented in Figure 118.

6. Erosion Discussion

As noted above, liquid droplet impact erosion was observed in several places: on the advancing edge of the aft side of Rene' 41 blade clips in the first and second stages (the erosion was more significant in the second stage); on the Type 316 stainless steel second-stage honeycomb turbine shroud; and on the stationary U-700 erosion inserts installed behind the second-stage turbine blade tips. Of equal significance is the fact that erosion did not occur on

similar refractory alloy erosion inserts although they were subjected to identical liquid droplet impact conditions.

The fact that U-700 was eroded but that TZM, for example, was not, is of interest when their relative yield strengths, fatigue endurance limits, and strain energies are examined. In each case, the U-700 has properties which are superior to TZM. This is indicated in Figure 119 for yield and fatigue properties and in Table XIX and Figure 120 for strain energy values.* These properties are generally believed to be indicative of the resistance of a material to damage by impacting liquid droplets. While the exact nature of this correlation of materials properties with multiple drop impact damage may be in doubt, it is surprising to find that the impact damage experienced in the potassium vapor turbine bears an inverse relation to these materials properties.

It is recognized that the environmental conditions within the turbine may have modified the surface properties of the superalloy materials by depletion, mass transfer, and/or diffusion to render the eroded material less resistant to impact damage by liquid metal drops. The diffusion zones along the surface of the U-700 erosion inserts are indicative of this possibility.

* Thiruvengadam and Preiser (NASA CR-72035) showed a correlation between the strain energy of a material and its resistance to cavitation damage in liquid sodium at 1000°F. Assuming a straight line relationship, the high temperature strain energies of refractory alloys and of U-700 are also plotted as solid data points in Figure 120 to indicate their expected relative resistance to liquid metal cavitation damage.

C. PERFORMANCE

1. Validity of Measurements

Most of the instrumentation which malfunctioned was replaced or repaired and recalibrated during the shutdown periods. Correlations relating some of the measurements were made so that turbine performance could be monitored continuously. The water brake torque meter signal was read out on both the digital data system and on a Sanborn recorder in the control room. For the first 600 hours of the endurance test the digital signal was not obtained and the water brake torque was read from the Sanborn recorder.

In attempting to reduce high vibrations during the first 600 hours, the water brake torque meter calibration was invalidated. Therefore, the water brake torque was obtained from heat balance calculations during much of the first 600 hours. A correlation between the heat balance calculation and the torque meter reading obtained during previous testing, is shown in Figure 121.

Shown in Figure 122 is a correlation of steam turbine torque with steam turbine inlet pressure, obtained during previous testing. This correlation was used to determine steam turbine torque during part of the first 600 hours of testing when the torque meter signal was not obtained.

At the instant of zero speed during each shutdown of the turbine, both the water brake and steam turbine torque meters were read. These "zero" readings were used to correct the torque meter readings just prior to each shutdown for a more accurate determination of turbine performance. Shown in Figure 123 is the correlation between the vapor flow rate as measured by the

electromagnetic flow meter and the bullet nose differential pressure system. The open circles are the points used to draw the correlation line shown. These data were all taken early in the 3000-hour endurance test. Because of difficulty with the bullet nose system, it was read rather infrequently during the latter part of the test. However, the last four readings are shown as the darkened circles. These points indicate that the correlation had probably changed and the flow rates being obtained from the correlation are low by about 0.05 pounds per second.

The turbine exit pressure probe did not function properly. Few readings were obtained, due to plugging of the probe, and the readings that were obtained did not appear to be correct. No way was found to correlate these data with the results of the previous 2000-hour endurance test or the performance testing.

2. History

The nominal set point for the endurance test was inlet temperature of 1500 $\pm$ 5°F, exit temperature of 1240 $\pm$ 5°F, and for the major portion of the test, rotative speed of 18,800 rpm. An exit temperature of 1240°F was selected to set a total-to-static pressure ratio of 3.47 across the turbine. A digital scan of the performance instrumentation was made at four hour intervals to verify that the test point was being held and that the performance was not deteriorating.

Shown in Figure 124 are plots of the more significant performance parameters for the 3000-hour endurance test. The points plotted were all taken

at about 0830 hours each day. The first strip shows the speed which was held within ± 100 rpm of the desired value most of the time. The next two strips show the turbine inlet and exit temperatures. There were four thermocouples at the inlet and five at the exit of the turbine whose readings were averaged to determine the turbine inlet and exit temperatures. During the course of the test the reading from one of the inlet thermocouples was dropped from the average because it was reading about eight degrees higher than the other three. One of the exit thermocouples became inoperable and the use of another one was discontinued because it was reading about sixteen degrees lower than the other three. The next two strips are the inlet and exit static pressures measured by Taylor pressure transducers. The next strip shows the net blading torque and the last strip shows the vapor flow rate. Circles indicate flow rate obtained from the bullet nose pressure measurements and the triangles indicate flow rate obtained from the electromagnetic flow meter-bullet nose correlation.

Using the zero shifts to correct the net blading torque measured for the six digital data readings taken during the last 24 hours before the end of the test gives an average net blading torque of 513 inch-pounds. The net blading torque after the original start in April, 1966 was 514 inch-pounds. The endurance test had to be interrupted three times to repair the facility on May 13, June 9, and August 7, 1966. Torque meter zero readings were obtained at each shutdown. The following table summarizes the net blading torque measured just after each startup and prior to each shutdown. The torque readings prior to each shutdown have been corrected by the appropriate torque meter zero shifts. Also listed are the average turbine inlet and exit temperatures and the rotative

speed. The values given are averages of six digital data scans taken in a 24-hour period except for the first point. Because of the excessive water brake vibration condition during the first 600 hours, the test point was varied considerably in an attempt to find a stable operating condition; however, one point was obtained which was similar to the eventual endurance test condition.

Date	Inlet Temp., °F	Exit Temp., °F	Rotative Speed, rpm	Net Torque, in-lb	Torque Zero Shift, in-lb
4/20	1504.6	1235.2	18,610	514	----
5/13	1502.9	1228.7	19,095	509	+ 40
6/3	1502.6	1244.6	18,845	526	----
6/9	1501.4	1240.1	18,840	531	- 4
6/14	1502.2	1240.4	18,900	517	----
8/7	1503.0	1237.0	18,880	509	- 7
8/18	1501.2	1240.9	18,933	508	----
9/19	1503.4	1240.1	18,782	513	- 10

These data indicate that the turbine performance as indicated by the net blading torque did not substantially change during the 3000 hours of operation.

VI. CONCLUSIONS

The two-stage turbine was endurance tested for an additional 3000 hours, making a total of 5000 hours for many of the important parts. The endurance test was carried out at an inlet temperature of 1500°F, a second-stage inlet vapor quality calculated to be 96.7 percent, an exit temperature of 1240°F, and a rotative speed of 18,800 rpm. The test had but three interruptions, after 600, 814 and 2175 hours. Not one of these interruptions was caused by the two-stage turbine itself. The following conclusions are drawn from the evaluation of the test data for the 3000-hour endurance test:

1. The turbine mechanical design, material selection and fabrication techniques were demonstrated to have been durable.
2. There was no damage to the turbine by the potassium vapor or other cause which compromised its safety or reliability.
3. With some improvements in the test-turbine load train and with inspection and preventative maintenance of the facility, the test turbine could have a high probability of operating continuously for 5000 hours.
4. The cleanliness of the potassium in the facility, which was good at the initiation of the test, improved as the test proceeded.
5. Only minimal blade corrosion was observed on both 2000- and 3000-hour tests; the lesser corrosion noted in the 3000-hour test is believed to be the result of (1) a cleaner potassium

vapor environment in that test and (2) the incorporation of new turbine nozzles which provided better vapor flow conditions into the turbine blades.

6. The room temperature ductility of the U-700 blades in the first stage was reduced because of sigma phase formation, and the room temperature ductilities of the refractory alloys were in some instances likewise reduced, however, the use of 700°F turbine preheat should assure adequate warm ductility to permit safe turbine startup, should further testing be desired.

7. Mass transfer and alloy depletion effects were observable, but minor in consequence, extending usually less than one mil into the surface of the blades. The long-range consequences of such effects are not considered to be of a serious nature.

8. Liquid droplet impact erosion was observed on the Rene' 41 blade clips of both the first- and second-stage turbine rotors after 3000 hours operation; while this erosion was greater in the second stage, it was not of sufficient magnitude to represent a hazard to further turbine operation.

9. Very minor erosion of the Type 316 stainless steel honeycomb turbine shrouds was observable only by magnified binocular inspection of the first- and second-stage shrouds and could not be considered to have affected the performance characteristics of the turbine.

REFERENCES

1. R.J. Rossbach and G.C. Wesling: "Two-Stage Potassium Test Turbine - Vol. I Fluid Dynamic Design and Performance". NASA CR-722.

2. R.W. Fink and H.E. Nichols: "Two-Stage Potassium Turbine - Vol. II Mechanical Design and Development". NASA CR-723.

3. D.S. Engleby; R.B. Hand; J.W. Semmel, Jr.; and W.F. Zimmerman: "Two-Stage Potassium Test Turbine - Vol. IV Materials Support of Performance and Endurance Tests". NASA CR-725.

4. S.E. Eckard: "Two-Stage Potassium Test Turbine - Vol. III Test Facilities". NASA CR-724.

PRECEDING PAGE BLANK NOT FILMED.

TABLE I

COMPONENTS USED IN 3000 KW TURBINE ASSEMBLY

Description	Serial Number	Identification No.
Exhaust Scroll	1*	SK56131-426G1
Inlet Duct (Bullet Nose)	1*	SK56131-475G1
Bearing Housing Assy	1*	
Casing Assy	2*	SK56131-414G1
2nd Stage Nozzle Diaphragm	2**	4012000-646G1
1st Stage Nozzle Diaphragm	2**	4012000-700G1
Outlet Guide Vane	1*	4012000-651G1
Interstage Seal	3*	4012000-656P1
Koppers Coupling	781924*	165A5637P1
Ball Bearing Housing	1*	119C2773P1
Carbon Seal Housing	1*	119C2772P1
Screw Seal Retainer	1**	4012000-823P1
Screw Seal Retainer	2**	4012000-823P1
Rotating Cup Seal	2**	263-E781G1
Ball Bearing	27**	4012000-676P1
Ball Bearing	28**	4012000-676P1
Pad Bearing Assy	1**	119C2788G1
Pad Sleeve	4**	142B1765P2
Shim	1*	4012000-660P3
Shim	1*	4012000-660P2
Shim	1*	142B1759P4
Speed Pickup & Coupling	772574**	142B1879P1
Disc Brake & Coupling	1**	263E843
Sleeve	2*	165A5633P2
Carbon Seal Face	1**	165A5634P1
Locknut & Washer	3*	142B1709P1
Capnut	3*	4012000-682P2
Bearing Housing Heat Shield	3*	941D799
Shaft	3*	SK56131-178P1
Turbine Wheel 3rd Stage	3**	4012000-639P2
Turbine Wheel 4th Stage	3**	4012000-640P2
Belleville Spring Retainer	1**	142B1671P1
Koppers Coupling	817160*	
Locknut	3*	142B1687P1
Tie Bolt	5*	4012000-822P2
Instrumentation Ring	1**	941B110
Rotor Blades	See Table VI	

* Parts used in 2000 hour test and 3000 hour test - 5000 hours total

** Parts used in 3000 hour test only

TABLE II

INSTRUMENTATION

POTASSIUM TURBINE TESTING - 3000 KW FACILITY

ITEM NO.	PARAMETER	LOCATION	STATION	RANGE	SENSOR	CONTROL ROOM READOUT	CATS No. / Digital No.	CHANNEL OR POSITION
1	Vapor Total Temperature, °F	045-1	1	1400-1650°F	CA T/C	Digital	4 / 113	
2	Vapor Total Temperature, °F	135-1	1	1400-1650°F	CA T/C	Digital	5 / 114	
3	Vapor Total Temperature, °F	235-1	1	1432-1682°F	CA T/C	Sanborn		5-B
4	Vapor Total Temperature, °F	315-1	1	1400-1650°F	CA T/C	Digital	7 / 115	
5	Vapor Total Temperature, °F	315-2	1	1400-1650°F	PtPtRh T/C	Digital	/ 160	
13	Calorimeter Temperature, °F	Calorimeter 010-1	1	1400-1650°F	CA T/C	Digital	1 / 112	
20	Delta P Bullet Nose-2 Vapor Total Pres.	Inlet Duct 280-3	3	0-50 psia	Wiancko	Digital	/ 99	
23	Delta P Bullet Nose-1 Vapor Static Pres.	Inlet Duct 270-1	3	0-50 psia	Wiancko	Digital	/ 100	
28	Vapor Temperature	Wheel Space 120	4	1450-1650°F	CA T/C	Digital	10 / 140	
29	Vapor Temperature	Wheel Space 330	4	650-1650°F	CA T/C	Digital	11 / 141	
46	Vapor Temperature	OGV 128	7	650-1650°F	CA T/C	Digital	12 / 120	
47	Vapor Temperature	OGV 142	7	650-1650°F	CA T/C	Digital	13 / 121	
48	Vapor Temperature	OGV 156	7	650-1650°F	CA T/C	Digital	14 / 122	
49	Vapor Temperature	OGV 230	7	650-1650°F	CA T/C	Digital	15 / 123	
50	Vapor Temperature	OGV 45	7	650-1650°F	PtPtRh	Digital	/ 161	
51	Vapor Temperature	OGV 308	7	650-1650°F	CA T/C	Sanborn		6-B
52	Vapor Temperature	SW-1	8	650-1650°F	PtPtRh	Digital	/ 162	
53	Vapor Temperature	SW-2	8	650-1650°F	CA T/C	Cond. Control		
54	Vapor Temperature	SE-1	8	650-1650°F	CA T/C	Digital	20 / 128	
55	Vapor Temperature	NE-1	8	650-1650°F	CA T/C	Digital	21 / 129	
56	Vapor Temperature	NW-1	8	650-1650°F	CA T/C	Digital	22 / 130	
62	Vapor Static Pressure	N-1 Main Cond.	8	0-50 psia	Taylor Statham	Digital & Sanborn	/ 90	4-C

TABLE II (Continued)

ITEM NO.	PARAMETER	LOCATION	STATION	RANGE	SENSOR	CONTROL ROOM READOUT	CATS No. / Digital No.	CHANNEL OR POSITION
81	Condenser Liquid Level	Condenser	11	0-6 inches	Ohmart & Brown	Sanborn		3-C
82	Main Condenser Flow	Main EmFm	11	0-10 MV	EmFm	Digital	101,102, 106,107	103 108
83	Flow Temperature of Main Condenser	Main EmFm	11	432-932°F	CA T/C	Digital	2 / 131	
85	Speed	Steam Turbine	11	0-25,000 rpm	Magnetic Pickup	Berkeley		
86	Speed	Steam Turbine	11	0-25,000 rpm	Magnetic Pickup	Sanborn & Digital	91 Note #1	1-A
87	Steam Turbine Torque	Steam Turbine	11	0-200 in/lb	Bytrex	Dial & Digital	110 Note #3	
88	Potassium Turbine Torque	Potassium Turbine	11	0-1250 in lb Bytrex	Sanborn	Dial & Digital	109 Note #2	Sanborn 2-A
89	Condenser Liquid Temperature	Condenser	11	300-1300°F	CA T/C	Digital	30 / 148	
90	R.T.D. C.A.T.S. Block Temperature	CATS Block			R.T.D.	Digital	/ 104	
94	Standard Resistor R.T.D. Network			5.6 MV		Digital	/ 105	
	TURBINE PAD BEARING							
95	Pad Bearing Temp. Pad #2	Pad Bearing		250°F	CA T/C	TR#3-6		
96	Pad Bearing Temp. Pad #2	Pad Bearing		250°F	CA T/C	TR#3-5		
97	Pad Bearing Temp. Pad #1	Pad Bearing		250°F	CA T/C	TR#3-4		
98	Pad Bearing Temp. Pad #5	Pad Bearing			CA T/C	Sanborn		4-A
99	Pad Bearing Cavity Temperature				CA T/C	TR#3-3		
100	Pad Bearing Lube Inlet Pressure	Pad Bearing			Gauge	Visual & Wrng.Sig.		
101	Pad Bearing Lube Flow	Pad Bearing		0-200"H_2O (3 gpm)	Foxboro D.P.Cell	Dial & Sanborn		6-A
102	Potassium Turbine Brg. Lube Temp. Out			250°F	CA T/C	Digital & TR#3-2	38 / 149	
103	Potassium Turbine Brg. Lube Temp. In			250°F	CA T/C	Digital & TR#3-1	39 / 150	
104	Stabilizer Bearing Temperature			250°F	CA T/C			
	TURBINE BALL BEARING							
105	Rear Ball Thrust Bearing Temperature			32-282°F	CA T/C	TR#3-9 & Sanborn		3-A
106	Forward Ball Thrust Bearing Temperature			250°F	CA T/C	Sanborn & TR#3-8		3-A

TABLE II (Continued)

ITEM NO.	PARAMETER	LOCATION	STATION	RANGE	SENSOR	CONTROL ROOM READOUT	CATS No. / Digital No.	CHANNEL OR POSITION
107	Ball Bearing Lube Oil Pressure In			200 psig	Bourdon Gauge	Visual & Wrng.Sig.		
108	Ball Bearing Lube Oil Flow			0-200"H_2O (3 gpm)2	Foxboro D.P.Cell	Dial & Sanborn		5-A
	S T E A M T U R B I N E	B E A R I N G						
109	Temp. Steam Turbine Bearing Forward			250°F	CA T/C	TR#3-15		
110	Temp. Steam Turbine Bearing Middle			250°F	CA T/C	TR#3-16		
111	Temperature Steam Turbine Bearing Aft.			250°F	CA T/C	TR#3-17		
112	Temperature Steam Turbine Lube In			250°F	CA T/C	TR#3-13		
113	Temperature Steam Turbine Lube Out			250°F	CA T/C	TR#3-14		
114	Steam Turbine Lube Oil Pressure			80 psig	Bourdon Gauge	Warning Light		
115	Steam Turbine & H20 Brake Lube Oil Flow			1 gpm	Flow-rator	Warning Light		
	W A T E R B R A K E							
116	H20 Brake, Water Inlet Temperature			60°F	CA T/C	Digital	40 / 151	
117	H20 Brake Water Outlet Temperature			150°F	CA T/C	Digital+ TR#3-20	41 / 152	
118	Temperature H20 Brake Bearing Forward			180°F	CA T/C	TR#3-18	42 / 153	
119	Temperature H20 Brake Bearing Aft.			180°F	CA T/C	TR#3-19	43 / 154	
120	H_2O Brake Water Flow			0-50 gpm	D.C. Generator	Gauge		
121	H20 Brake Lube Oil Flow			1 gpm	Flow-rator	Warning Light		
	V I B R A T I O N							
122	Displacement SteamTur-bineAftBearing Vert.			0-5 mils.	Vib.P/U	Sanborn	No	7-A
123	Displacement SteamTur-bine Aft Bearing Hor.			0-5 mils.	Vib.P/U	Sanborn	No	7-A
124	Displacement Aft "K" Turbine Vert.			0-5 mils.	Vib.P/U	Sanborn	No	8-A
125	Displacement Aft "K" Turbine Hor.			0-5 mils.	Vib.P/U	Sanborn	No	8-A
126	Accel. Pad Bearing Vert.			0-10 g's	Accel.	Visual	No	
127	Accel.Pad Bearing Hor.			0-10 g's	Accel.	Visual	No	
	H Y D R O D Y N A M I C	S E A L						
128	Temp. Seal "K" In			500°F	CA T/C	Digital & TR2-9		
129	Temp. Seal "K" Out			1000°F	CA T/C	Digital & TR2-10		
130	Slinger Seal Turbine Inlet Pressure P-11			0-150 psig	Taylor Gage	Visual	No	
131	P-8 Oil Side Seal Pressure			0-30 psig	Taylor & Wiancko	Sanborn	No	8-B
132	"K" Seal Flow			0-25MW See Curve	Face+ Emrm	FlowRec. & Dig.	93	

TABLE II (Continued)

ITEM NO.	PARAMETER	LOCATION	STATION	RANGE	SENSOR	CONTROL ROOM READOUT	CATS No. / Digital No.	CHANNEL OR POSITION
133	Temperature Argon Seal In			500°F	CA T/C			
134	Turbine Argon Inlet Pressure P-7	Lab Seal Inlet at Man		100 psig	Pressure Gauge	Visual	No	
135	Bearing Sump Wall Temperature			500°F	CA T/C		No	
136	Lube Cart Pressure Out			200 psig	Gauge	Visual	No	
137	Stabilizer Bearing Lube Pressure			200 psig	Gauge	Visual	No	
138	Stabilizer Bearing Piston Actuating Pres.			200 psig	Gauge	Visual	No	
139	P-8 Potassium Side Seal Pressure			-30"Hg to 100 psig	Taylor & Pace	Sanborn & Visual	No	7-B
140	Argon Header Pressure P-1			0-60 psig	Taylor Gauge	Visual	No	
141	Argon Extraction Flow	Downstream of VPL-8	11	0-10 MV	EmFm	Sanborn	No	2-C
142	Boiler Drum Pressure	Boiler Inlet			Wiancko & Tylr G.	Sanborn	No	2-B
143	Turbine Shaft 270° Movement Radial	Stabilizer Bearing			Bently Gauge	Oscillo-scope	No	
144	Turbine Bearing Housing Temp. (Fwd)	Bearing Housing	Sec. E		CA T/C	TR#2-11	No	
145	Turbine Bearing Housing Temp. (Aft)	Bearing Housing	Sec. F		CA T/C	TR#2-12	No	
146	Turbine Casing Forward Temperature	Turbine Casing	3	1400°F	CA T/C	TR#2-14	No	
147	Turbine Casing Aft Temperature	Turbine Casing	5	1400°F	CA T/C	TR#2-15	No	
148	8-inch Vapor Line Temperature	6"Aft of Spray Line	2	1400°F	CA T/C		No	
149	8-inch Vapor Line Temperature	14"Aft of Spray Line	2	1400°F	CA T/C		No	
150	Pad Bearing Ring Temp.#1 T/C 24°	Pad Brg. Ring			CA T/C	TR#3-7	No	
151	Pad Bearing Ring Temp.#2 T/C 50°	Pad Brg. Ring			CA T/C		No	
152	Bullet Nose Delta P	Between Itm 20 and 23	3	0-1.5 psid	Efflux & Pace	Digital	92	
154	Boiler Feed Temperature	At Boiler Feed EmFm			CA T/C		No	
155	Boiler Feed Flow	Boiler Input			EmFm	Sanborn	No	1-C
156	Exit Calorimeter Htr. "B" Power Input	Exit Cal-orimeter	8	0-5 KW	Hall X-Ducer	Dial		

TABLE II (Continued)

ITEM NO.	PARAMETER	LOCATION	STATION	RANGE	SENSOR	CONTROL ROOM READOUT	CATS No. / Digital No.	CHANNEL OR POSITION
157	Exit Calorimeter Htr 'A' Power Input	Exit Calorimeter	8	0-5 KW	Hall X-Ducer	Dial		
158	Compensating Heater Power Input	Compensating Heater	2	0-5 KW	Hall X-Ducer	Dial		
159	Vapor Static Pressure		1		Taylor & Pace	Sanborn & Digital	95	4-B
160	Vapor Static Pressure		7		Taylor & Pace	Digital	96	
161	Turbine Shaft Movement Radial 180°	Stabilizer Bearing			Bently Gauge	Oscilloscope	No	
162	Boiler Liquid Level	Boiler			"J" Tube		No	
163	Boiler Liquid Level	Boiler			Ohmart Gauge	Recorder & Sanborn	No	3-B
164	VPL-11 Valve Stem Position	VPL-11	1		Lin. Mot.Pot.		No	
165	Water Brake Valve Stem Position	Water Brk. Valve			Lin. Mot.Pot.		No	
166	Boiler Discharge Temperature	Upstream VPL-11		1650°F	Skin CA T/C	Digital	44 155	
167	Vapor Temperature	Midstream .022°	3	1650°F	CA T/C	Digital	45 139	
168	Water Brake Vibration Vertical				Vib. Pickup	GE Vib. Meter	No	
169	Water Brake Forward Vibration Horizontal				Vib. Pickup	GE Vib. Meter	No	
170	Water Brake Water Flow	Water Brk Inlet			Potter	Digital	94	
171	Vapor Drum Separator Heat Exch. T/C 47	Vapor Drum			CA T/C		No	
172	Vapor Drum Separator Heat Exch. T/C 48	Vapor Drum			CA T/C		No	
173	Delta P at Bullet Nose	Itm 20 & Itm 24	3	0-1.5 psid	Wiancko Efflux			
174	200 lb Bytrex Temp. - Rear Flange	Body of 200 lb Bytrex		150°F	Skin CA T/C	Digital	9 116	
175	200 lb Bytrex Temp. - Fwd. Flange	Top of Fwd Flange		150°F	Skin CA T/C	Digital	17 124	
176	1250 lb Bytrex Temp. - Fwd. Flange	Top of Fwd Flange		150°F	Skin CA T/C	Digital	3 132	
177	1250 lb Bytrex Temp. - Rear Flange	Top of Rear Flange		150°F	Skin CA T/C	Digital	46 156	
178	Bearing Housing Forward	Bottom Centerline	Sec. F		Skin CA T/C	TR#3-10		
179	Bearing Housing Mid	Bottom Centerline	Sec. F		Skin CA T/C	TR#3-11		

TABLE II (Continued)

ITEM NO.	PARAMETER	LOCATION	STATION	RANGE	SENSOR	CONTROL ROOM READOUT		CHANNEL OR POSITION
180	Bearing Housing Aft	Bottom Centerline	Sec. F		Skin CA T/C	TR#3-12		
181	Vapor Total Temperature	Inlet Duct	3	1550°F	CA T/C	Digital	35 136	
182	Vapor Total Temperature	Inlet Duct	3	1550°F	CA T/C	Digital	36 137	
183	Vapor Total Temperature	Inlet Duct	3	1550°F	CA T/C	Digital	37 138	
184	Throttling Calorimeter - Taylor Gage	Inlet Calorimeter	1		Taylor Gage	Digital	97	
185	Steam Turbine Inlet Pressure	Inlet to Steam Turbine			Pace X-duce	Digital	98	
186	Vapor Total Temperature	Upstream Noz. Tip 340°	5		CA T/C	Digital	6 142	
187	Vapor Total Temperature	Upstream Noz. Tip 355°	5		CA T/C	Digital	23 143	
188	Vapor Total Temperature	Upstream Noz. Tip 20°	5		CA T/C	Digital	24 144	
189	Turbine rpm	Fwd. Koppers Coupling			Magnetic Pickup	Dial & Sanborn		1-B
190	S.S. Loop Potassium Supply Pressure	S.S. Loop Supply			Taylor Gage	Dial		
191	Pad Bearing #3 Temperature	Pad Bearing			CA T/C	Simply-Trol		

TABLE
SANBORN INSTR

Item No.	Parameter	Sanborn No.	Station Location #	Location	Sens
86	R.P.M.	1A	11	Steam Turbine	6 Toothge Magnetic
88	Water Brake Torque	2A	11	Aft of Potassium Turbine	Strain Gag
106	Forward Ball Bearing Temperature	3A		Potassium Turbine	CA T/C
195	Rear Ball Bearing Temperature	3A		Potassium Turbine	CA T/C
98	Pad Bearing Temperature	4A		Potassium Turbine	CA T/C
108	Ball Bearing Lube Flow	5A		Lube Inlet	Foxboro D/
101	Pad Bearing Lube Flow	6A		Lube Inlet	Foxboro D/
122	Steam Turbine Vib. Vert.	7A		Aft Face of Steam Turbine	Velocity P
123	Steam Turbine Vib. Horiz.	7A		Aft Face of Steam Turbine	Velocity P
124	Potassium Turbine Vib. Vert.	8A		Flange of Potassium Turbine Bearing Housing	Velocity P
125	Potassium Turbine Vib. Horiz.	8A		Flange of Potassium Turbine Bearing Housing	Velocity P
189	RPM	1B		Potassium Turbine	6 Tooth Ge Magnetic P
142	Boiler Vapor Drum Pressure	2B		Boiler Drum	Taylor Gag Pace
163	Boiler Liquid Level	3B		Boiler	Ohmart Rad Gage
159	Station #1 Taylor Gage	4B	1	Downstream of VPL-11	Taylor Gag Pace
3	Turbine Inlet Temperature	5B	1	Inst. Section 235-1	CA T/C
51	Turbine Exit Temperature	6B	7	O.G.V. Inlet	CA T/C
139	Potassium Side Seal Pressure P-8	7B		Potassium Side Seal Manifold	Taylor Gag Pace
131	Oil Side Seal Pressure P-6	8B		Oil Sump at Bearing	Foxboro & 70756
155	Boiler Feed Flow	1C		Boiler Input	Em Fm
141	Argon Extraction Flow	2C		Downstream VPL-8	Em Fm
81	Condenser Liquid Level	3C		Condenser	Ohmart Rad Gage
62	Station #8 Taylor Gage	4C	8	N-1	Taylor Gag Pace

FOLDOUT FRAME 36

r	Range In Units	Digital Channel	Calibration	Turbine System No.	Cell Wiring	Attenuation
and ckup	0-25,000 RPM		0-2500 CPS			
Bytrex	0-1250 in/lbs		0-640 in/lbs			
	32°-282°F	NO	32°-282°F			
	32°-282°F	NO	32°-282°F			
	32°-282°F	NO	32°-282°F			
Cell	0-200" H_2O See Curve	NO	3-15 psig			
Cell	0-200" H_2O See Curve	NO	3-15 psig			
ckup	0-5 mils	NO	110 MV RMS at 100 cps			
ckup	0-5 mils	NO	110 MV RMS at 100 cps			
ckup	0-5 mils	NO	110 MV RMS at 100 cps			
ckup	0-5 mils	NO	110 MV RMS at 100 cps			
& ckup	0-25,000		0-2500 cps			
&	0-60 psig	NO	3-15 psig			
ation	0-25 %	NO	0-25 %			
&	0-30 psia		See Calibration Curve			
	1332°-1532°F	NO	1332°-1532°F			
	1032°-1432°F	NO	1032°-1432°F			
&	-30" Hg - 35 psig	NO	0-10 psig			
iancko	0-30 psig	NO	3-15 psi			
	No Calibration	NO	0-10 MV			
	See Curve	NO	0-10 MV			
ation	0-6	NO	0-100 %			
&	-30" Hg - 30 psia		0-20 psia See Calib. Curve			

FOLDOUT FRAME

TABLE

MECHANICAL OPERATIONAL DATA MONITOR

Date	4/22/66	4/27/66	5/1/66	5/5/66	5/9/66	5/13/66	S D 5/
Time, hours	2020	2400	0400	0800	1200	1600	
Accumulated Test Time, hours	100	200	300	400	500	600	
Speed, rpm	19,000	18,800	19,400	19,000	18,500	18,900	
Potassium Turbine							
Horizontal Vibration, g's	1.6*	2.4*	1.9*	1.8*	1.75*	4.3*	
Vertical Vibration, g's							
T/P Casing Forward Temp., °F	1444	1448	1455	1448	1455	1432	
Casing Aft Temp., °F	1256	1292	1228	1247	1250	1250	
Bearing Housing Forward Temp., °F	944	963	960	970	975	979	
Bearing Housing Aft Temp., °F	780	803	800	812	815	824	
Pad Bearing Temp., °F	178	177	185	182	179.5	179.5	
Ball Bearing Temp., °F	197	195	205.5	194	194.5	195	
Oil Inlet Temp., °F	132	134	139	136	134	132	
Oil Outlet Temp., °F	190.5	188	191	189	186	198	
Potassium Liquid Inlet Temp, °F	243	268	269	267	265	268	
Potassium Liquid Outlet Temp., °F	788	830	830	833	838	850	
Pad Bearing Oil Flow, gpm	2.2	2.82	2.46	2.58	2.58	2.13	
Ball Bearing Oil Flow, gpm	.81	.81	.82	.83	.835	.8	
Water Brake							
Horizontal Vibration, mils	1.6	2.4	1.9	1.8	1.8	4.3	
Vertical Vibration, mils	1.5-2.0	1.8-4.3	1.5-4.0	1.8-2.5	1.7-4.0		
Forward Bearing Temp., °F	1.63	156	161	163	154	159	
Aft Bearing Temp., °F	122	120	119	119	116	117	
Steam Turbine							
Vibration, mils	.93	1.05	.38	.4	.4	.38	
Forward Bearing Temp., °F	155	155	155	156	153	155	
Aft Bearing Temp., °F	162	163	161	164	159	163	

*Measured in mils.

IV

D DURING 3000-HOUR ENDURANCE TEST

ut wn 3/66	Start Up 5/31/66	6/2/66	6/4/66	6/8/66	Shut Down 6/9/66	Start Up 6/11/66	6/12/66	6/15/66	6/19/66
		1500	1700	2100			2400	0200	0600
		650	700	800			850	900	1000
		17,100	18,500	18,750			18,800	18,550	18,500
		2.5	2.2	2.8			2.4	3.2	2.4
		1.0	1.2	1.6			1.7	1.7	1.9
		1440	1450	1455			1450	1449	1448
		1250	1253	1259			1260	1250	1251
		925	930	932			942	938	939
		770	782	785			791	789	789
		173	191	192			192	191	194.5
		162	177	182			171	172	169.5
		129	135	142.5			140	136	134
		183	187	191			182.5	180	181
		250	252	254			250	248	248
		763	767	772			781	780	782
		2.38	2.5	2.5			2.5	2.51	2.48
		.078	.825	.87			.82	.85	.85
		.5	.7	.7			.85	1.0	.9
		.7	.9	.8			1.6	1.65	1.6
		163	159.5	162.5			160	162.5	158
		123	120	123			118	121	117
		.12	.21	.18			.21	.22	.14
		157	154.5	156.5			150.5	150	148
		163	158	161			154.5	155	153

Shut down at 600 accumulated hours due to vibrations in water brake coupling and potassium turbine disc brake.

Shut down at 813 accumulated hours due to weld-leak in test facility main throttle valve.

PART 1 OF 2

TABLE IV

(Continued)

Date	6/23/66	6/27/66	7/1/66	7/5/66
Time, hours	1000	1400	1800	2200
Accumulated Test Time, hours	1100	1200	1300	1400
Speed, rpm	18,750	18.900	18,750	18,800
Potassium Turbine				
Horizontal Vibration, g's	3.4	3.5	3.2	2.9
Vertical Vibration, g's	1.8	3.0	1.9	1.6
T/P Casing Forward Temp., °F	1448	1453	1451	1450
Casing Aft Temp., °F	1250	1247	1247	1246
Bearing Housing Forward Temp., °F	943	951	946	957
Bearing Housing Aft Temp., °F	800	803	812	810
Pad Bearing Temp., °F	192.5	187	190.5	192
Ball Bearing Temp., °F	172	158	171	171
Oil Inlet Temp., °F	137	130	134	133
Oil Outlet Temp., °F	180	180	183	182
Potassium Liquid Inlet Temp., °F	252	253	252	248
Potassium Liquid Outlet Temp., °F	785	796	798	800
Pad Bearing Oil Flow, gpm	2.55	2.57	2.52	2.52
Ball Bearing Oil Flow, gpm	.85	.825	.83	.835
Water Brake				
Horizontal Vibration, mils	.8	.8	.7	.7
Vertical Vibration, mils	1.4	1.6	1.35	1.18
Forward Bearing Temp., °F	164	164.5	165	163
Aft Bearing Temp., °F	122	121	121	121
Steam Turbine				
Vibration, mils	.18	.1	.18	.2
Forward Bearing Temp., °F	154	155.5	154	152
Aft Bearing Temp., °F	159	162	160	158

FOLDOUT FRAME

PART 2 of 2

Shut Down 8/7/66	Start Up 8/16/66	9/11/66	9/15/66	9/19/66	Shut Down 9/19/66	
		1200	1600	2000		
		2800	2900	3000		
		18,500	19,000	19,000		
		2.0	2.0	2.2		
		1.6	1.6	1.6		
		1462	1478	1460		
		1266	1273	1260		
		960	963	978		
		798	815	830		
		192	197	192		
		177	174	175		
		135	136	135		
		186	184	186		
		280	280	273		
		821	818	828		
		2.62	2.63	2.66		
		.83	.82	.83		
		.55	.65	.5		
		.6	.8	.6		
		154	150	154		
		118	115	118		
		.15	.20	.19		
		154	150	151		
		162	155	157		

Shut down at 2176 accumulated hours due to failure of water brake forward bearing.

End of 3000-hour endurance test.

FOLDOUT FRAME

TABLE V

TURBINE DIMENSIONAL INSPECTION RECORDS

	Before	After
ROTOR		
First Stage Wheel		
Over Blade Diameter	8.8150*	8.8155
Second Stage Wheel		
Over Blade Diameter	9.6225	9.6230
Interstage Seal Teeth Diameter	4.071	4.070
Screw Seal Diameter	3.450	3.454
Shaft		
Screw Seal Diameter	3.844	3.842
Hydrodynamic Seal		
Labyrinth Teeth Diameters		
Inner	3.749/3.750	3.752/3.753
Outer	4.720/4.721	4.719/4.718
STATOR		
Inlet Duct		
Diameter at 0°	10.270	10.261
Diameter at 90°	10.271	10.262
Scroll		
O.D. of Bearing Housing Flange		
at 0°	7.589	7.589
at 90°	7.590	7.581
Bearing Housing and Internal Parts		
Bearing Housing O.D. of Aft Diameter		
at 0°	6.192	6.1865
at 90°	6.191	6.1885
O.D. of Pad Bearing Seat Diameter		
at 0°	4.538	
at 90°	4.538	
Socket Ring O.D.		
at 0°	5.1221	5.122*
at 90°	5.1229	5.125

TABLE V (Continued)

PAD BEARING		
Journal Sleeve	3.429	3.429
Bearing Pads	3.4345	3.436
ROTOR BALANCE (Residual Unbalance)		
Forward Bearing, gm-in	0.5	1.05
Aft Bearing, gm-in	0.5	0.35

*Unless specified, dimensions given in inches.

TABLE VI

TURBINE ASSEMBLY NO. 8: BUCKET WEIGHTS FOR 3000-HOUR ENDURANCE TEST

STAGE 1 U700 BUCKETS

Bucket No.*	Set No.	Weight Before Testing, grams	Weight After Testing & Brush Cleaning, grams	Percent Change	Weight After Vapor Blast, grams	Percent Change
1	II	16.0713	16.0712	-.0006	16.0554	-.009
1	III	16.1136	16.1146	+.006	16.0845	-.181
2	III	16.4715	16.4728	+.008	16.4537	-.108
3	II	16.1379	16.1336	-.027	16.1126	-.151
4	III	16.0879	16.0862	-.011	16.0621	-.160
5	III	16.1355	16.1335	-.012	16.1054	-.186
6	II	16.1624	16.1590	-.021	16.1421	-.126
6	III	16.0148	16.0122	-.016	15.9935	-.133
9	III	16.2194	16.2193	-.0006	16.1870	-.198
10	III	16.1016	16.1013	-.002	16.0768	-.154
11	III	16.2141	16.2137	-.002	16.1898	-.150
15	III	16.0318	16.0315	-.002	16.0061	-.160
16	III	16.3276	16.3251	-.015	16.3076	-.122
17	III	16.2109	16.2086	-.014	16.1913	-.121
18	II	16.0632	16.0622	-.006	16.0394	-.148
18	III	16.2208	16.2198	-.006	16.1953	-.157
20	III	16.2192	16.2185	-.004	16.2024	-.104
21	II	16.3012	16.3016	+.002	16.2764	-.152
21	III	16.1873	16.1860	-.008	16.1683	-.117
22	III	16.1935	16.1931	-.002	16.1792	-.088
23	III	16.3793	16.3773	-.012	16.3553	-.146
26	III	16.0952	16.0944	-.005	16.0748	-.127
27	III	16.2055	16.2039	-.010	16.1780	-.170
28	III	16.0049	16.0025	-.015	15.9774	-.172
30	III	16.1918	16.1900	-.011	16.1712	-.127
33	III	15.9247	15.9233	-.009	15.9021	-.142
36	III	16.2604	16.2601	-.002	16.2340	-.162
39	III	16.3049	16.3032	-.010	16.2809	-.147
41	III	15.9256	15.9238	-.011	15.9094	-.102
43	III	15.8243	15.8241	-.001	15.7968	-.174
44	III	16.3346	16.3335	-.007	16.3156	-.116
47	II	16.2529	16.2587	+.036	16.2315	-.132
48	III	16.3455	16.3450	-.003	16.3328	-.078
49	III	16.3947	16.3930	-.010	16.3714	-.142
50	III	16.2955	16.2948	-.004	16.2690	-.163
51	III	15.9932	15.9938	+.004	15.9754	-.111
52	III	16.1913	16.1869	-.027	16.1692	-.136
54	III	16.1974	16.1969	-.003	16.1819	-.096

TABLE VI (Continued)

Bucket No.*	Set No.	Weight Before Testing, grams	Weight After Testing & Brush Cleaning, grams	Percent Change	Weight After Vapor Blast, grams	Percent Change
55	III	16.0255	16.0255	.000	16.0093	-.101
57	III	16.2733	16.2735	+.001	16.2563	-.104
61	III	16.0241	16.0237	-.002	16.0067	-.108
62	III	16.0125	16.0111	-.009	15.9911	-.134
64	III	16.3394	16.3395	+.0006	16.3182	-.130
65	III	16.1171	16.1165	-.004	16.0901	-.167
67	III	16.1373	16.1359	-.009	16.1087	-.177
68	III	16.2309	16.2283	-.016	16.2104	-.126
70	III	16.3591	16.3593	+.001	16.3356	-.144
71	III	15.9123	15.9112	-.007	15.8866	-.161
73	III	16.0411	16.0420	+.006	16.0268	-.089
74	II	16.1096	16.1071	-.015	16.0714	-.237
74	III	16.2261	16.2250	-.007	16.2011	-.154
75	III	16.1369	16.1349	-.012	16.1134	-.146
77	III	16.1606	16.1578	-.017	16.1341	-.164
78	II	16.1261	16.1258	-.002	16.1076	-.115
81	II	16.1326	16.1317	-.006	16.1078	-.154
7**	III	16.3111	16.3086	-.015	16.2946	-.101
12**	III	16.3022	16.2963	-.036	16.2833	-.116
25**	III	16.1855	16.1826	-.018	16.1615	-.148
29**	III	16.3179	16.3146	-.020	16.3008	-.105
31**	III	16.2374	16.2338	-.022	16.2144	-.142
34**	III	16.4313	16.4287	-.016	16.4160	-.093
53**	III	15.8895	15.8862	-.021	15.8733	-.102
				Average of All Buckets		-.137
				Average of All Used Buckets		-.139
				Average of All New Buckets		-.115

TABLE VI(Continued)

STAGE 2 U700 BUCKETS

Bucket No.*	Set No.	Weight Before Testing, grams	Weight After Testing & Brush Cleaning, grams	Percent Change	Weight After Vapor Blast, grams	Percent Change
2	I	21.7461	21.7706	+.113	21.7340	-.056
4	I	21.9207	21.9467	+.119	21.9254	+.021
5	I	21.8112	21.8365	+.116	21.8073	-.013
6	I	22.0539	22.0788	+.113	22.0522	-.008
7	I	22.0529	22.0783	+.115	22.0483	-.021
8	I	22.3101	22.3378	+.124	22.3071	-.013
9	I	21.9078	21.9315	+.108	21.9073	-.002
10	I	22.1136	22.1392	+.118	22.1093	-.019
12	I	21.9545	21.9792	+.112	21.9398	-.067
13	I	22.3181	22.3442	+.117	22.3177	-.002
14	I	21.4629	21.4877	+.115	21.4665	+.017
16	I	22.0054	22.4393	+.197	22.9881	-.079
17	I	21.5932	21.6199	+.124	21.5872	-.028
18	I	21.6837	21.7138	+.139	21.6800	-.017
19	I	21.7553	21.7833	+.133	21.7467	-.039
21	I	21.6131	21.6416	+.132	21.6264	+.061
22	I	21.9088	21.9348	+.118	21.8967	-.055
24	I	22.0225	22.0484	+.118	22.0152	-.033
25	I	21.5516	21.5789	+.127	21.5515	-.0005
26	I	21.6419	21.6692	+.126	21.6472	+.024
27	I	21.1071	21.1301	+.109	21.1014	-.027
29	I	20.9146	20.9392	+.118	20.9169	+.011
30	I	20.9882	21.0158	+.131	20.9886	+.002
31	I	21.5697	21.5961	+.122	21.5631	-.030
32	I	21.3908	21.4188	+.131	21.3960	+.024
33	I	21.6521	21.6775	+.117	21.6450	-.033
35	I	21.3017	21.3252	+.110	21.3047	+.014
36B	I	21.4342	21.4583	+.112	21.4259	-.039
36A	I	21.2089	21.2349	+.123	21.2023	-.031
37	I	21.7351	21.7608	+.118	21.7435	+.039
38	I	21.2242	21.2476	+.110	21.2230	-.006
39	I	21.3968	21.4249	+.131	21.3986	+.008
40	I	21.3301	21.3567	+.122	21.3322	+.009
41	I	21.5963	21.6264	+.139	21.6034	+.033
42	I	21.1086	21.1329	+.115	21.1078	-.004
44	I	21.2654	21.2861	+.097	21.2634	-.009
45	I	21.6767	21.7056	+.133	21.6655	-.052
47	I	21.1098	21.1361	+.125	21.1083	-.007
49	I	21.4261	21.4504	+.113	21.4303	+.019
51	I	21.2659	21.2922	+.124	21.2663	+.002

TABLE VI (Continued)

STAGE 2 U700 BUCKETS

Bucket No.*	Set No.	Weight Before Testing, grams	Weight After Testing & Brush Cleaning, grams	Percent Change	Weight After Vapor Blast, grams	Percent Change
60	I	21.6078	21.6317	+.111	21.6046	-.015
61	I	21.3245	21.3479	+.110	21.3264	+.009
62	I	21.4219	21.4447	+.106	21.4288	+.032
63	I	21.1051	21.1297	+.116	21.1056	+.002
64	I	21.5493	21.5746	+.117	21.5491	-.0009
6**	II	22.4879	22.5047	+.075	22.4753	-.056
23	II	22.4808	22.4959	+.067	22.4913	+.047
28	II	22.3744	22.3904	+.071	22.3840	+.043
29	II	22.7885	22.8077	+.084	22.8013	+.056
30	II	22.4551	22.4724	+.077	22.4444	-.048
55	II	22.6861	22.7057	+.086	22.6977	+.051
66	II	22.3104	22.3287	+.082	22.2947	-.070
				Average of All U700 Buckets		+.013
				Average of Used Buckets		+.017
				Average of New Buckets		+.0033

STAGE 2 TZM BUCKETS

19**	I	27.6231	27.6244	+.005	27.6120	-.040
22**	I	27.6249	27.6222	-.009	27.6130	-.043
23*	I	27.9279	27.9260	+.007	27.9181	-.024
21*	I	27.7907	27.7905	+.001	27.7811	-.034
				Average		-.035

STAGE 2 TZC BUCKETS

11*	I	28.4657	28.4657	.000	28.4573	-.029
1	I	28.2838	28.2809	+.010	28.2735	-.036
2	I	28.3379	28.3387	+.003	28.3277	-.036
12	I	28.3752	28.3746	+.002	28.3642	-.039
				Average		-.035

* These buckets were used previously in the 2000-hour test and were subsequently cleaned and re-tip ground for use in the 3000-hour test. The weight changes listed above are those incurred only during the 3000-hour test.

** These are new buckets which ran only in the 3000-hour test.

TABLE VII

AVERAGE BLADE WEIGHT CHANGES AFTER 2000-HOUR AND 3000-HOUR ENDURANCE TESTS

Material	Test Duration, Hours	No. of Blades*		Change in Weight, %			
				After Cleaning		After Vapor Blasting	
		New	Old	New	Old	New	Old
First Stage:							
U-700	2000	61**	0	+0.038	N.A.	-0.304	N.A.
	3000	7	55	-0.021	-0.006	-0.115	-0.139
Second Stage:							
U-700	2000	52**	0	+0.147	N.A.	-0.019	N.A.
	3000	7	45	+0.077	+0.120	+0.003	+0.017
TZM	2000	4**	0	-0.044	N.A.	-0.105	N.A.
	3000	2	2	-0.002	+0.004	-0.042	-0.029
TZC	2000	4**	0	-0.033	N.A.	-0.102	N.A.
	3000	0	4	N.A.	+0.004	N.A.	-0.035

Notes:

N.A. - Not applicable.

*New - Not previously used in endurance testing.

*Old - Used in 2000-hour endurance test.

**Brand new at beginning of 2000-hour test.

TABLE VIII

TENSILE PROPERTIES OF U-700 TURBINE BLADE MATERIALS BEFORE AND AFTER ENDURANCE TESTING

Blade Stage	Test Time, Hours	Turbine Test Temp., °F	Test Temp., °F	UTS, ksi	.2% YS, ksi	% E	% R.A.
Untested Blank	0	0	R.T.	185	124	19	18
	0	0	R.T.	190	129	17	18
	0	0	R.T.	188	125	20	18
First	2000	1407	R.T.	175	121	12	13
		1407	R.T.	175	125	12	10
		1407	R.T.	178	125	10	9
First	3000	1407	R.T.	190	131	15	12
		1407	R.T.	173	127	10	11
		1407	1450	137	117	20	37
		1407	1450	130	110	17	36
First	5000	1407	R.T.	145	122	7.5	8.5
		1407	R.T.	148	125	2.5	5
		1407	R.T.	152	120	5	7
		1407	1450	144	99.5	15	32
Second	2000	1314	R.T.	191	131	10	17
		1314	R.T.	198	130	12	19
		1314	R.T.	199	141	15	15
Second	3000	1314	R.T.	196	143	15	13
		1314	R.T.	195	141	10	14.5
		1314	1250	193	114	15	24
Second	5000	1314	R.T.	198	134	20	22
		1314	R.T.	200	132	20	19
		1314	R.T.	195	132	15	19
		1314	1250	168	121	20	24

TABLE IX

TENSILE PROPERTIES OF TZC TURBINE BLADE MATERIAL

BEFORE AND AFTER ENDURANCE TESTING

Test Time, Hours	Turbine Test Temp., °F	Test Temp., °F	UTS, ksi	.2% YS, ksi	% E	% R.A.
0(1)(2)	Not Tested	R.T.	103.1	97.8	1.0	1.0
0(1)(2)	Not Tested	150	107	83.7	6.0	9.0
0(1)(4)	Not Tested	250	69.0	61.2	11.0	53.0
5000(3)	1240	R.T.	96.1	91.0	0	3
5000(3)	1240	250	93.4	67.0	17	34

(1) Conventional Tensile Specimens

(2) As Rolled 2912°F

(3) Miniature Tensile Bar from Turbine Blade

(4) As Rolled and Pickled

TABLE X

BEND TEST RESULTS OF SPECIMEN FROM TZC, 5000-HOUR TEST BLADES

Blade No.	Test Temperature	Bend Angle	Ductility
12	125°F	> 95°	Fractured
1	250°F	> 90°	Ductile, No Cracks

TABLE XI

TENSILE PROPERTIES OF BARS EXPOSED TO POTASSIUM VAPOR UPSTREAM AND DOWNSTREAM OF THE TURBINE DURING ENDURANCE TESTING

Alloy	Test Time, Hours	Turbine Test Temp., °F	Test Temp., °F	UTS, ksi	.2% YS, ksi	% E	% R.A.
I. Upstream							
TZM*	0	0	R.T.	108	102	24	60
TZM*	0	0	1400	88	80	13	83
TZM	3000	1500	R.T.	118	118	0.2	0.0
TZM	3000	1500	R.T.	104	-	0.0	0.0
TZM	3000	1500	1400	78.5	77.2	15.1	89.5
TZM	3000	1500	1400	78.6	77.2	15.3	87.5
II. Downstream							
TZC*	0	0	150	107	83.7	6.0	9.0
TZC*	0	0	1400	66.4	58.7	14	74
TZC	1746	1240	150	109	89.4	5.5	6.0
TZC	1746	1240	250	100	81.1	9.8	22.4
TZC	1746	1240	250	91.5	73.6	5.0	7.0
TZC	1746	1240	1400	64.7	58.2	15.7	70.6
TZC	3000	1240	150	116.2	115.1	0.3	1.0
TZC	3000	1240	150	111.3	109	0.3	2.0
TZC	3000	1240	1400	91	87	10.7	59.3
TZC	3000	1240	1400	94	91.7	9.4	51.8
AS-30*	0	0	R.T.	127	100	13.0	30.0
AS-30*	0	0	1400	90	73	8.0	55.0
AS-30	3000	1240	R.T.	113.1	108	0.6	1.0
AS-30	3000	1240	R.T.	122.3	112.6	1.3	2.5
AS-30	3000	1240	1400	88.5	77	12.1	61.2
AS-30	3000	1240	1400	88.5	76.9	12.0	59.2

*Tensile test data from as-received material for comparison purposes.

TABLE XII

WEIGHT CHANGE AND CHEMICAL ANALYSIS EVALUATION OF REFRACTORY ALLOY PROBE SPECIMENS AFTER FIRST 814 HOURS OF TURBINE TESTING

(Probe I Located at Turbine Inlet - 1500°F)

Specimen No.	Material	Original Weight -gr.	Weight Change -gr.	Chemical Analysis				
					Quantity, ppm			
				Location	C	O	N	H
1	TZC	9.7604	+0.0001					
2	TZM	9.9617	-0.0019					
3	F-48	8.8440	-0.0025					
4	TZC	9.4964	+0.0001					
5	TZM	9.7961	-0.0005					
6	F-48	9.1666	-0.0052	Surface	340/360	190	116	7
				Core	200/250	54	20	7

TABLE XIII

WEIGHT CHANGE AND CHEMICAL ANALYSIS EVALUATION OF REFRACTORY ALLOY PROBE SPECIMENS AFTER A TOTAL OF 3000 HOURS OF TURBINE TESTING

(Probe I Located at Turbine Inlet - 1500°F)

Specimen No.	Material	Original Weight -gr.	Weight Change -gr.	Chemical Analysis				
					Quantity, ppm			
				Location	C	O	N	H
1	TZC	9.7605	+0.0001	Surface	934/987	26/4	11/7	< 1
				Core	1086/1104	11/18	4	< 1
2	TZM	9.9636	+0.0001	Surface	99/197	22	4	< 1
				Core	106/175	19	8	< 1
3	F-48	8.8415	+0.0005	Surface	366/429	66/17	248/162	1/5
				Core	202/218	9	28/22	6/5
4	TZC	9.4965	+0.0003	Surface	922/953	6/11	2	< 1
				Core	990/1075	11	2	< 1
5	TZM	9.7966	+0.0002	Surface	142/161	20	5	< 1
				Core	145/146	21	13/9	< 1
6A[1]	F-48	8.8940	-0.0009	Surface	413/416	39/29	101/98	7/6
				Core	317	14/26	21/27	8

[1] Installed after 814 hour shut-down; total exposure time was 2186 hours.

TABLE XIV

WEIGHT CHANGE AND CHEMICAL ANALYSIS EVALUATION OF REFRACTORY ALLOY PROBE SPECIMENS AFTER THE FIRST 2175 HOURS OF TURBINE TESTING

(Probe III Located in the Condenser - 1240°F)

Specimen No.	Material	Original Weight -gr.	Weight Change -gr.	Chemical Analysis				
					Quantity, ppm			
				Location	C	O	N	H
1	TZM & Cb	8.4141	-0.0001					
2	TZM	10.4703	-0.0104					
3	F-48	8.8496	-0.0037					
4	TZM & Cb	8.3280	-0.0001					
5	TZM	9.8578	-0.0024					
6	F-48	9.4610	-0.0106	Surface	270	63	58	10
				Core	280	50	19	4

TABLE XV

WEIGHT CHANGE AND CHEMICAL ANALYSIS EVALUATION OF REFRACTORY ALLOY PROBE SPECIMENS AFTER A TOTAL OF 3000 HOURS OF TURBINE TESTING

(Probe III Located in the Condenser - 1240°F)

Specimen No.	Material	Original Weight -gr.	Weight Change -gr.	Chemical Analysis				
					Quantity, ppm			
				Location	C	O	N	H
1	TZM & Cb	8.4142	+0.0001	Surface	197/338	51/64	49/36	2/4
				Core[2]	193/215	25/31	14	3/5
2	TZM	10.4807	+0.0002	Surface	179/202	21/26	4	< 1
				Core	159/174	17	4	< 1
3	F-48	8.8533	-0.0016	Surface	231/235	32/45	41/33	2/5
				Core	191/216	31	20	3/4
4	TZM & Cb	8.3281	-0.0001	Surface	511/768	33	14/19	< 1
				Core	587/590	17	8	< 1
5	TZM	9.8602	-0.0023	Surface	201/240	28	9	< 1
				Core	162/184	17	5	< 1
6A[1]	F-48	8.9520	-0.0038	Surface	476/481	50/22	14/4	< 1
				Core	432/487	25	7	< 1

[1] Installed after 2175-hour shut-down; total exposure time was 825 hours.

[2] Core analysis for O, N, H used as reference analysis; original carbon content was 650 ppm.

TABLE XVI

REFERENCE C, O, N, AND H ANALYSES FOR REFRACTORY METAL ALLOYS

Alloy*	Carbon, ppm	Oxygen, ppm	Nitrogen, ppm	Hydrogen, ppm
TZM	178	25	10	< 1
TZC	1305	28	4	3
F-48	204	27	17	< 1
TZM & Cb	650	28	14	4

*Typical Compositions:

TZM: Mo - 0.55 Ti - 0.09 Zr - 0.019C

TZC: Mo - 1.1 Ti - 0.13 Zr - 0.13C

F-48: Cb - 14.9 W - 4.5 Mo - 0.87 Zr - 0.027 C

TZM & Cb: Mo - 1.62 Cb - 0.50 Ti - 0.32 Zr - 0.965 C

TABLE XVII

EROSION INSERT TESTED IN THE POTASSIUM TURBINE

MATERIAL	COMPOSITION	CONDITION	SPECIMENS TESTED		
			2000-HOURS	3000-HOURS	5000-HOURS
U-700	0.06 C, 18.7 Co, 15.1 Cr, 4.48 Al, 3.40 Ti, 0.029 B, 5.15 Mo, Bal. Ni	2125°F - 2 Hrs. A.C. 1975°F - 2 Hrs. A.C. 1550°F - 2 Hrs. A.C. 1400°F - 2 Hrs. A.C.	A-1, A-2 A-3	A-1, A-2 A-4*, A-5*, A-6*	A-1, A-2
TZM	0.55 Ti, 0.09 Zr, 0.019 C, Bal. Mo	Recrystallized; 2850°F - 1 Hr.	B-1, B-2, B-3	None	None
TZM	0.55 Ti, 0.09 Zr, 0.19 C, Bal. Mo	Stress Relieved 2200°F - 1 Hr.	C-1, C-2, C-3	C-1, C-2	C-1, C-3
TZC	1.1 Ti, 0.13 Zr, 0.13 C, Bal. Mo	As-Rolled: 3092°F	D-1, D-2, D-3	D-1, D-3	D-1, D-3
AS-30	17.4 W, 0.98 Zr, 0.087 C, Bal. Cb	Stress Relieved 1900°F - 1 Hr.	None	E-1*, E-2*, E-3*	None

*Newly installed for 3000-hour test.

TABLE XVIII

EROSION INSERT WEIGHT CHANGES DURING 3000-HOUR ENDURANCE TEST

Alloy S/N	Original Weight - Gm.	Weight Change - Gm.
U-700		
A-1	22.2998	+0.0101
A-2	22.5790	+0.0118
A-4	22.1130	+0.0211
A-5	22.2138	+0.0148
A-6	21.9830	+0.0071
TZM		
C-1	28.6028	-0.0090
C-2	28.5091	-0.0104
TZC		
D-1	28.2019	-0.0057
D-3	27.9373	-0.0098
AS-30		
E-1	27.1080	-0.0437
E-2	26.8389	-0.0601
E-3	26.6915	-0.0574

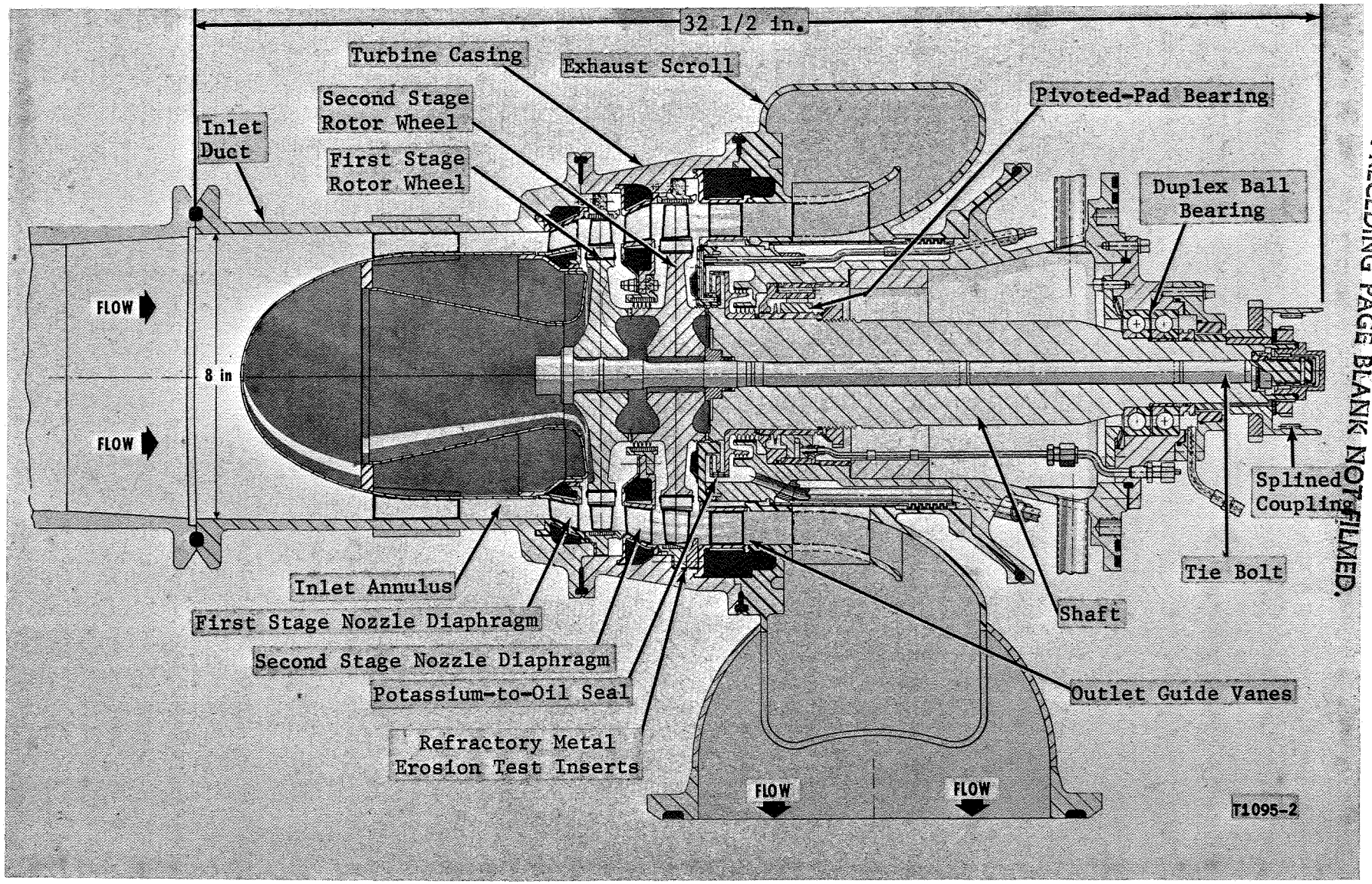
TABLE XIX

TENSILE PROPERTIES OF VARIOUS EROSION INSERT MATERIALS

Material	Condition	Test Temp. -°F	0.2% Yld. -ksi	Ult. -ksi	Elong. -%	Strain Energy -ksi
U-700*	As Heat Treated	1500	88	105	15	14.5
U-700	As Heat Treated	1250	130	180	8	12.4
U-700	As Heat Treated	1500	100	120	20	22.0
TZM*	SR	1400	80	88	13	10.9
TZM*	SR + 3000 Hr. Turbine Test at 1550°F	1400	77.2	78.5	15.1	11.8
TZC*	SR	1400	58	65	16	9.85
TZC*	SR + 3000 Hr. Turbine Test at 1260°F	1400	87	91	10.7	9.5
AS-30*	SR	1400	75	90	8	6.6
AS-30*	SR + 3000 Hr. Turbine Test at 1260°F	1400	76.9	88.5	12	9.9

*Data from heat used as inserts.





PRECEDING PAGE BLANK NOT FILMED.

Figure 1. Sectional View of Two-Stage Potassium Test Turbine.

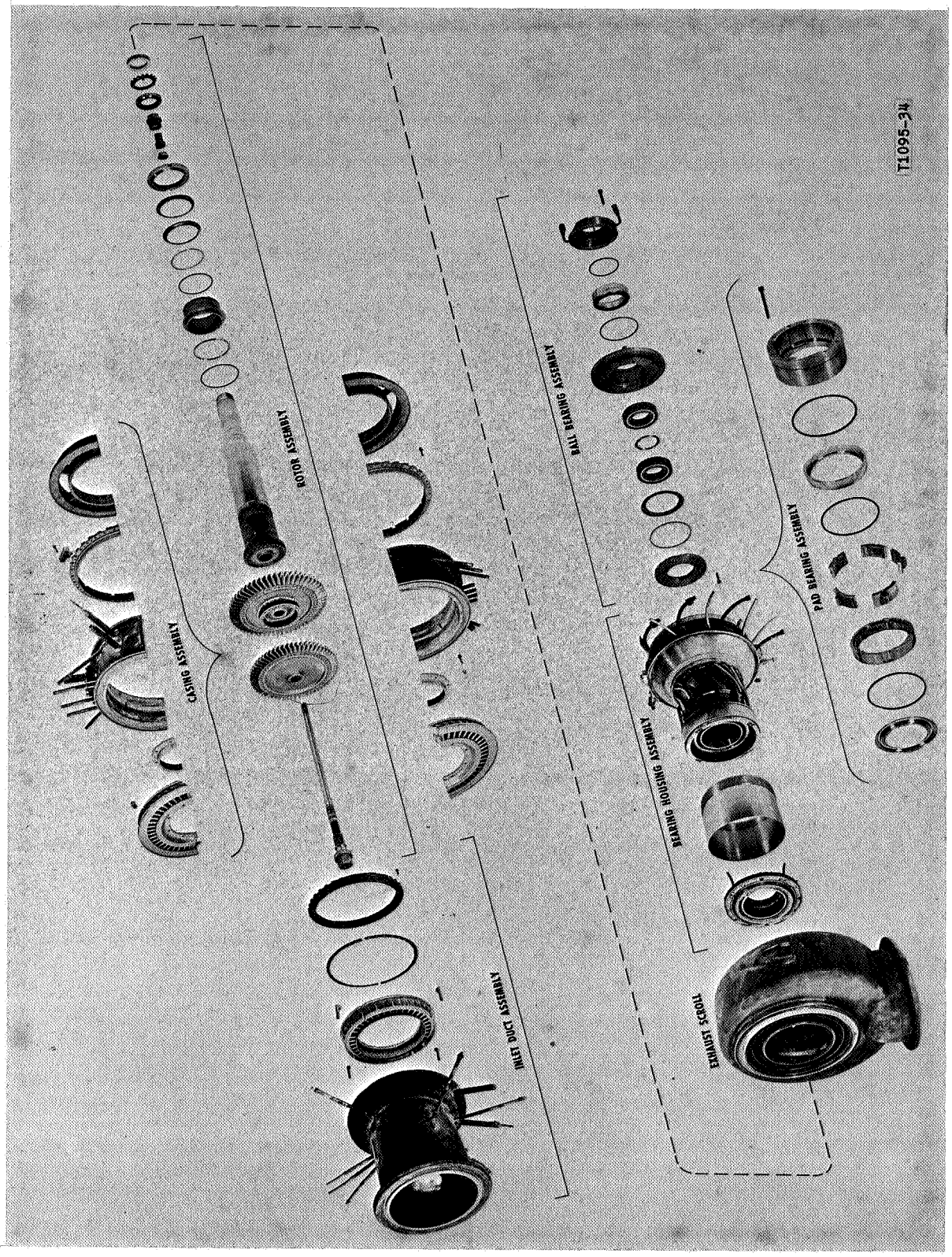
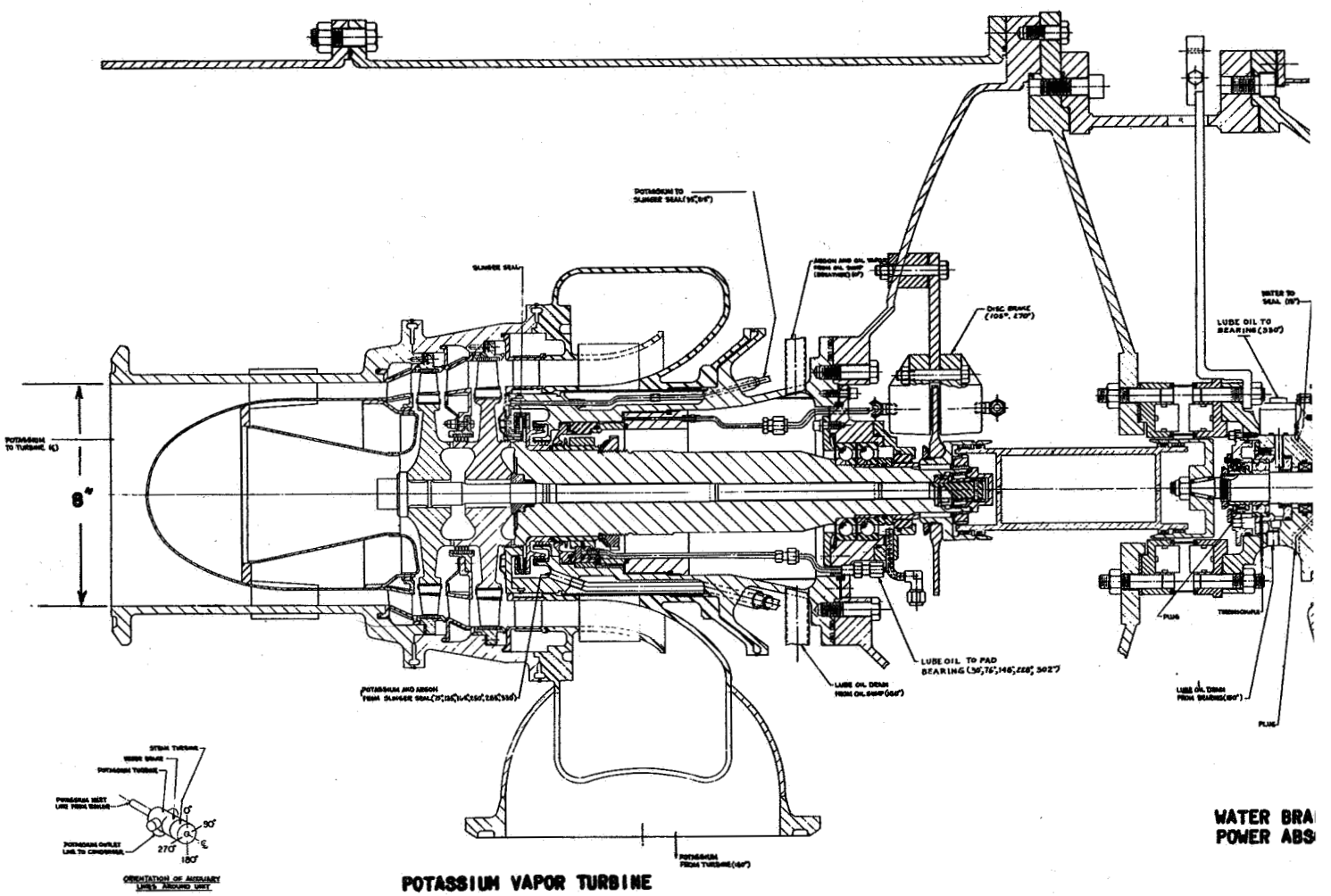


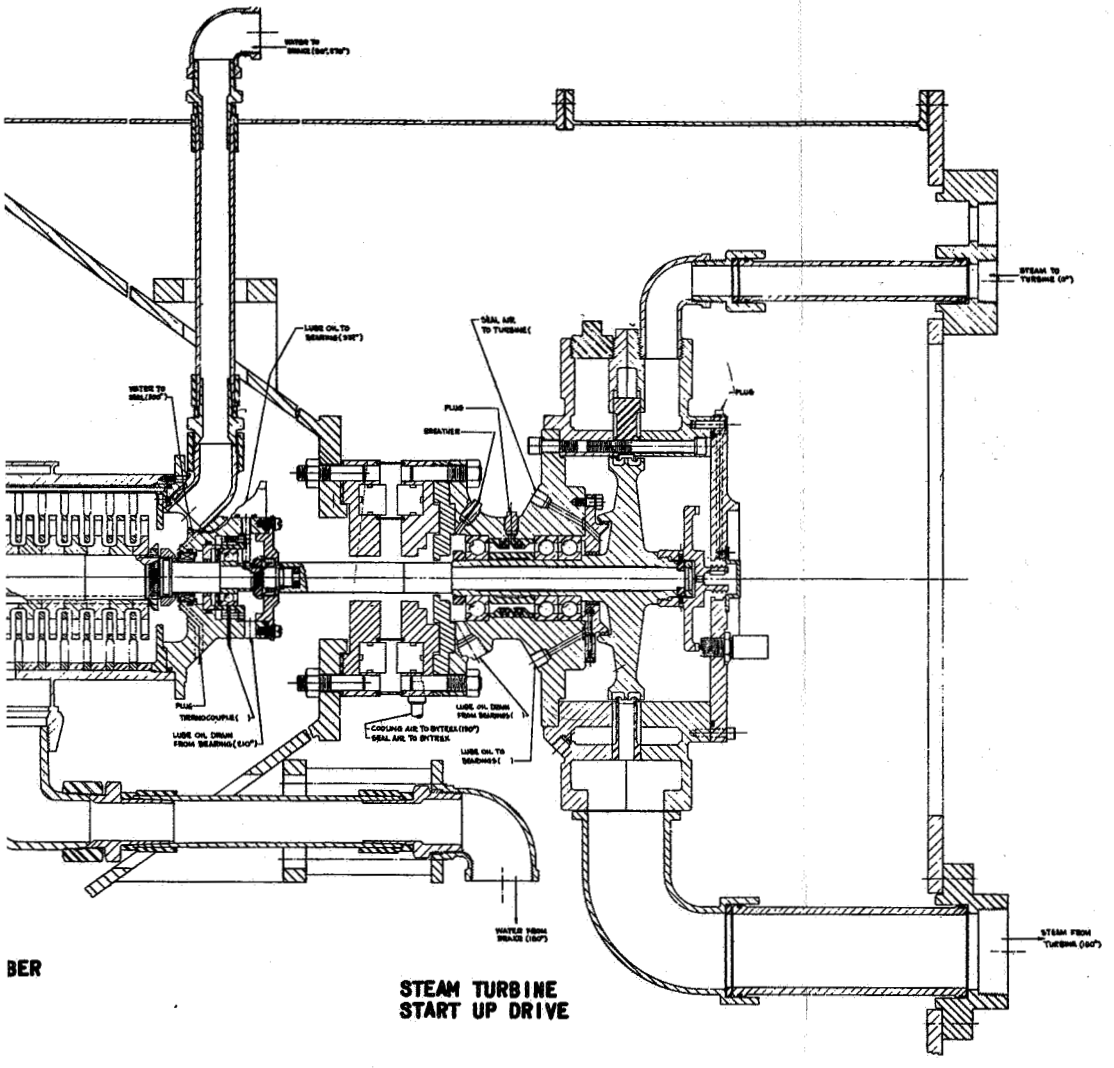
Figure 2. Exploded View of Turbine.



POTASSIUM VAPOR TURBINE

Figure 3. Overall Tes

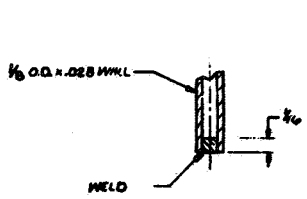
FOLDOUT FRAME



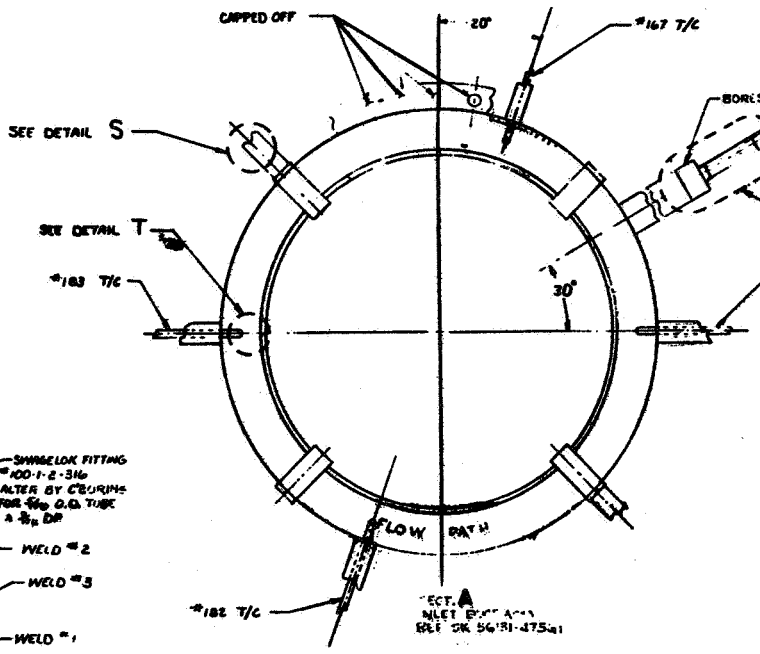
BER

Assembly Arrangement.

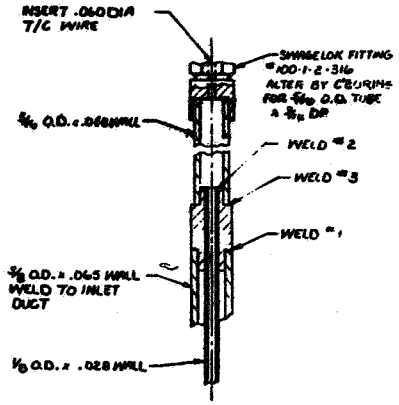
FOLDOUT FRAME



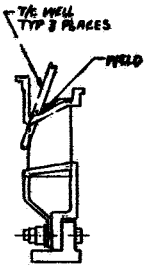
DETAIL T
TYP T/C WELL CONSTRUCTION
SCALE : NONE



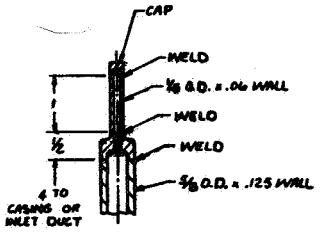
SECT. A
INLET DUCT ASSY
REF DR 56151-475-01



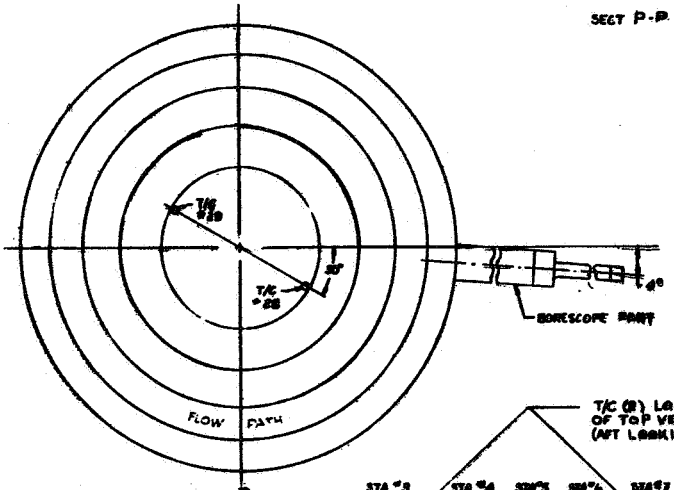
DETAIL S
TYP T/C INSTALLATION IN INLET DUCT
SCALE NONE



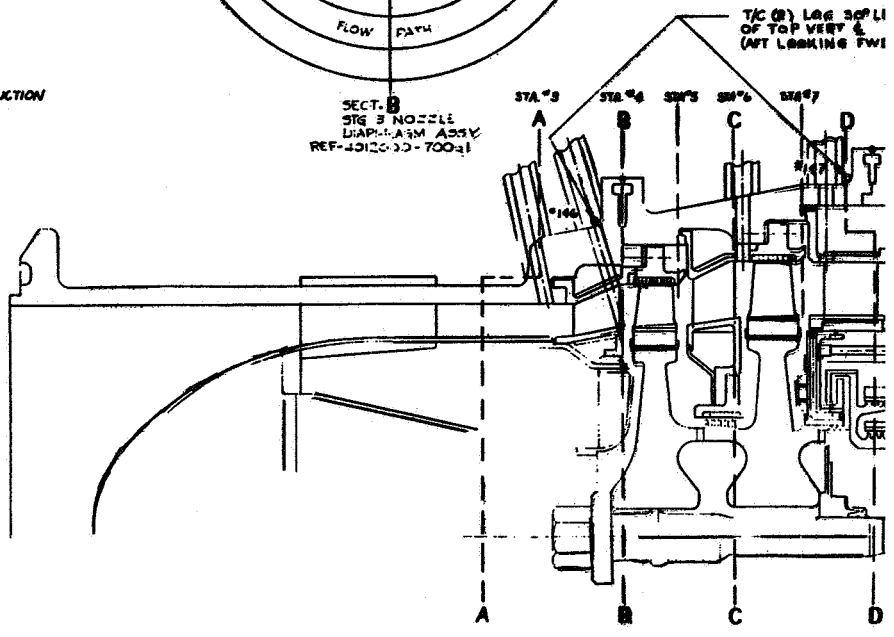
SECT P-P

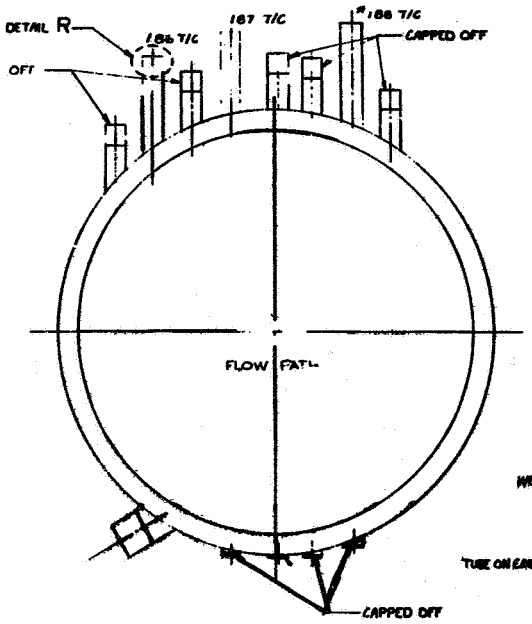


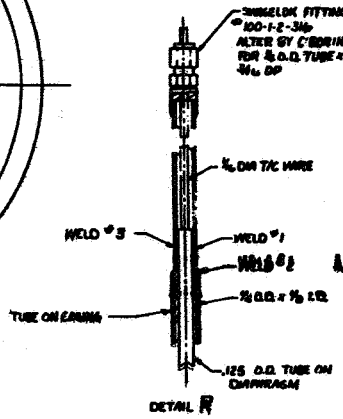
DETAIL V
TYP BORESCOPE PORT CONSTRUCTION
SCALE : NONE



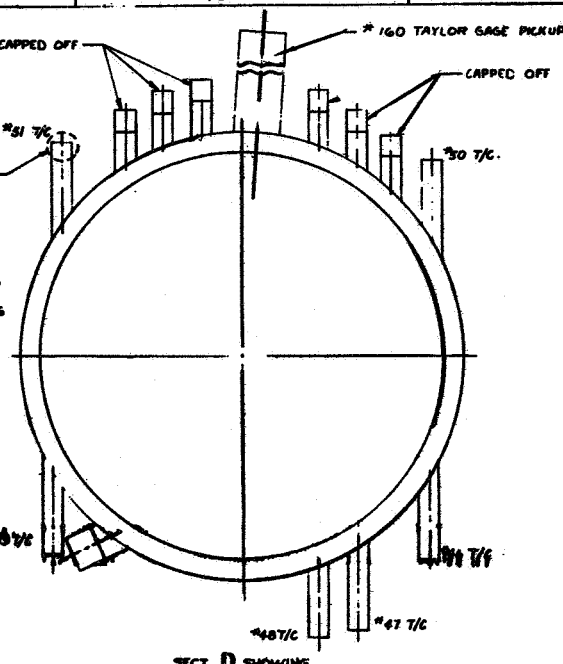
SECT. B
STG 3 NOZZLE DIAPHRAGM ASSY
REF-40126-00-700-01



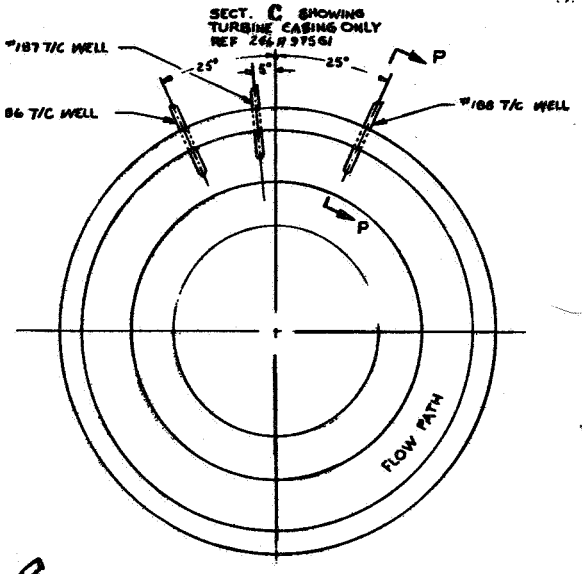


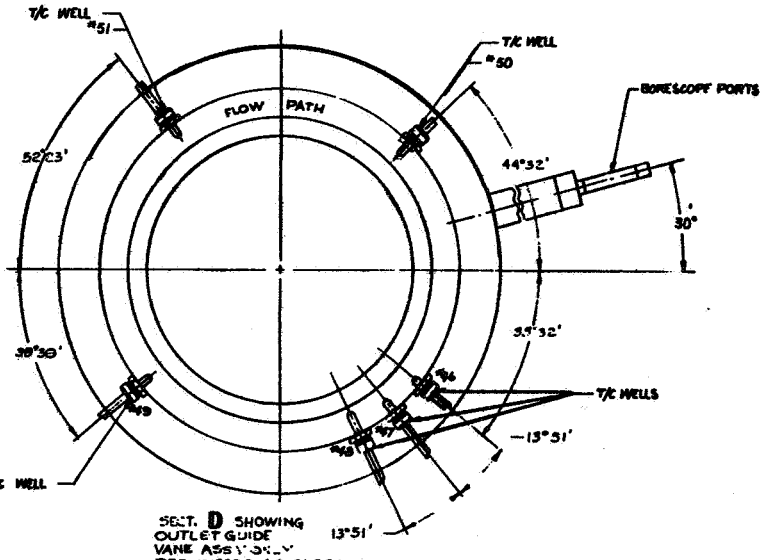


DETAIL R
TYP T/C INSTALLATION
SCALE: NONE



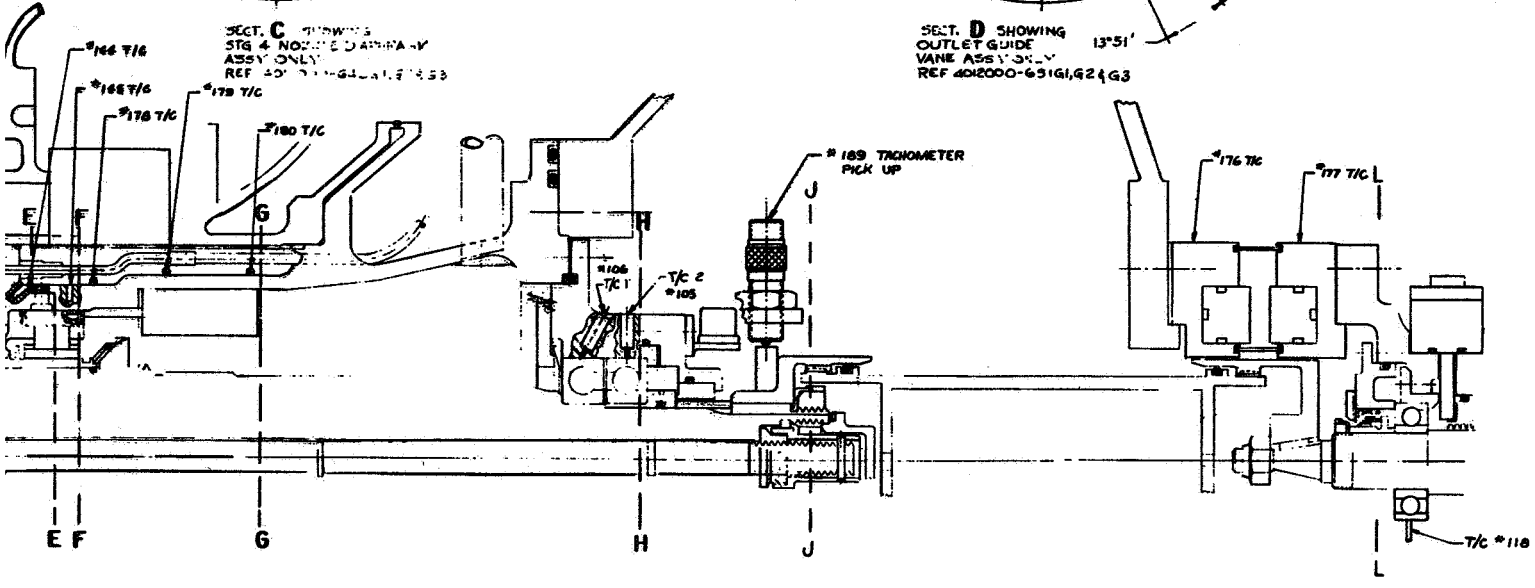
SECT. D SHOWING
TURBINE CASING
ONLY
REF 246R975G1

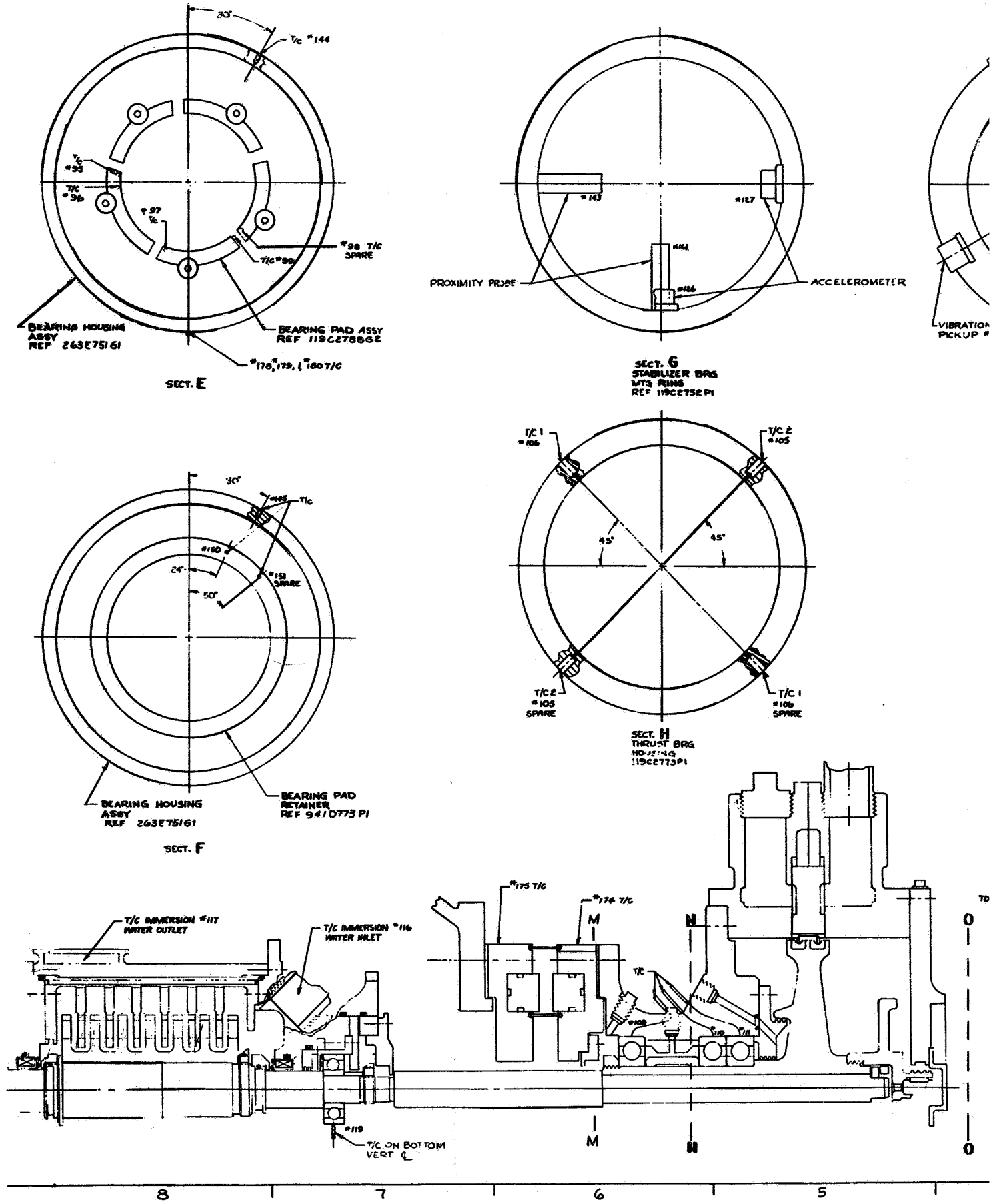




SECT. C SHOWING
STG 4 NOZZLE DIAPHRAGM
ASSY ONLY
REF 401200-631G1,G2 & G3

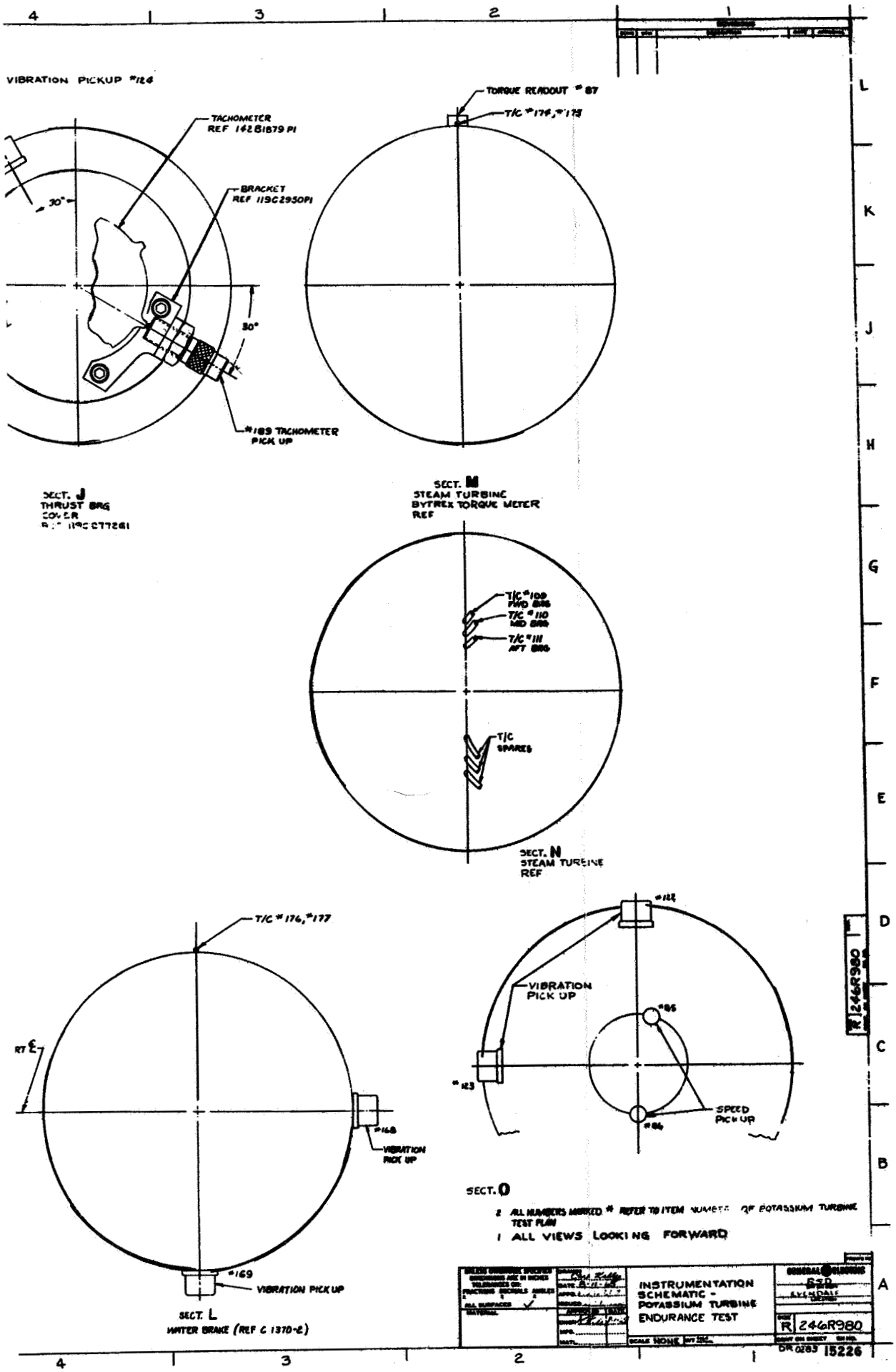
SECT. D SHOWING
OUTLET GUIDE
VANE ASSY ONLY
REF 401200-631G1,G2 & G3





FOLDOUT FRAME

Figure 4. Instrumentation



Schematic for Potassium Turbine Endurance Test.

FOLDOUT FRAME



PRECEDING PAGE BLANK NOT FILMED.

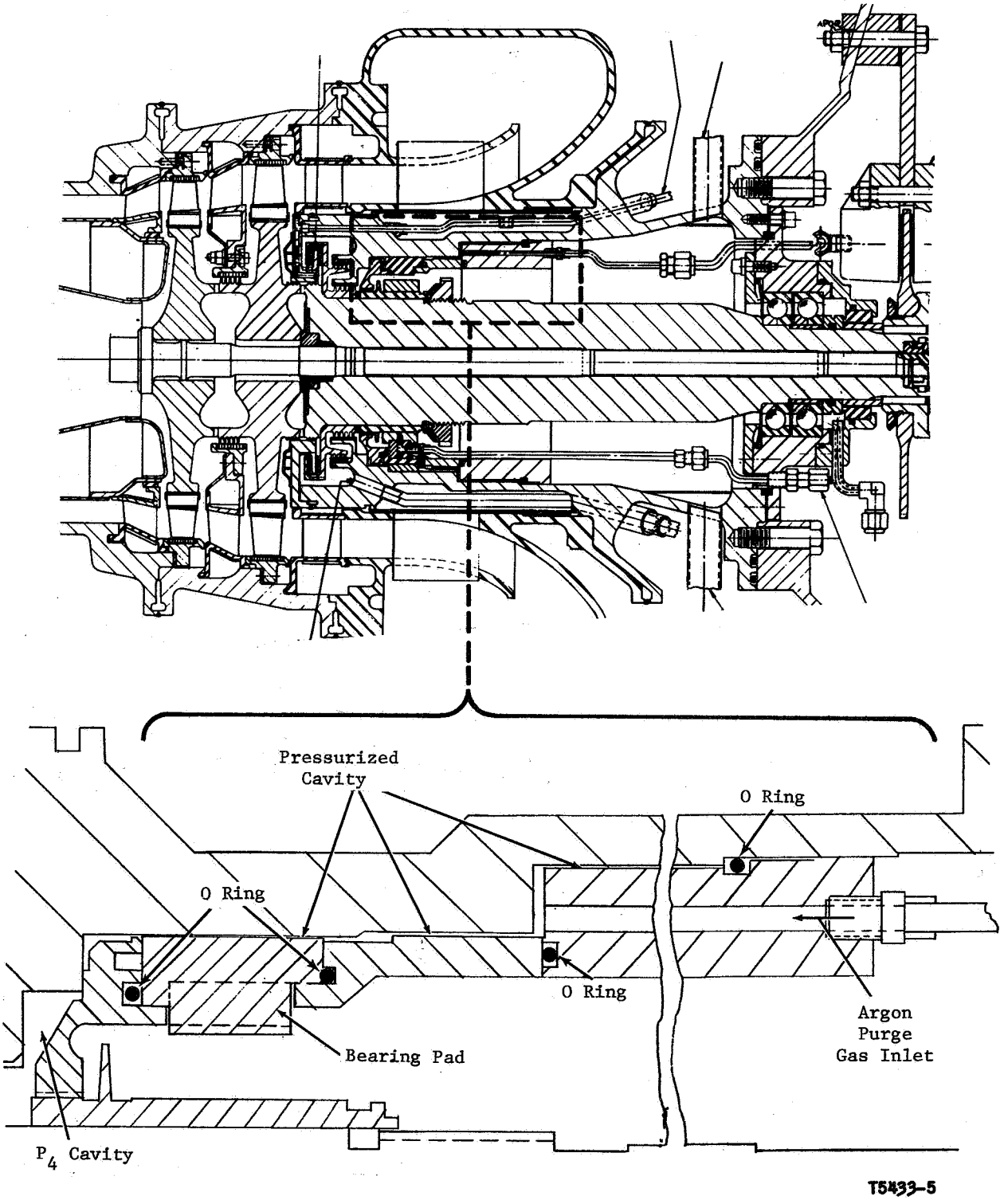


Figure 5. Bearing Housing Internal Assembly Showing **Argon Pressurized** Oil Seal.

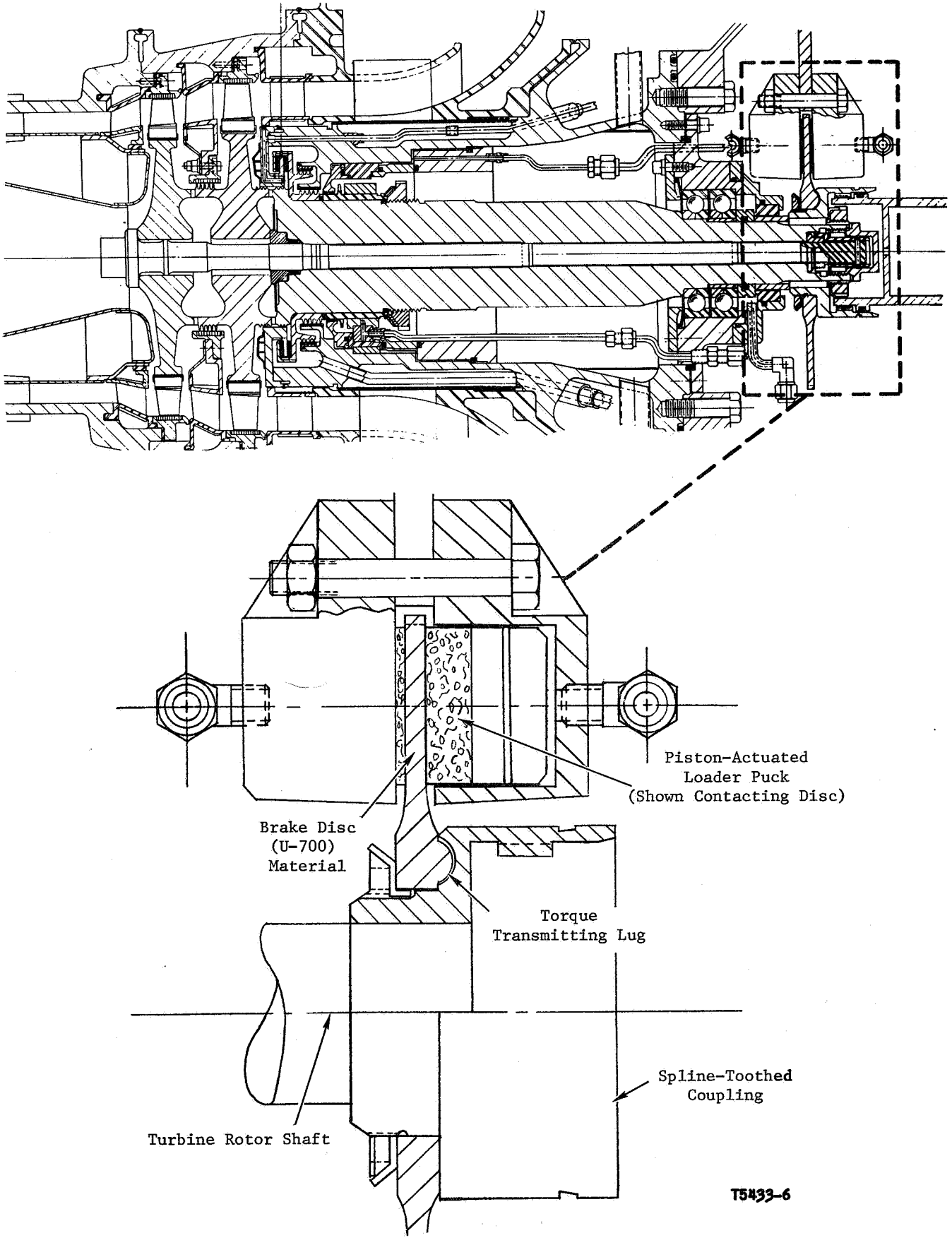
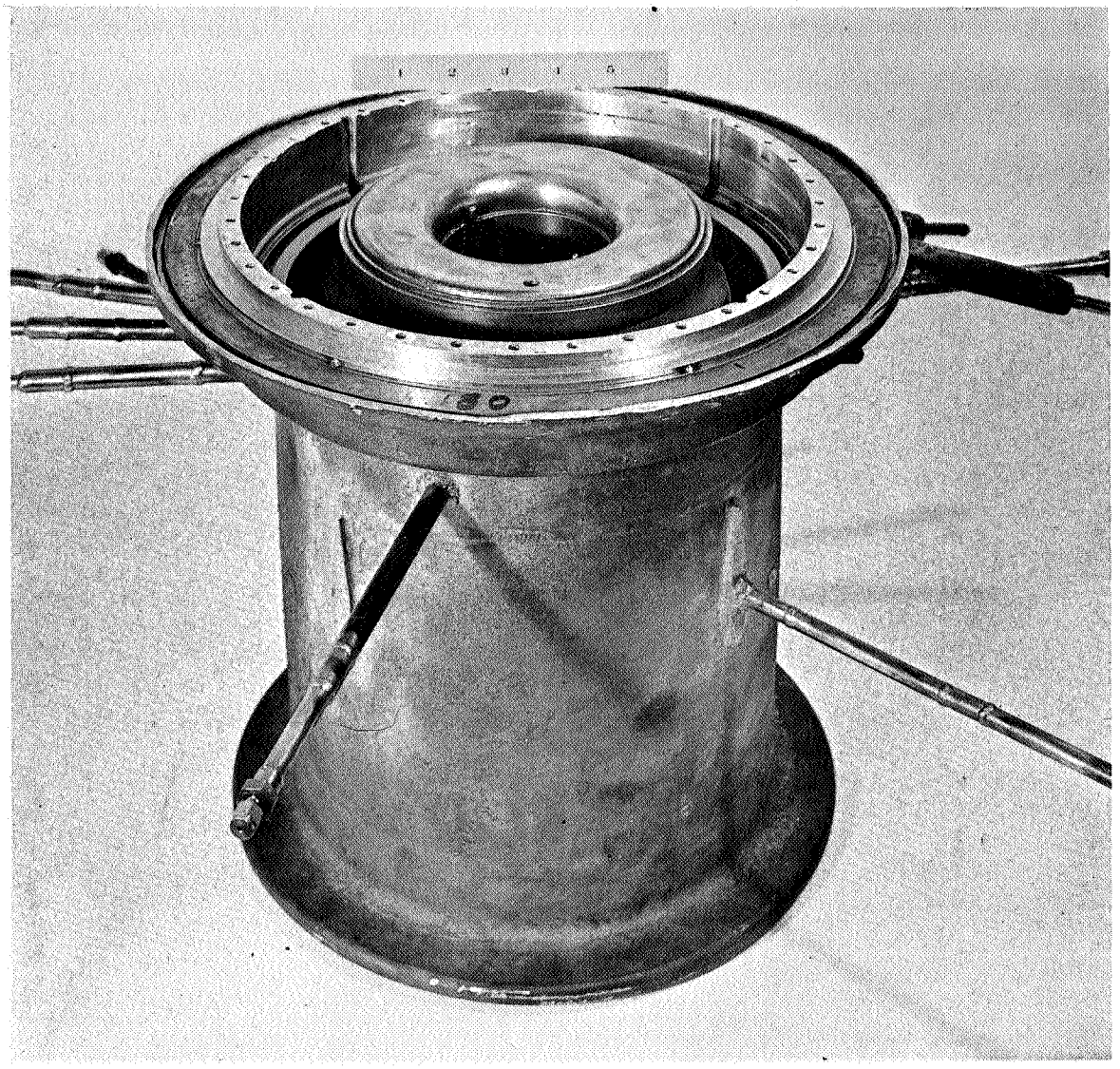
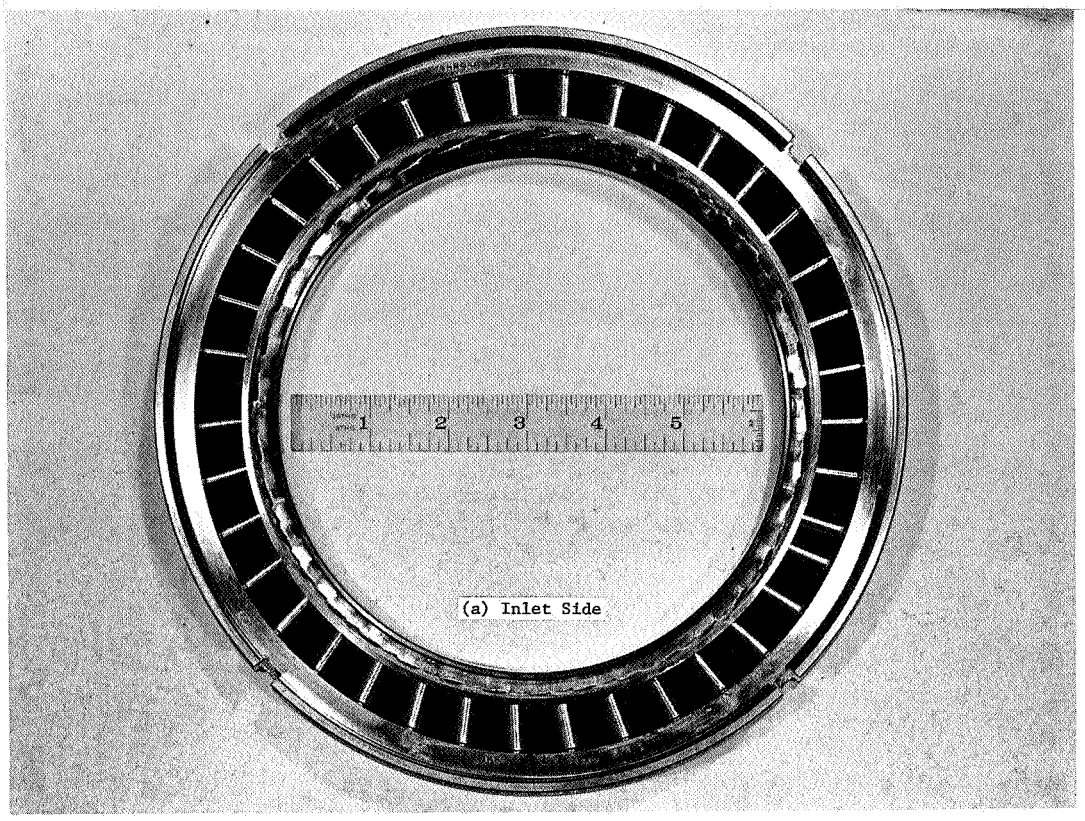


Figure 6. Installation of the Disc Brake on Two-Stage Turbine.



T5433-7

Figure 7. Inlet Duct.



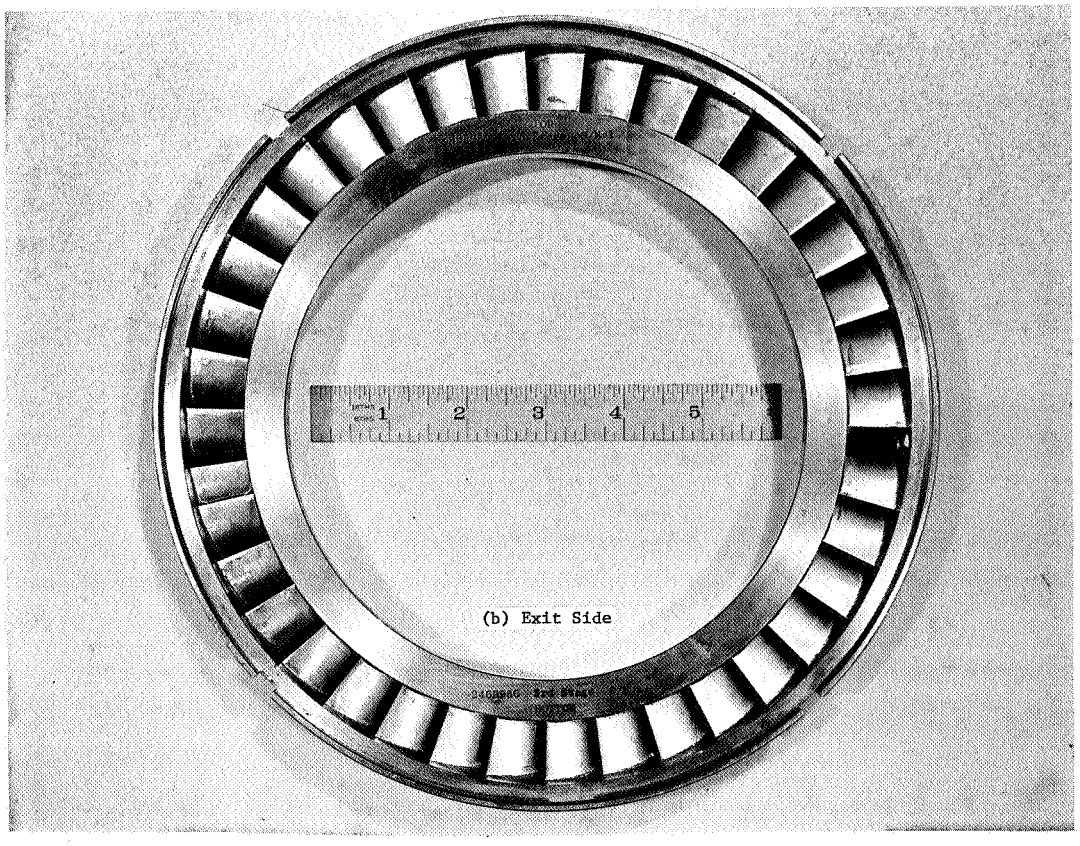
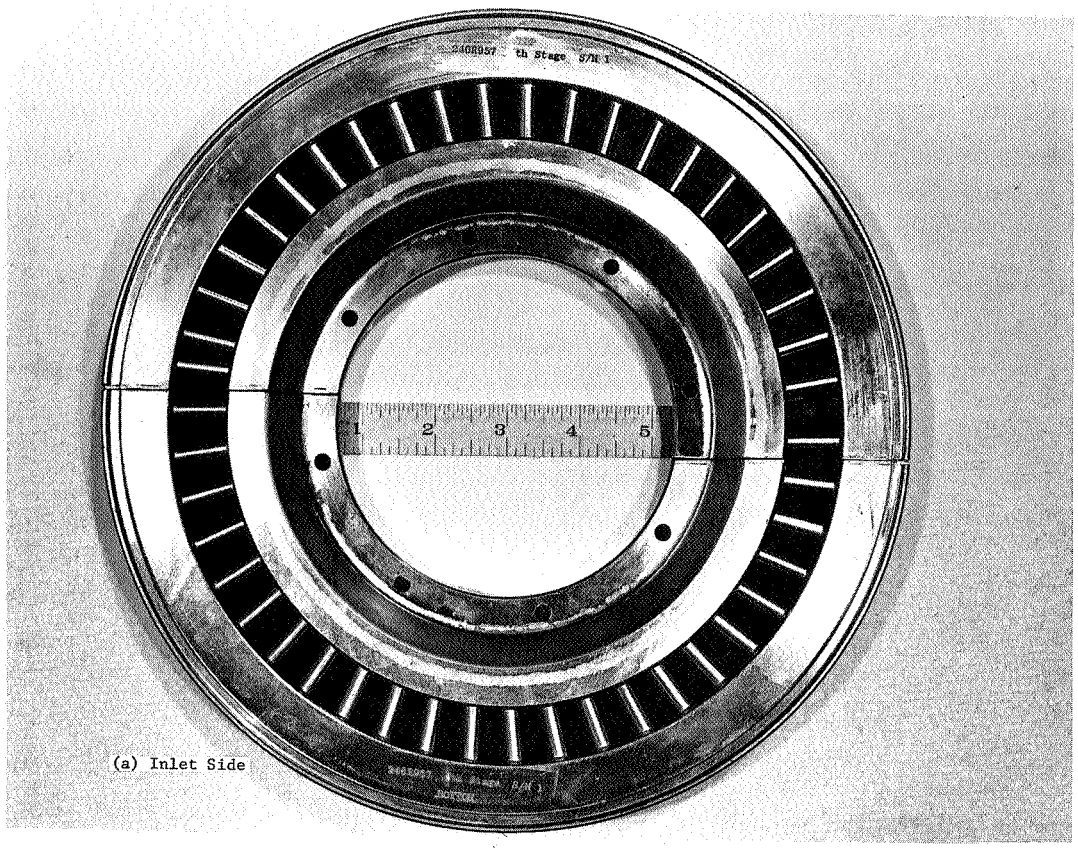
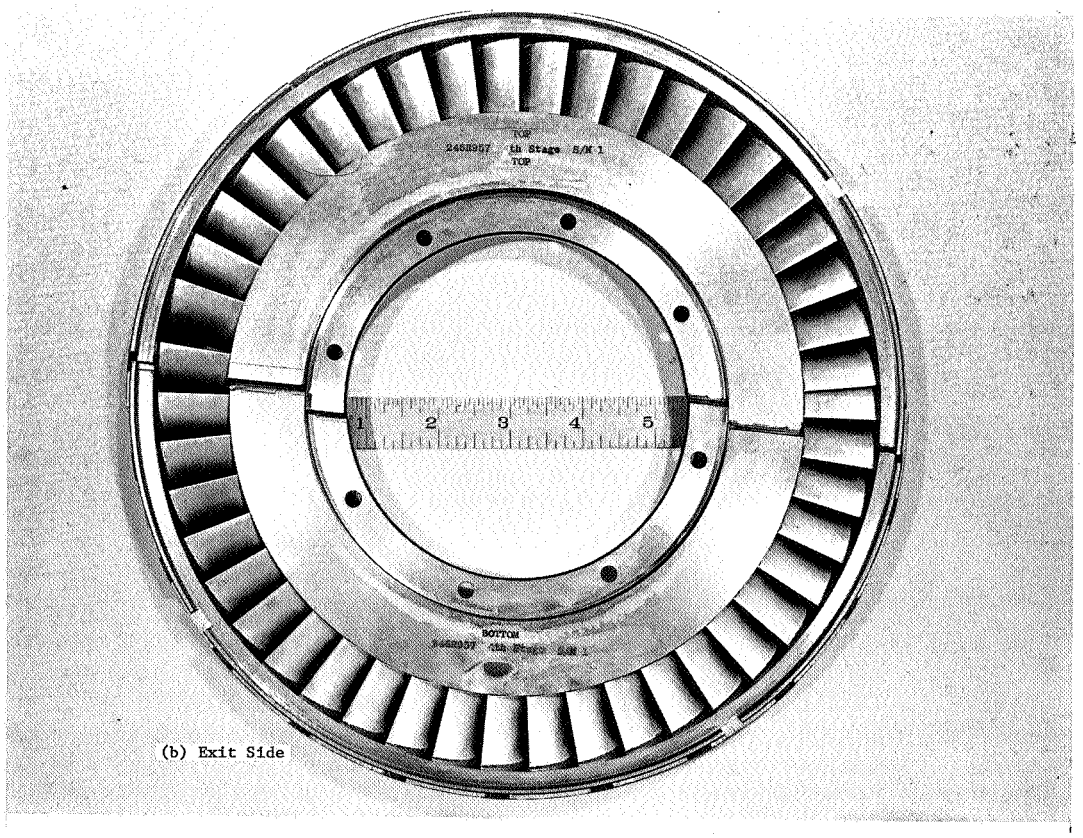


Figure 8. First Stage Nozzle Diaphragm. T5433-8

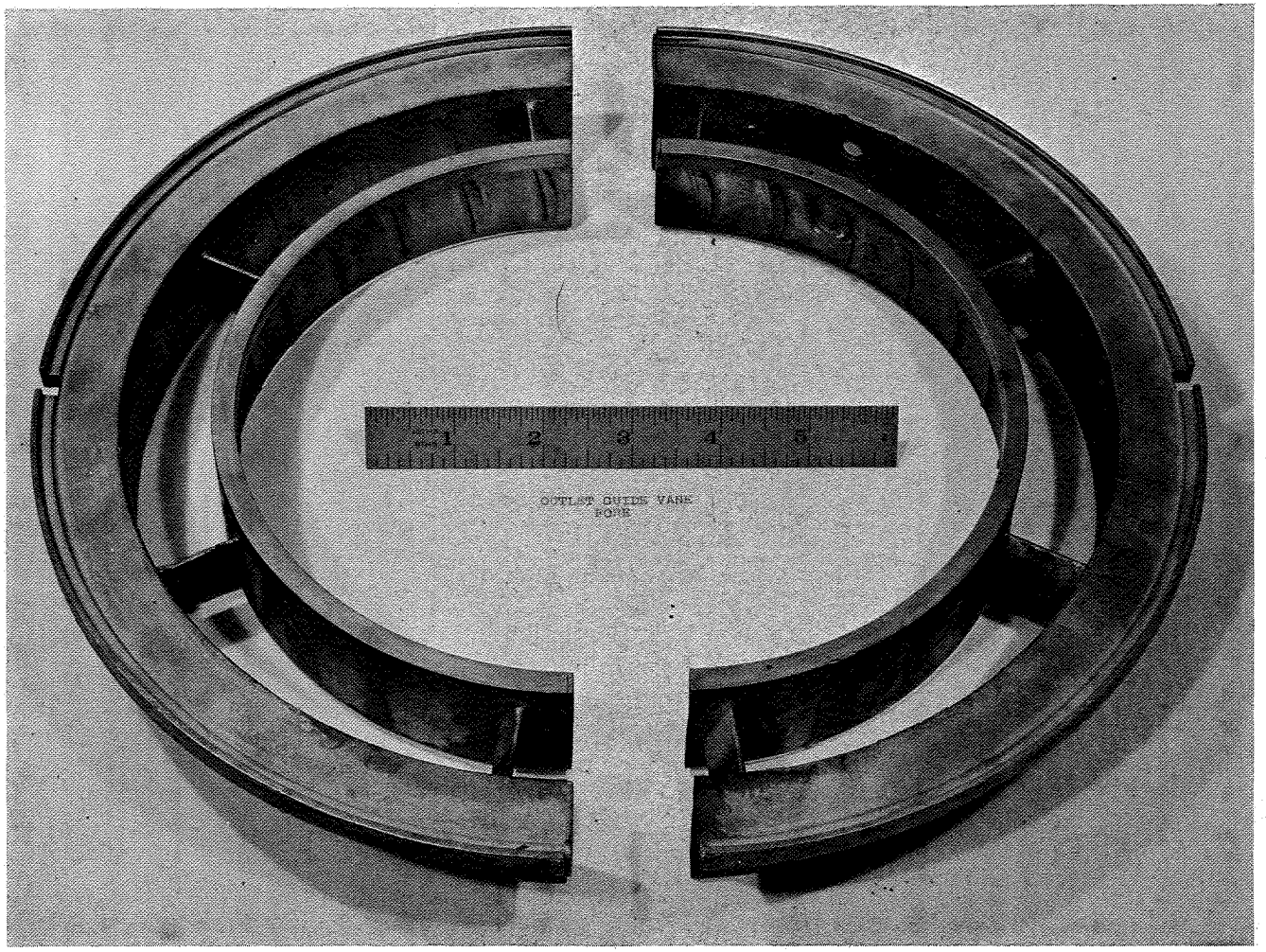




(b) Exit Side

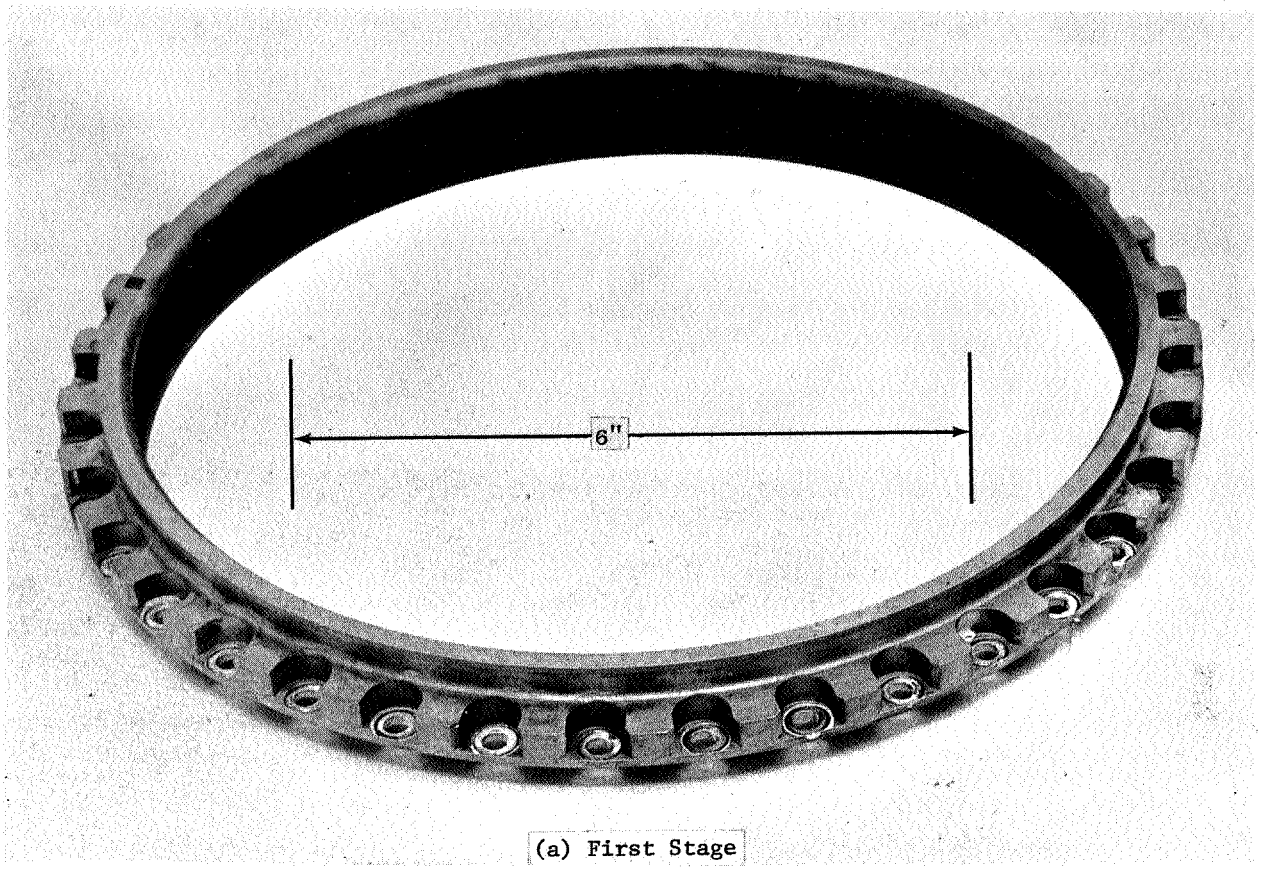
T5433-9

Figure 9. Second Stage Nozzle Diaphragm.

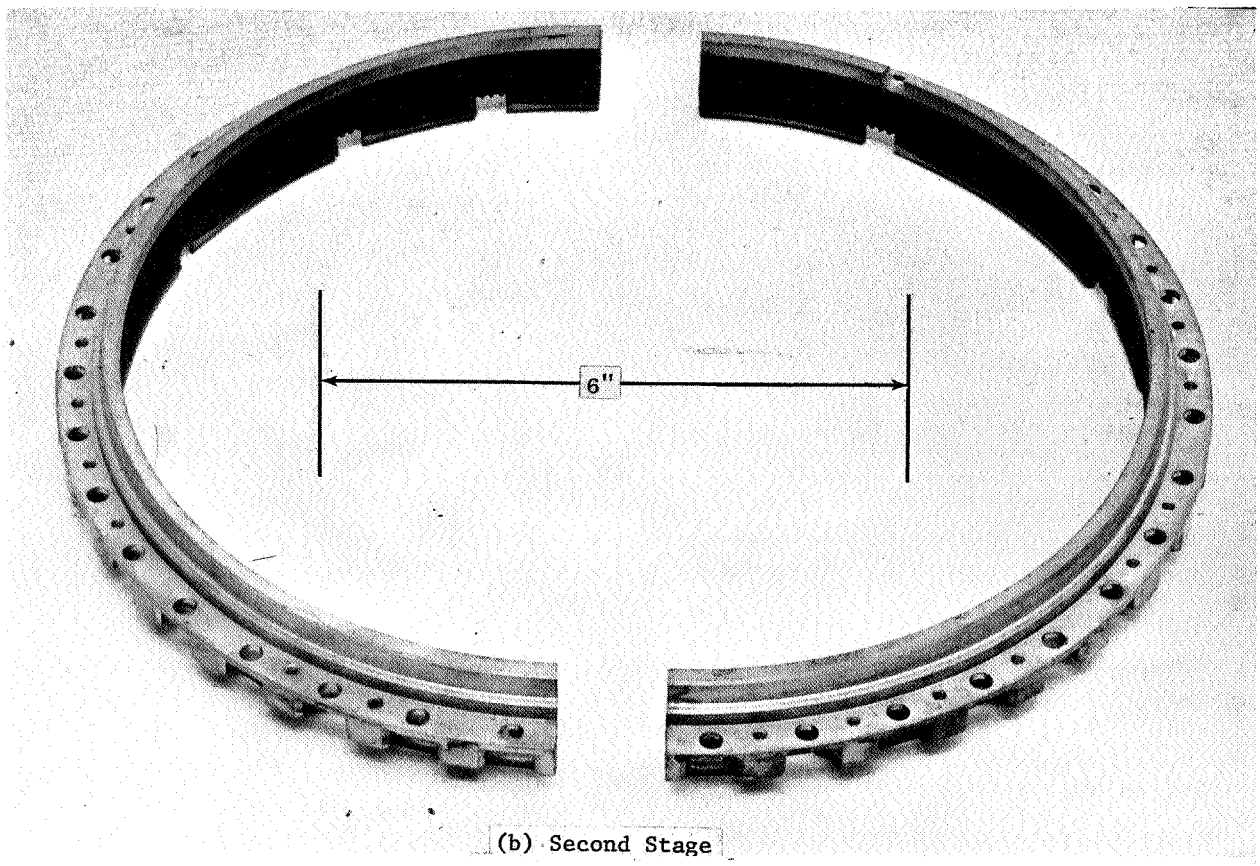


T5433-10

Figure 10. Outlet Guide Vane.



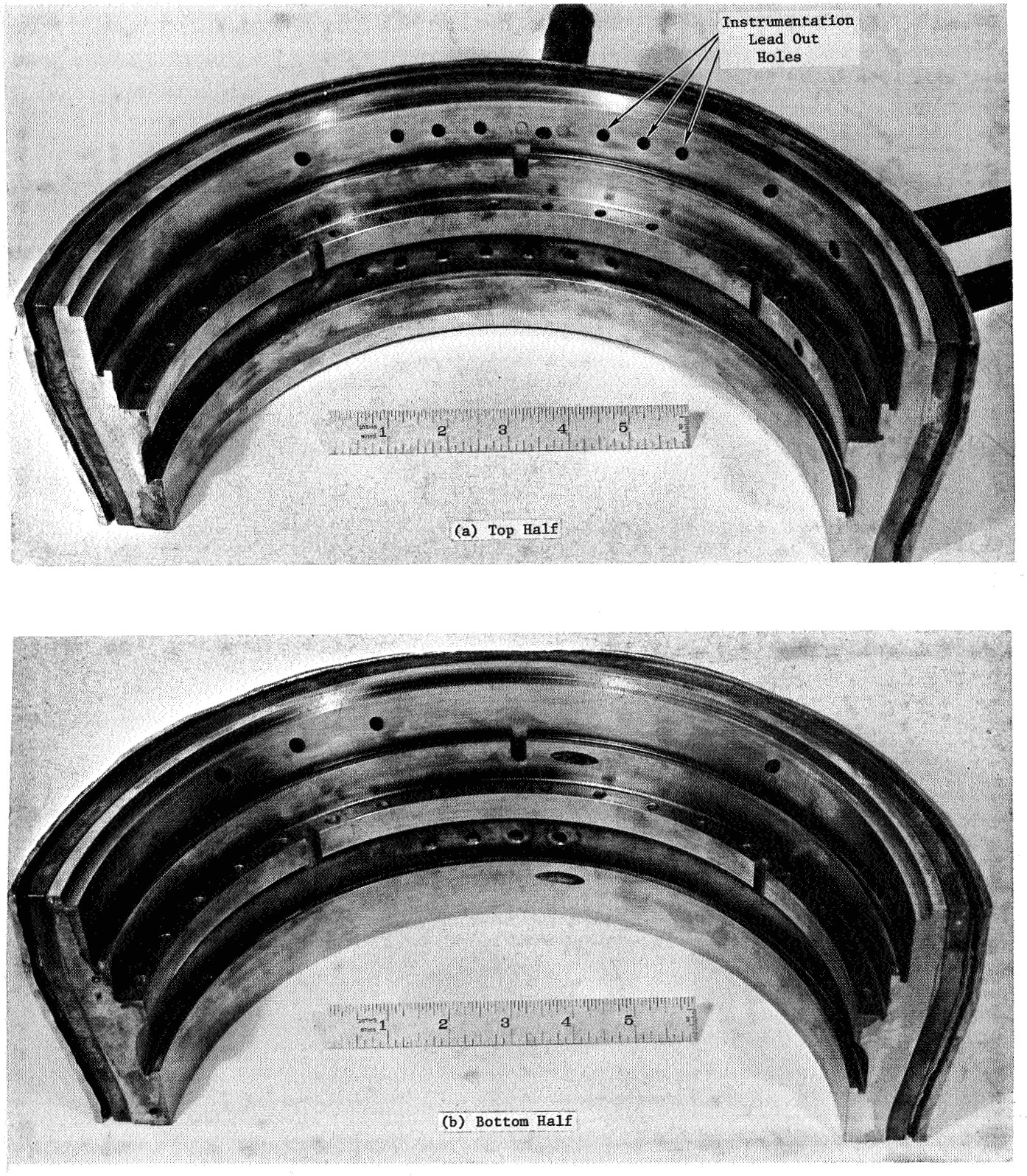
(a) First Stage



(b) Second Stage

T5433-11

Figure 11. Turbine Tip Seal.



T5433-12

Figure 12. Turbine Casing.

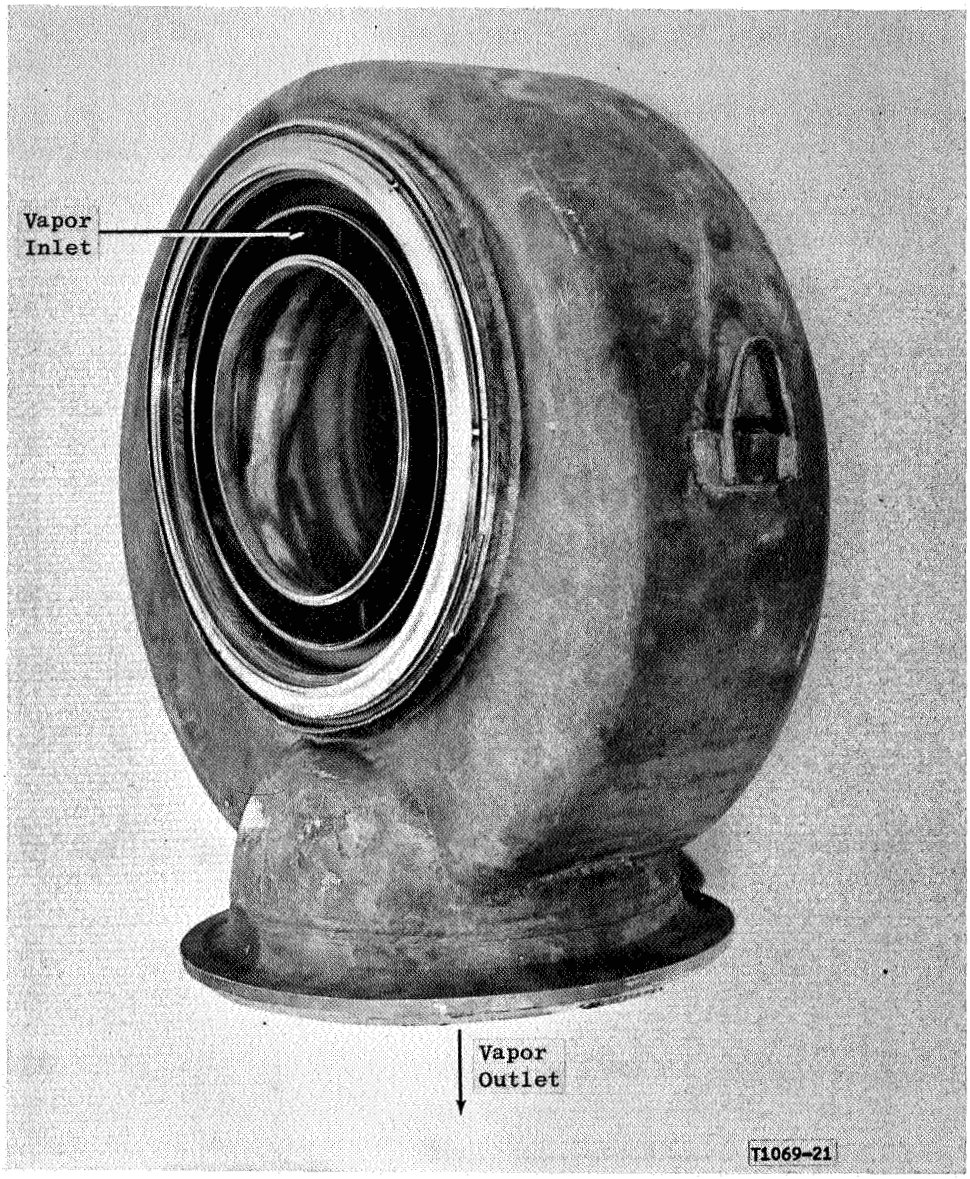


Figure 13. Turbine Exhaust Scroll.

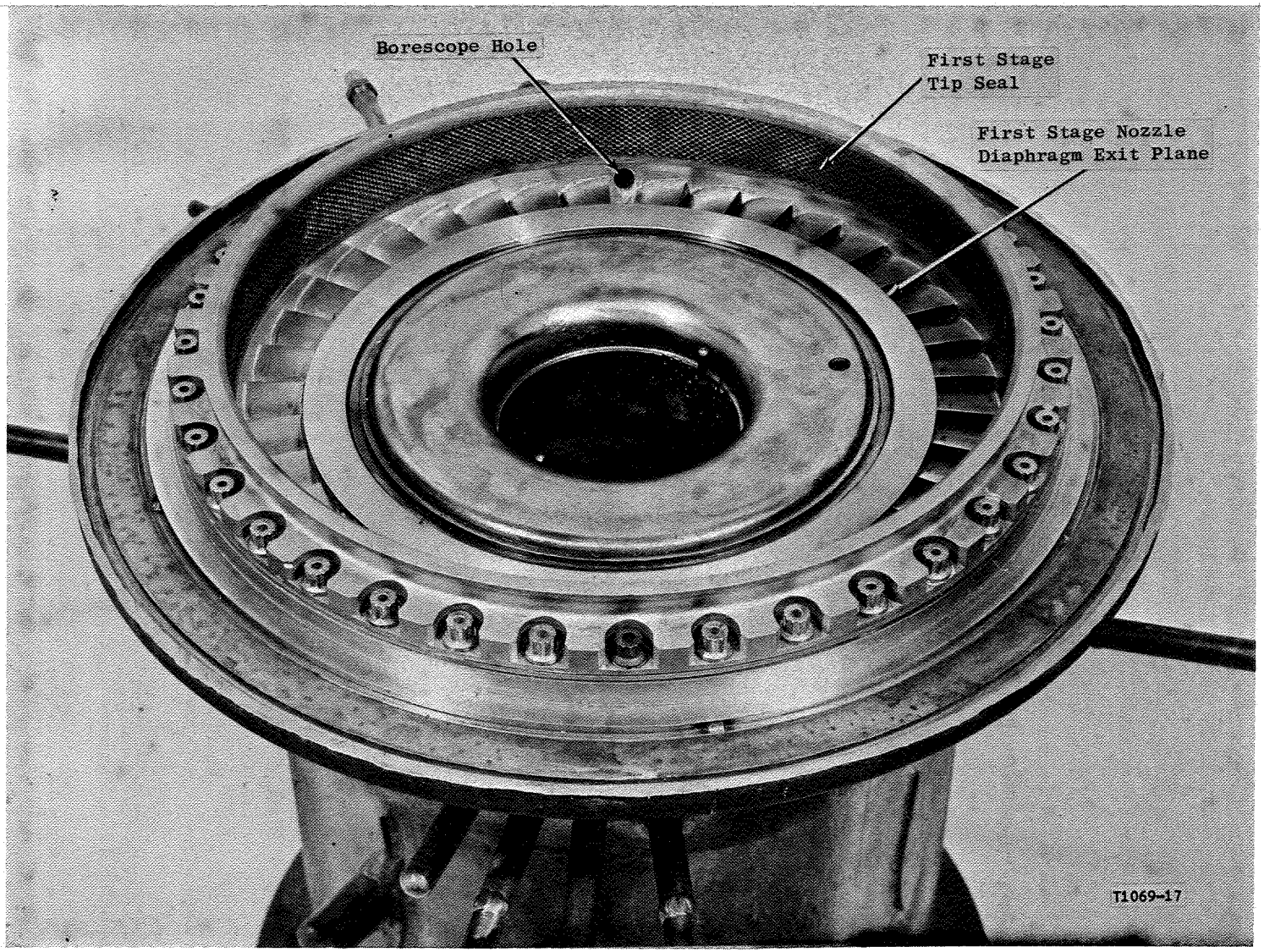
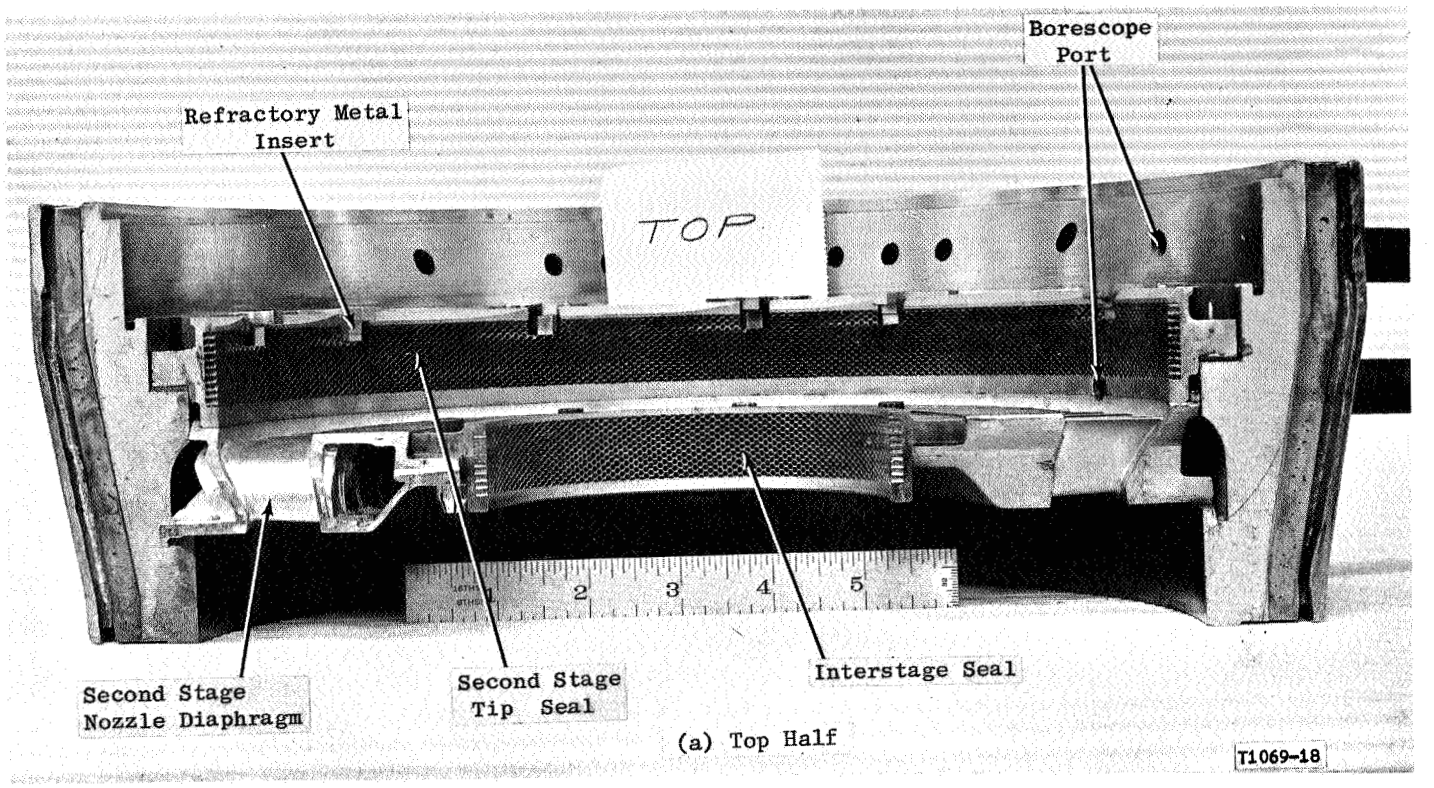


Figure 14. Inlet Duct Assembly.



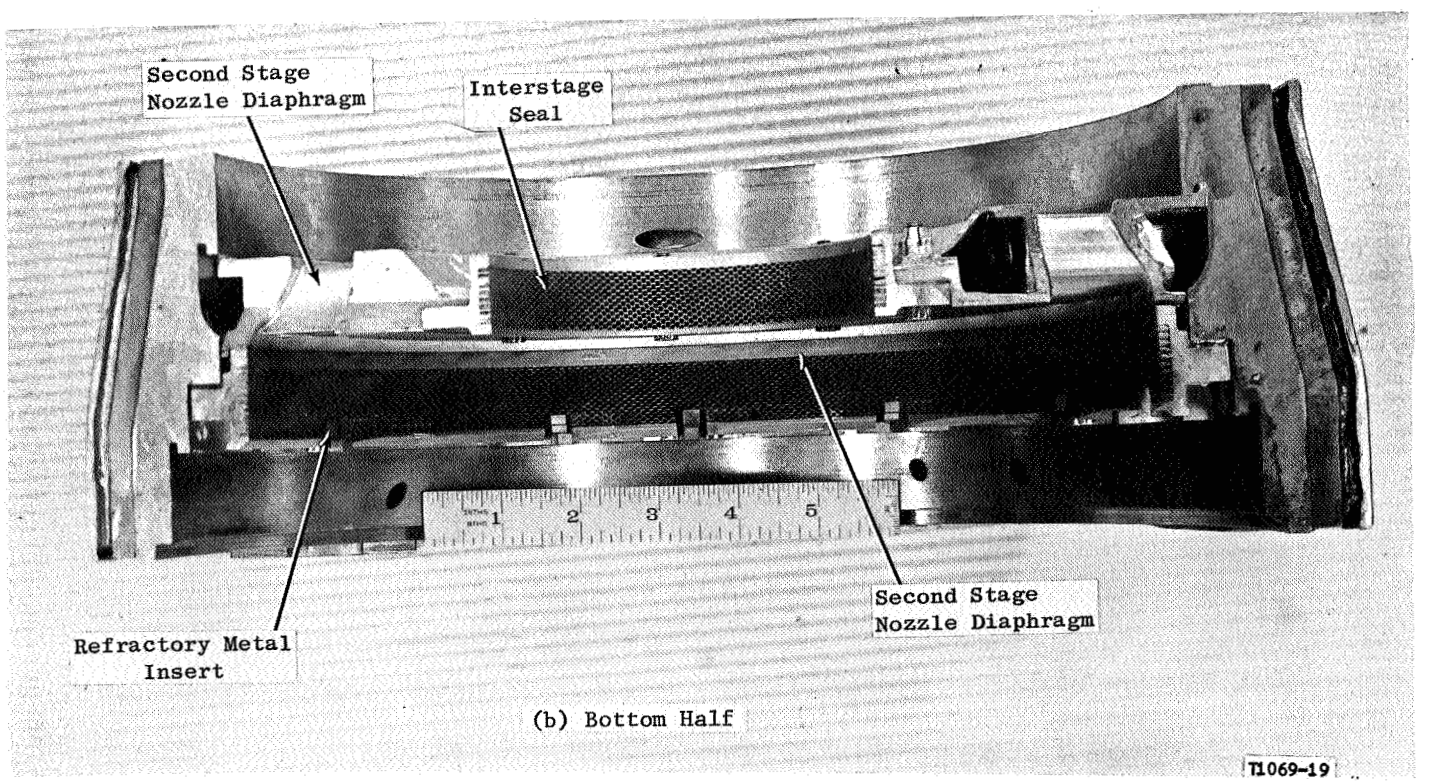


Figure 15. Turbine Casing Assembly.

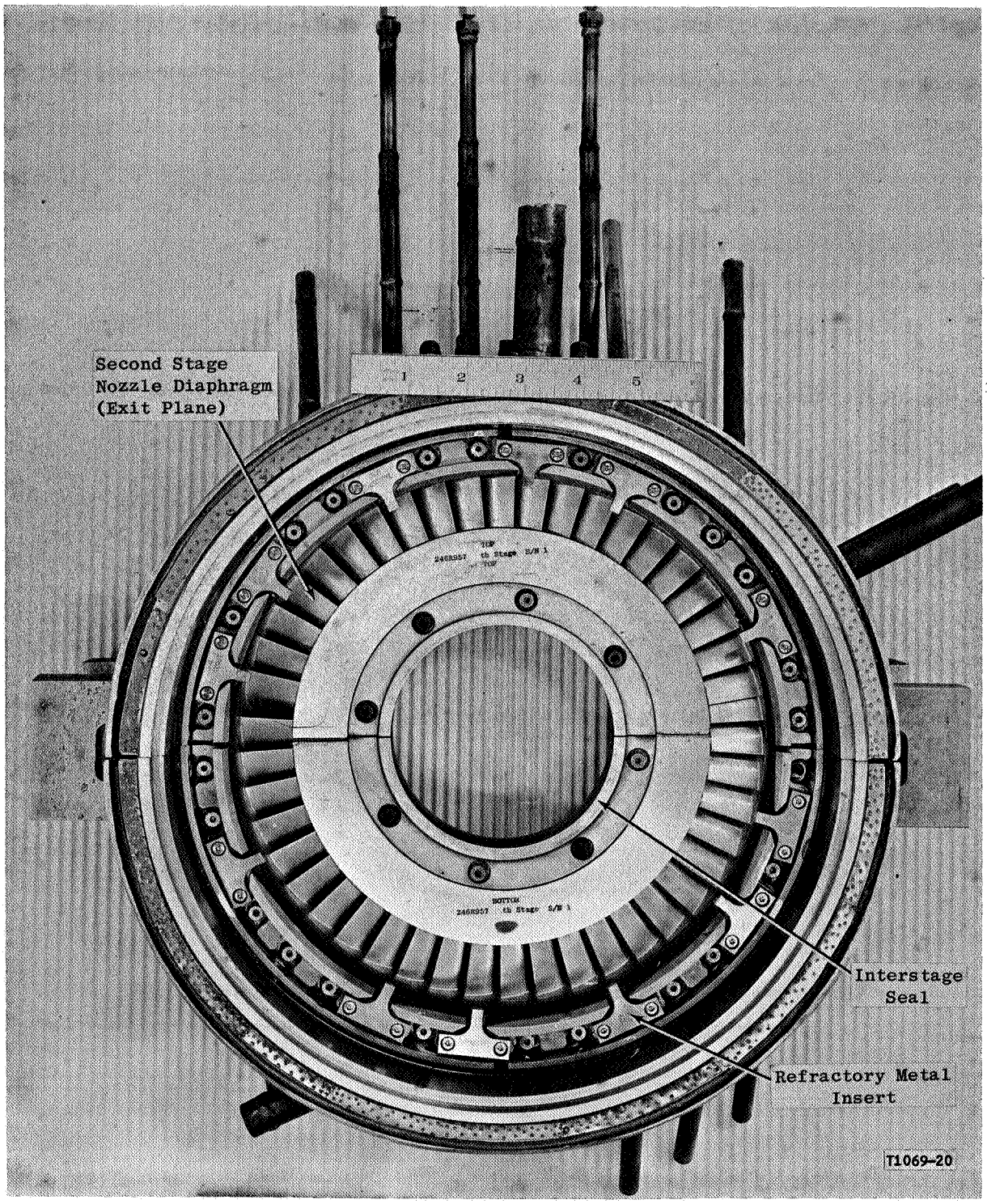


Figure 16. Turbine Casing Assembly.

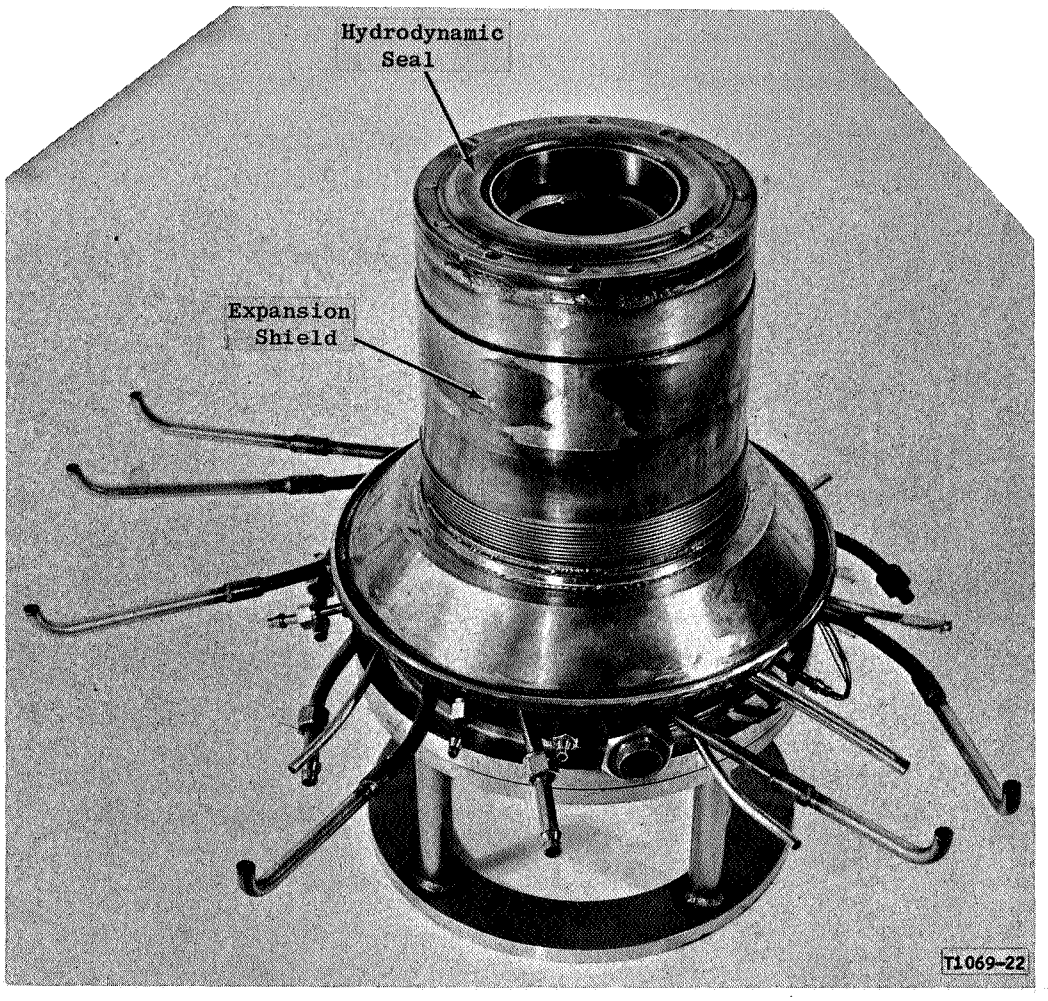


Figure 17. Bearing Housing.

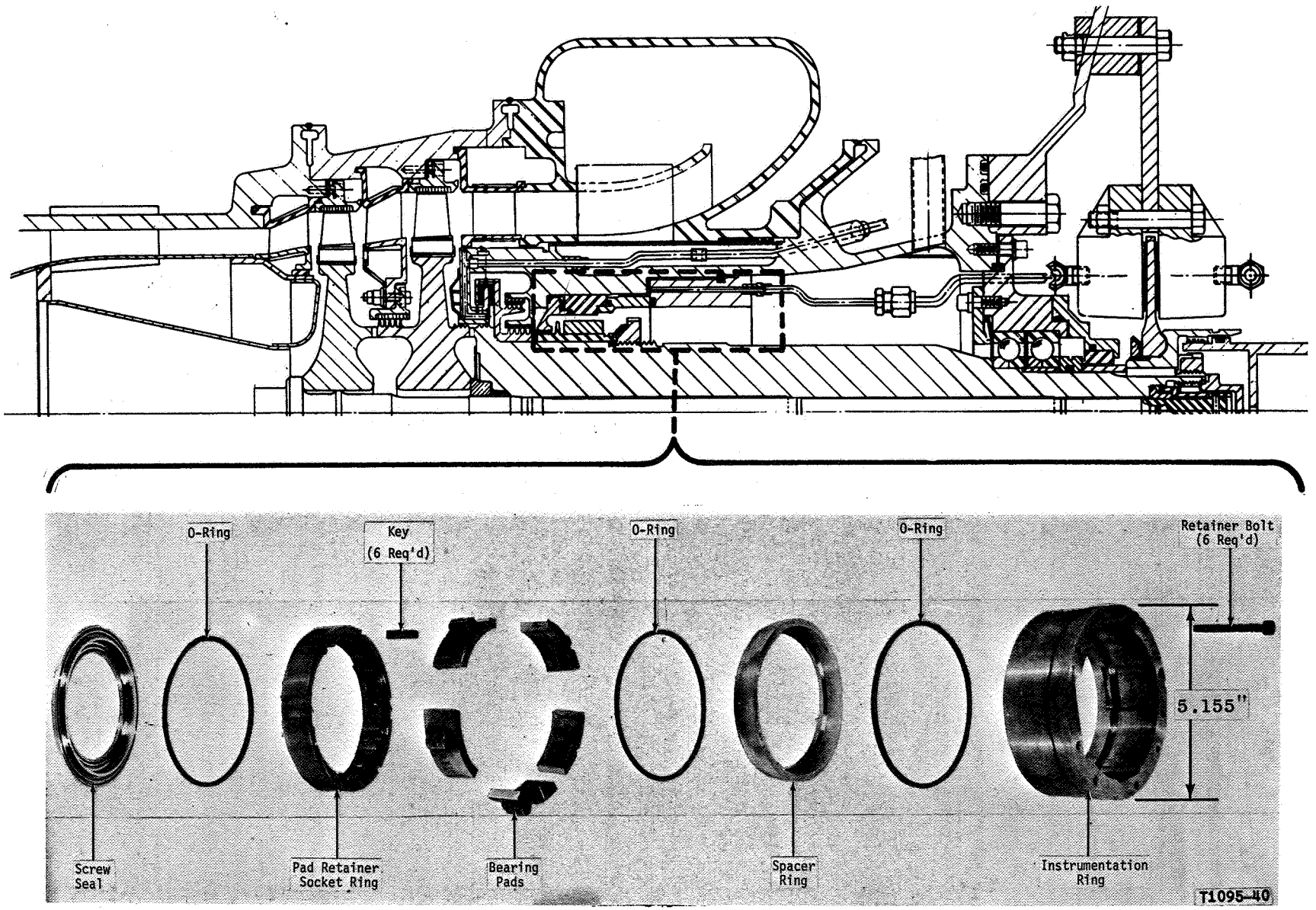


Figure 18. Pad Bearing Assembly.

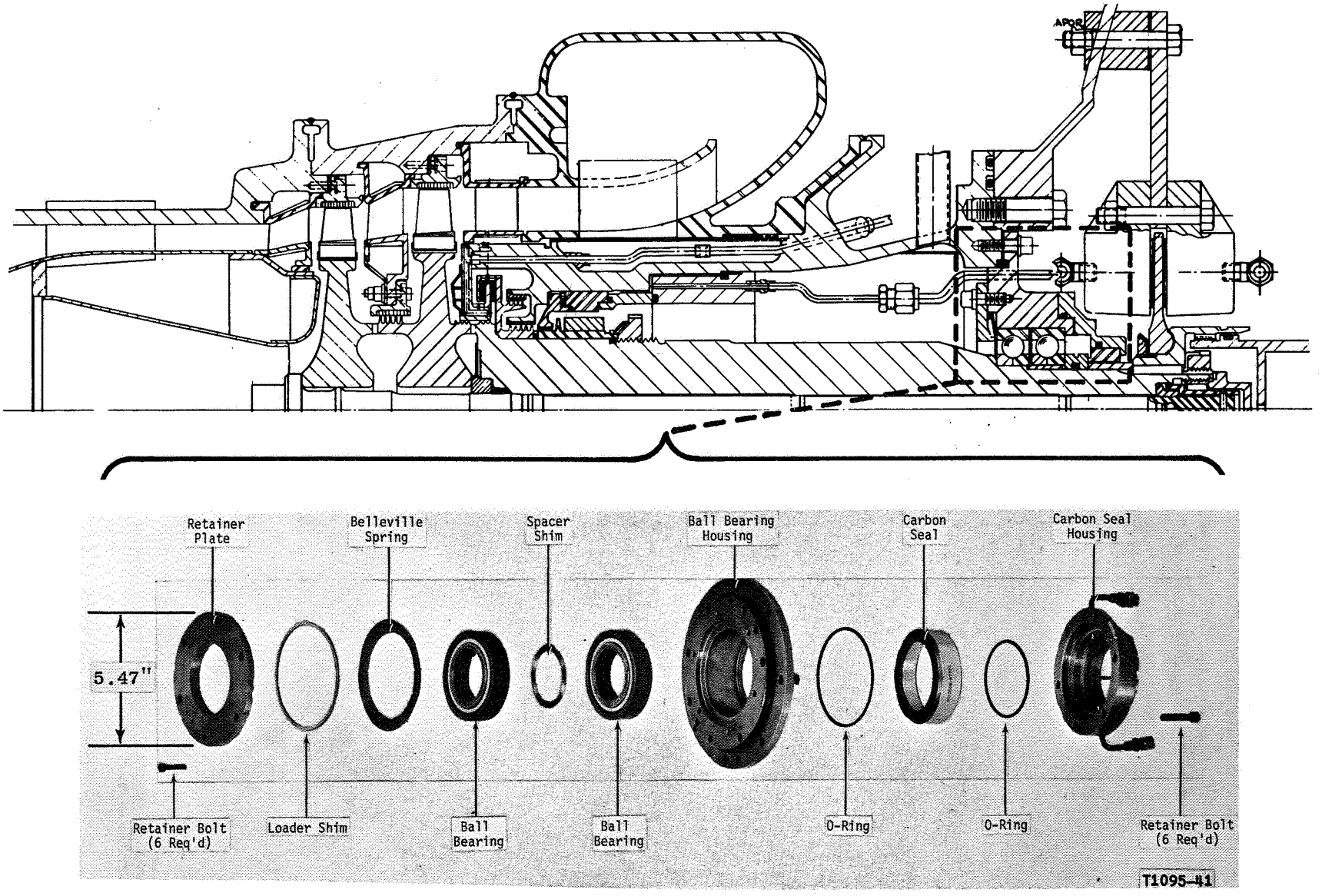


Figure 19. Ball Thrust Bearing Assembly.

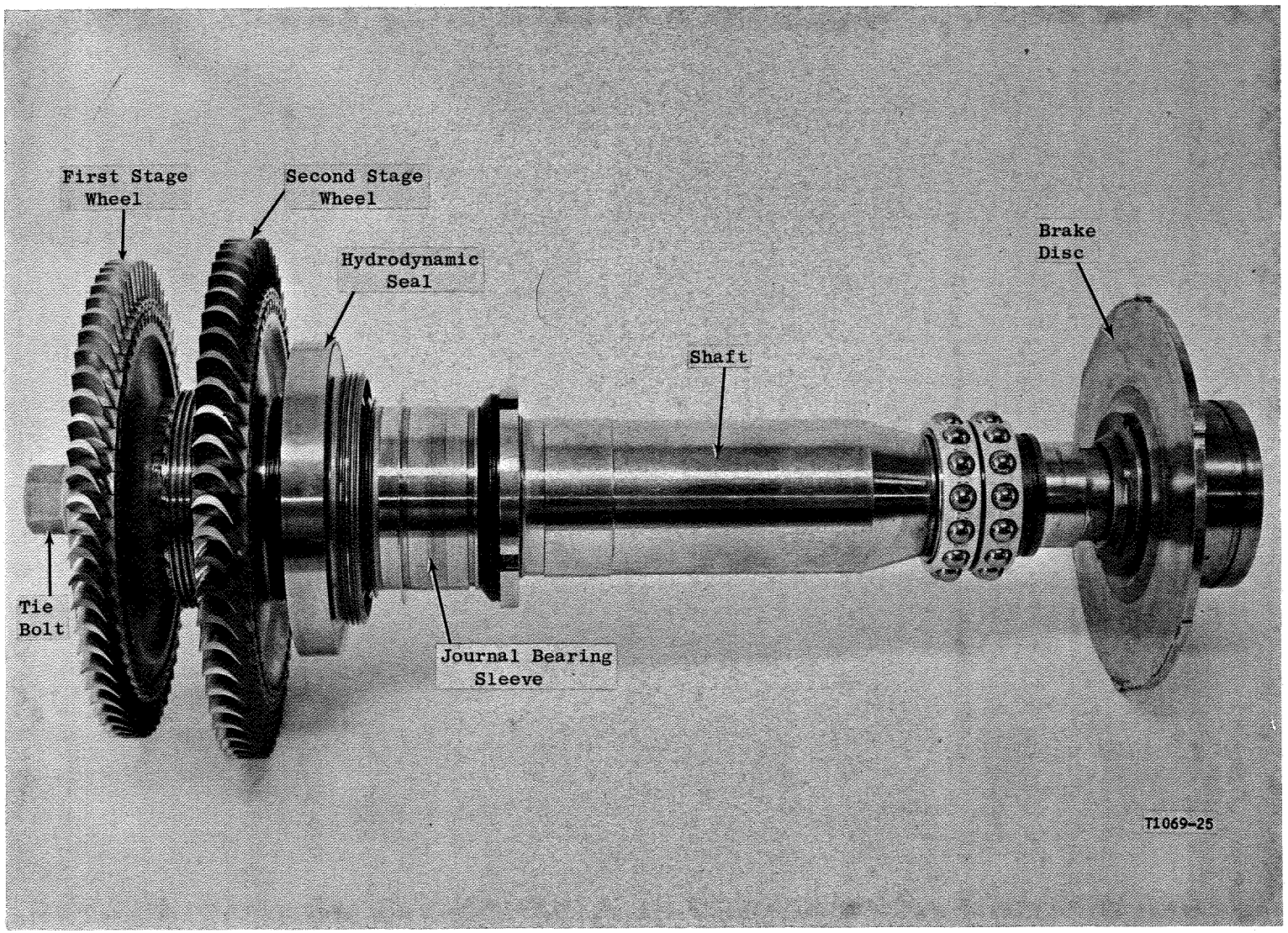


Figure 20. Turbine Rotor Assembly.

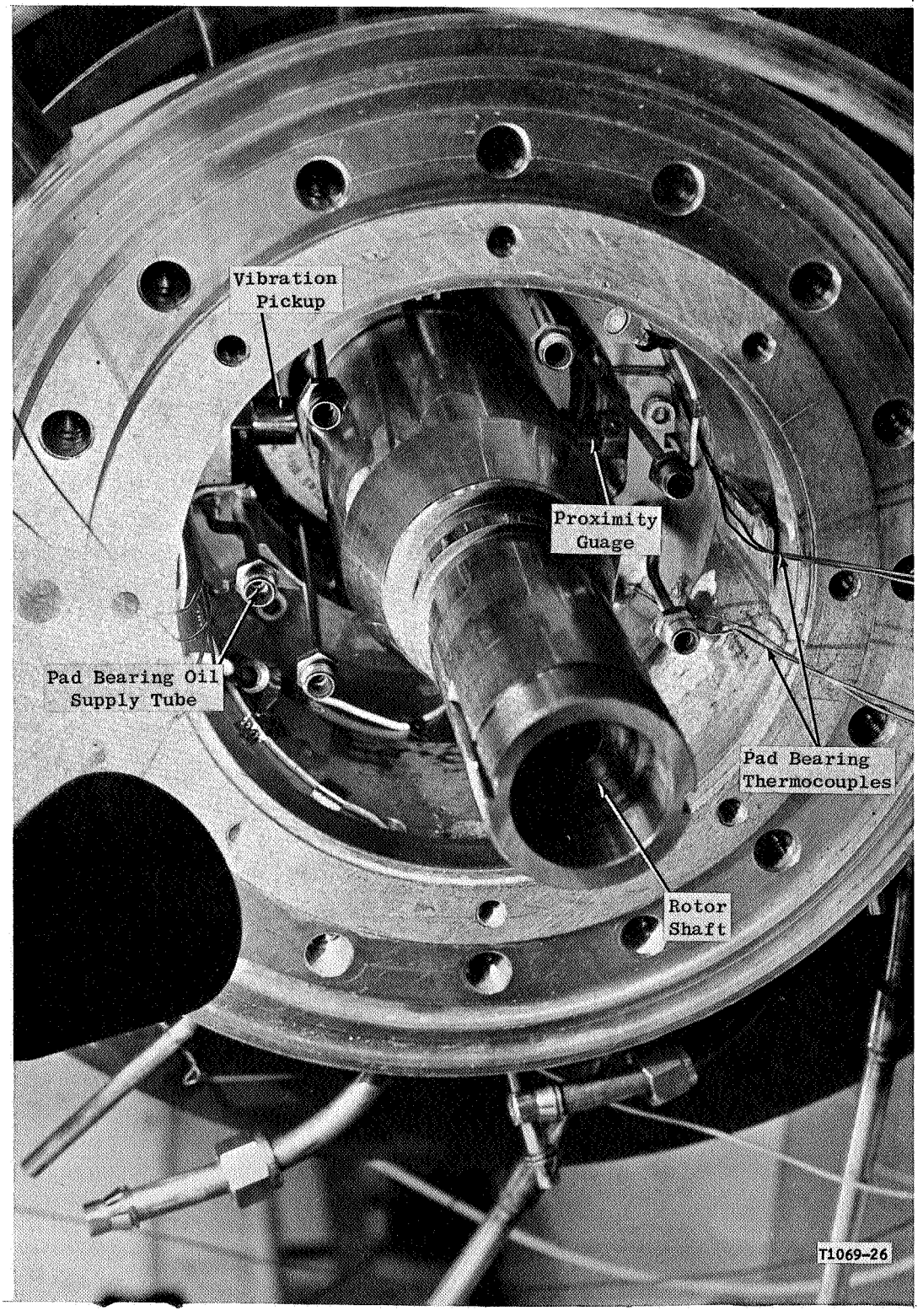
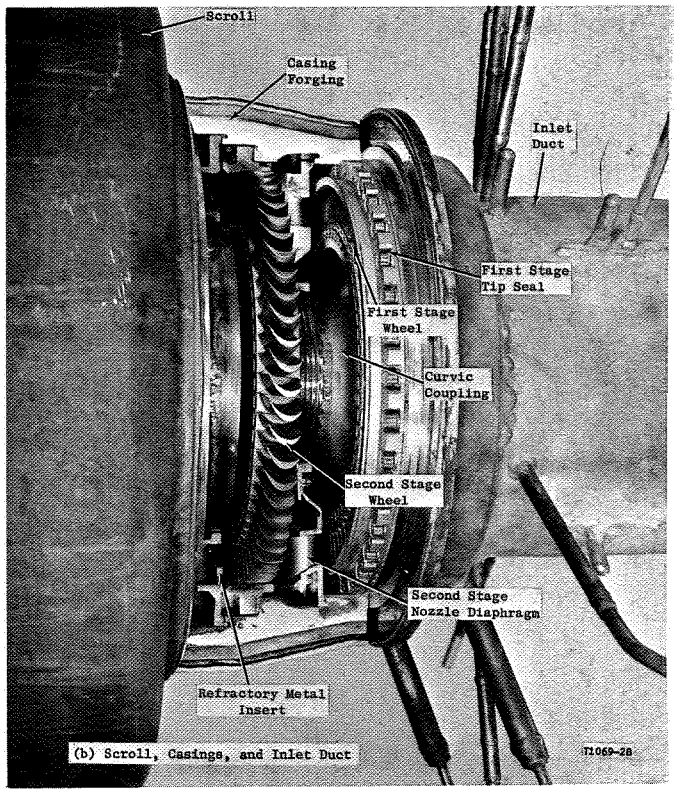


Figure 21. Bearing Housing Bore.



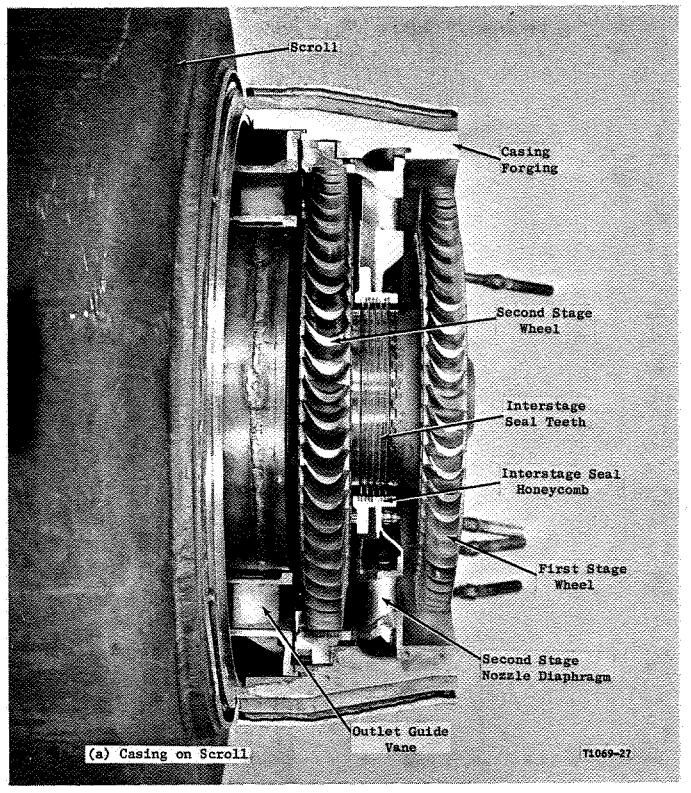
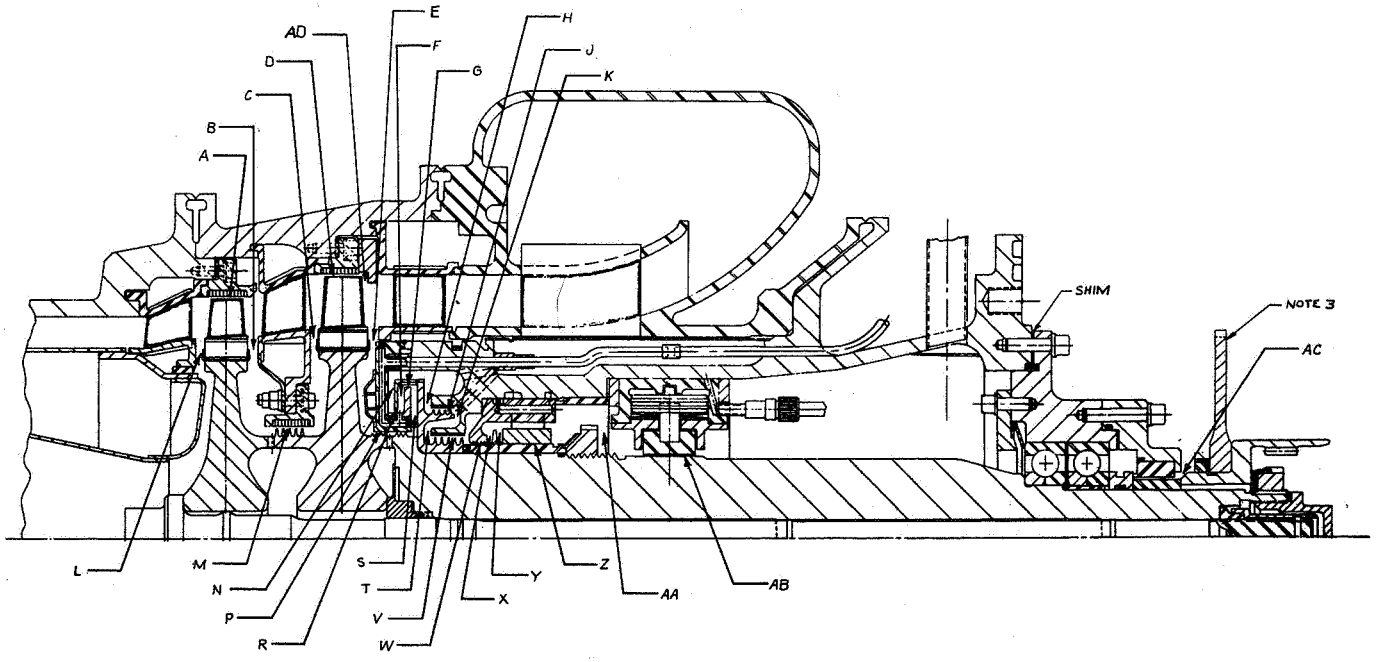


Figure 22. Trial Assembly of Sub-Assembled Turbine Components For Observation and Measurement of Critical Fits and Clearances.



BUILD-UP NO.	CLEARANCE DIMENSIONS																										
	A RAD	B	C	D RAD	E	F	G	H	J	K	L	M	N	P	R	S	T	V	W	X	Y	Z	AA	AB	AC	SHIM THK	AD
8 COLD	.021 MIN	.189	.101	.028 MIN	.174	.128	.026	.135	.016	.124	.144	.027	.050	.017	.070	.054	.127	.014	.013	.081	.095	.0052	—	—	.100	.031	.163
8 HOT	.037 MIN	.109	.181	.044 MIN	.174	.128	.026	.135	.016	.124	.222	.042	.050	.017	.070	.054	.127	.014	.013	.081	.095	.0052	—	—	.100	—	.087

T5433-23

Figure 23. Clearance Dimensions for Potassium Test Turbine.

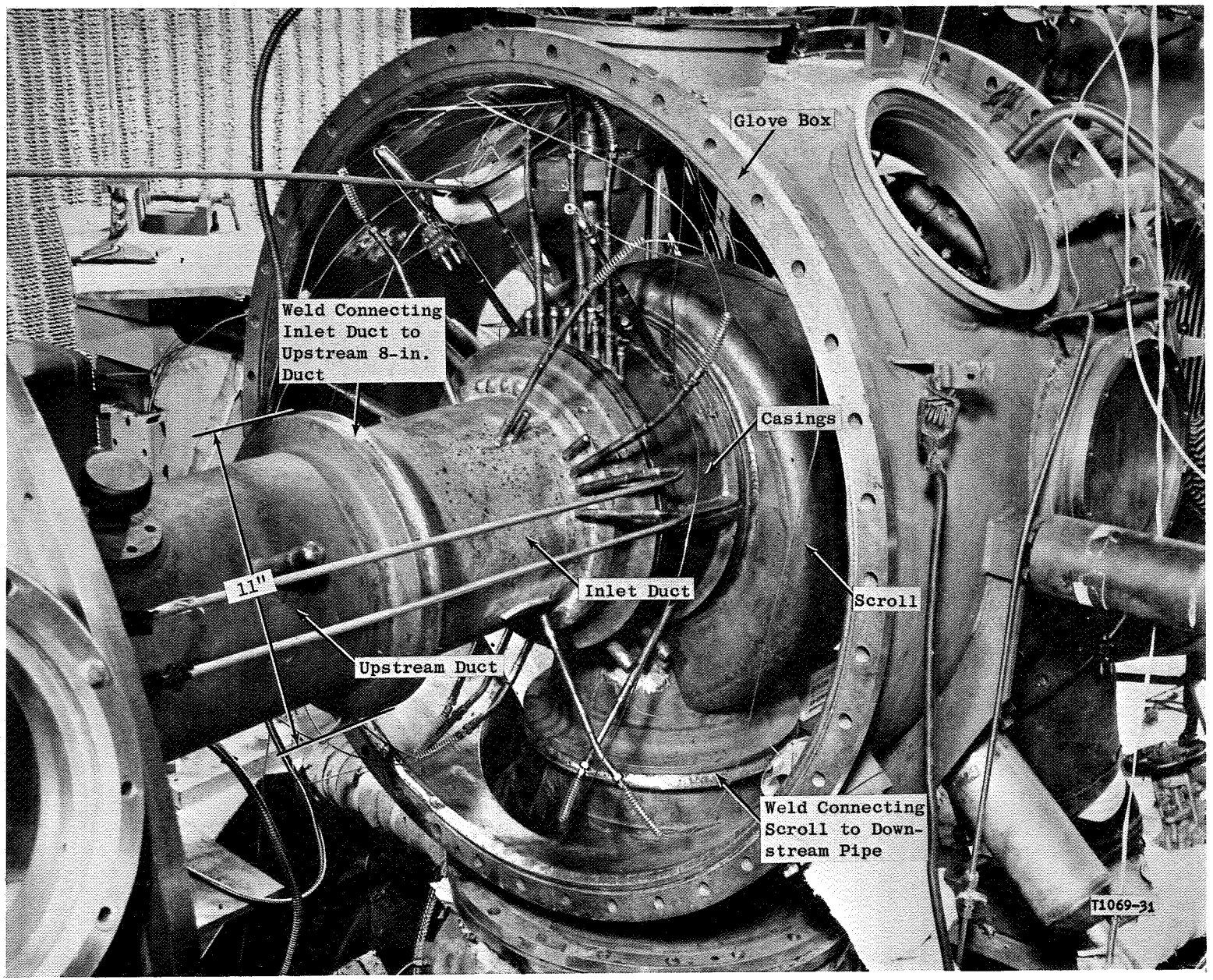


Figure 24. Forward View of Installed Turbine.

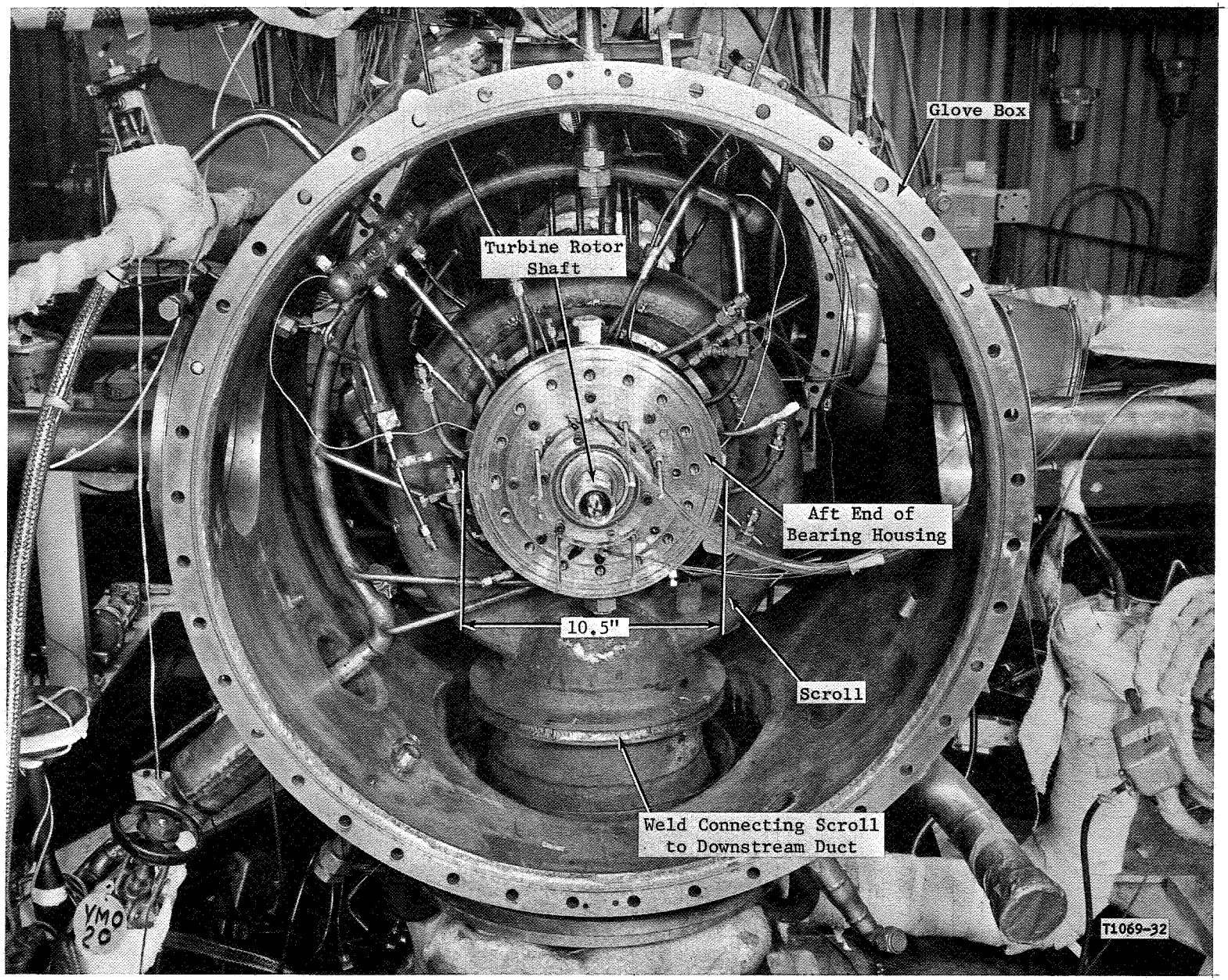


Figure 25. Aft View of Installed Turbine.

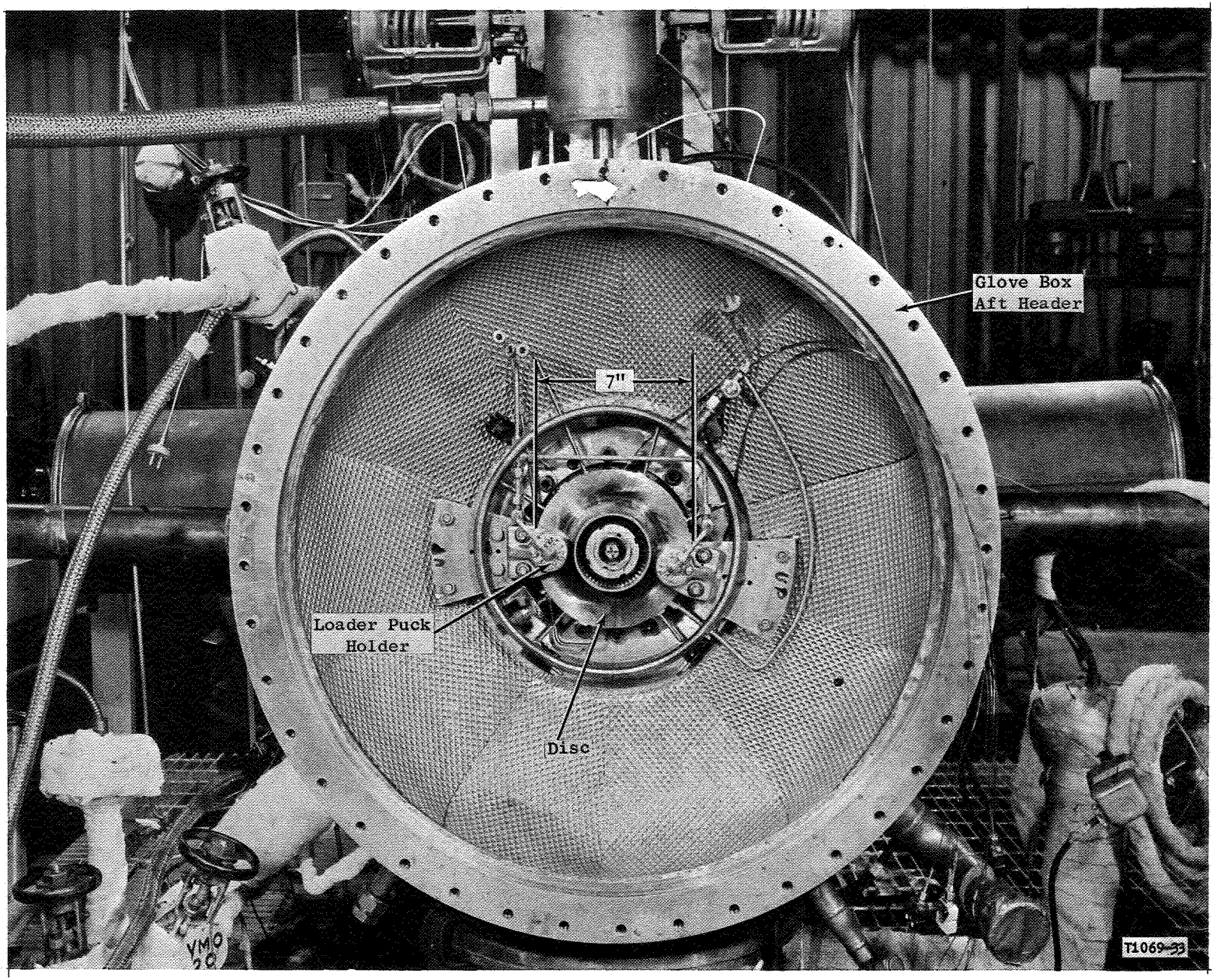


Figure 26. Aft View of Turbine.

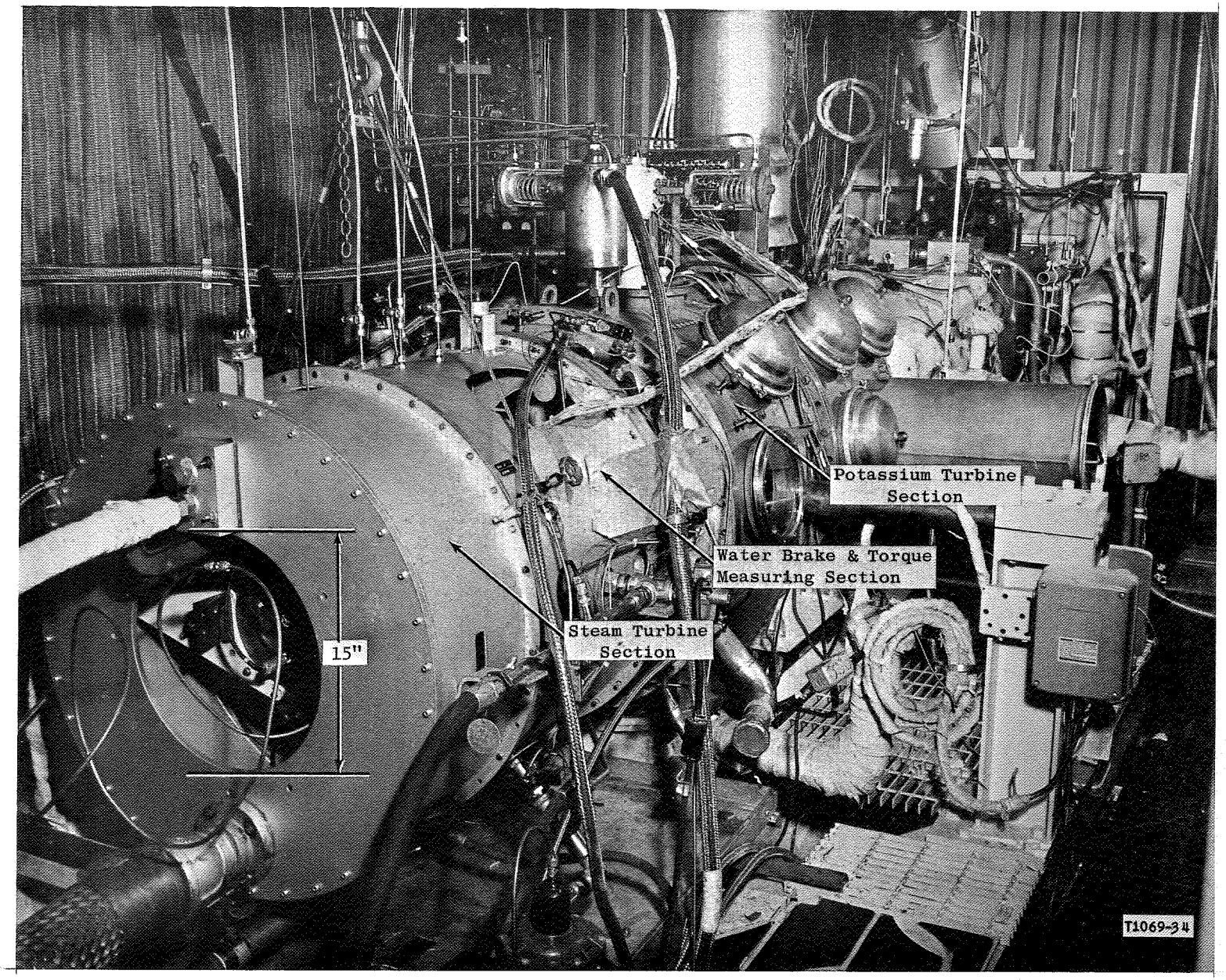


Figure 27. Turbine Test Assembly.

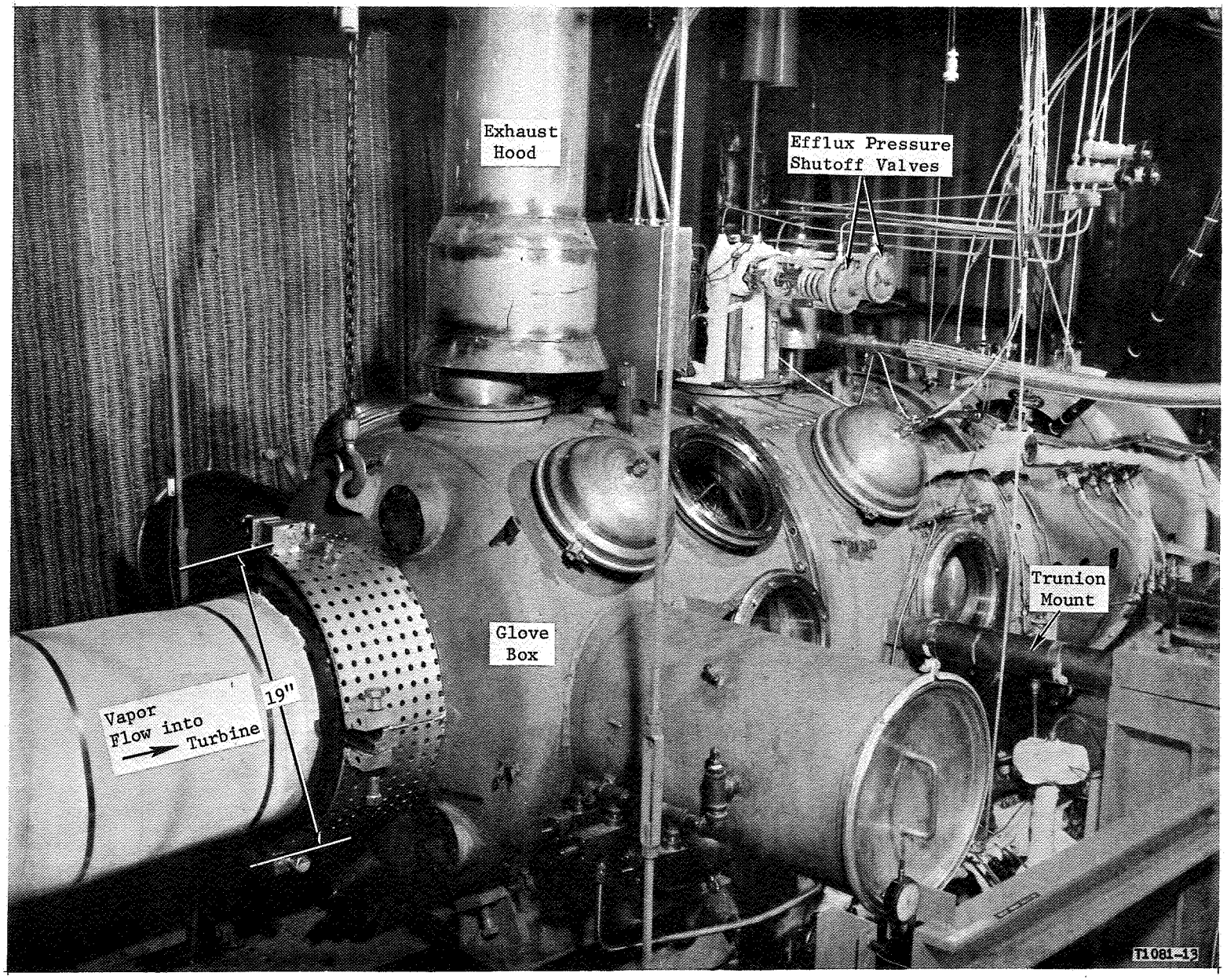
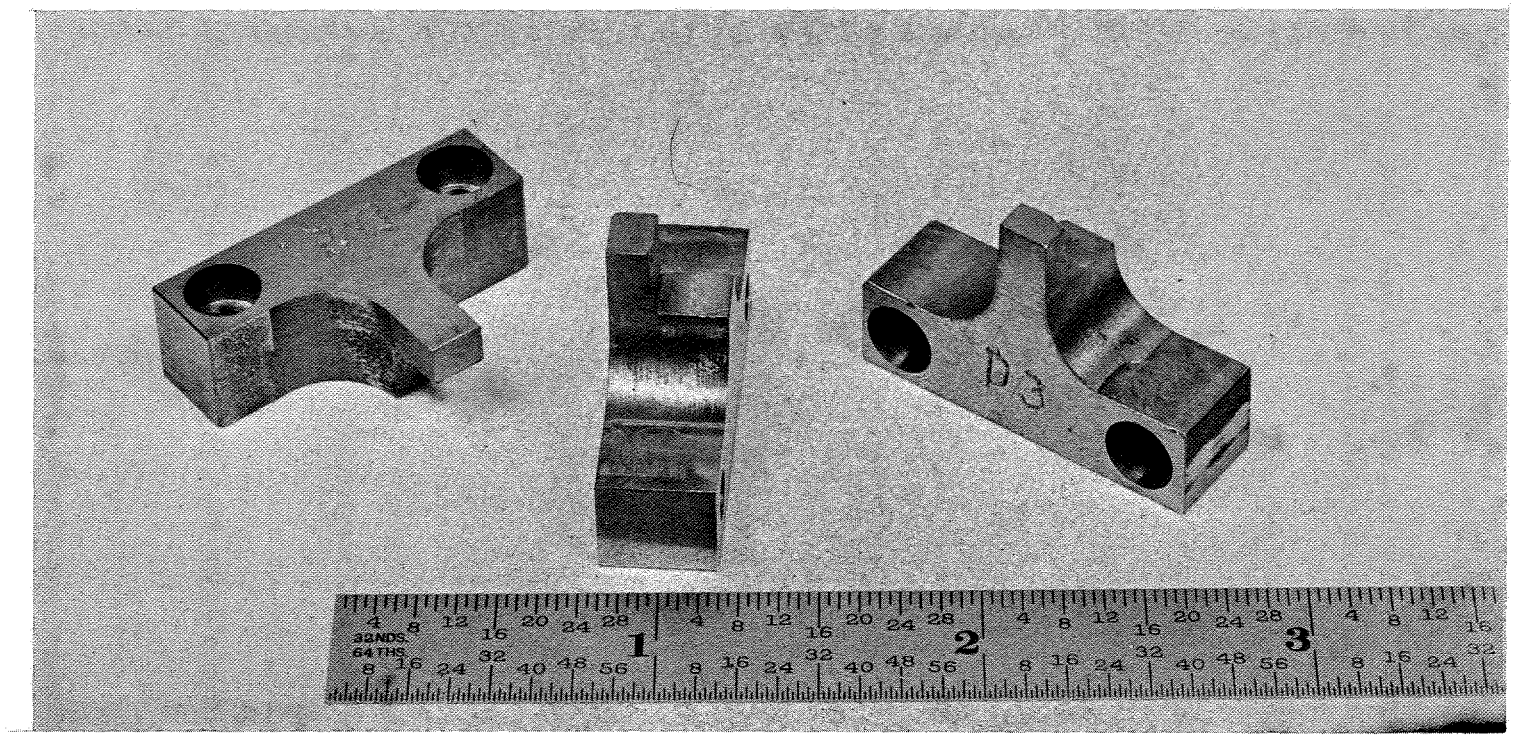
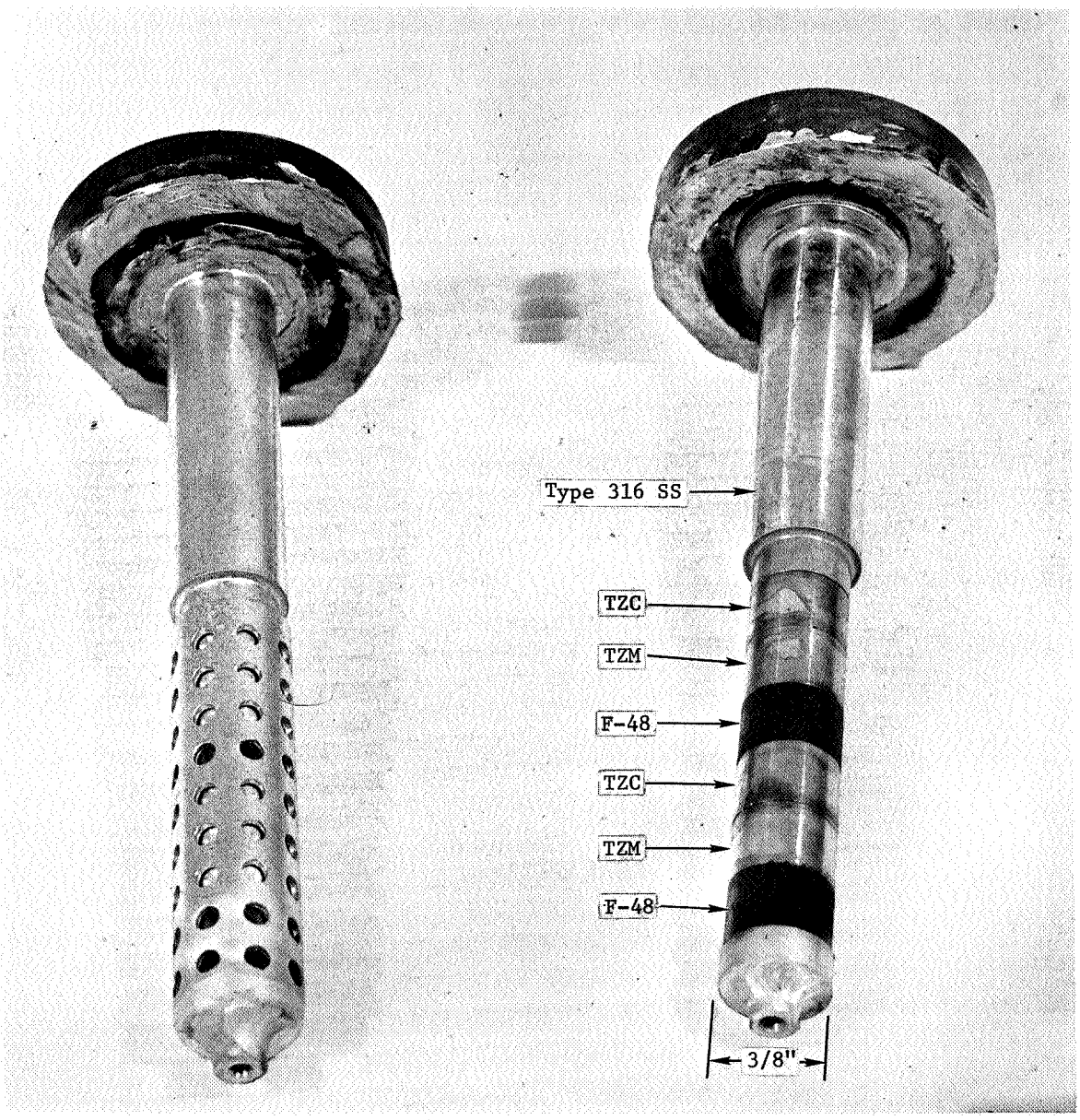


Figure 28. Turbine and Load Train Assembly (South View).



T5433-29

Figure 29. Molybdenum Alloy TZC Erosion Inserts Before Installation for 2000-Hour Endurance Test. (C65082408)



T5433-30

Figure 30. Refractory Alloy Specimen Probes From Station One, Left, and Condenser, Right (Note Darkening of F-48 Specimens). Mag: 1X

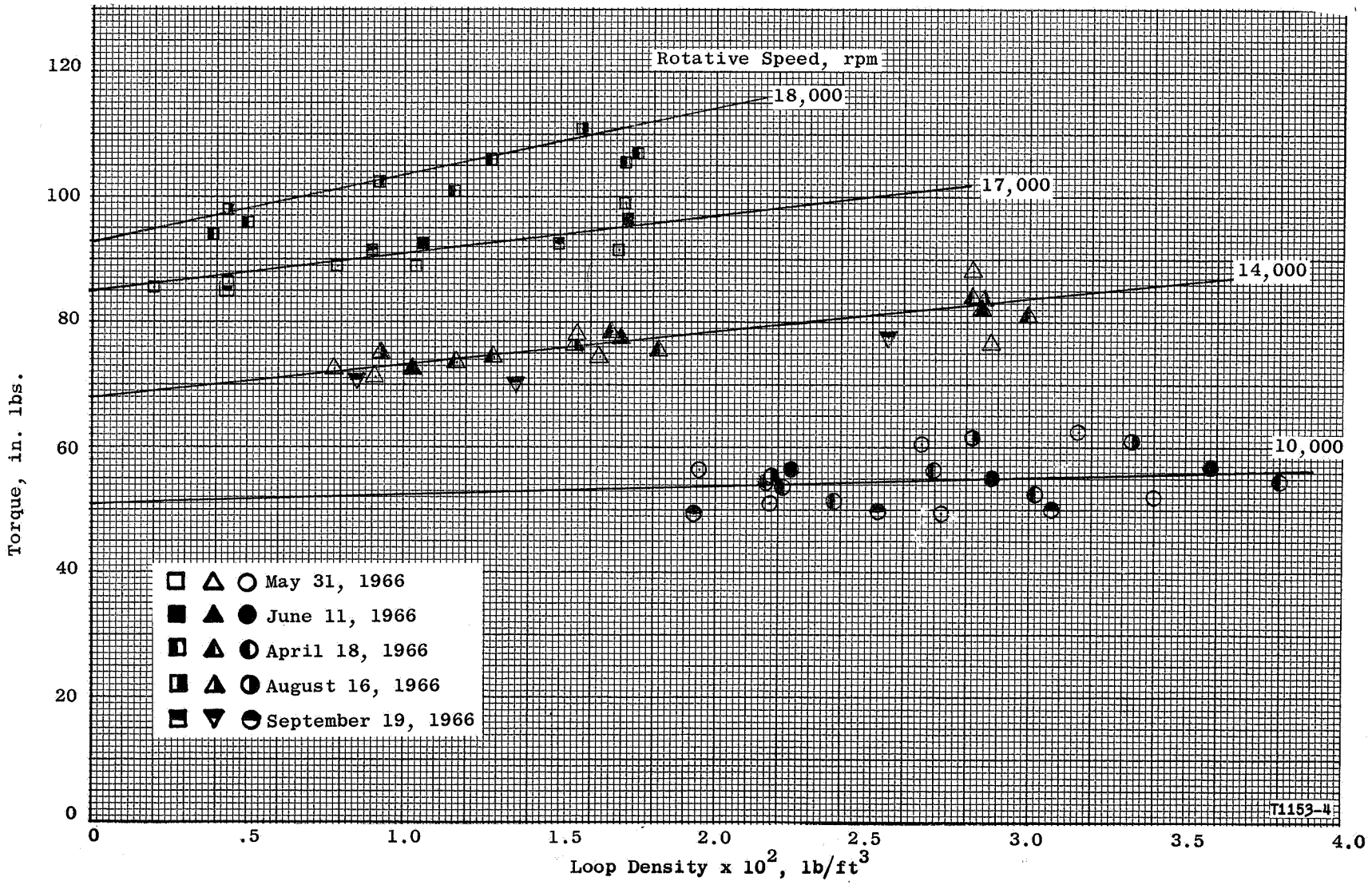


Figure 31. Comparison of Parasitic Torque For All Parasitic Torque Tests During 3000-Hour Endurance Test.

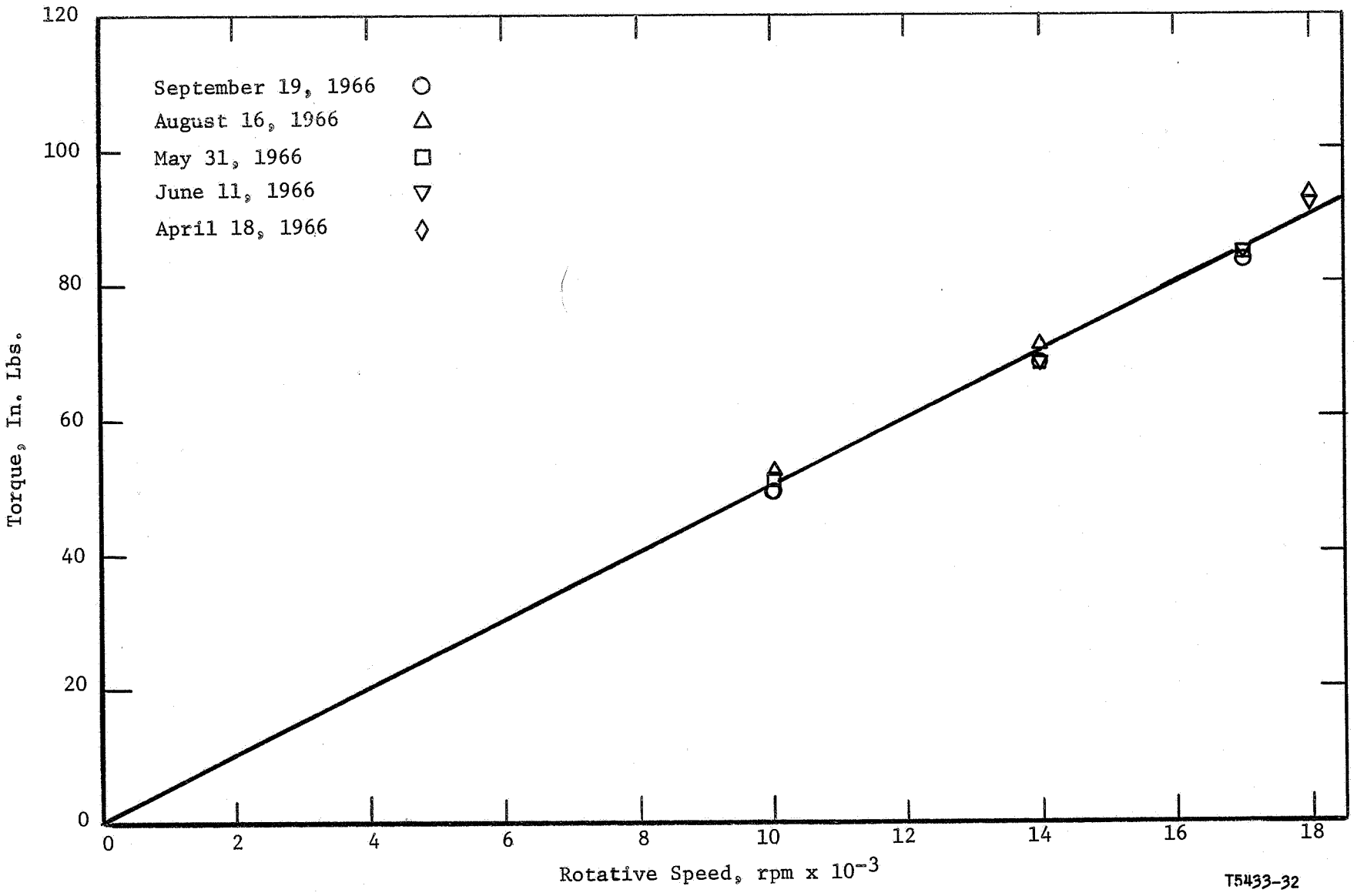
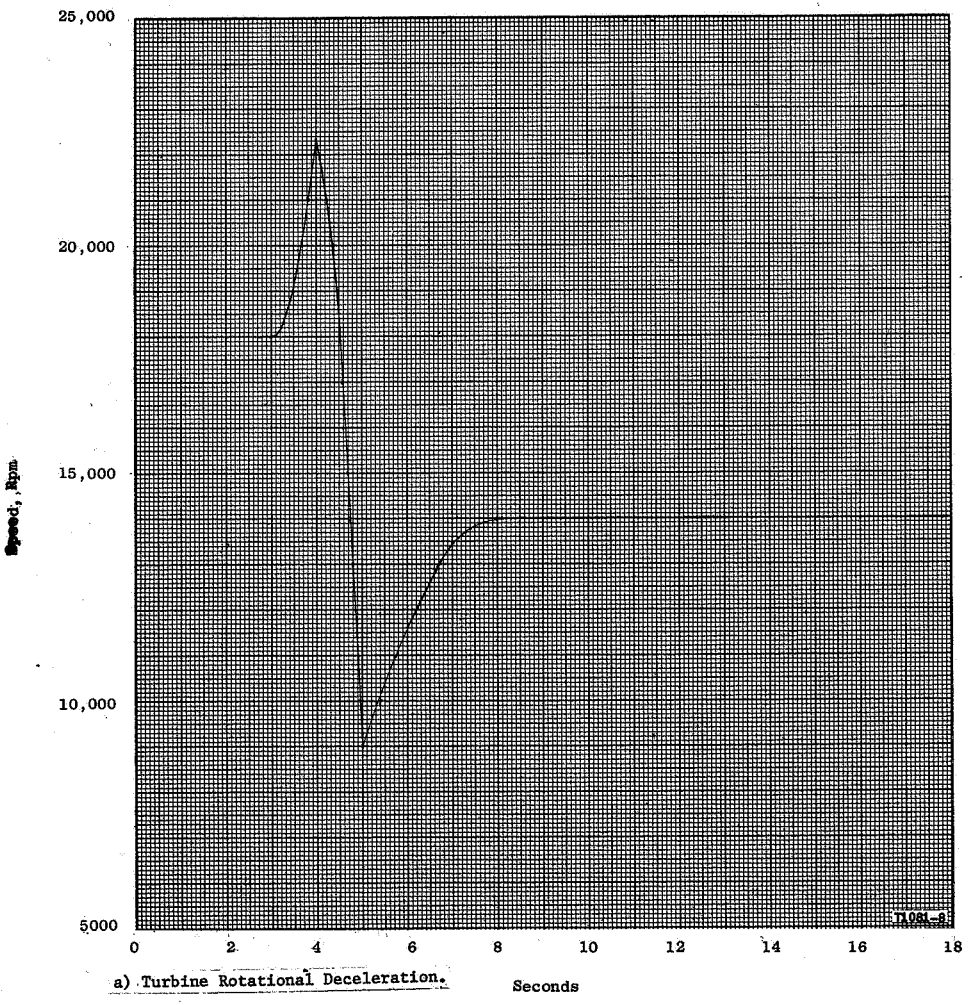
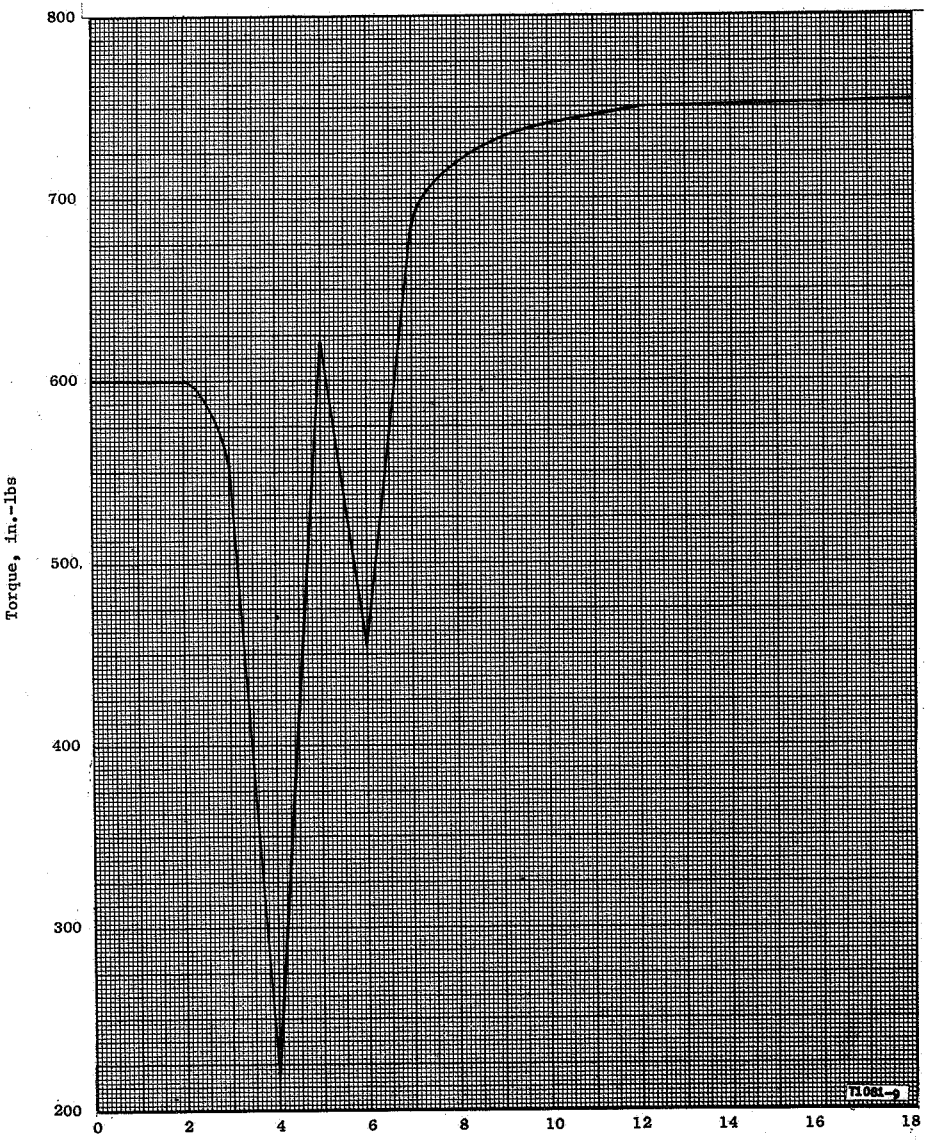


Figure 32. Parasitic Torque as a Function of Rotative Speed.



a) Turbine Rotational Deceleration.



b) Water Brake Torque.

Figure 33. Application of Disc Brake on 5/19/66.

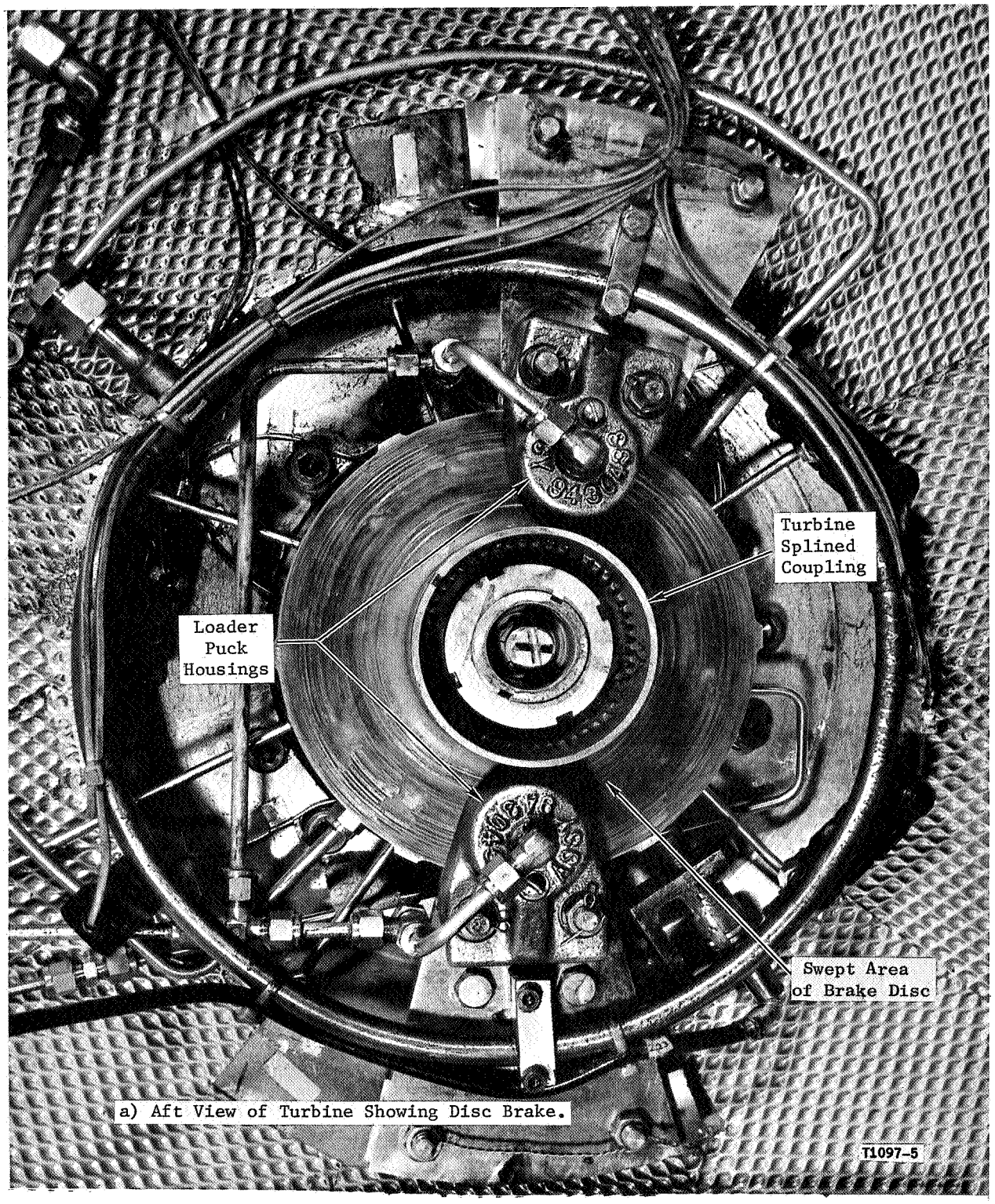


Figure 34a. Turbine Disc Brake.

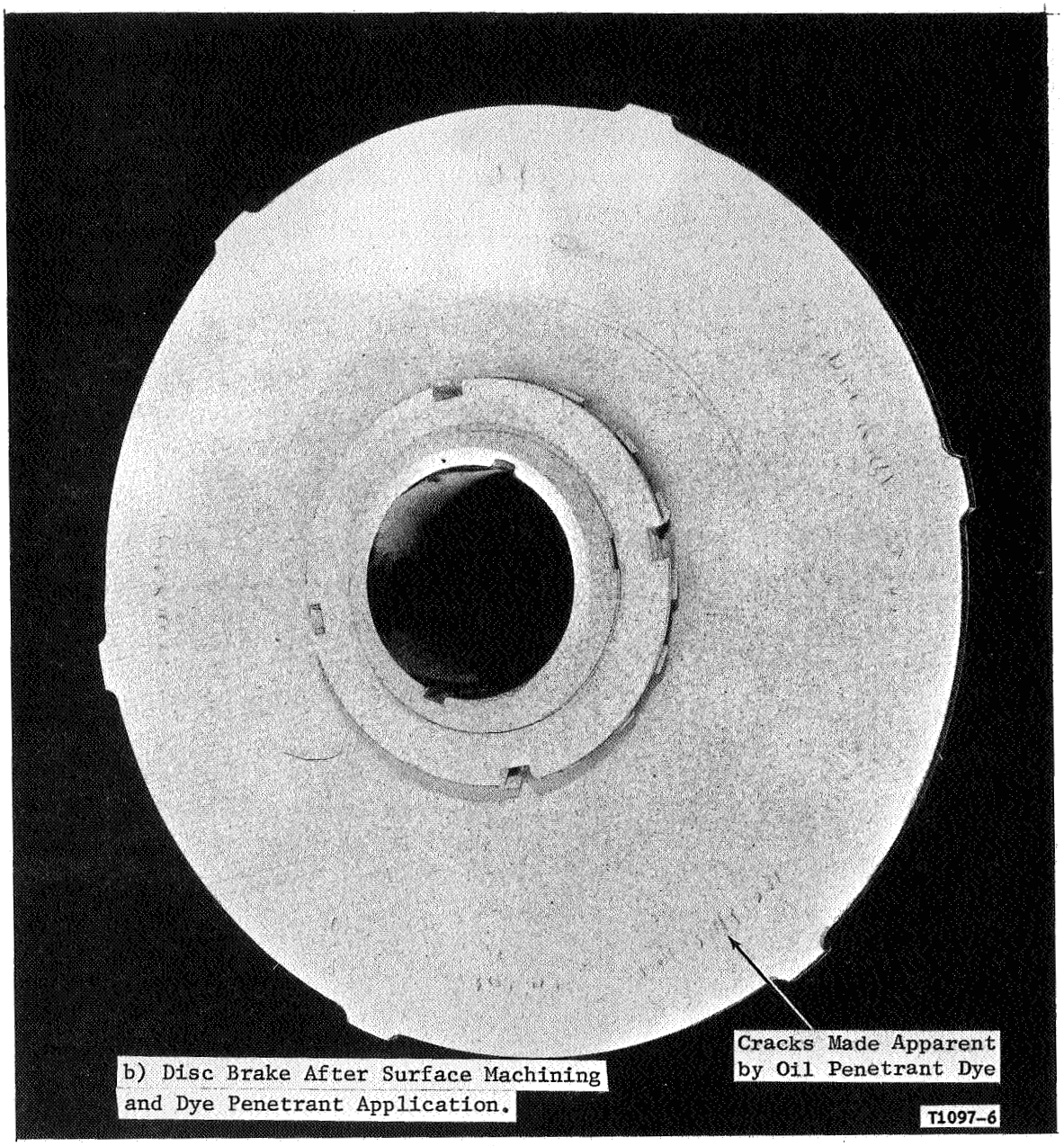


Figure 34b. Turbine Disc Brake.

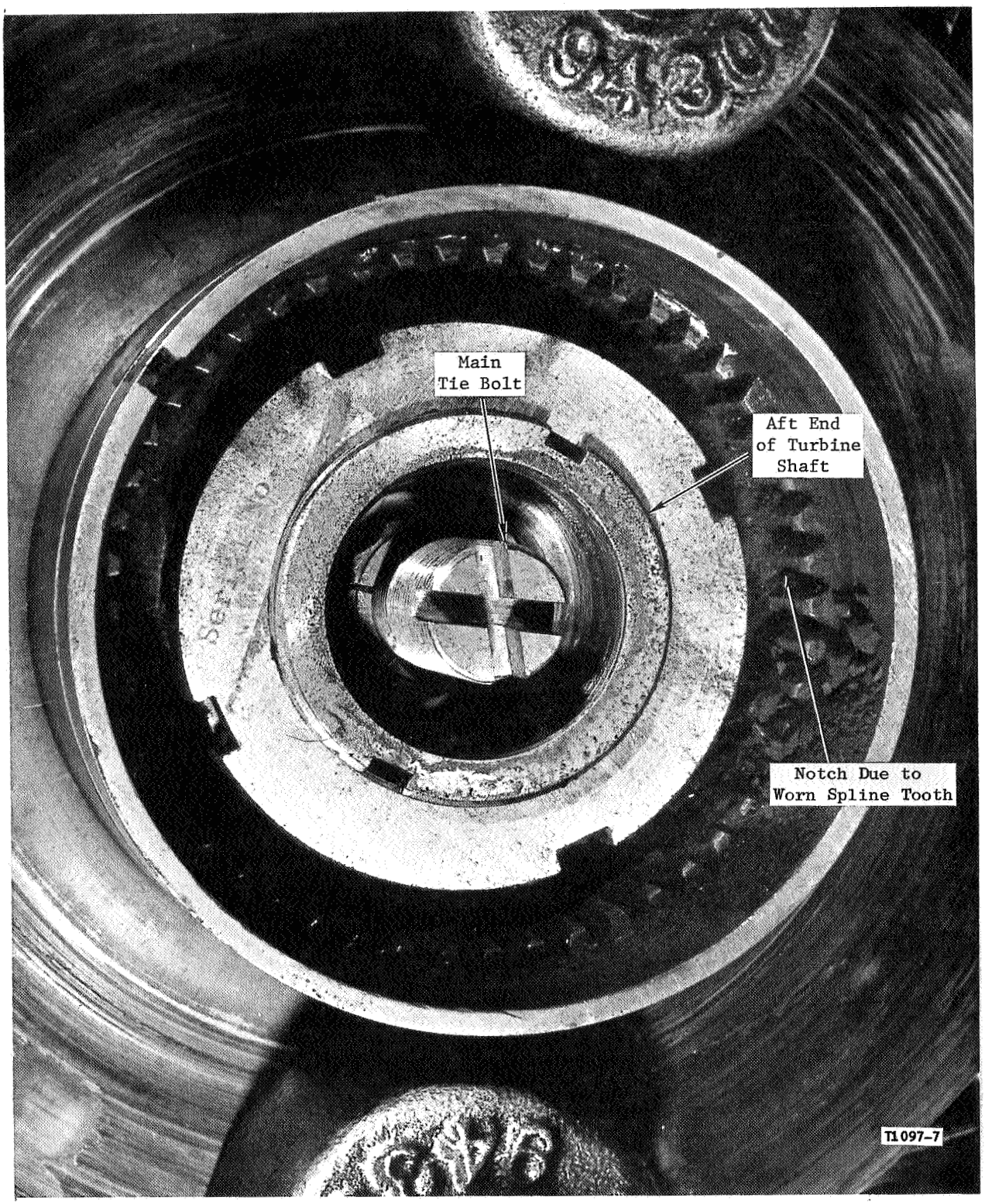


Figure 35. Spline Coupling, Potassium Turbine End, Showing Tooth Wear.

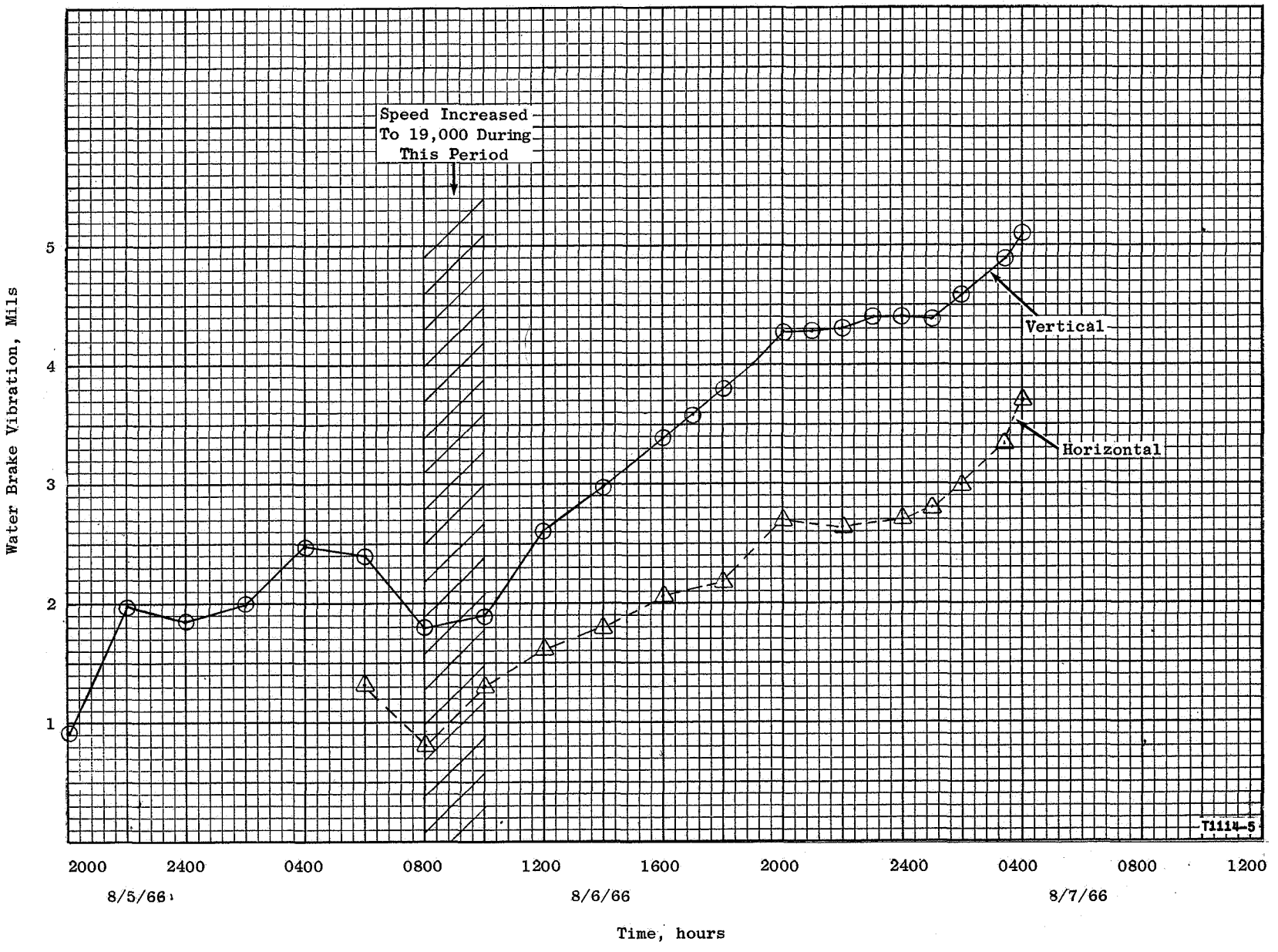


Figure 36. Water Brake Vibration Prior to Shutdown.

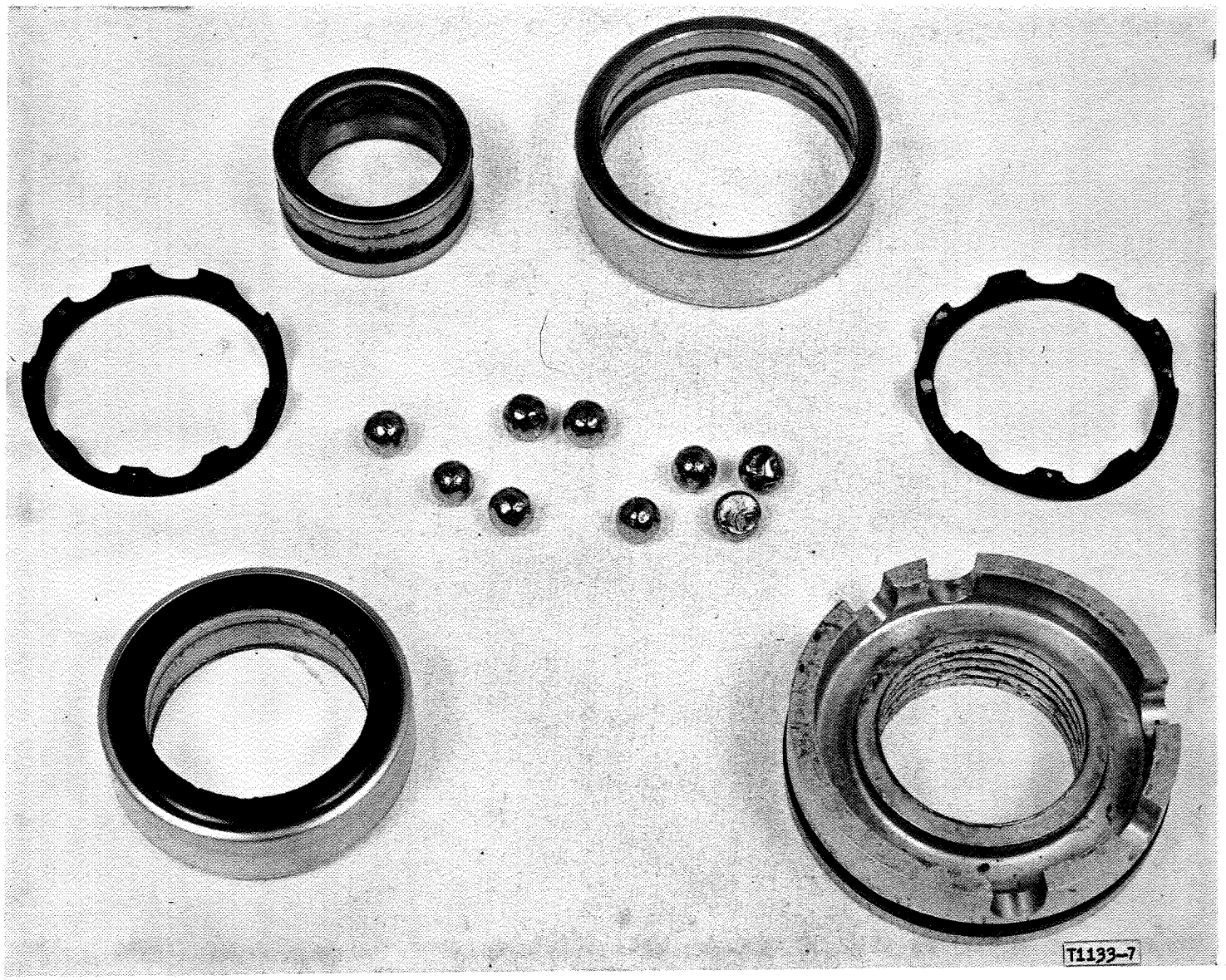


Figure 37. Destroyed Water Brake Front Bearing and Seal Parts.

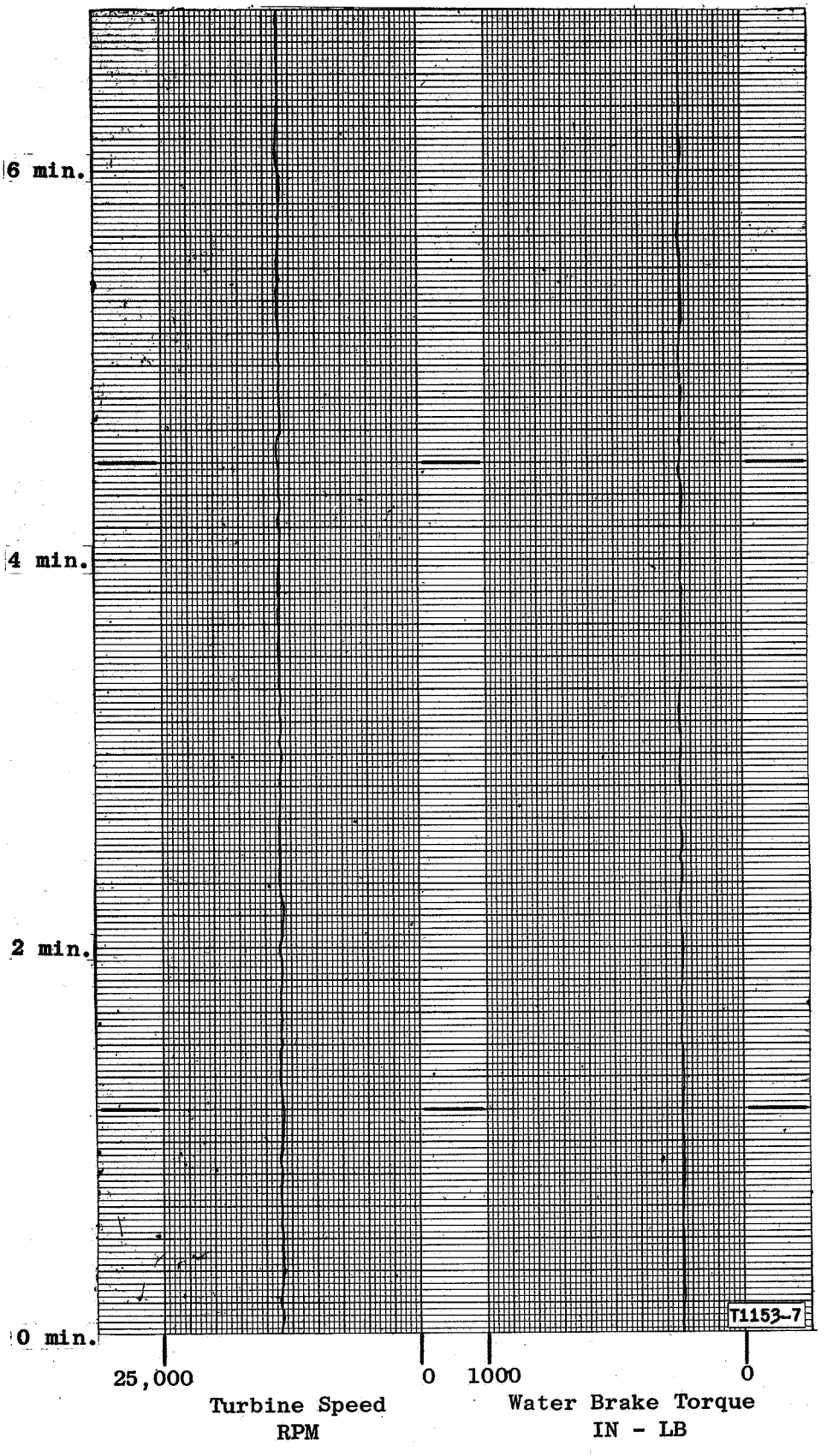
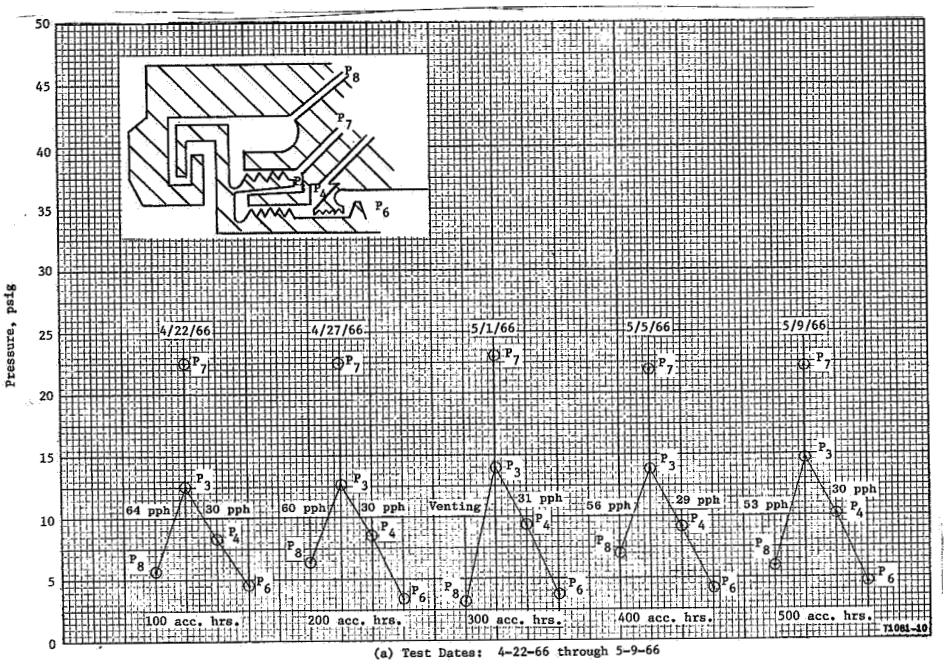
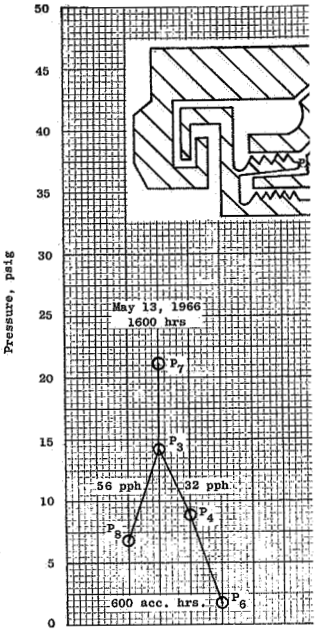
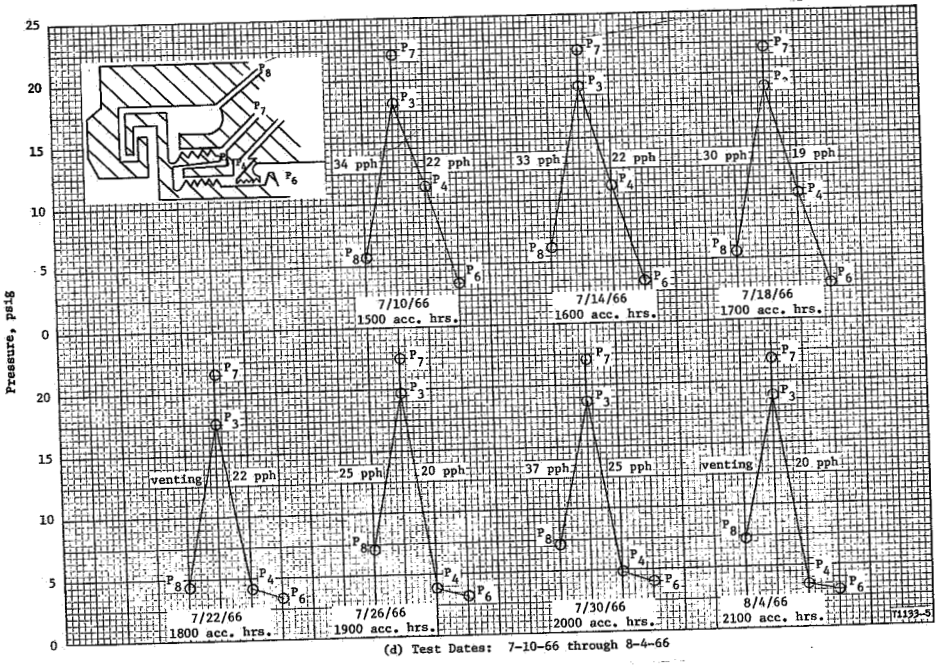


Figure 38. Turbine Speed and Water Brake Torque During 3000 Hour Endurance Test.



(a) Test Dates: 4-22-66 through 5-9-66





(d) Test Dates: 7-10-66 through 8-4-66

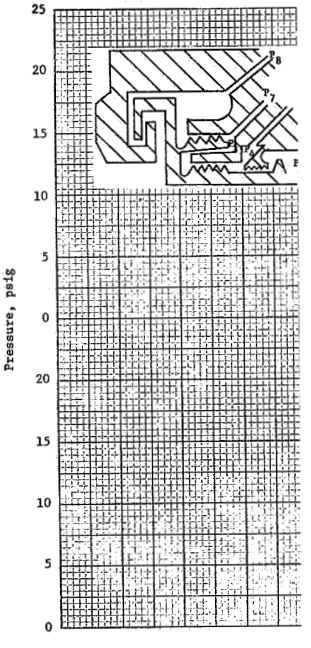
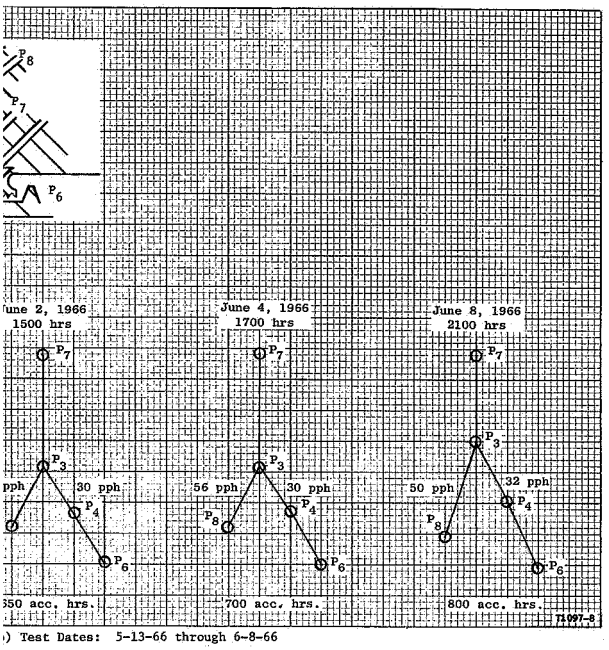


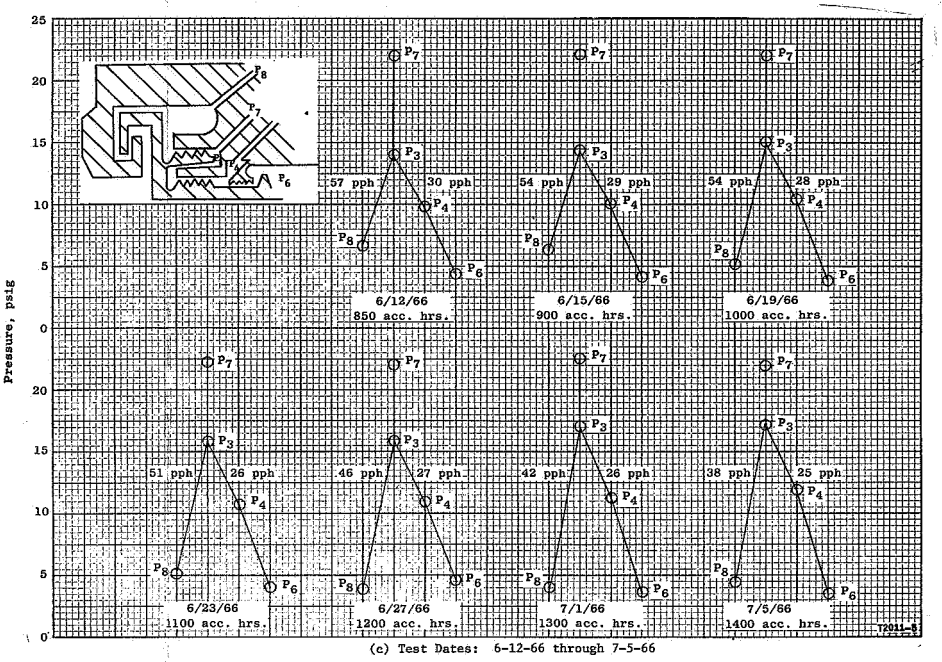
Figure 39. Seal Cavit

FOLDOUT FRAME

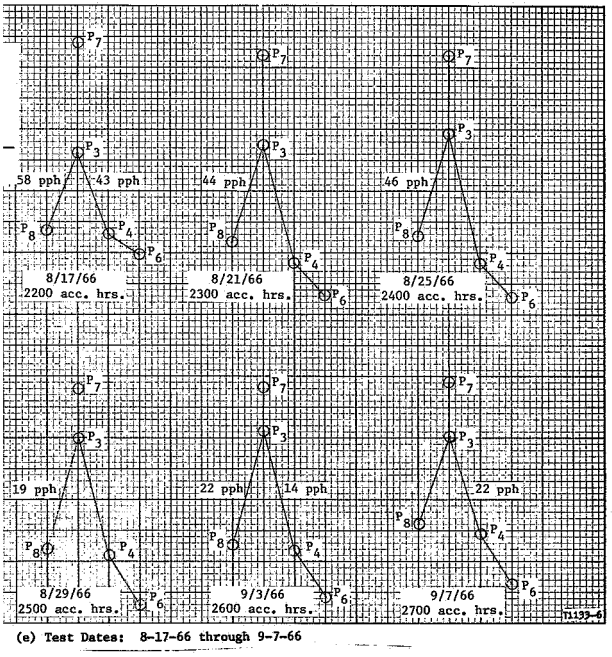
152



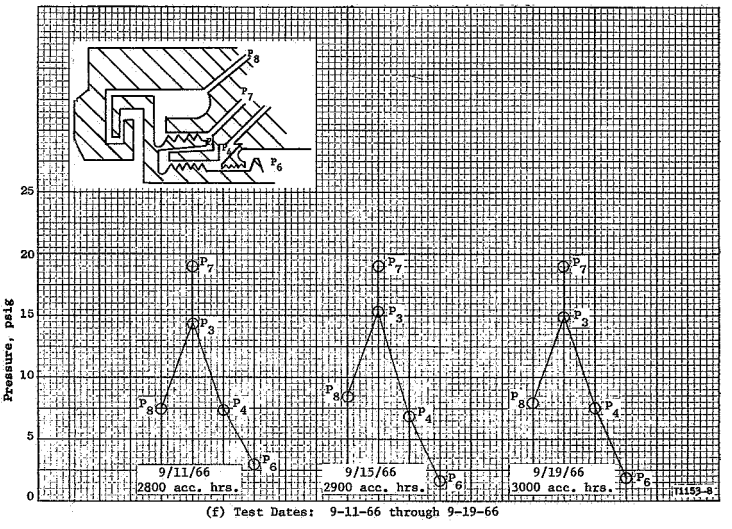
(b) Test Dates: 5-13-66 through 6-8-66



(c) Test Dates: 6-12-66 through 7-5-66



(e) Test Dates: 8-17-66 through 9-7-66



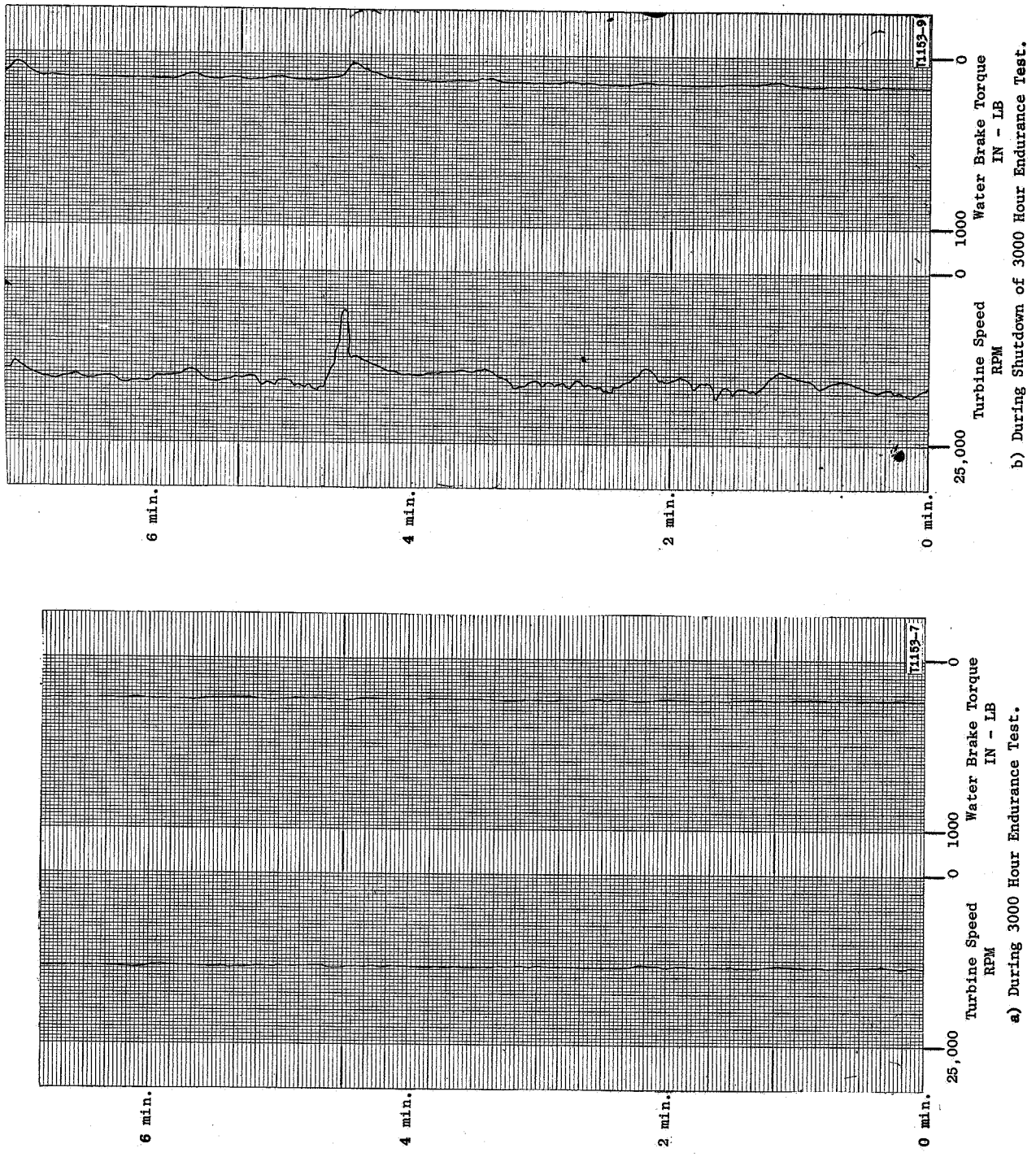
(f) Test Dates: 9-11-66 through 9-19-66

Figure 8. Seal Cavity Pressures During Endurance Testing in September of 1966.

Pressures During Endurance Testing.

FOLDOUT FRAME

PRECEDING PAGE BLANK NOT FILMED.



b) During Shutdown of 3000 Hour Endurance Test.

a) During 3000 Hour Endurance Test.

Figure 40. Turbine Speed and Water Brake Torque.

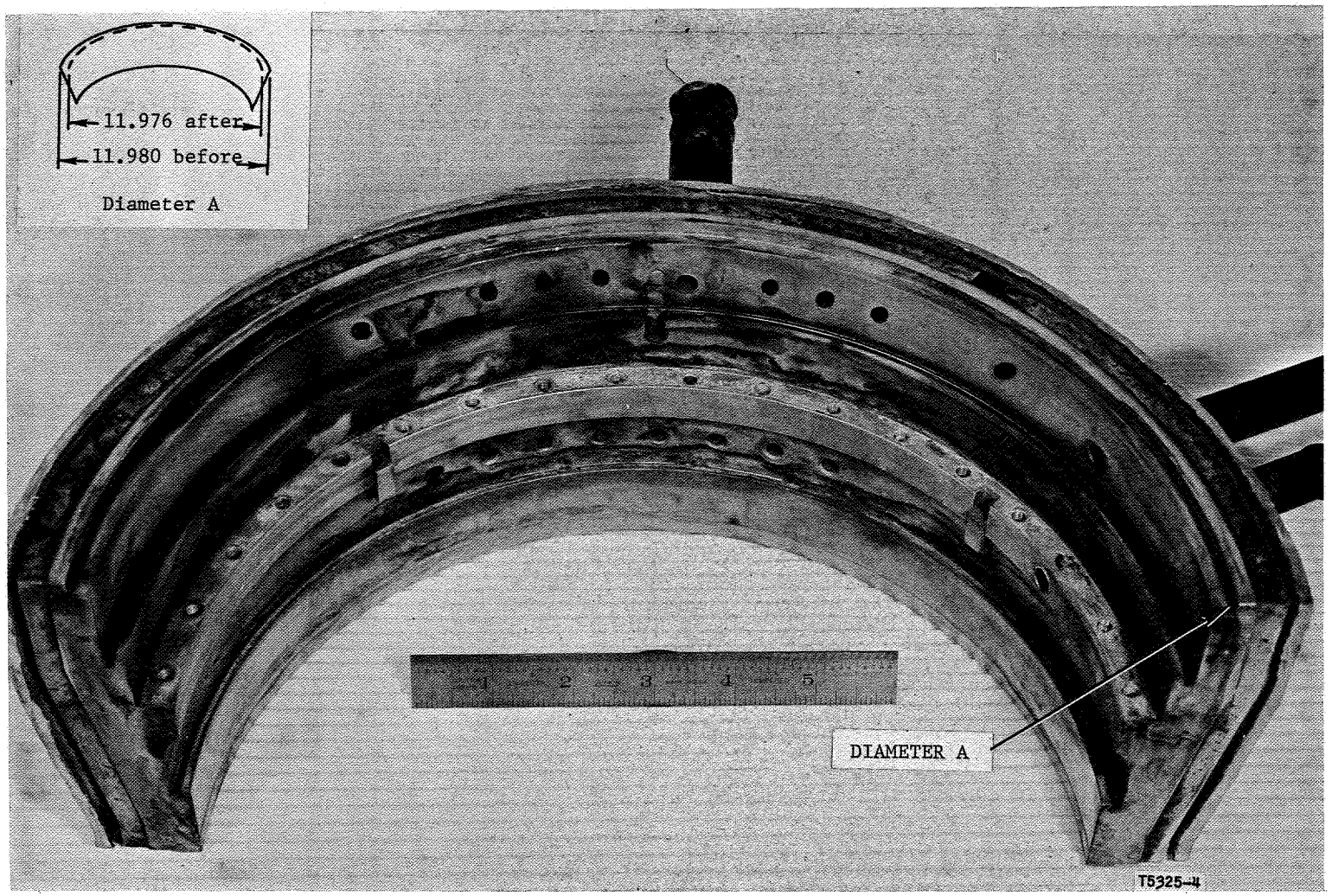


Figure 41. Top Half of Turbine Casing After 3000 Hour Test.

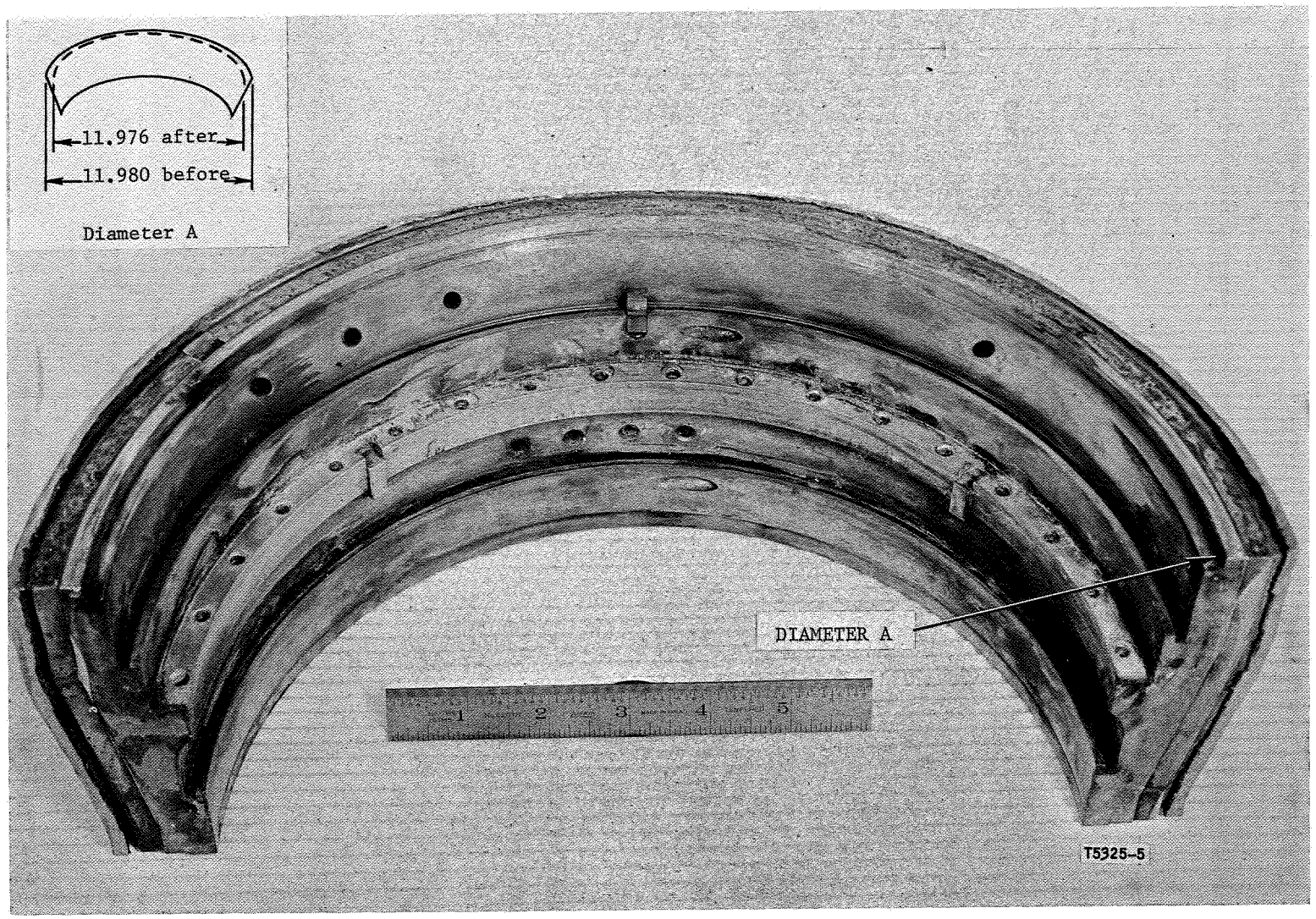


Figure 42. Bottom Half of Turbine Casing After 3000 Hour Test.

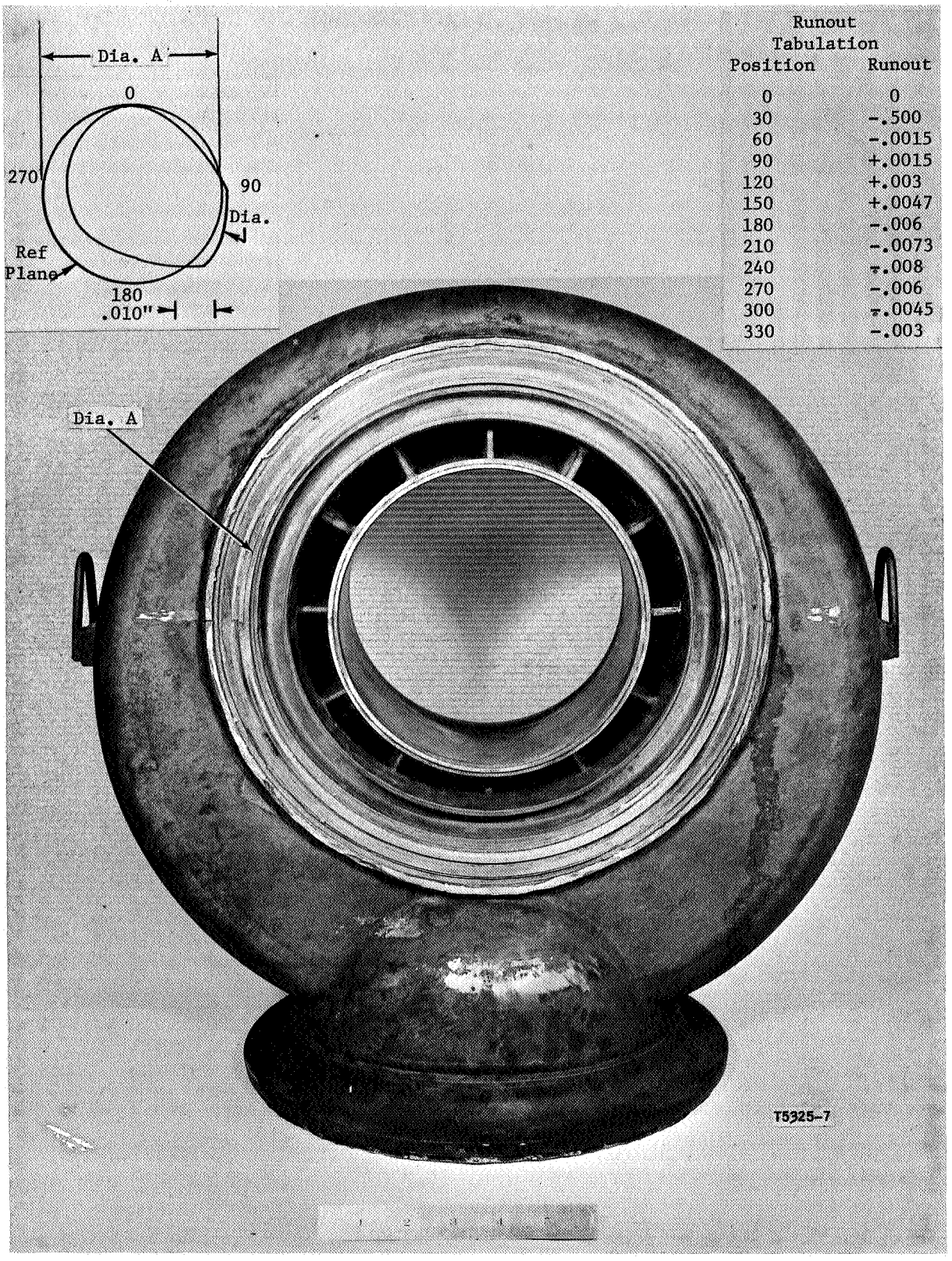


Figure 43. Surface Flange Runout Inspection of Turbine Exhaust Scroll. (Roundness)



Figure 44. Surface Flange Runout Inspection of Turbine Exhaust Scroll. (Squareness)

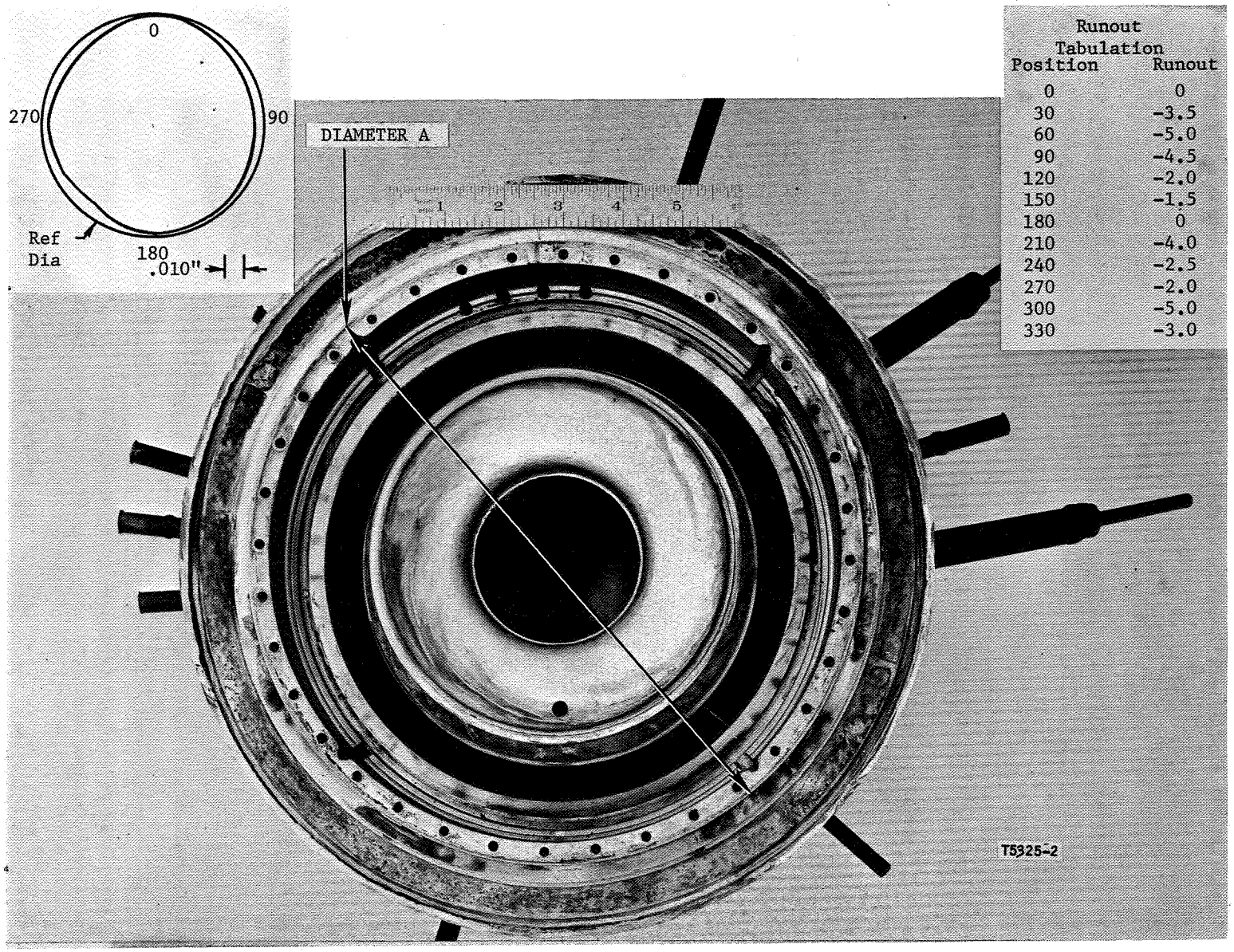


Figure 45. Inlet Duct After 3000 Hour Test Showing Distortion of Diameter A (Rabbet to Casings) Due to Thermal Cycling.

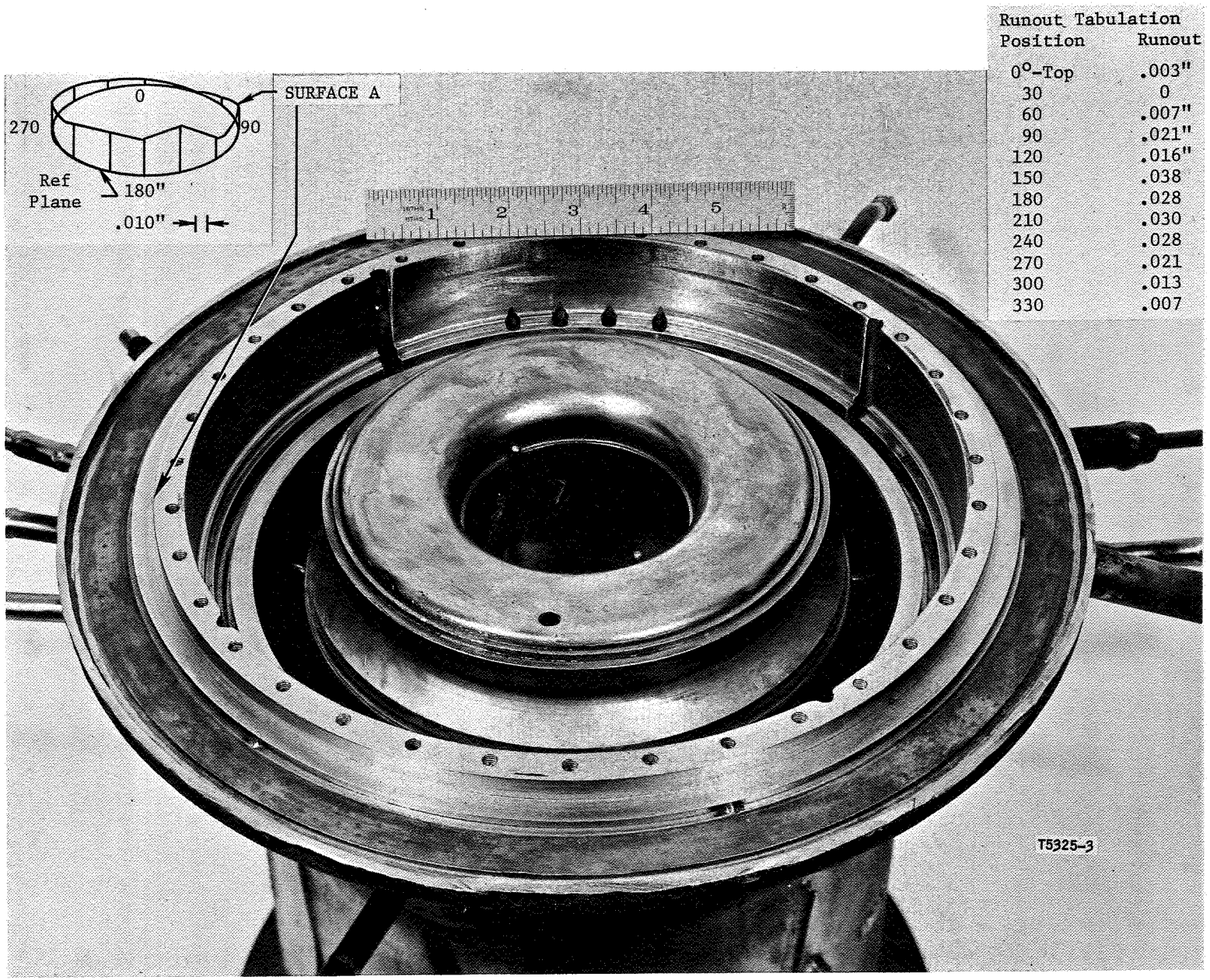


Figure 46. Inlet Duct After 3000 Hour Test Showing Distortion of Surface A (Butt Face to Casings) Due to Thermal Cycling.

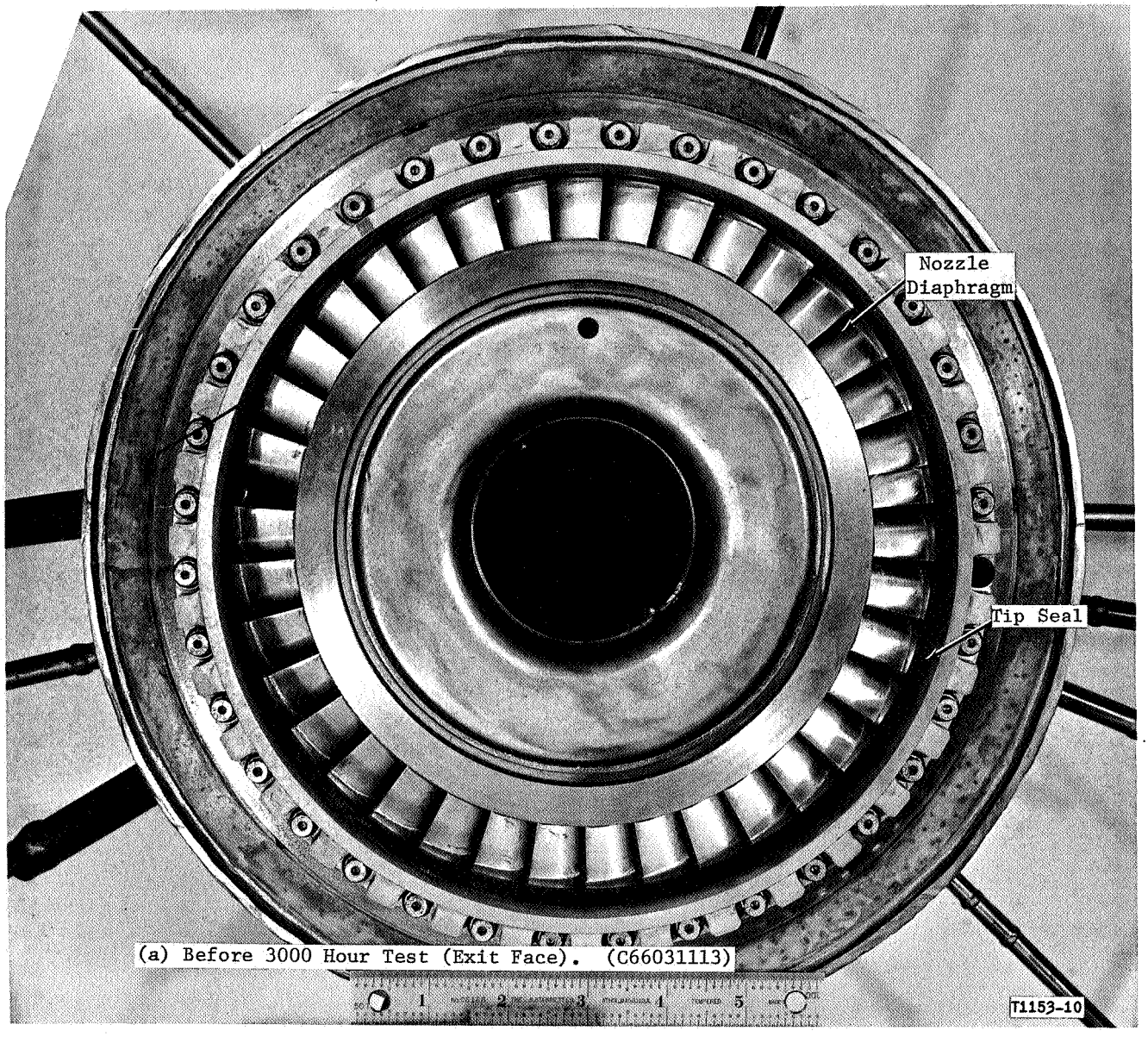


Figure 47a. Inlet Duct Assembly.

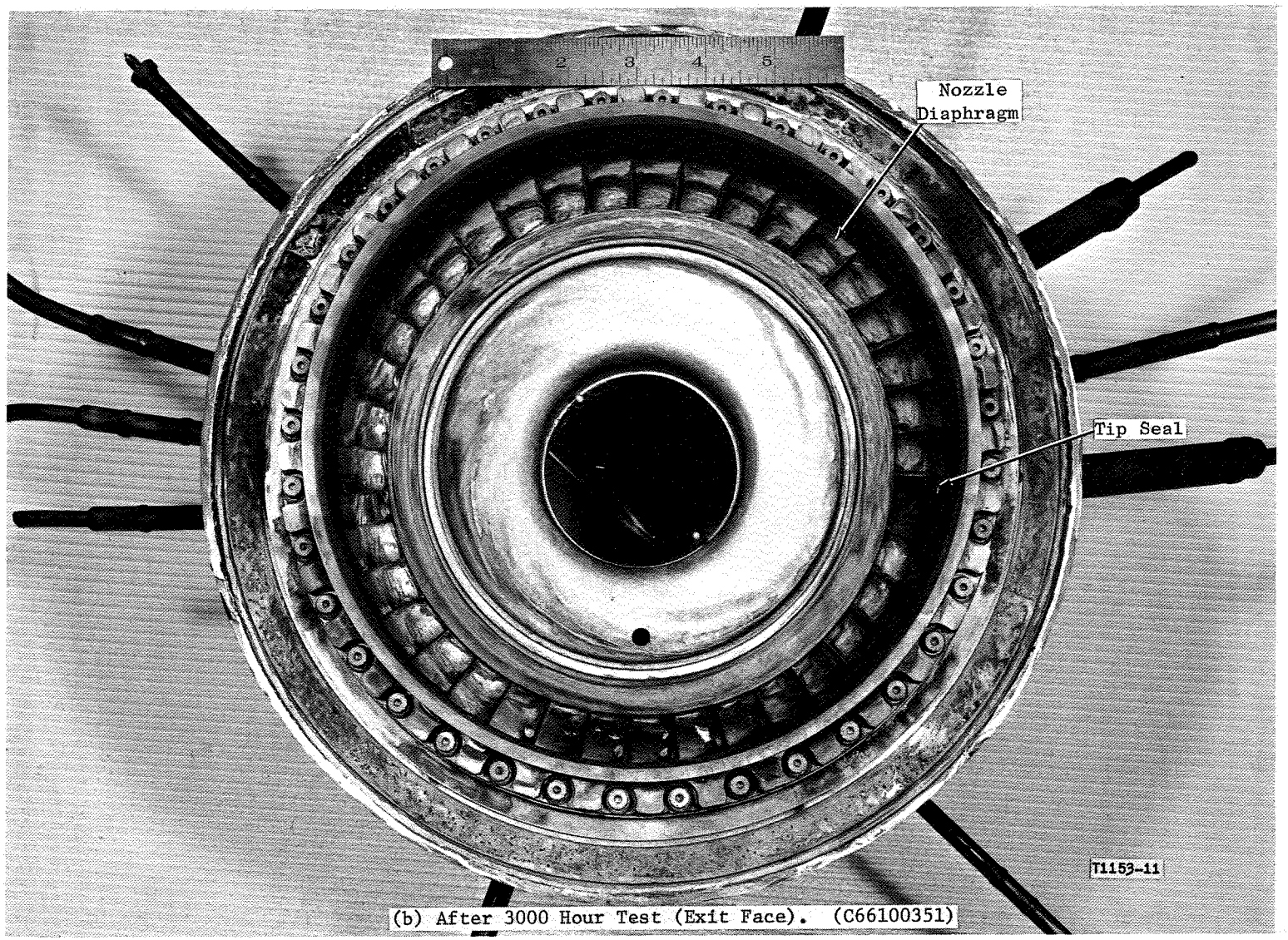


Figure 47b. Inlet Duct Assembly.

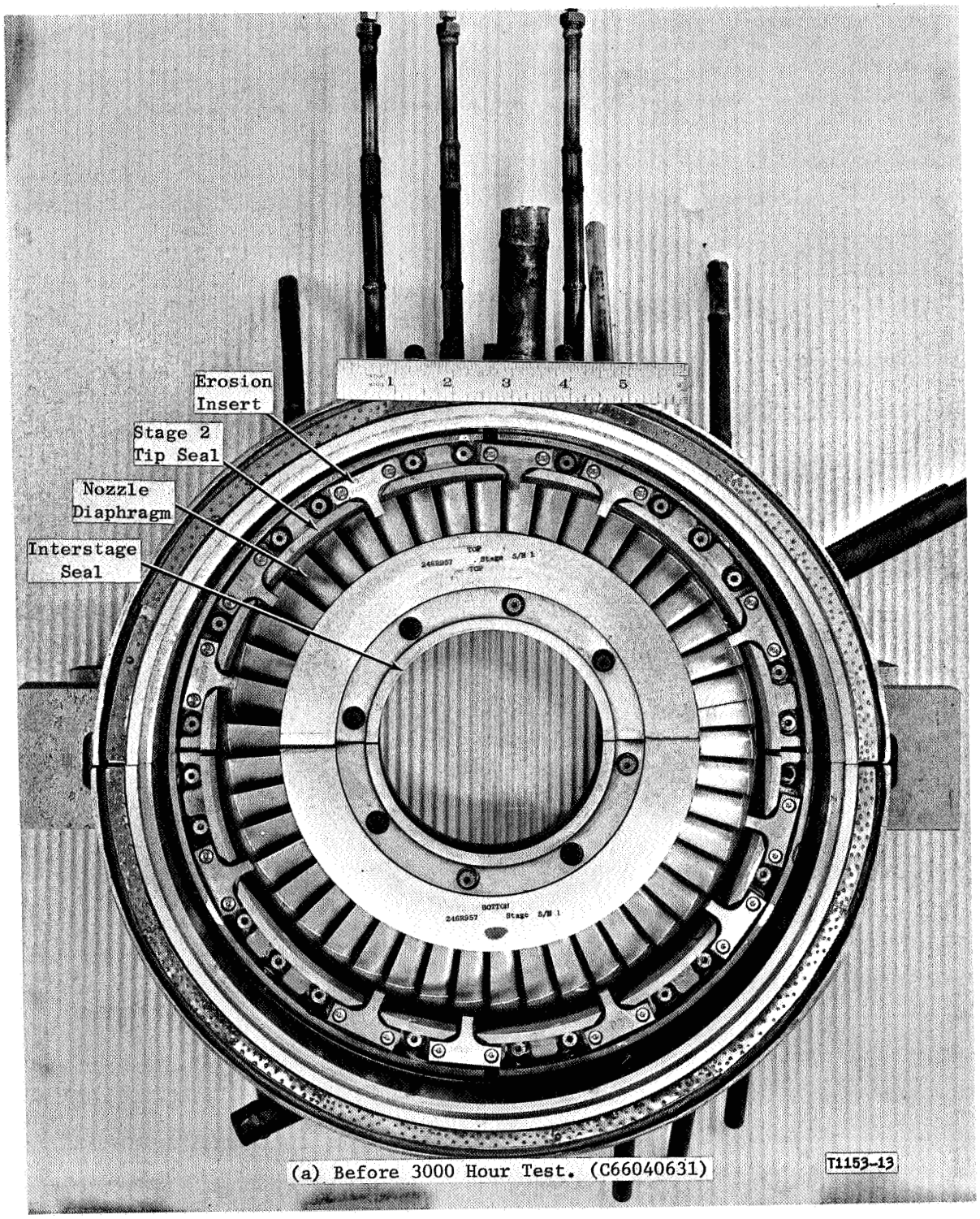


Figure 48a. Aft View of Turbine Casing Assembly.

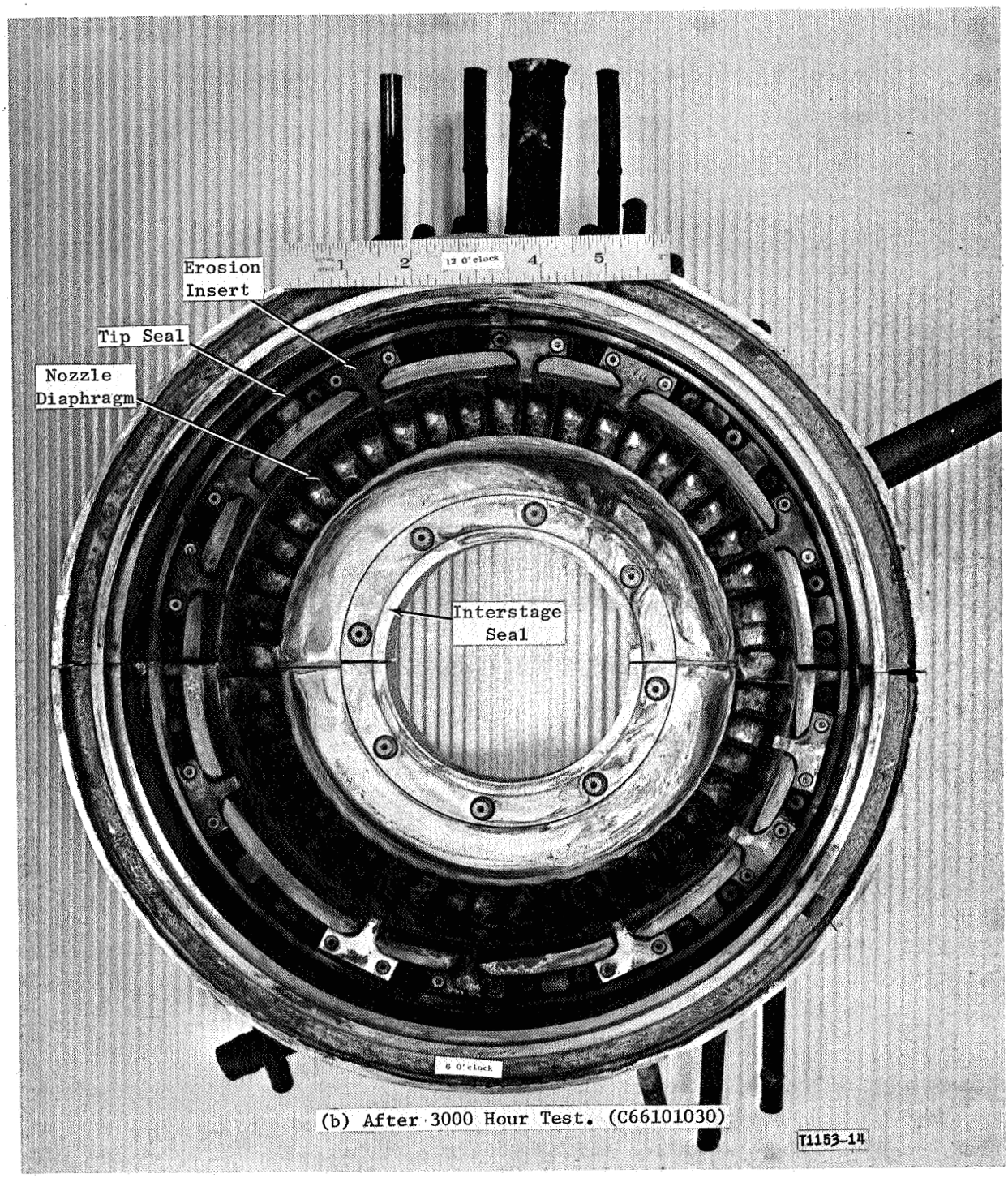
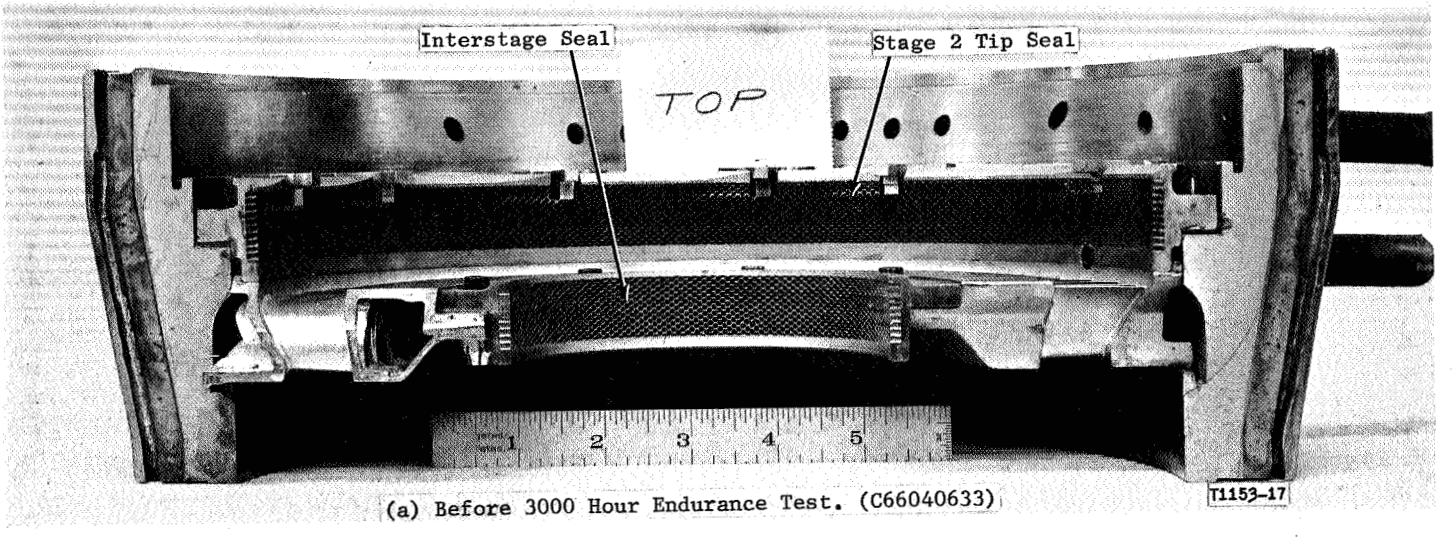
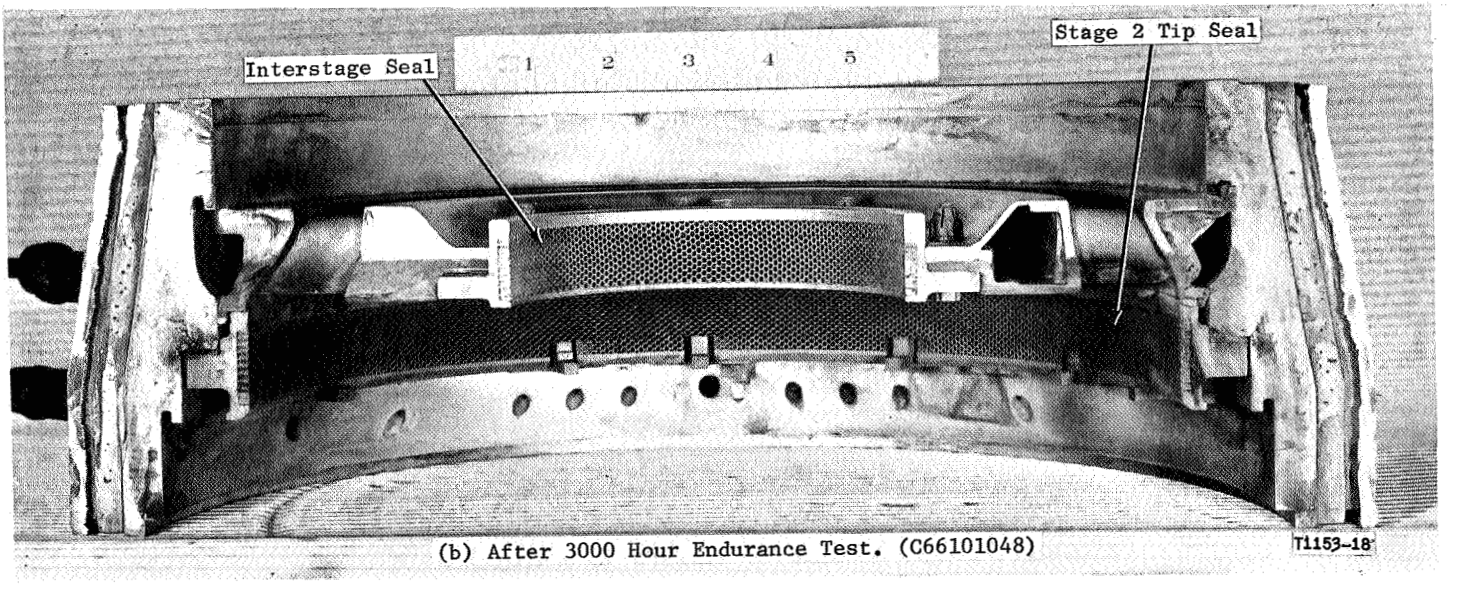


Figure 48b. Aft View of Turbine Casing Assembly.

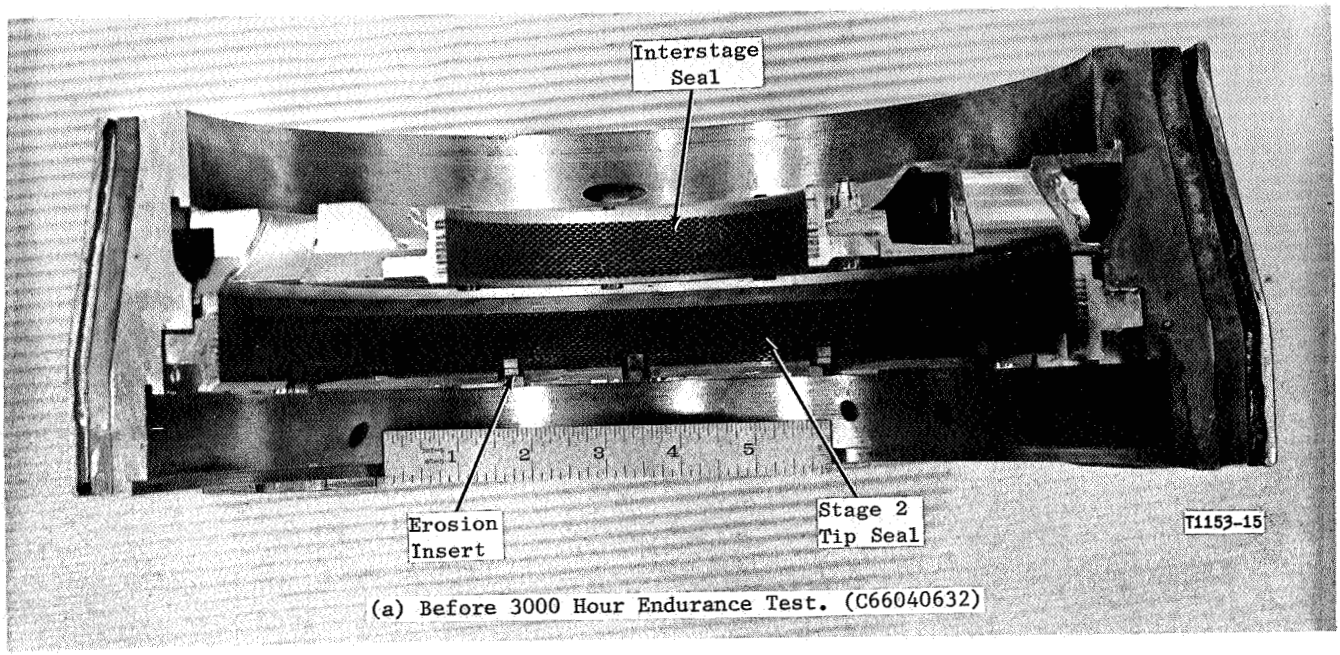


(a) Before 3000 Hour Endurance Test. (C66040633)

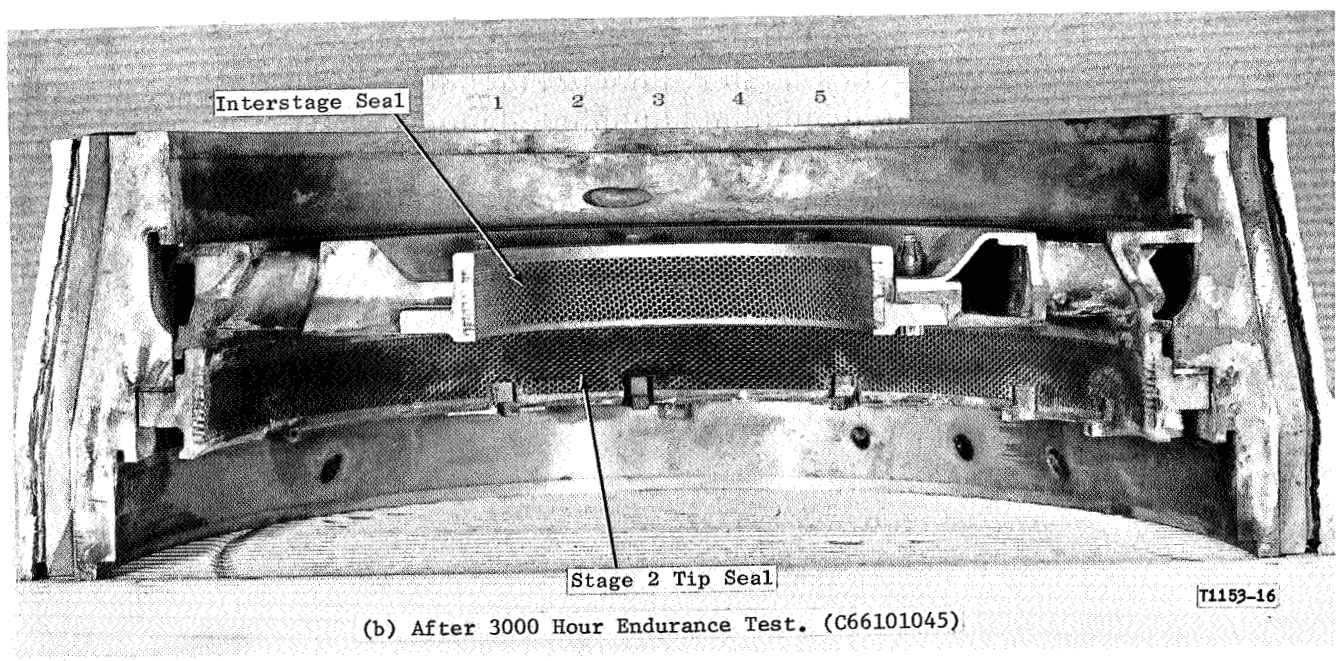


(b) After 3000 Hour Endurance Test. (C66101048)

Figure 49. Top Half of Turbine Casing Assembly.

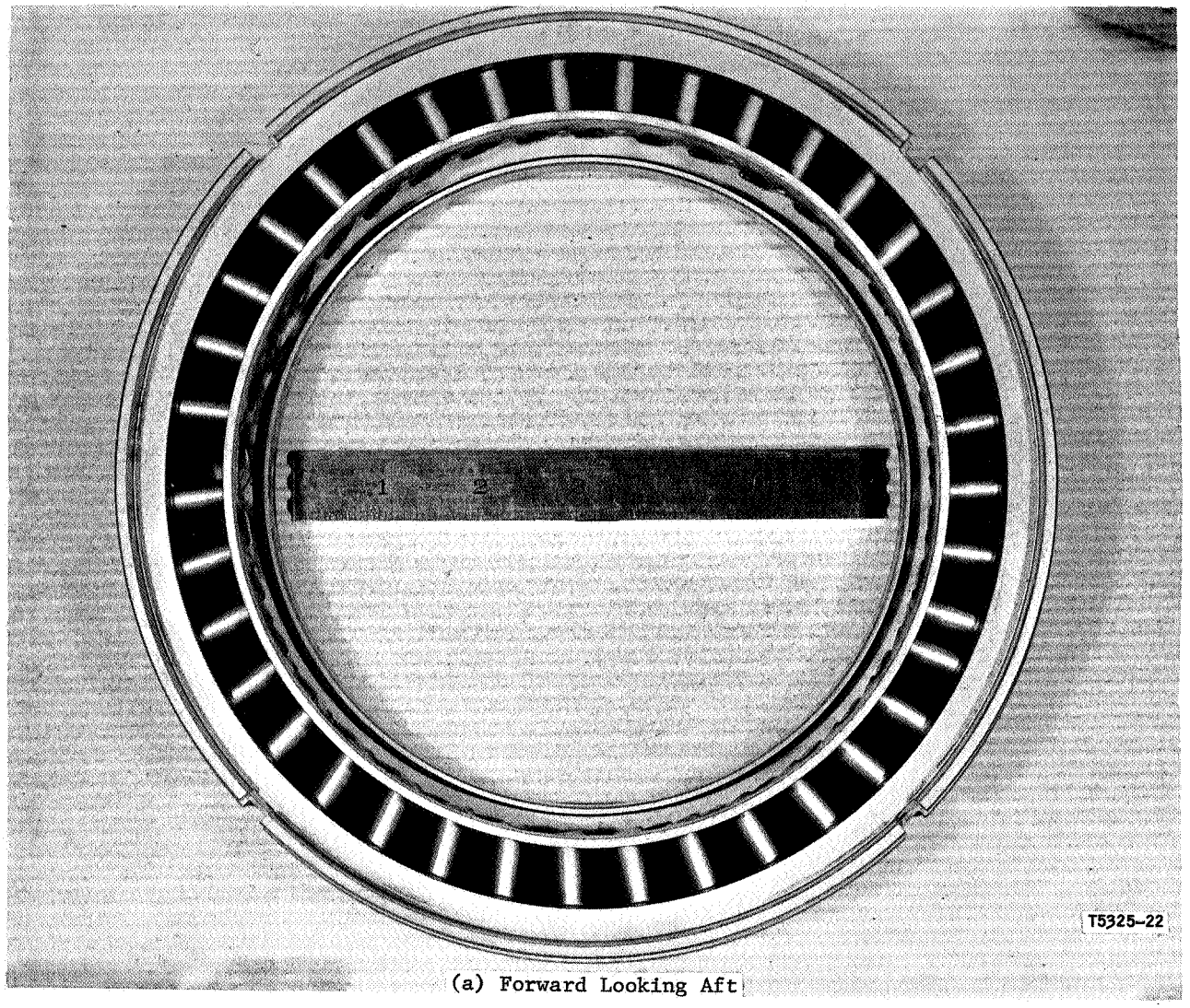


(a) Before 3000 Hour Endurance Test. (C66040632)



(b) After 3000 Hour Endurance Test. (C66101045)

Figure 50. Bottom Half of Turbine Casing Assembly.



(a) Forward Looking Aft

Figure 61a. First Stage Nozzle Diaphragm Assembly Following 3000 Hour Endurance Test and Vapor Blast Cleaning.

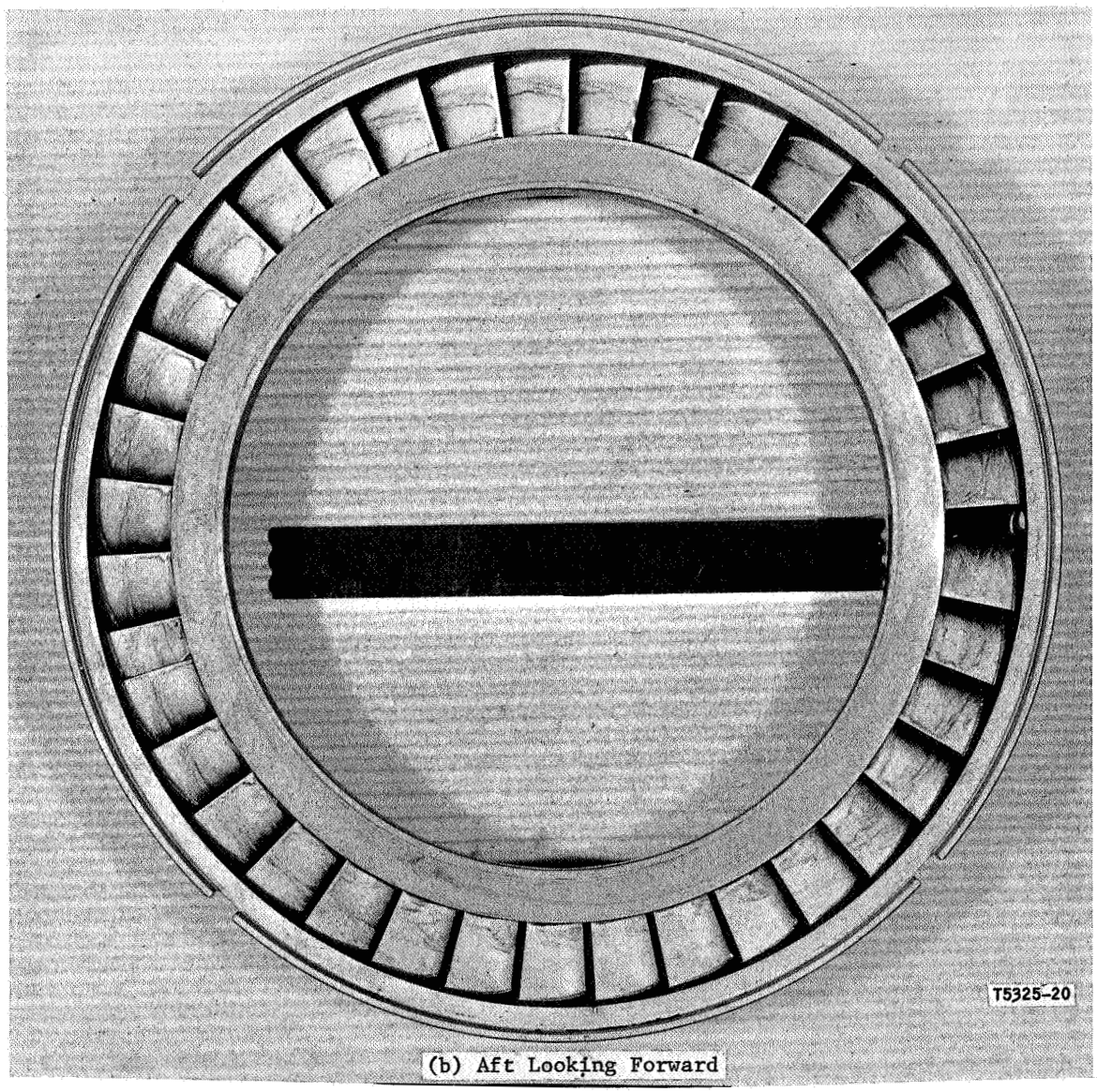


Figure 51b. First Stage Nozzle Diaphragm Assembly Following 3000 Hour Endurance Test and Vapor Blast Cleaning.



PRECEDING PAGE BLANK NOT FILMED.

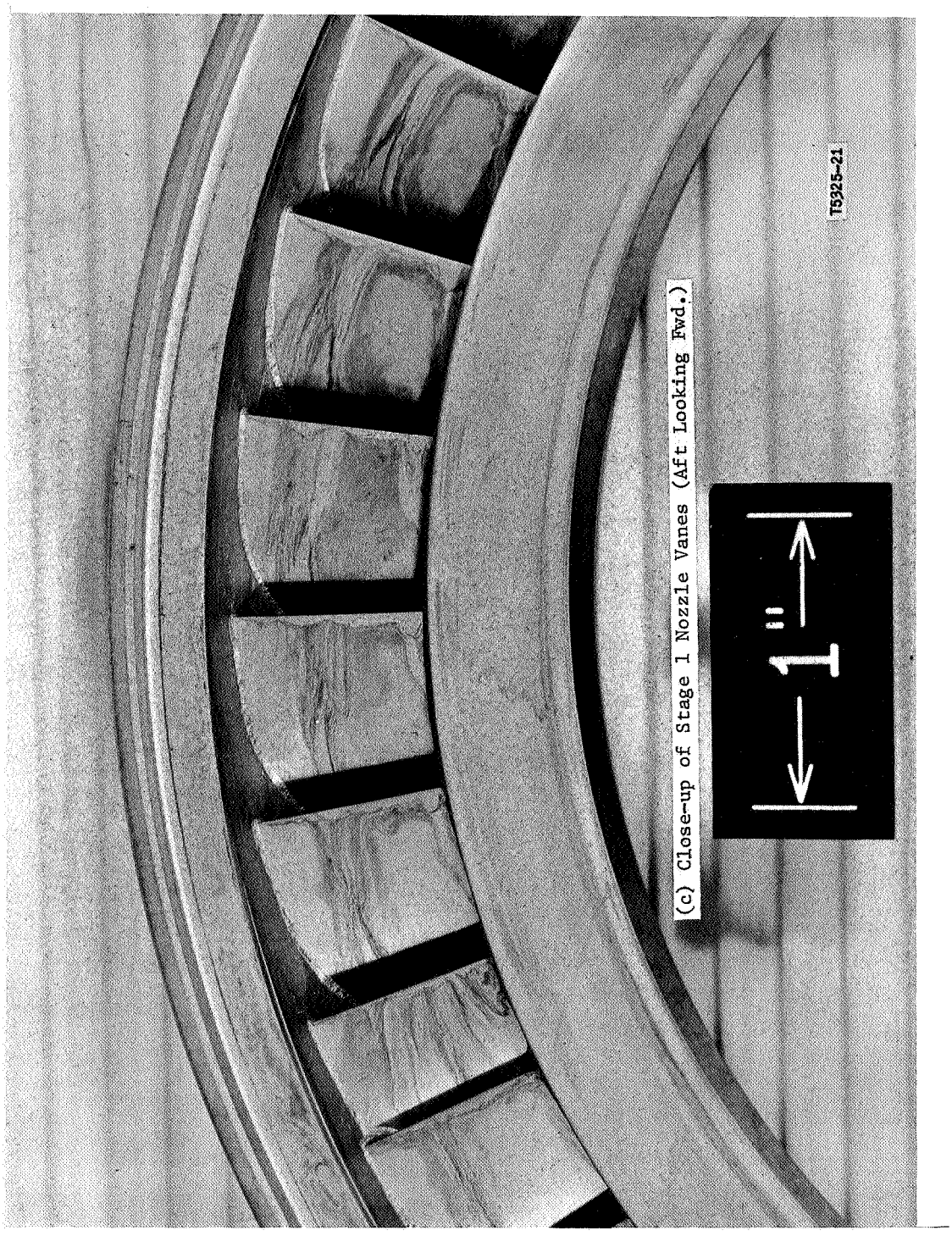
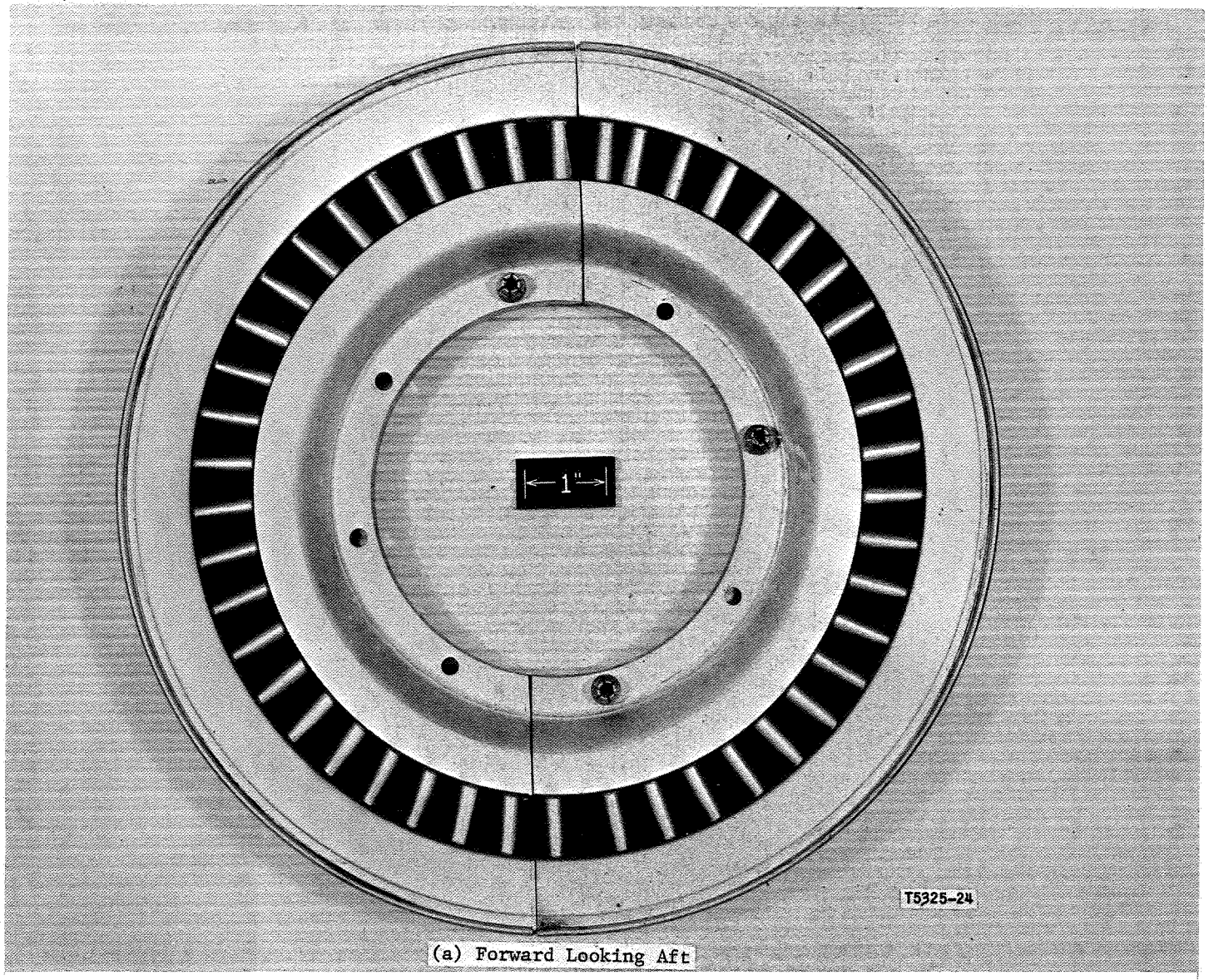


Figure 51. First Stage Nozzle Diaphragm Assembly Following 3000 Hour Endurance Test and Vapor Blast Cleaning.



(a) Forward Looking Aft

Figure 52a. Stage Two Nozzle Diaphragm Assembly Following 3000 Hour Endurance Test and Vapor Blast Cleaning.

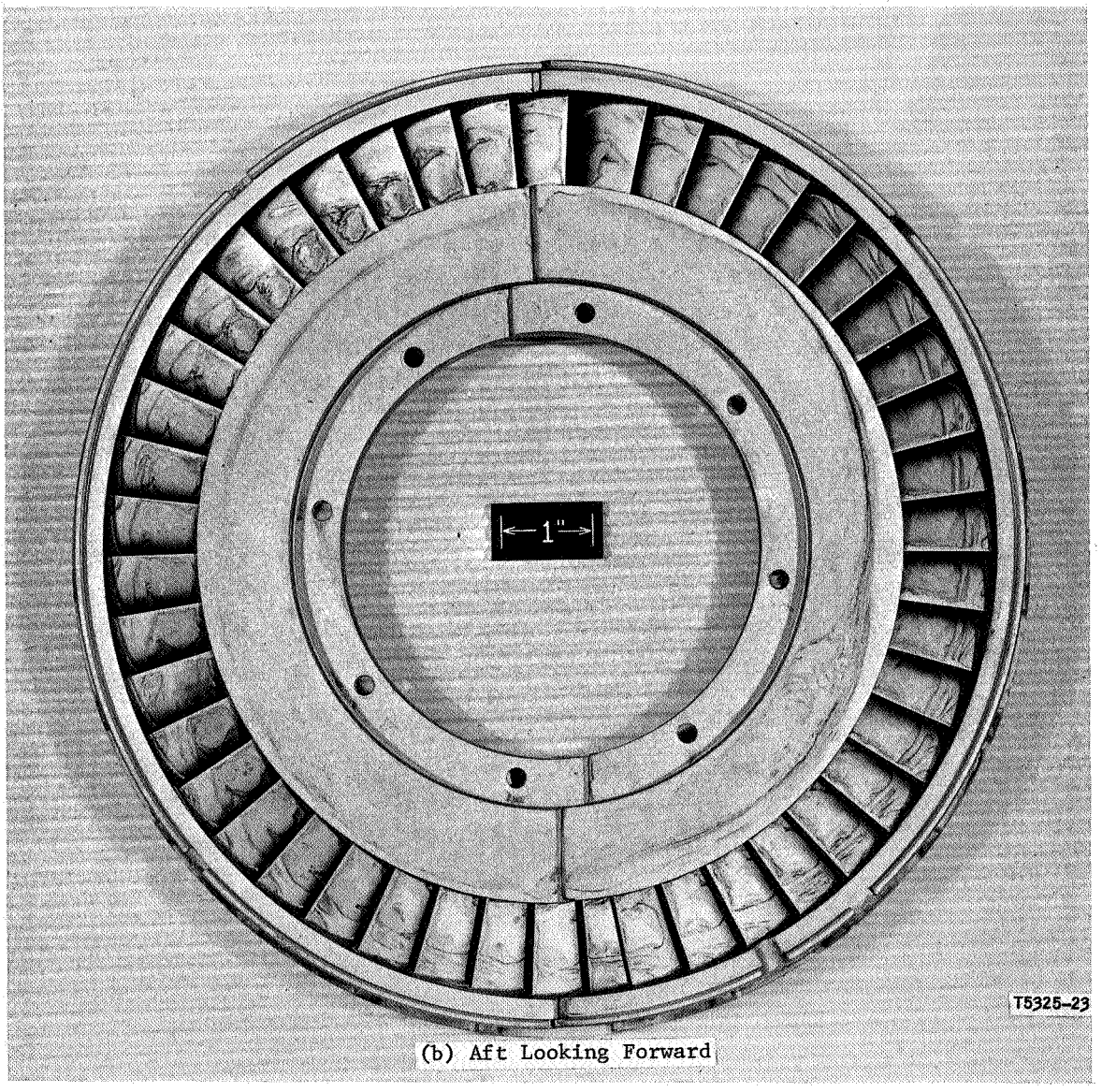


Figure 52b. Stage Two Nozzle Diaphragm Assembly Following 3000 Hour Endurance Test and Vapor Blast Cleaning.

PRECEDING PAGE BLANK NOT FILMED.

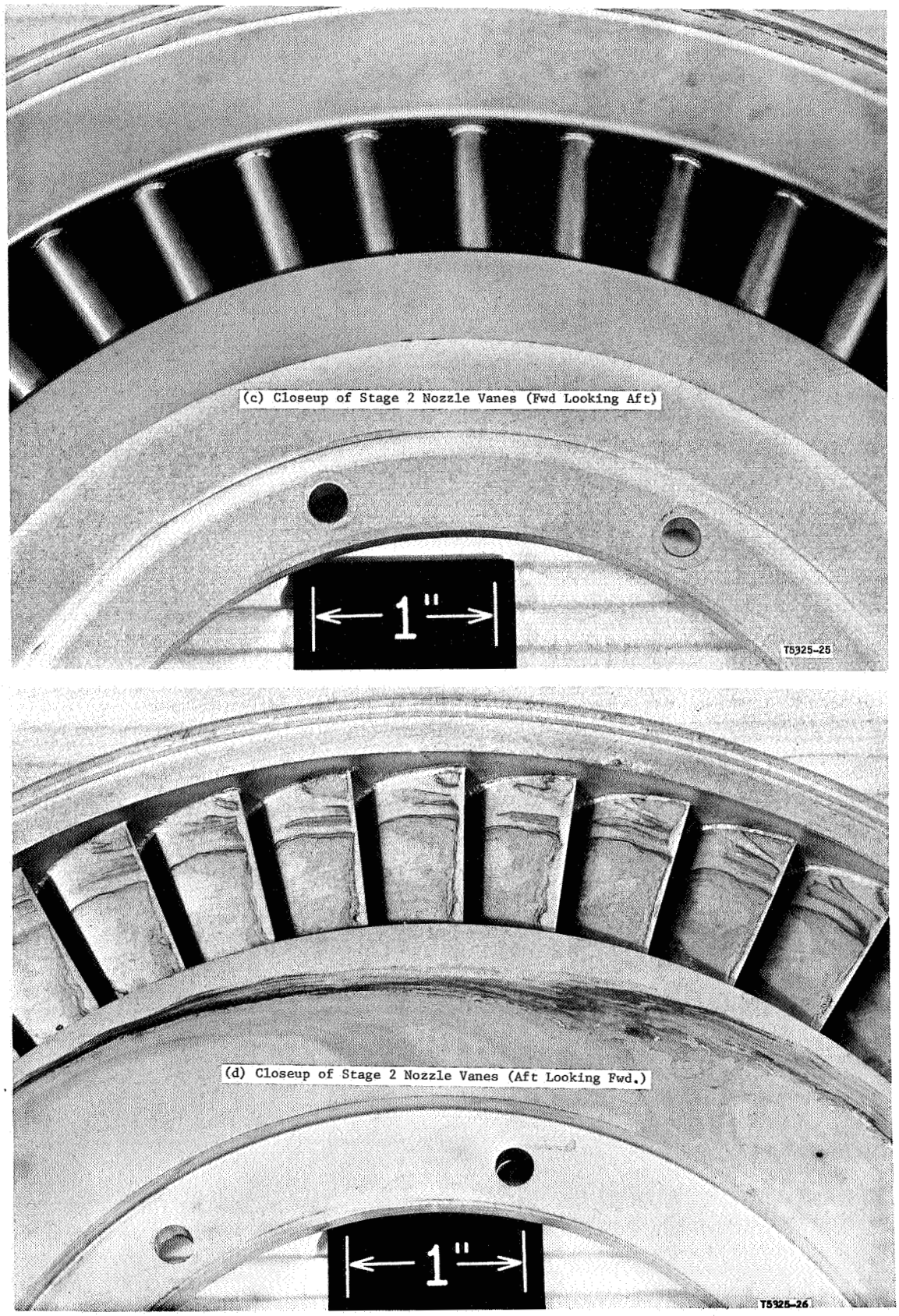


Figure 52c. Stage Two Nozzle Diaphragm Assembly Following 3000 Hour Endurance Test and Vapor Blast Cleaning.

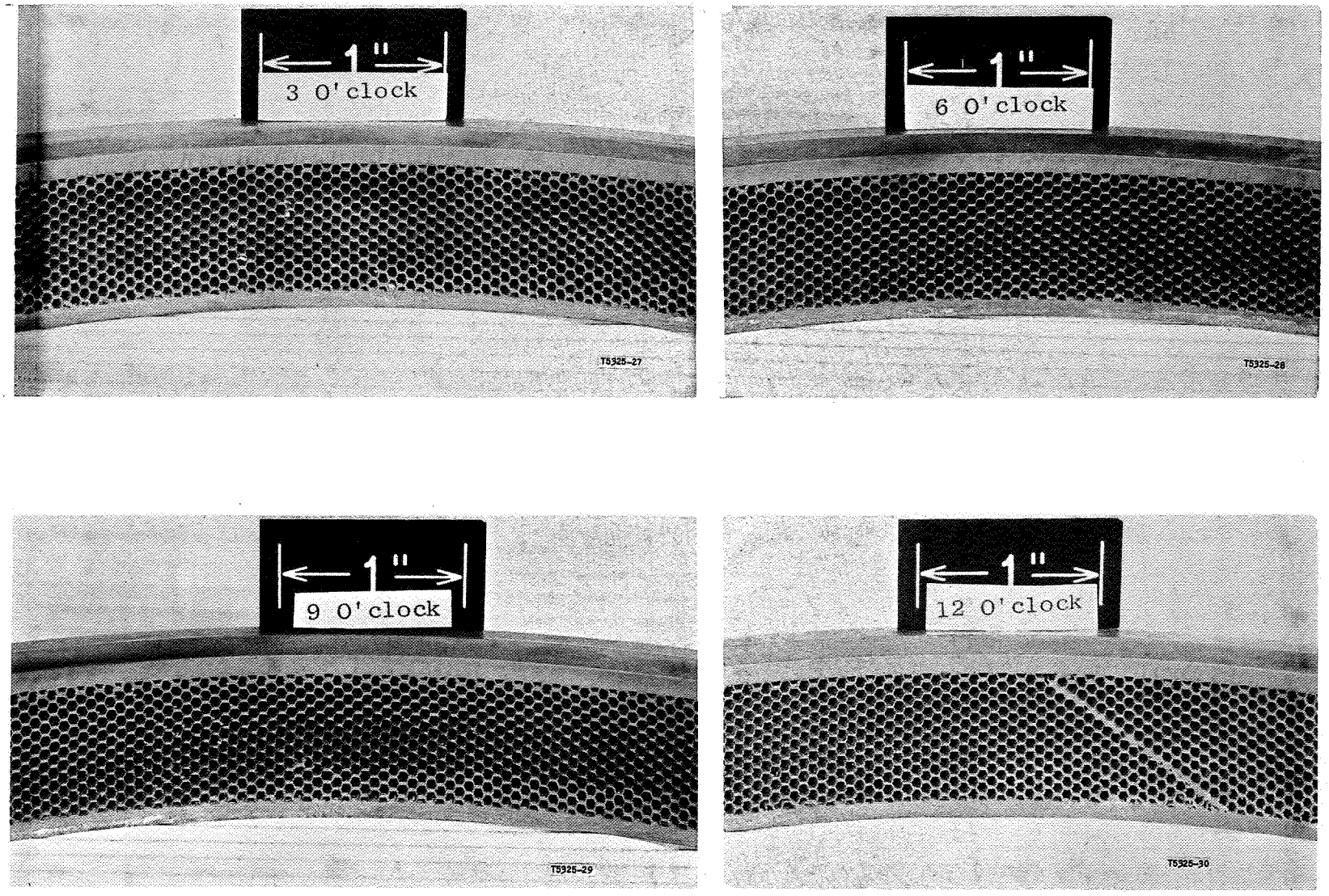


Figure 53a. Honeycomb Tip Seals Following 3000-Hour Endurance Test; Stage One.

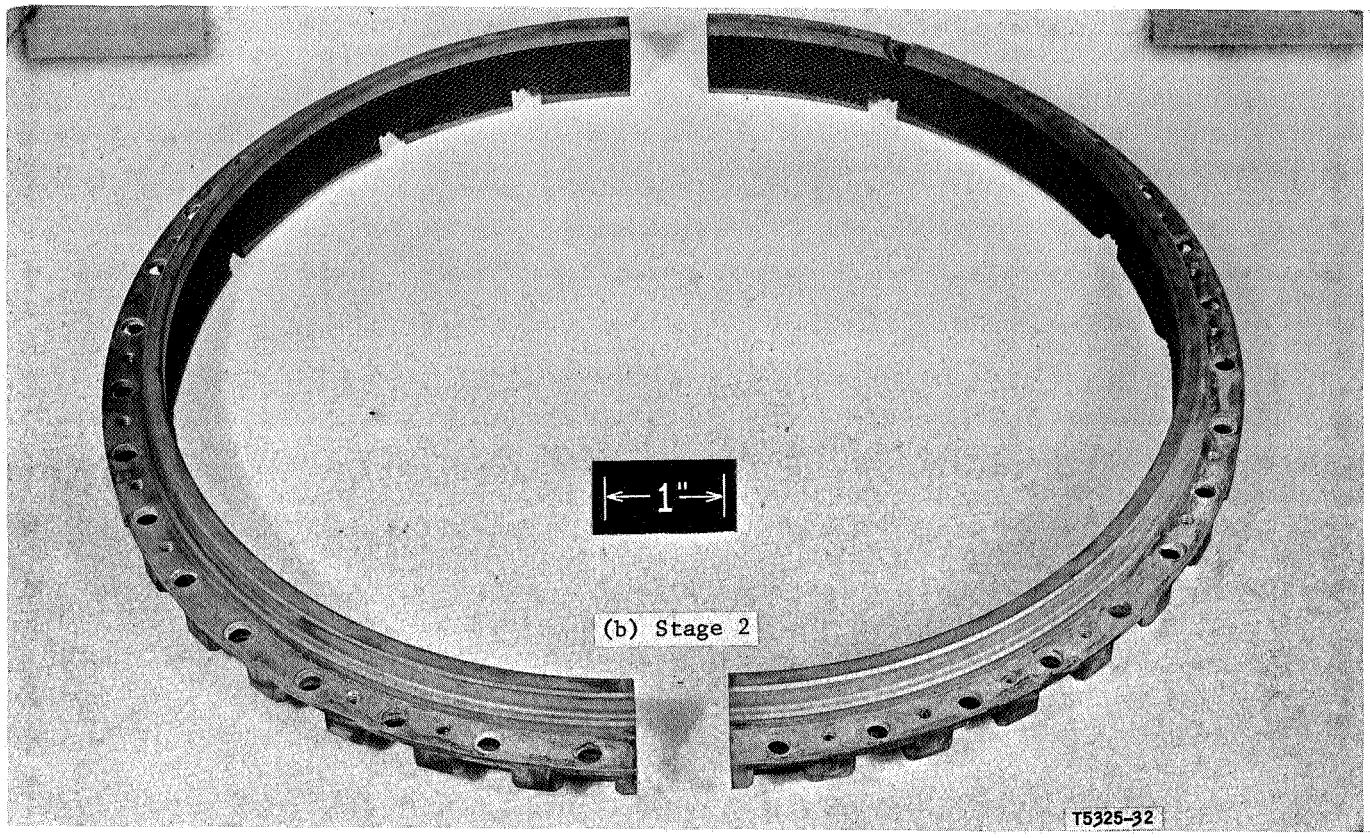


Figure 53b. Honeycomb Tip Seals Following 3000-Hour Endurance Test; Stage Two.

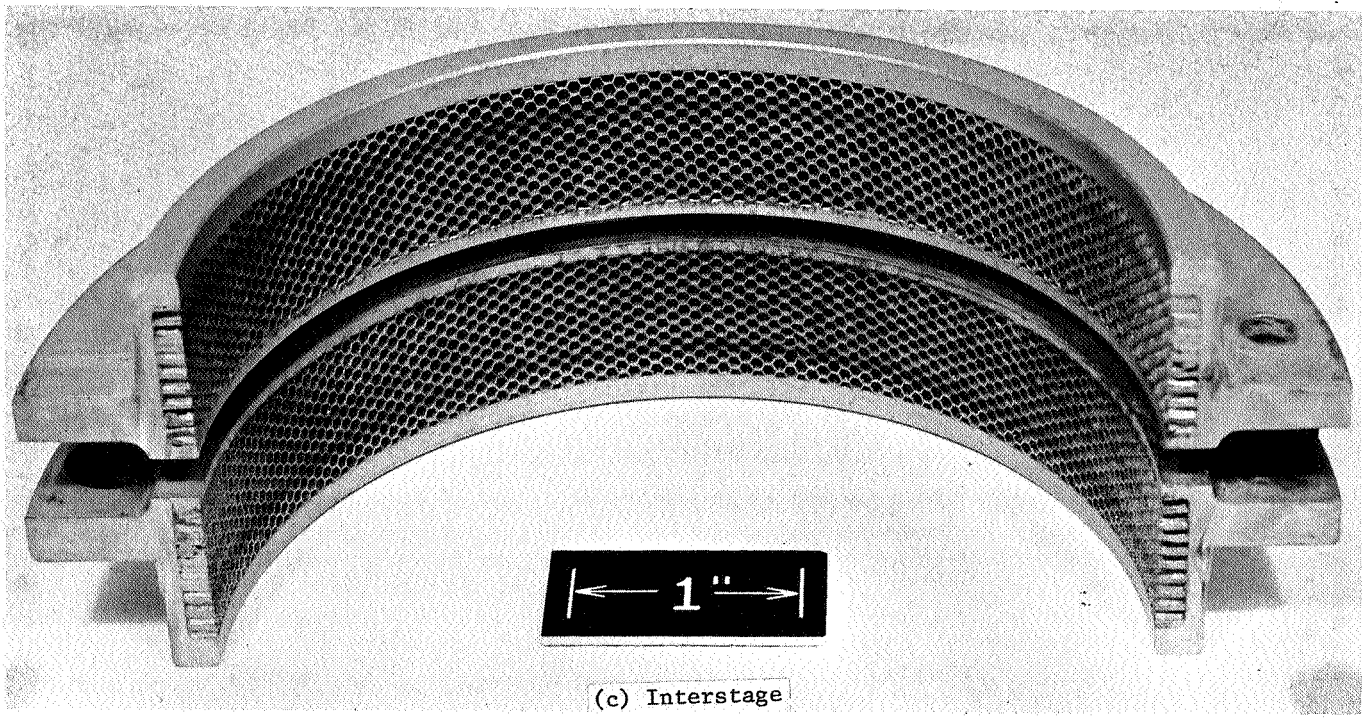
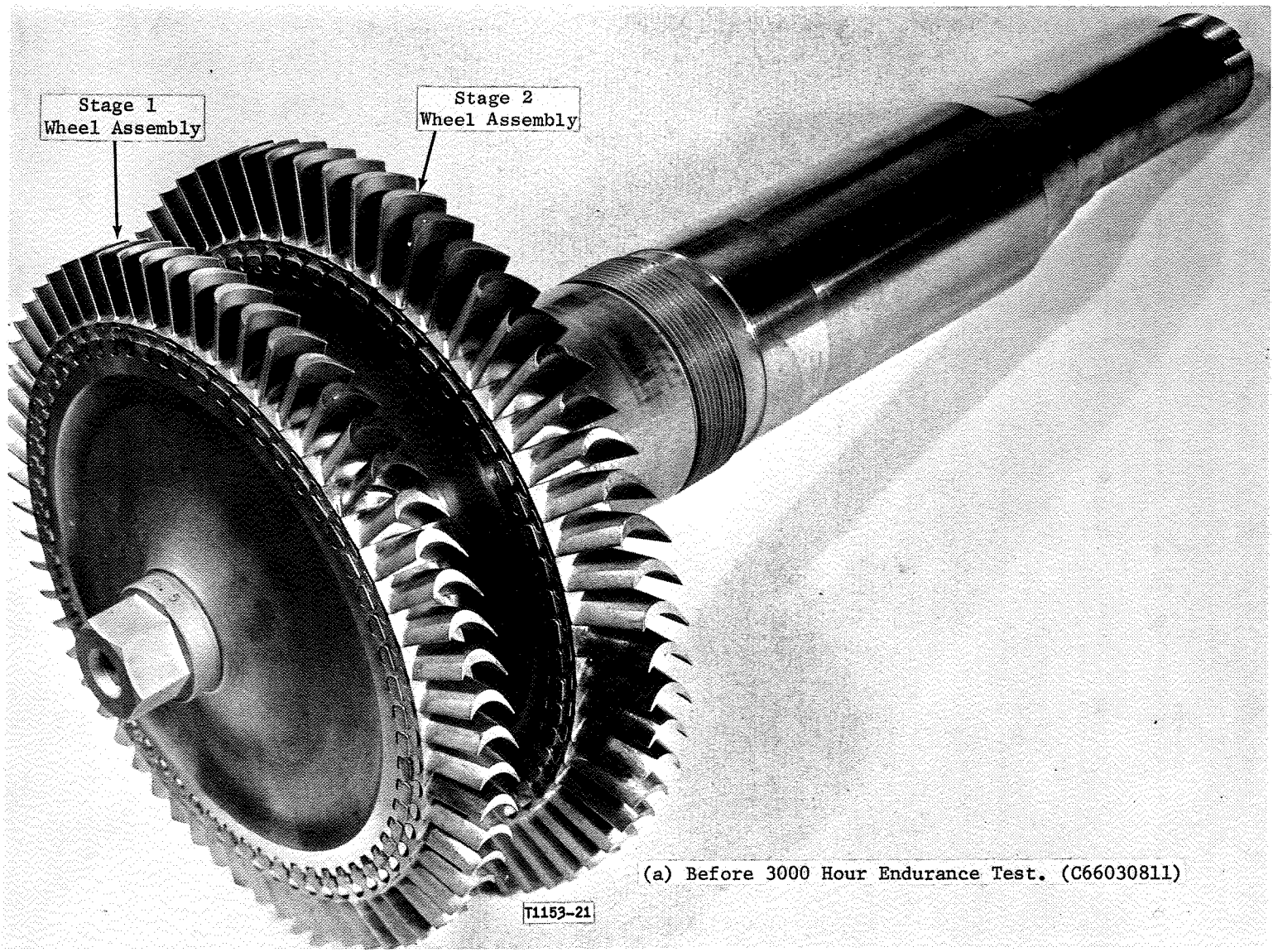


Figure 53c. Honeycomb Tip Seals Following 3000-Hour Endurance Test; Interstage.



(a) Before 3000 Hour Endurance Test. (C66030811)

Figure 54a. Two-Stage Turbine Rotor Assembly.

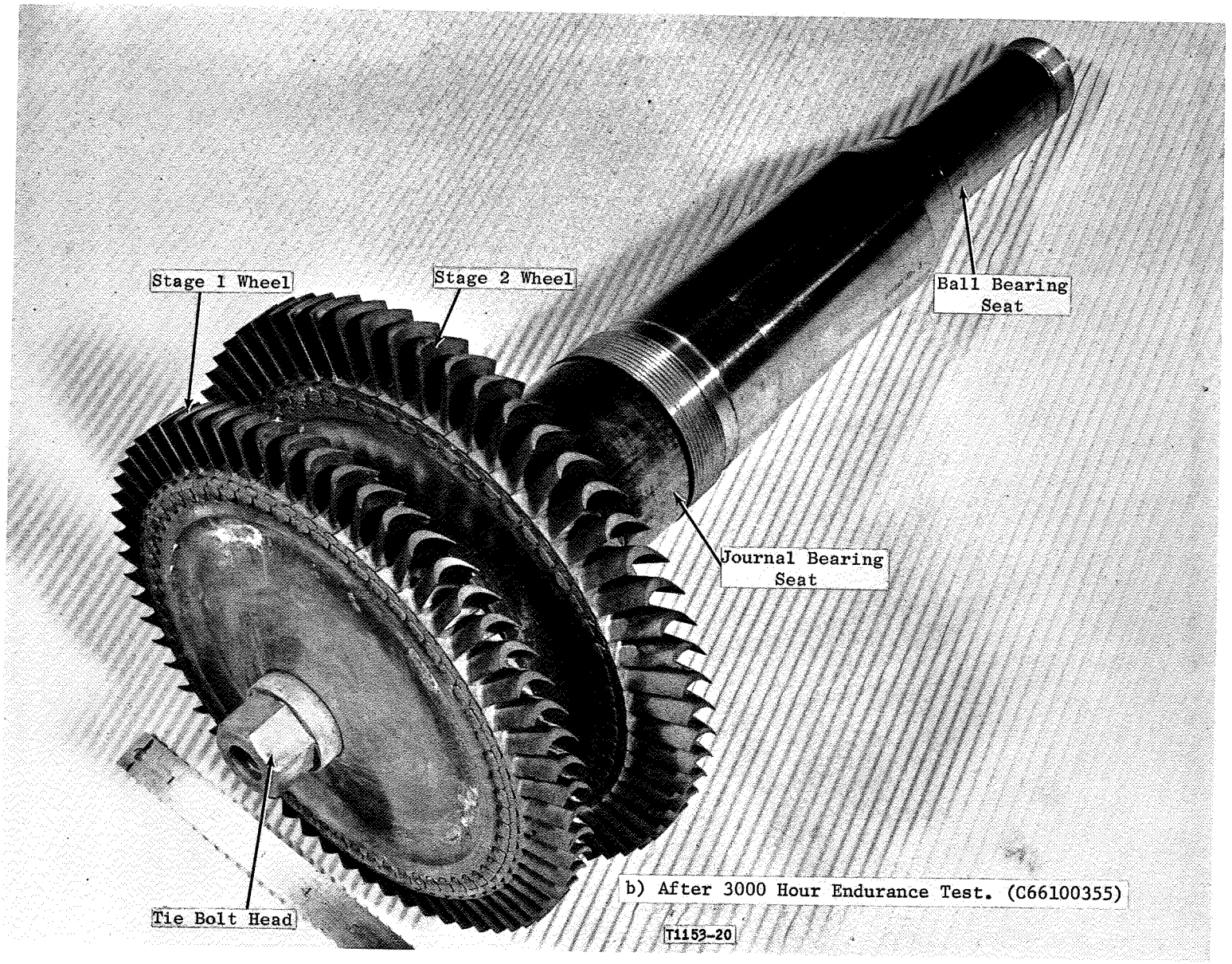
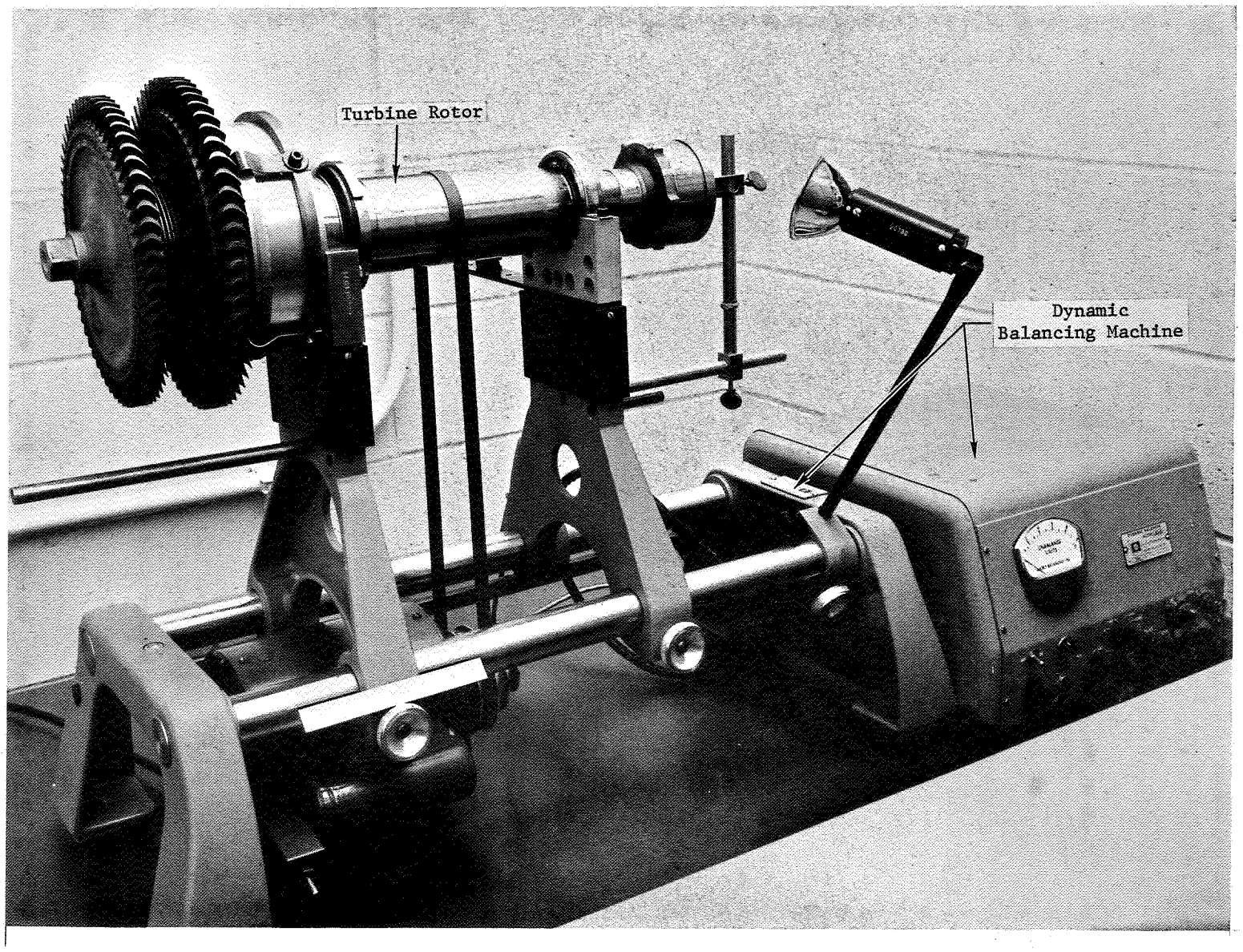


Figure 54b. Two-Stage Turbine Rotor Assembly.



T5433-55

Figure 55. Turbine Rotor in Balance Machine Following 3000 Hour Endurance Test and Prior to Disassembly.

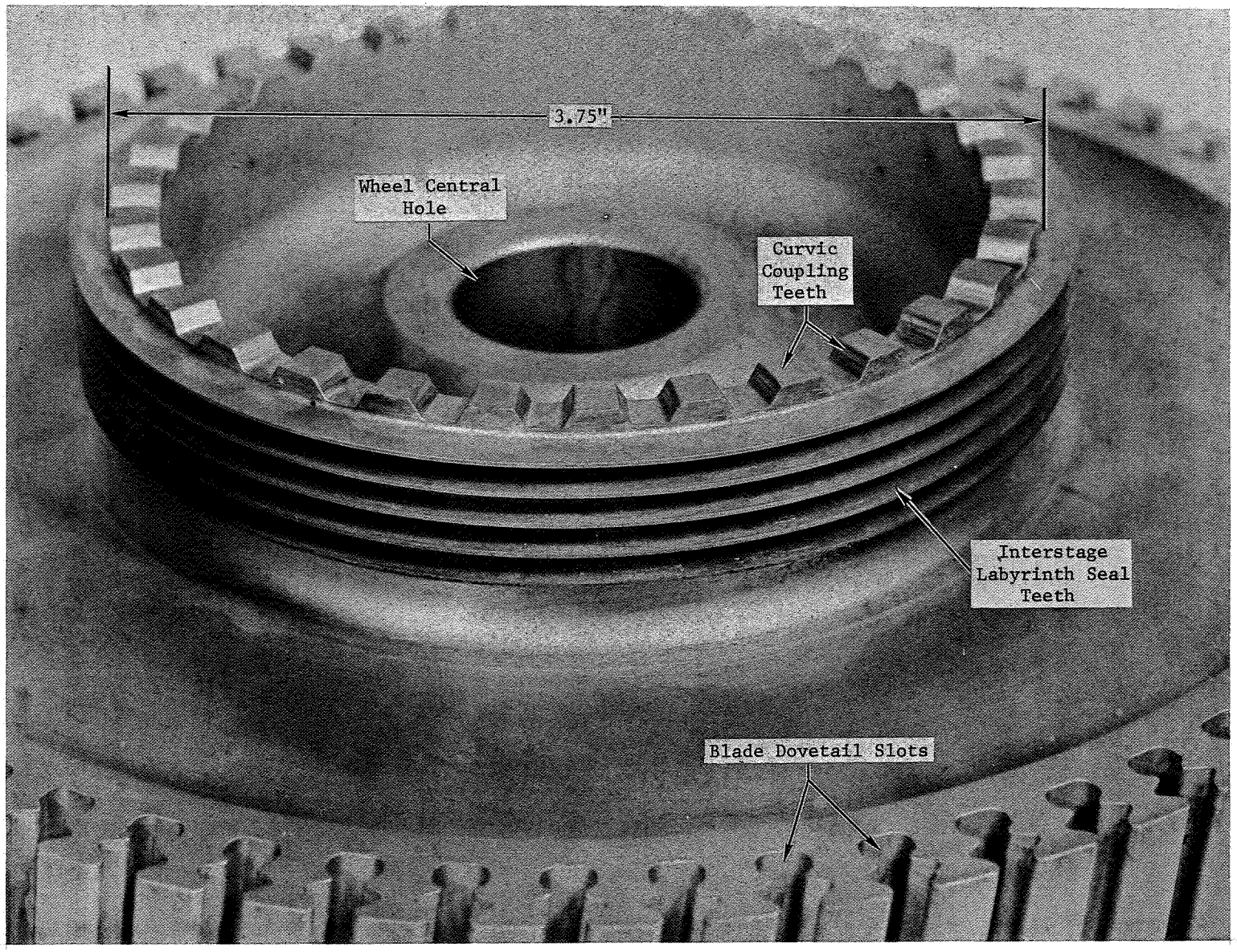


Figure 56. Forward Face of Stage Two Wheel Showing Curvic Coupling and Seal Teeth Following 3000-Hour Endurance Test.

T8439-86

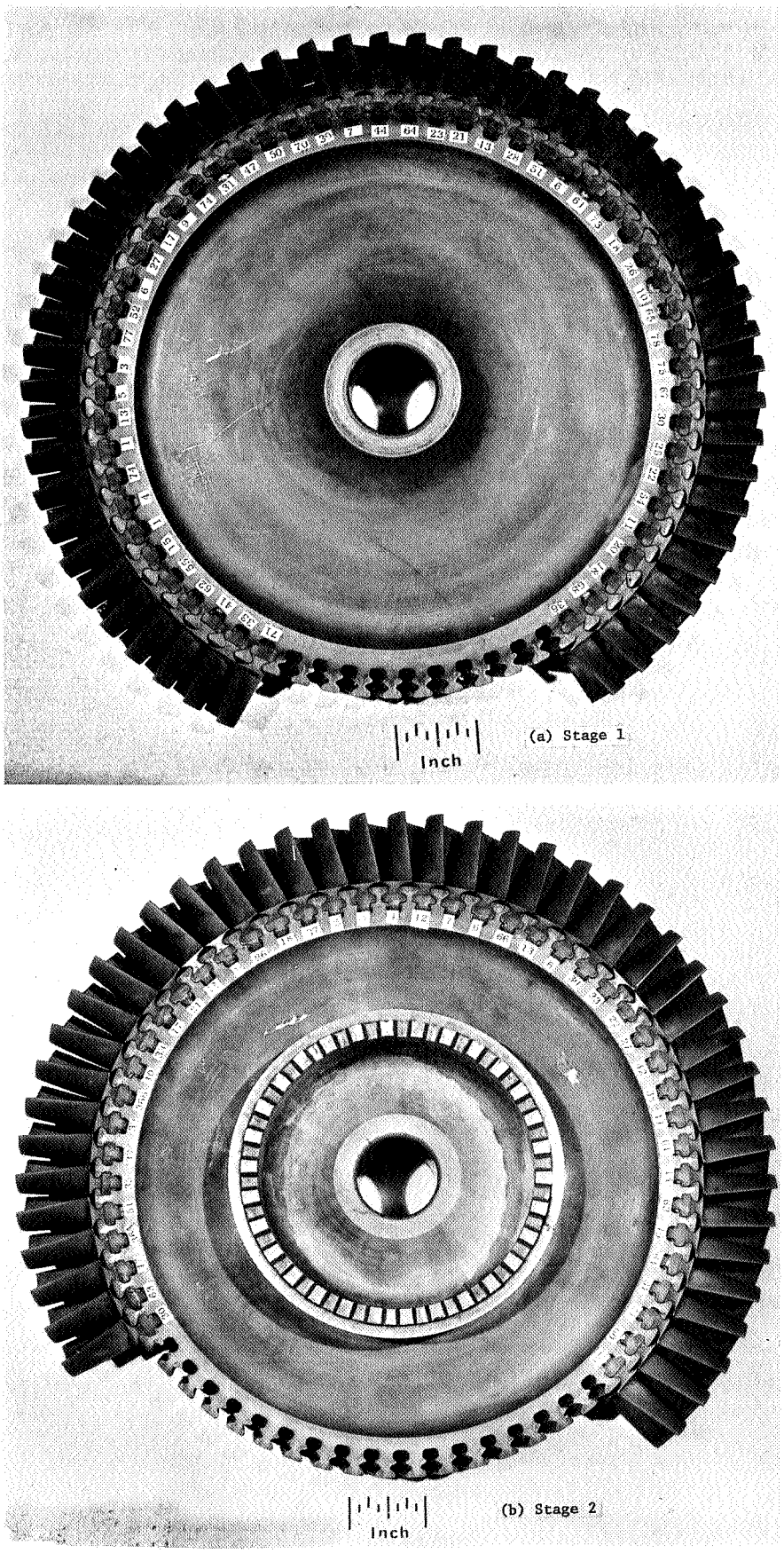
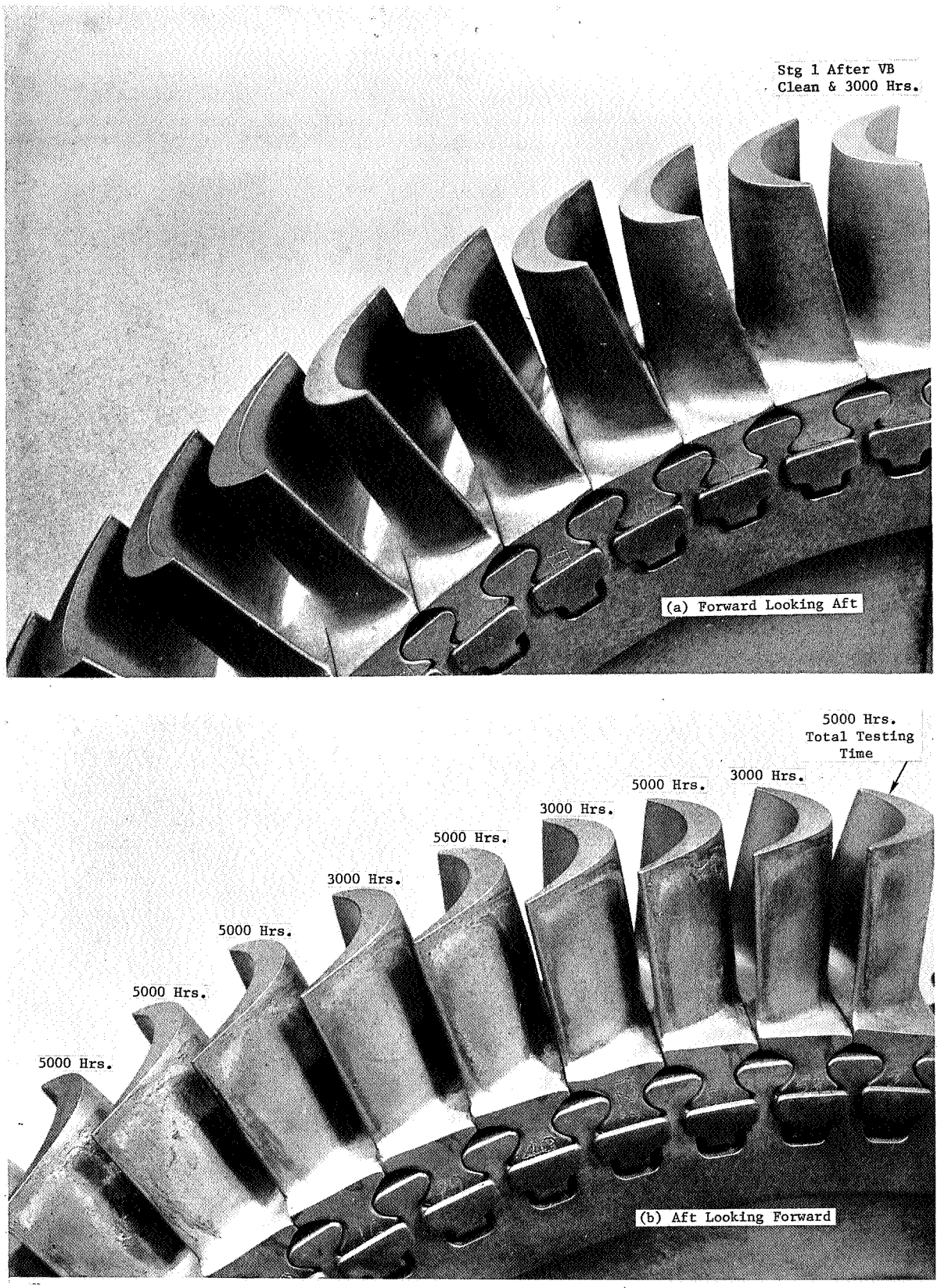
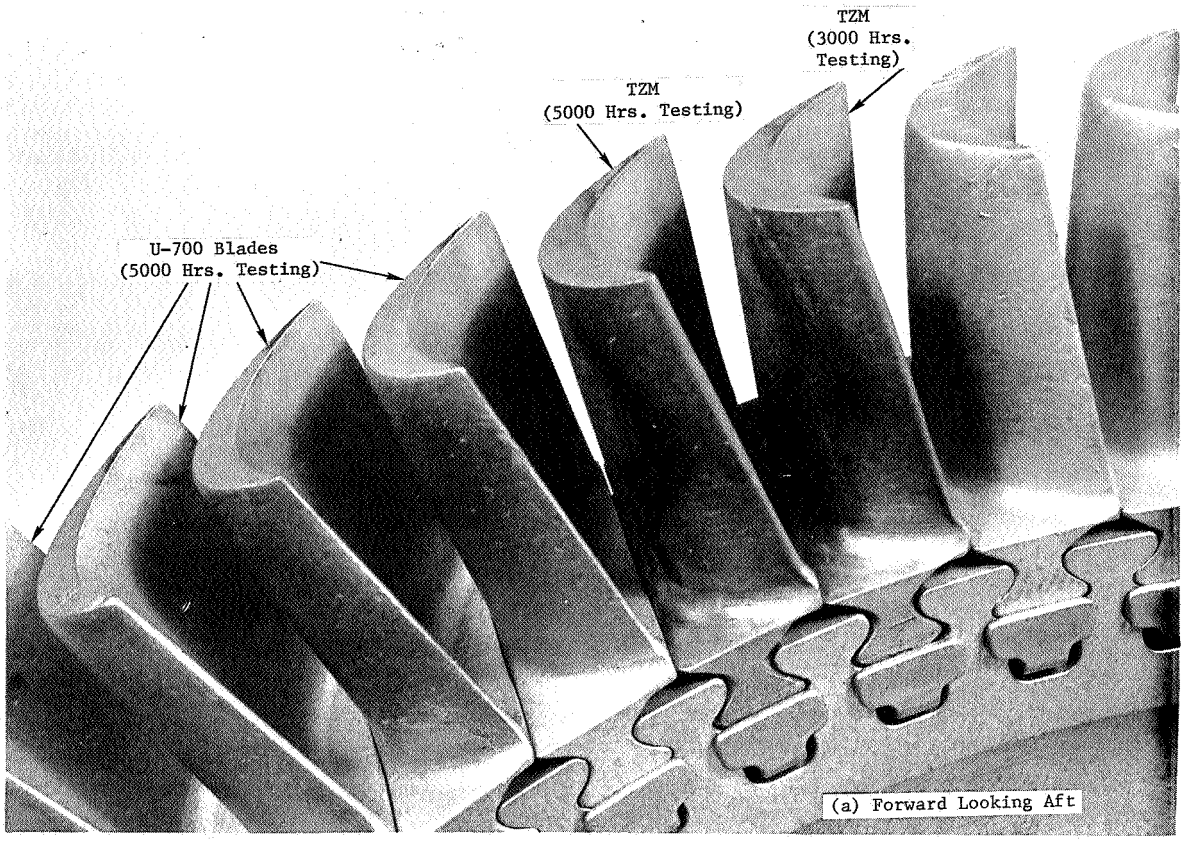


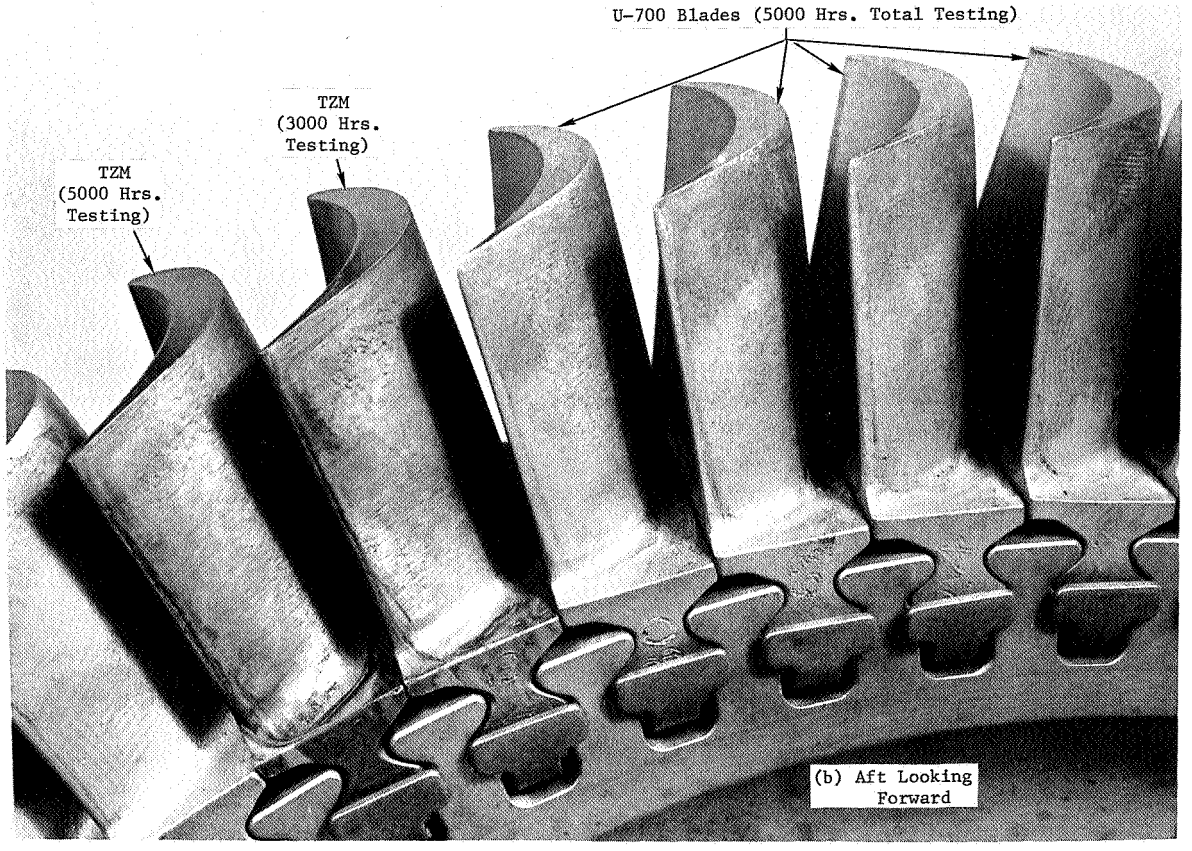
Figure 57. Partially Disassembled Wheel Following 3000 Hour Endurance Test.



T5433-58

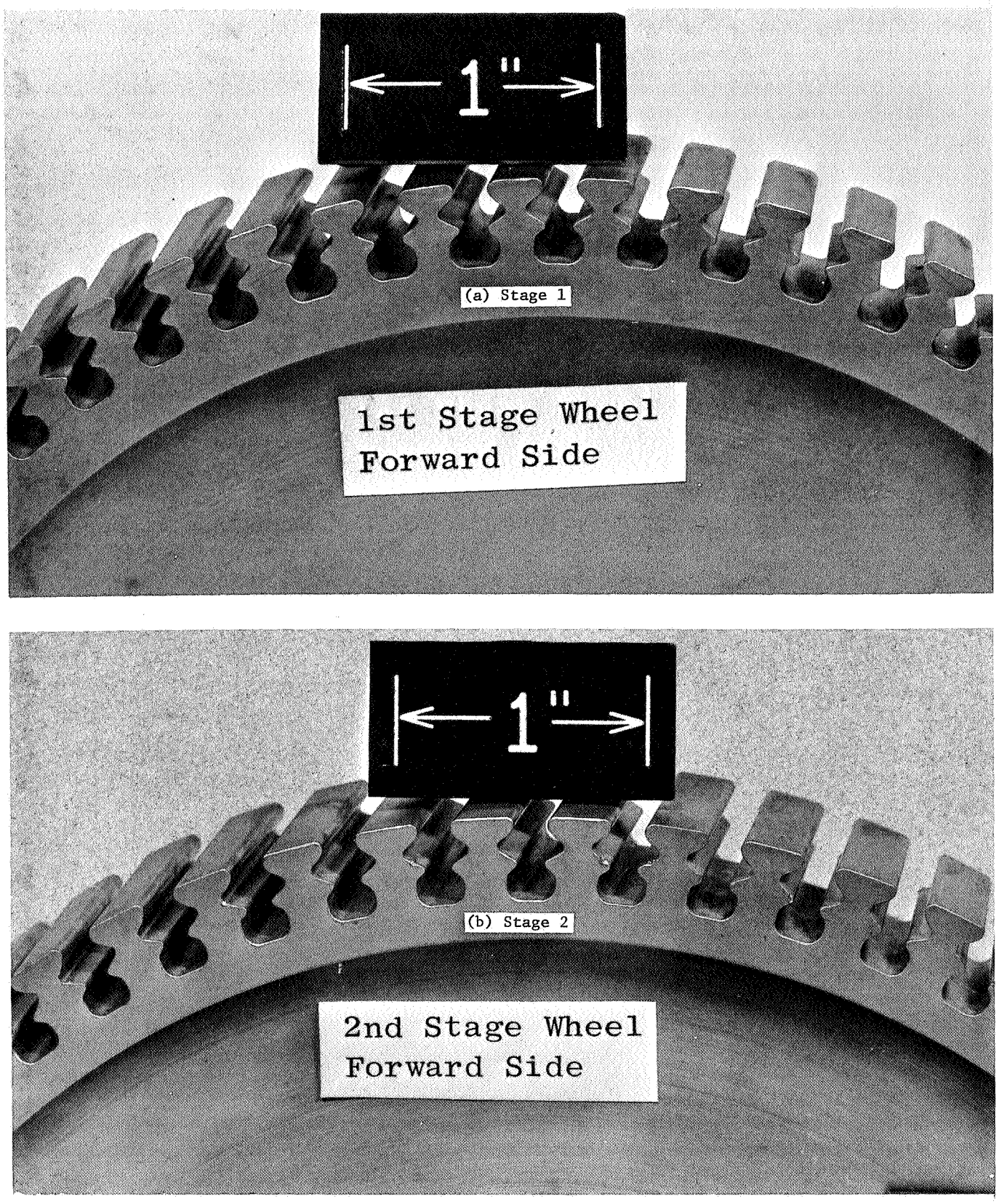
Figure 58. **Stage One Blade-Wheel** Assembly Following 3000 Hour **Endurance Test and Vapor Blast** Cleaning.





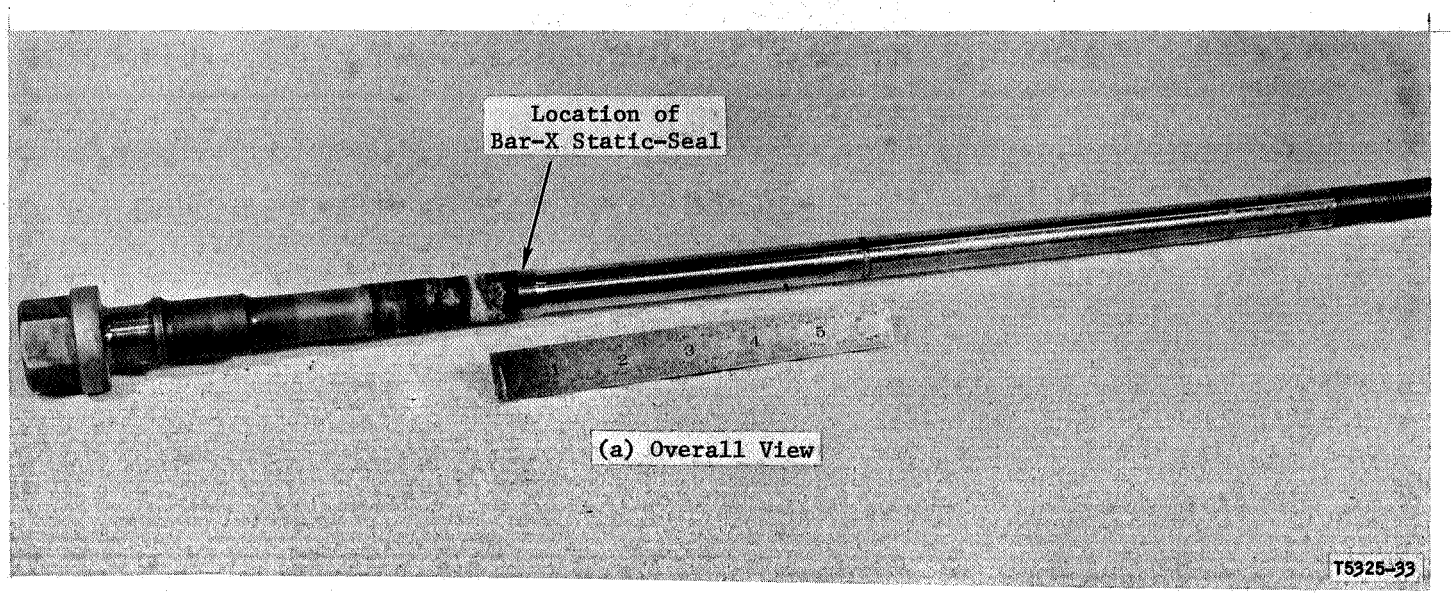
10433-59

Figure 59. Stage Two Blade-Wheel Assembly Following 3000 Hour Endurance Test and Vapor Blast Cleaning.



T5433-60

Figure 60. **Turbine Wheel Segment** Following 3000 Hour Endurance Test.



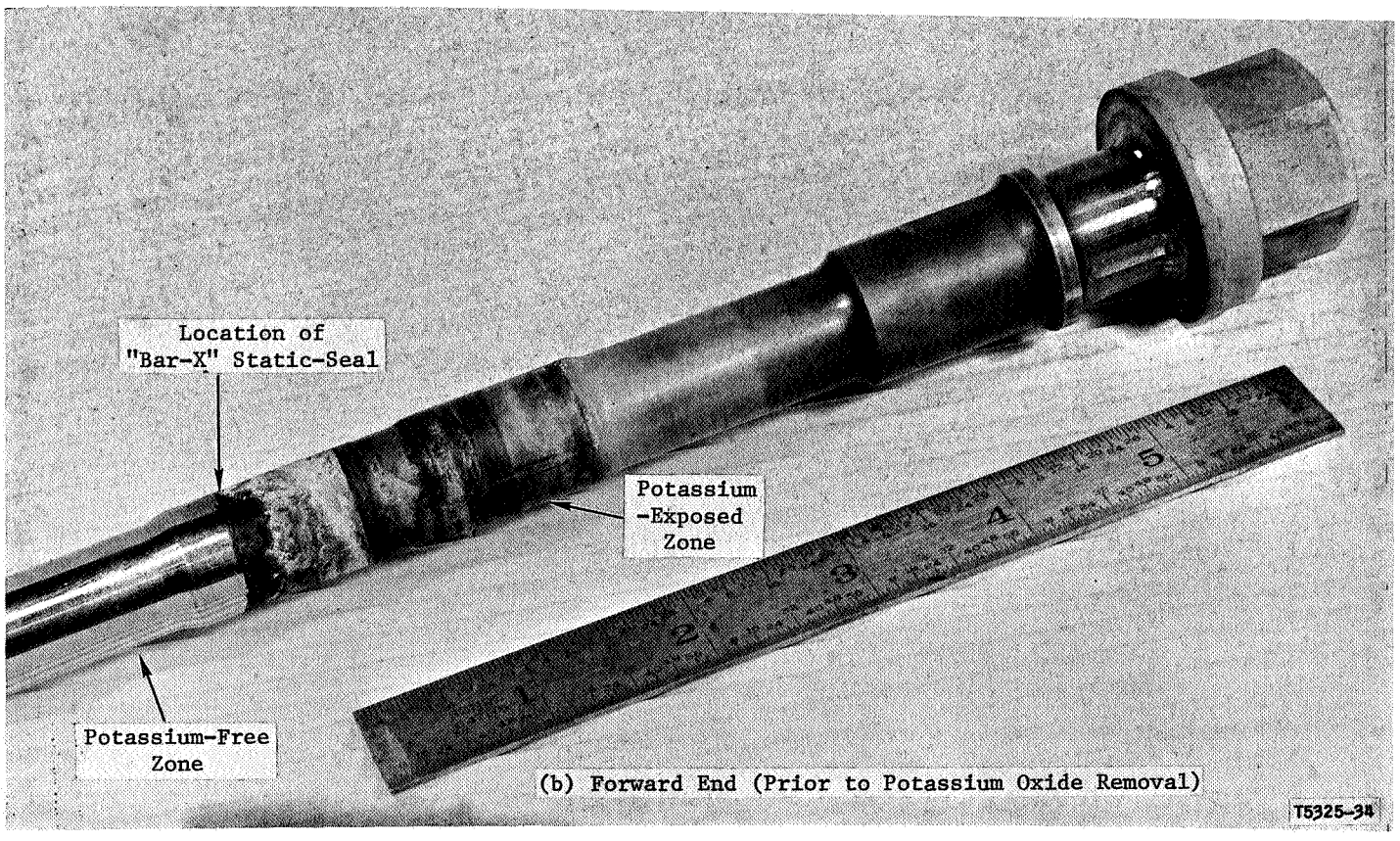
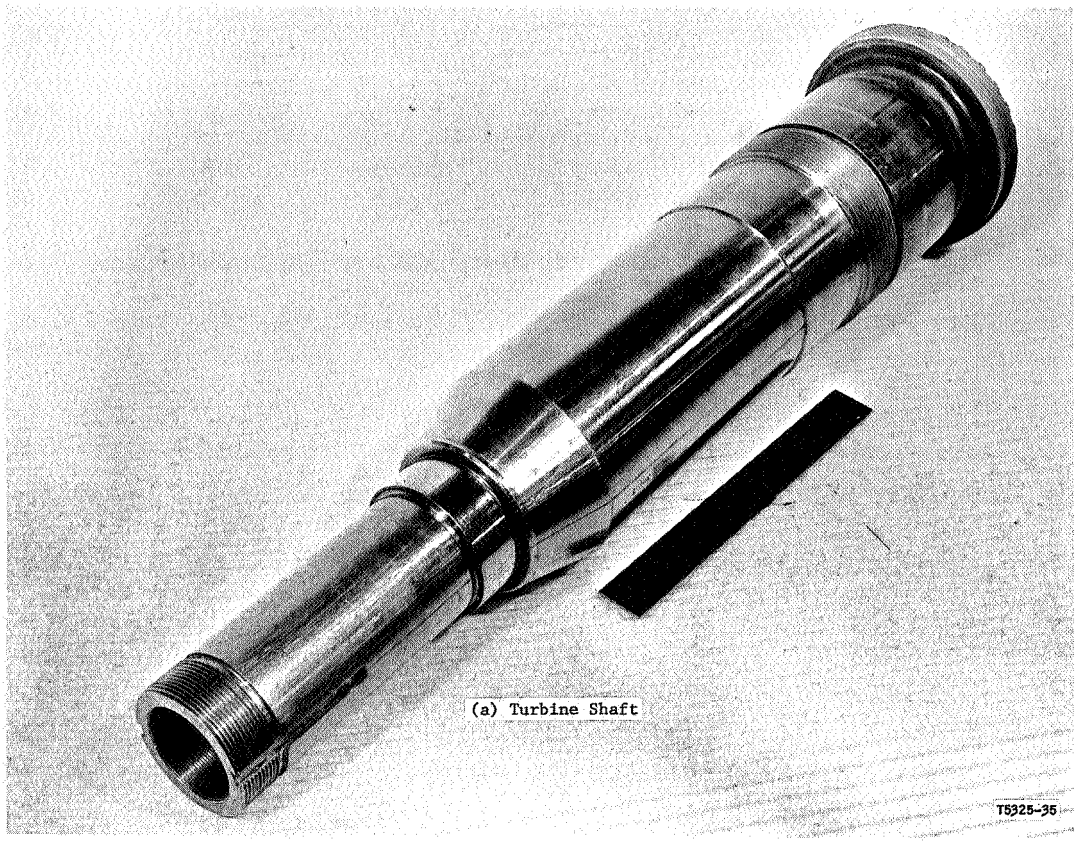


Figure 61. Tie Bolt Following 3000 Hour Endurance Test.



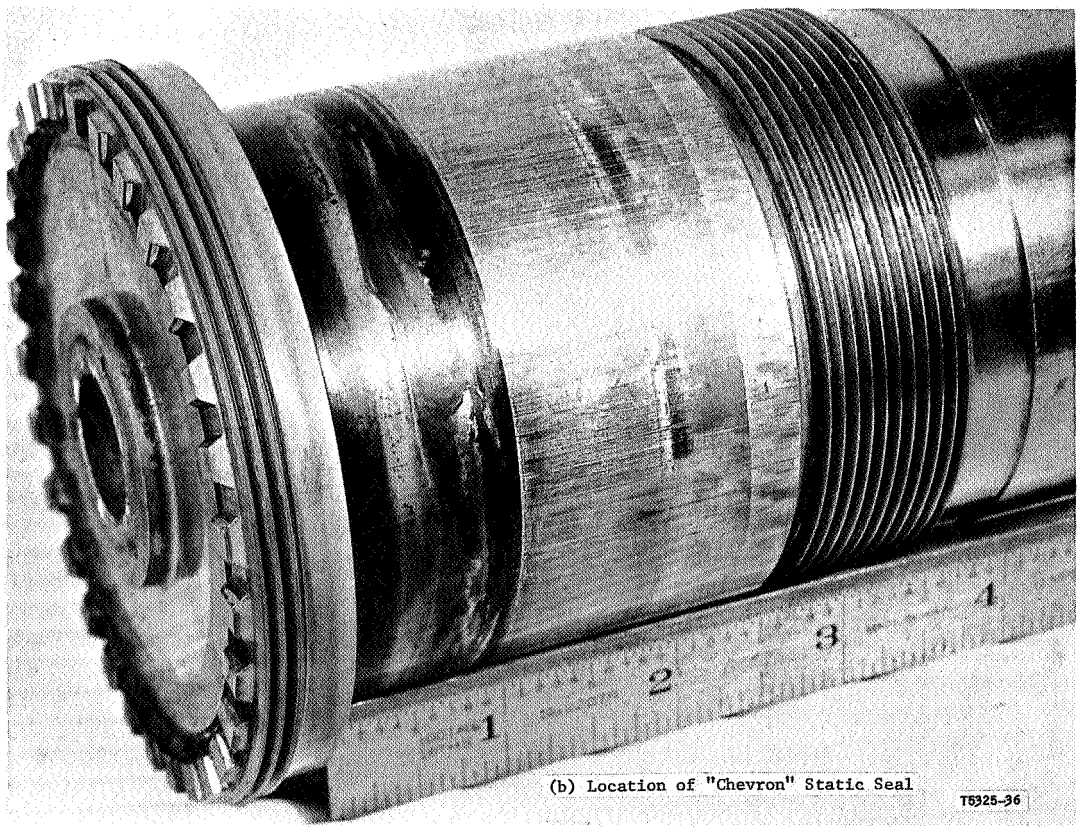


Figure 62. Turbine Shaft Following 3000 Hour Test (Matl: A286).

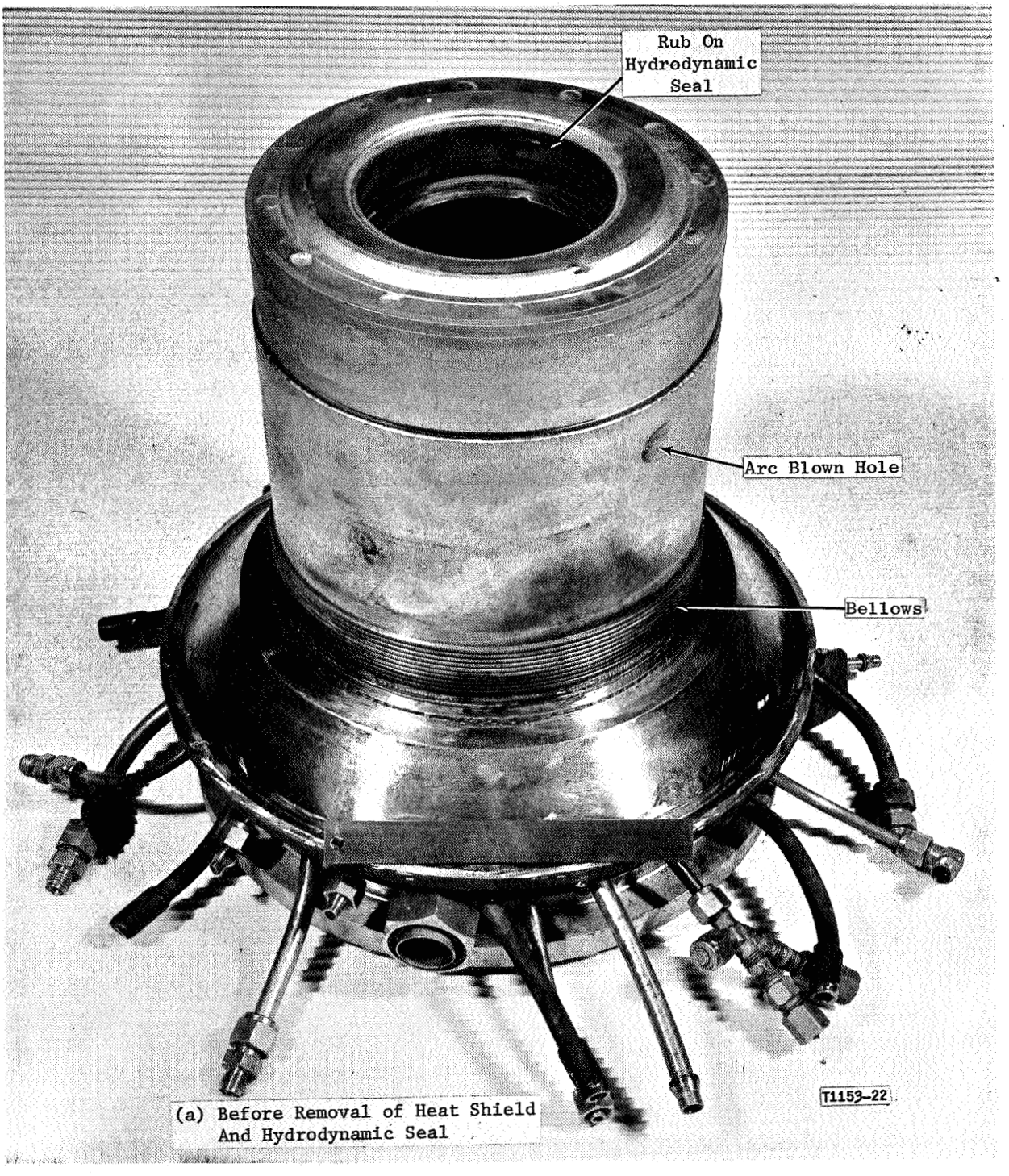


Figure 63a. Bearing Housing Assembly After the 3000-Hour Test.

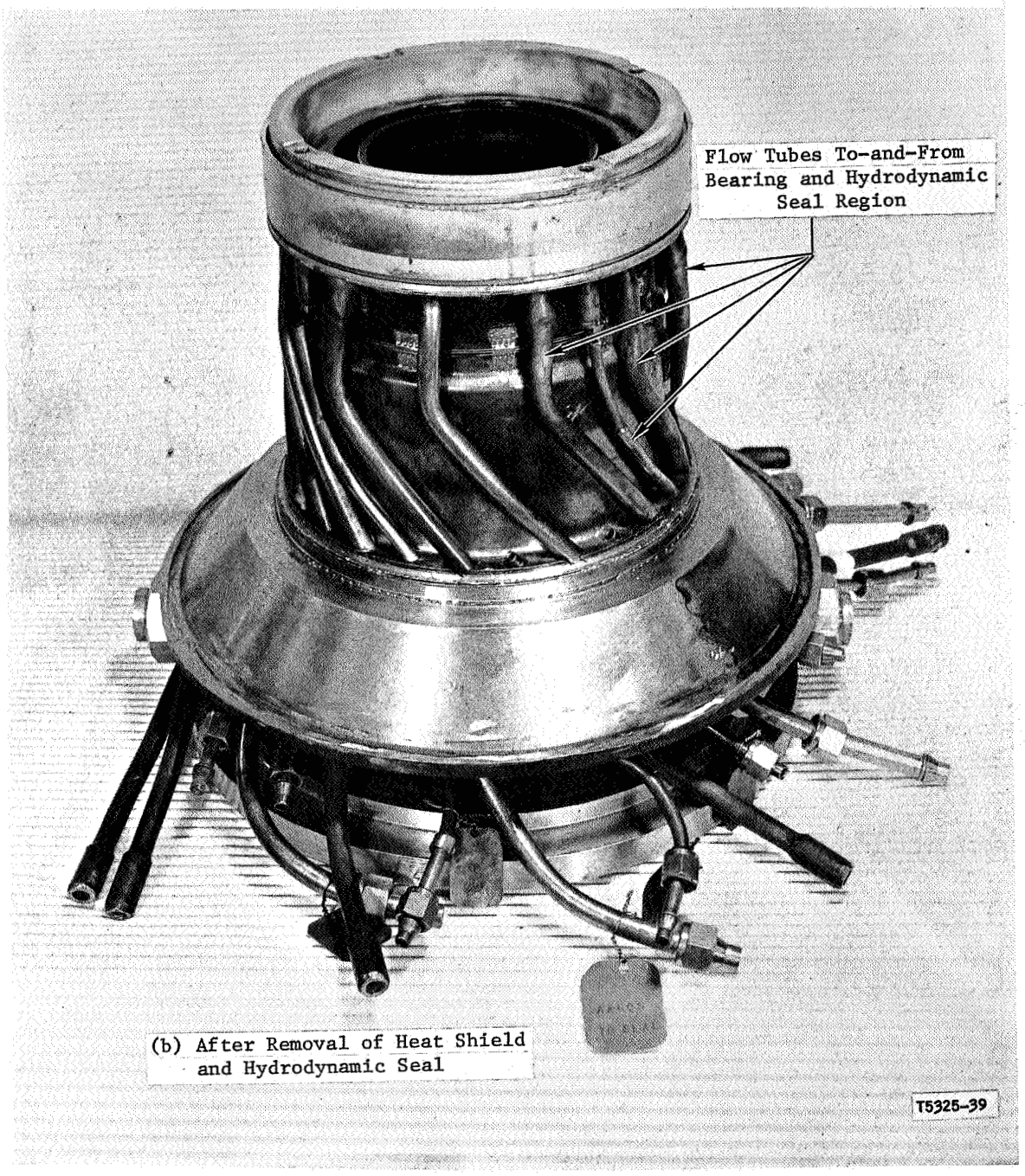


Figure 63b. **Bearing Housing** Assembly After the 3000-Hour Test.

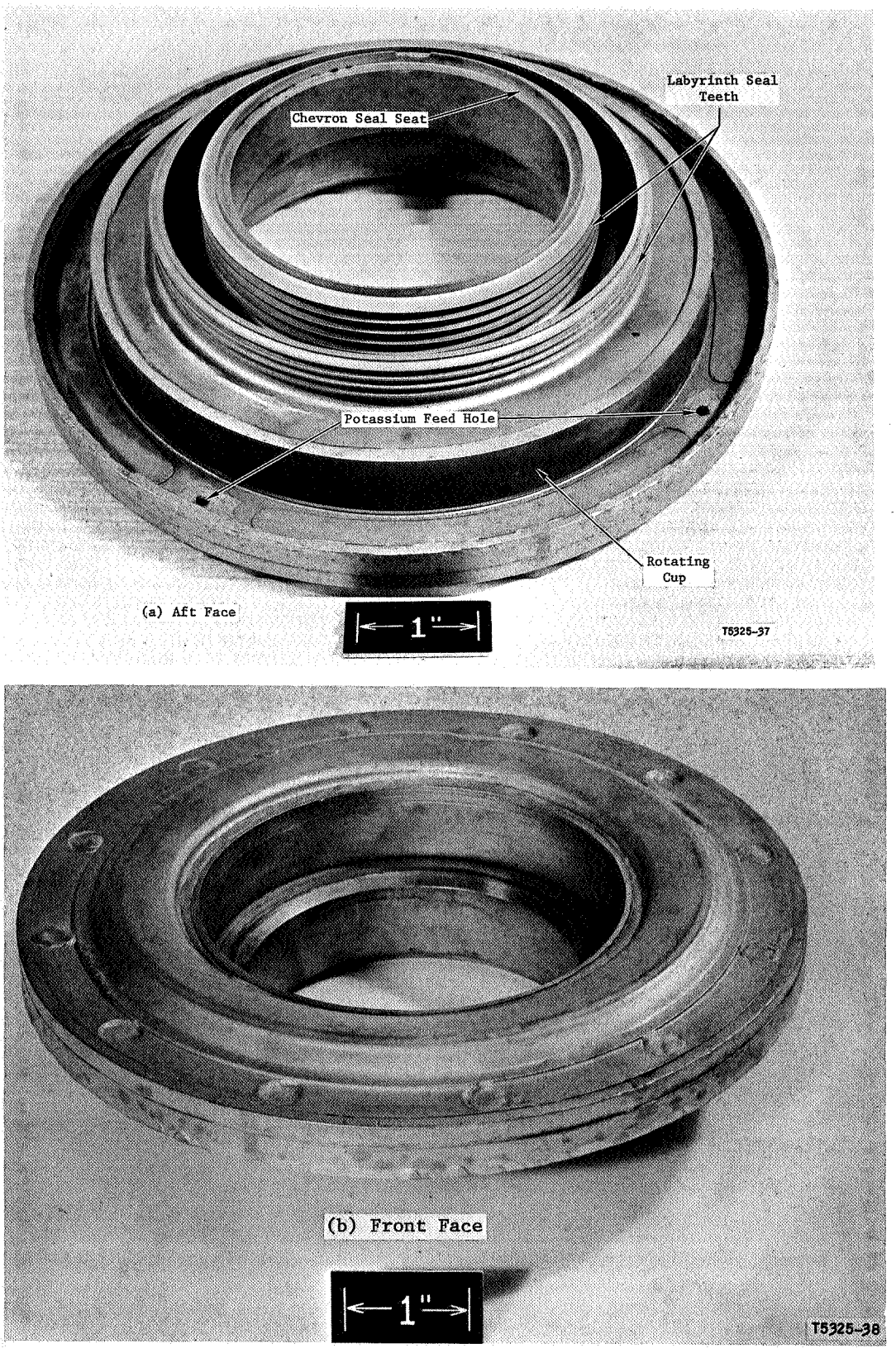


Figure 64. **Hydrodynamic** Seal Following 3000 Hour Endurance Test.

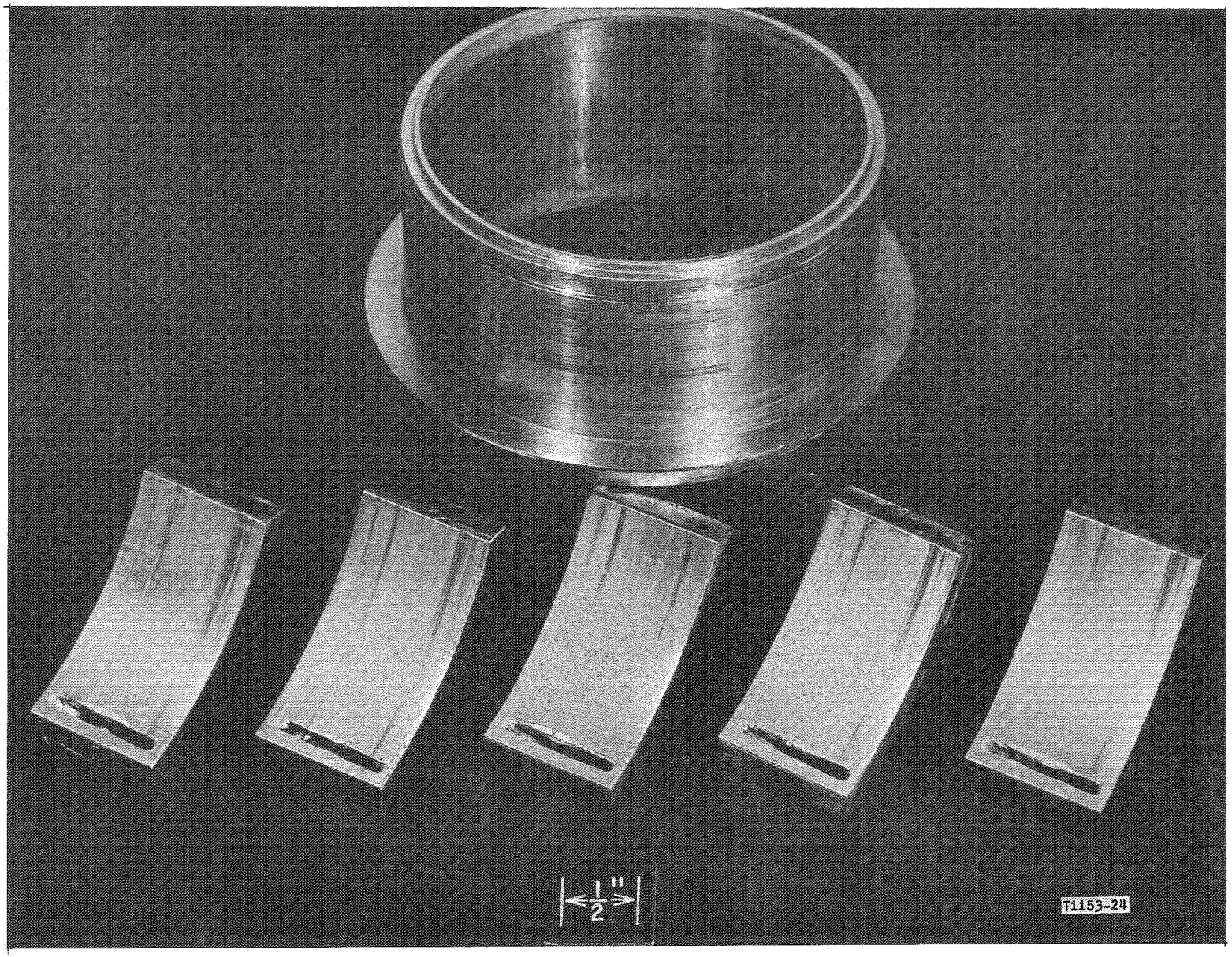


Figure 65. Bearing Pads and Journal Sleeve After 3000 Hour Endurance Test. (CDC 6655)

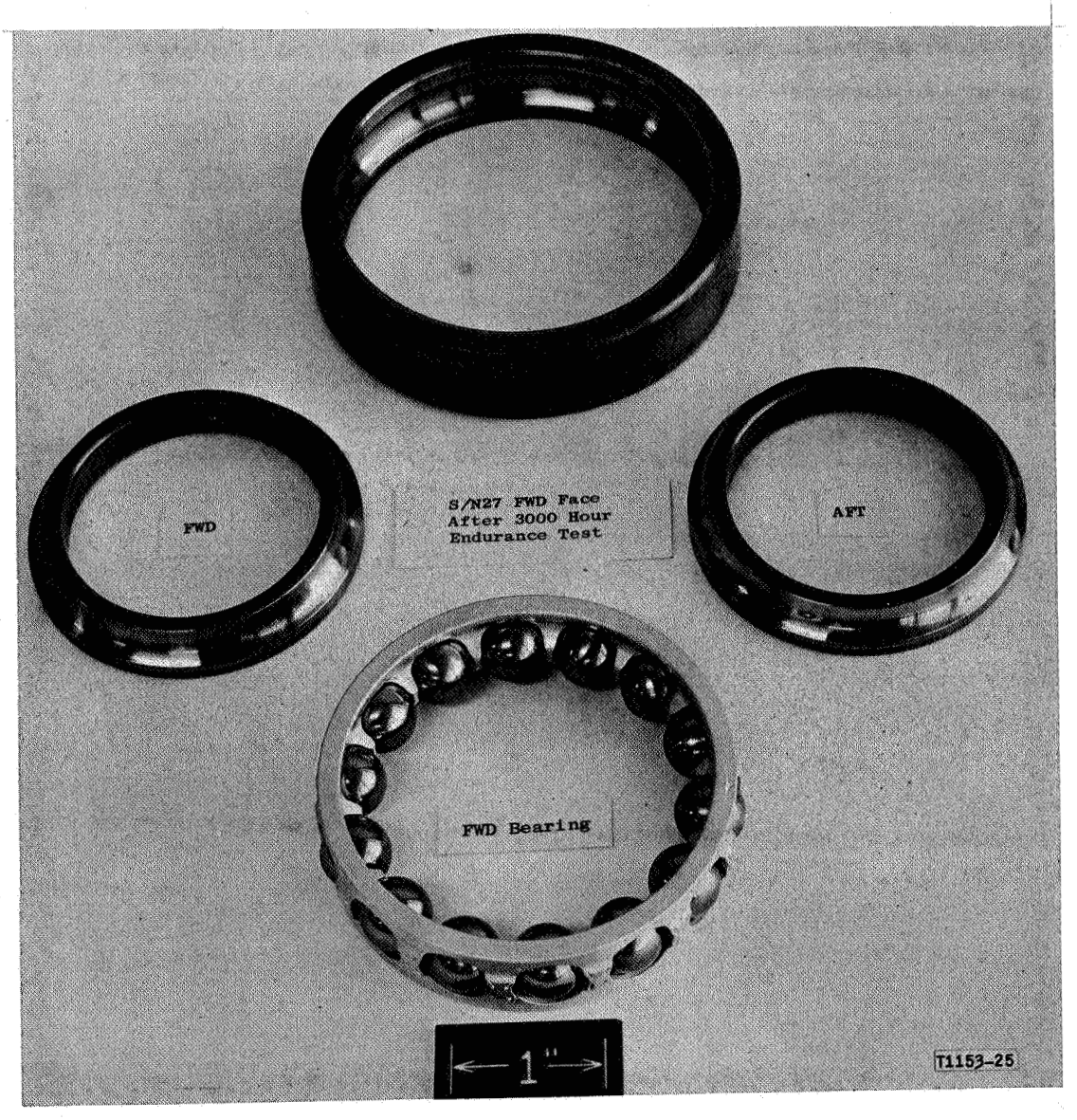
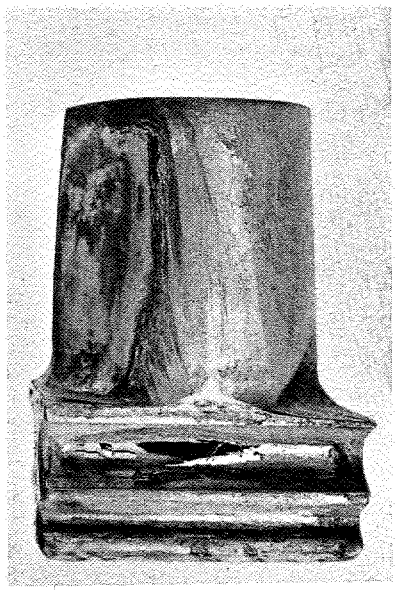


Figure 66. Ball Thrust Bearing After 3000 Hour Test. (C66100363)

TYPE OF TEST: 2000 Hr. 3000 Hr. 5000 Hr.

MATERIAL:

U-700



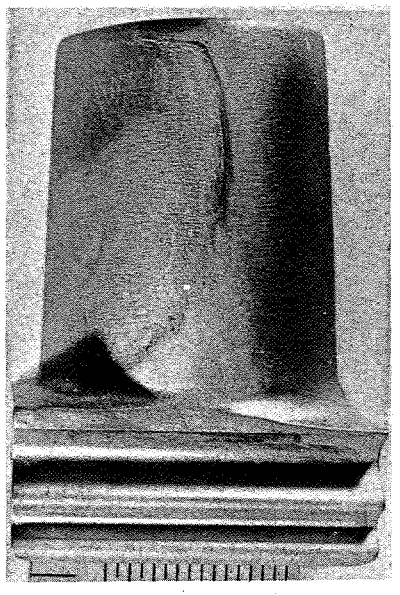




FIRST STAGE Mag: 1.5X

U-700



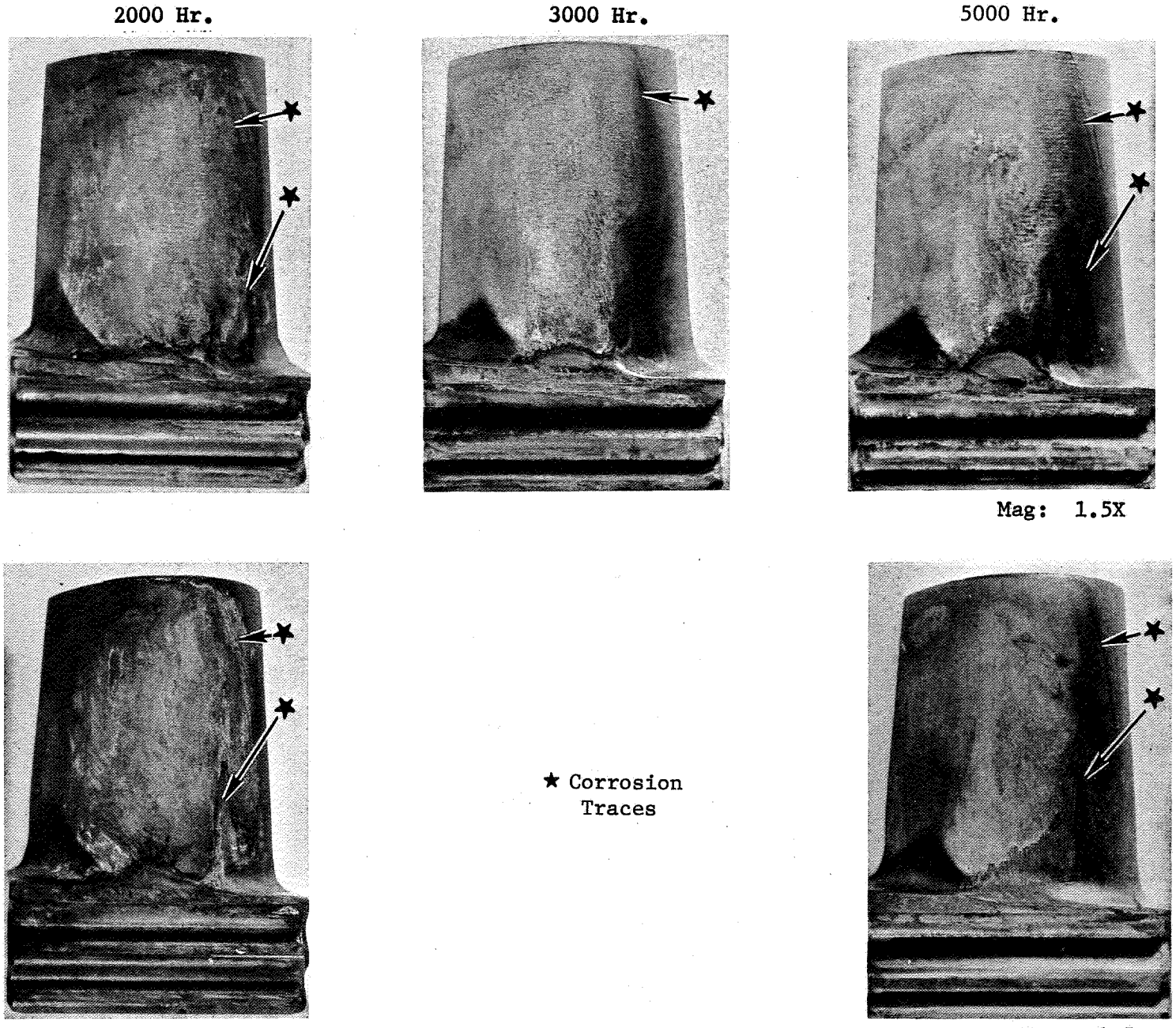




SECOND STAGE Mag: 1.5X

Figure 67. Convex Blade Surfaces After Potassium Turbine Test.

T5433-67



T5433-68

Figure 68. Convex Blade Surfaces After Potassium Turbine Test, Second Stage.

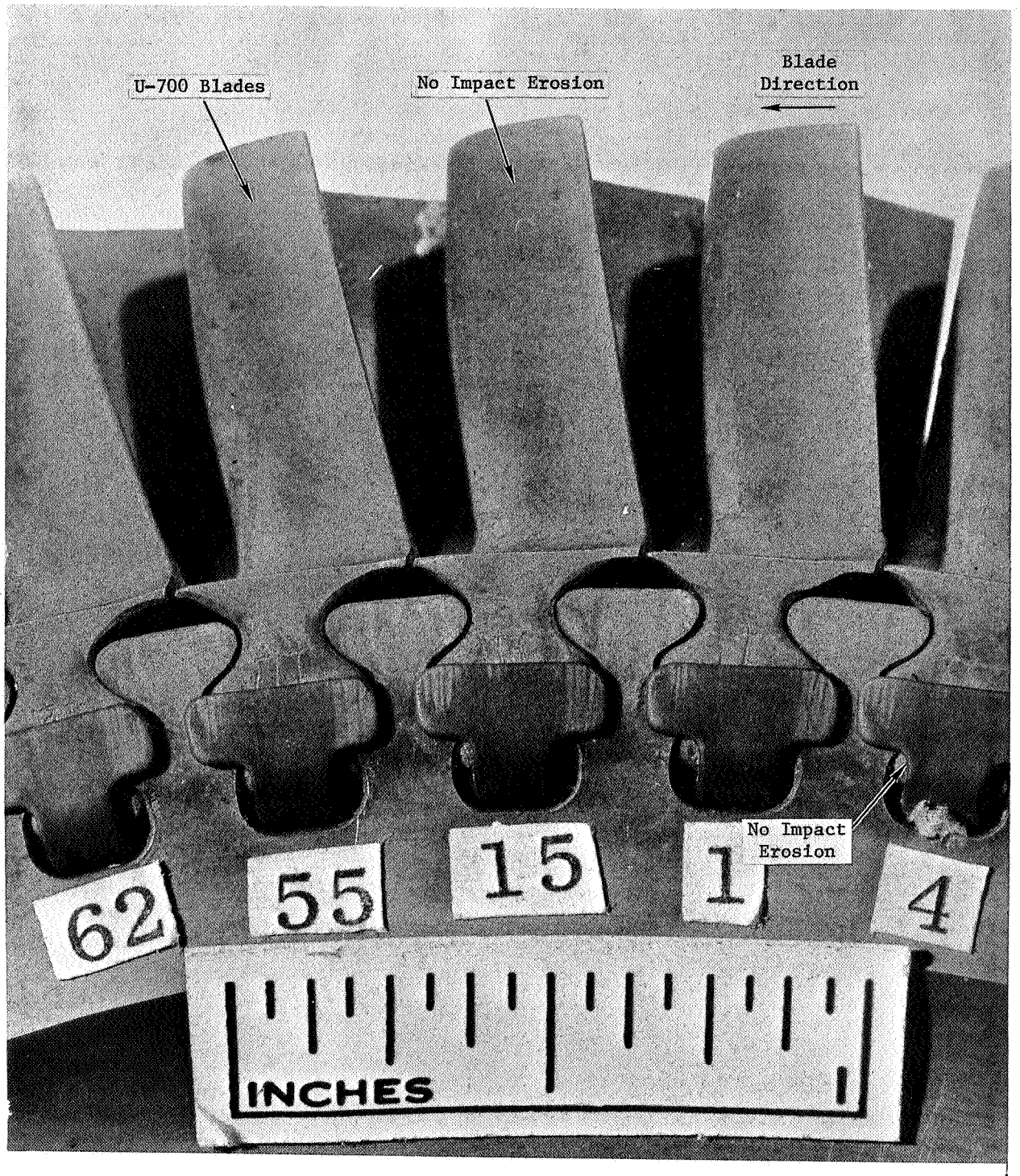
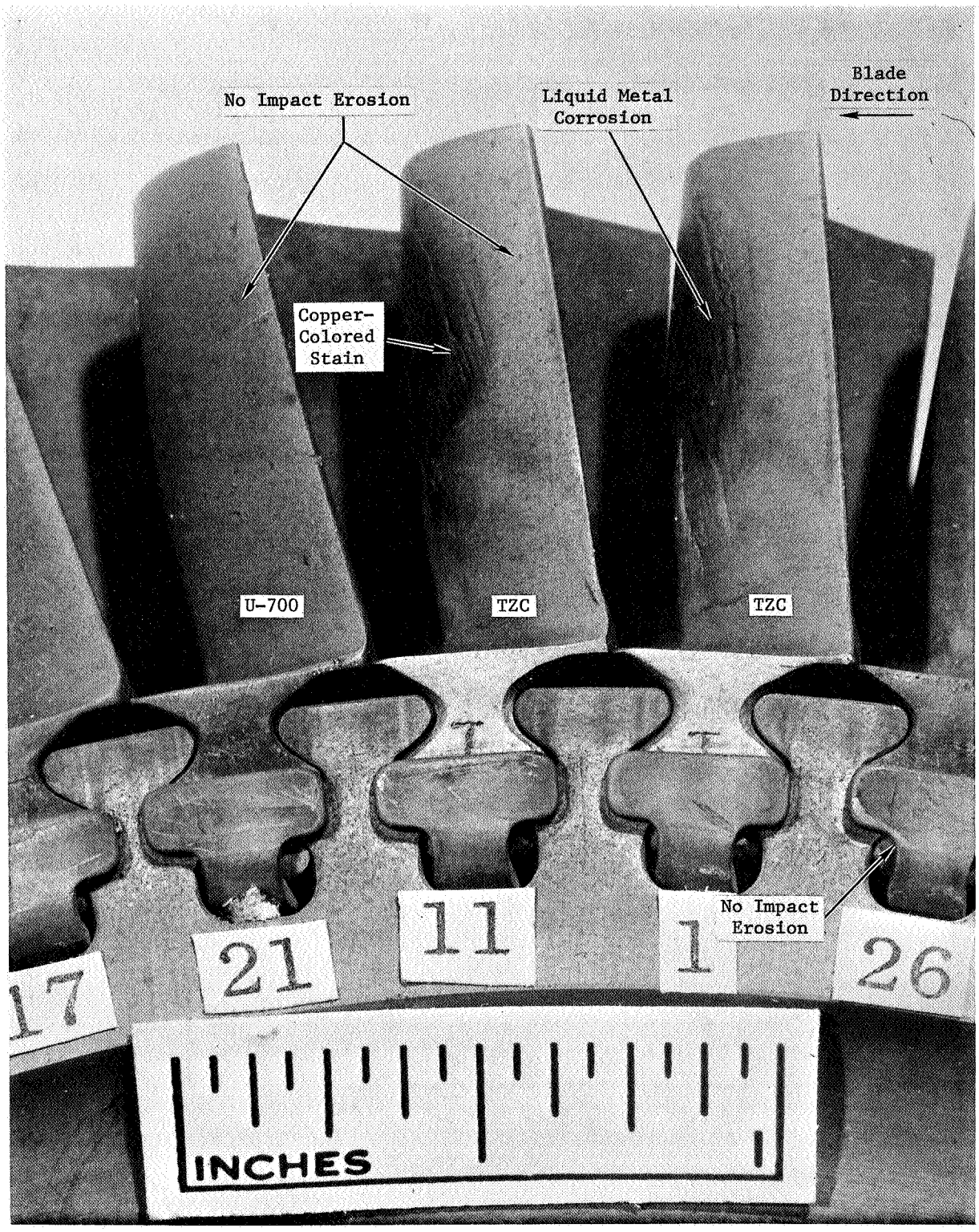


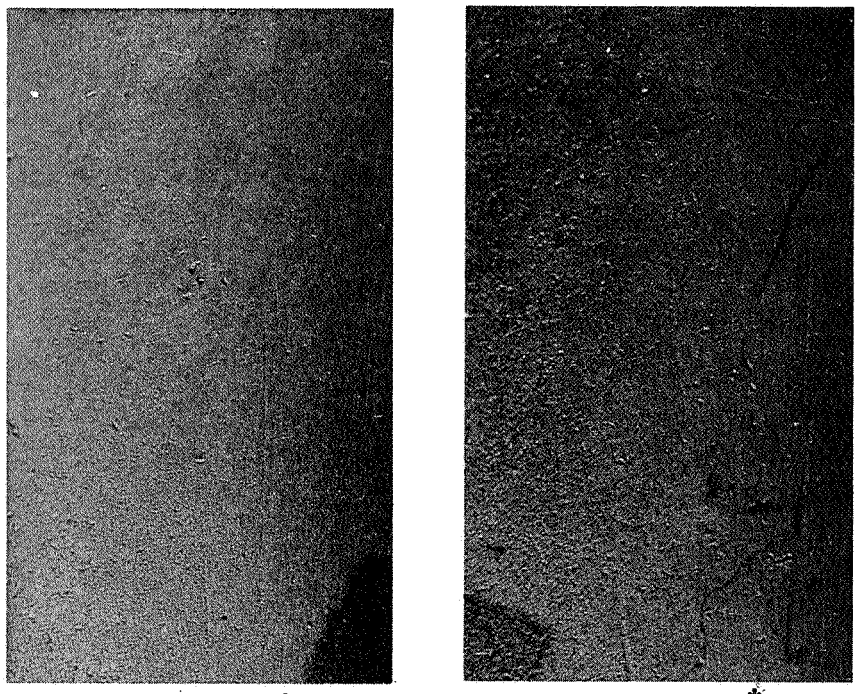
Figure 69. Convex Leading Edges of First Stage U-700 Turbine Blades After 3000-Hour Turbine Test. Note Absence of Impact Erosion Damage on These Cleaned and Lightly Vapor Blasted Airfoils. 433-69



T5433-70

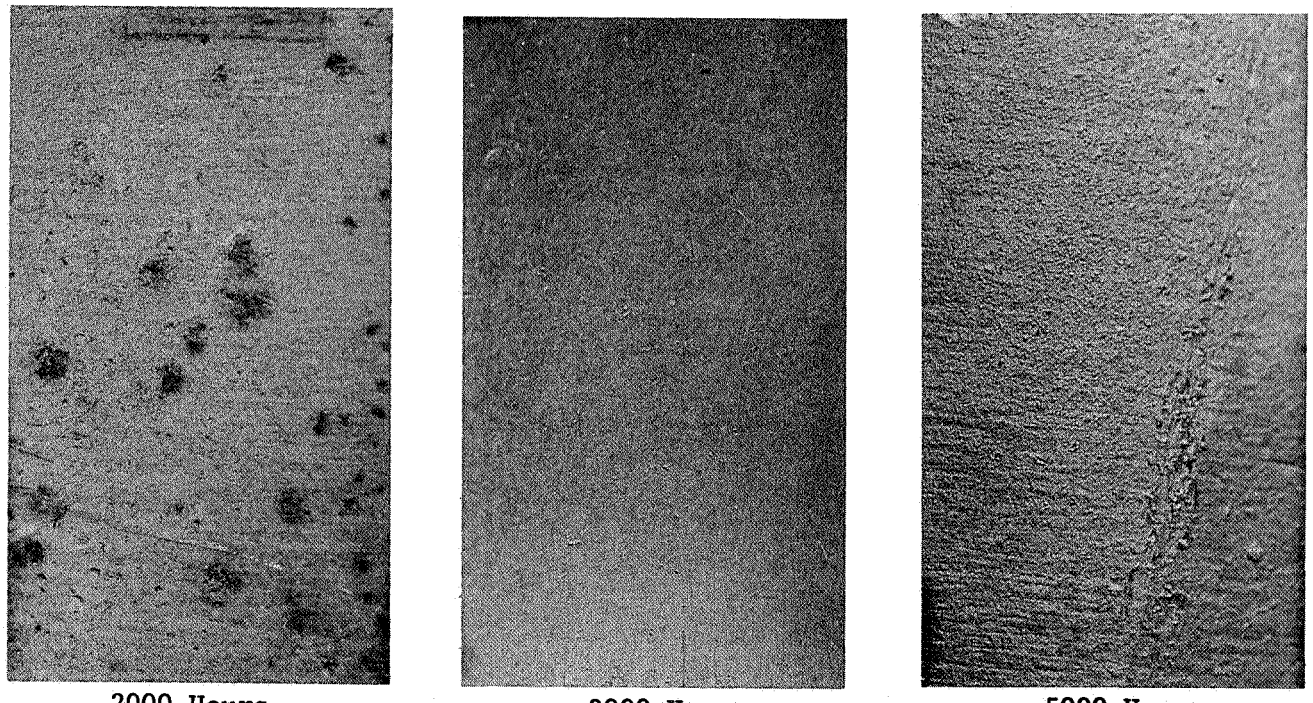
Figure 70. Convex Leading Edges of Second Stage U-700 and TZC Blades. Note Absence of Impact Erosion Damage on These Cleaned and Lightly Vapor Blasted Blades and the Presence of Corrosion Traces on the Two TZC Blades.

FIRST STAGE:



3000 Hours* 5000 Hours*

SECOND STAGE:



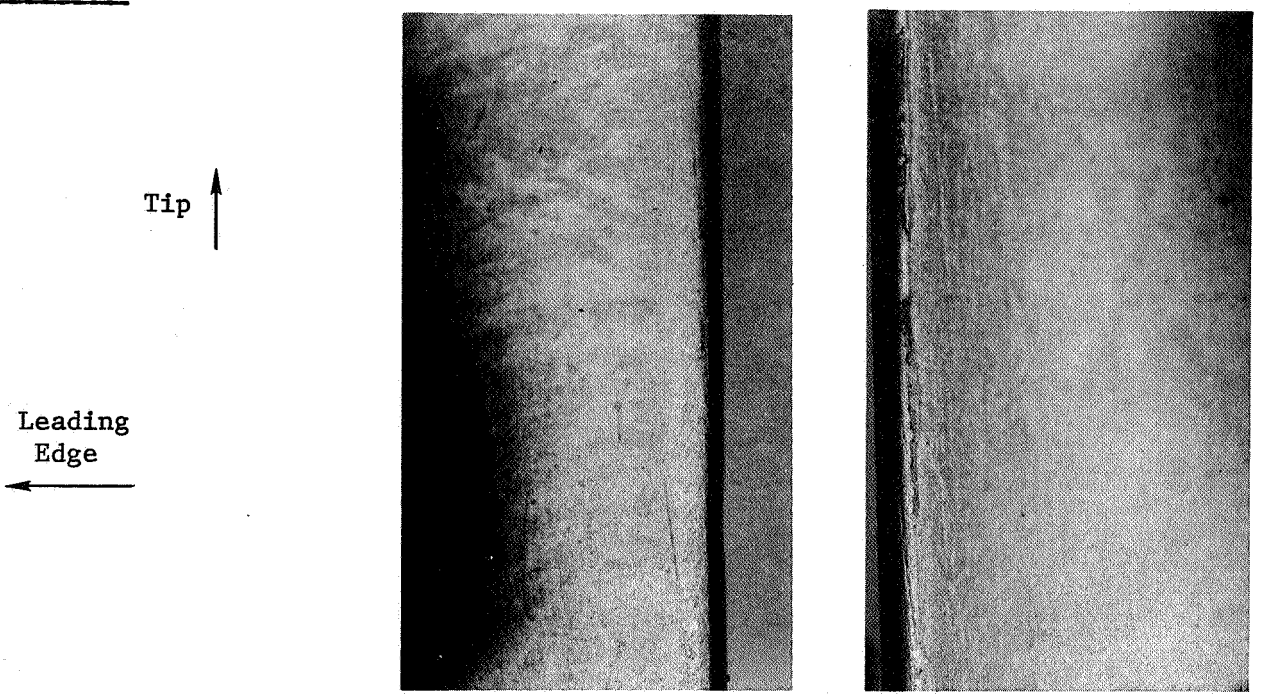
2000 Hours 3000 Hours 5000 Hours

T5433-71

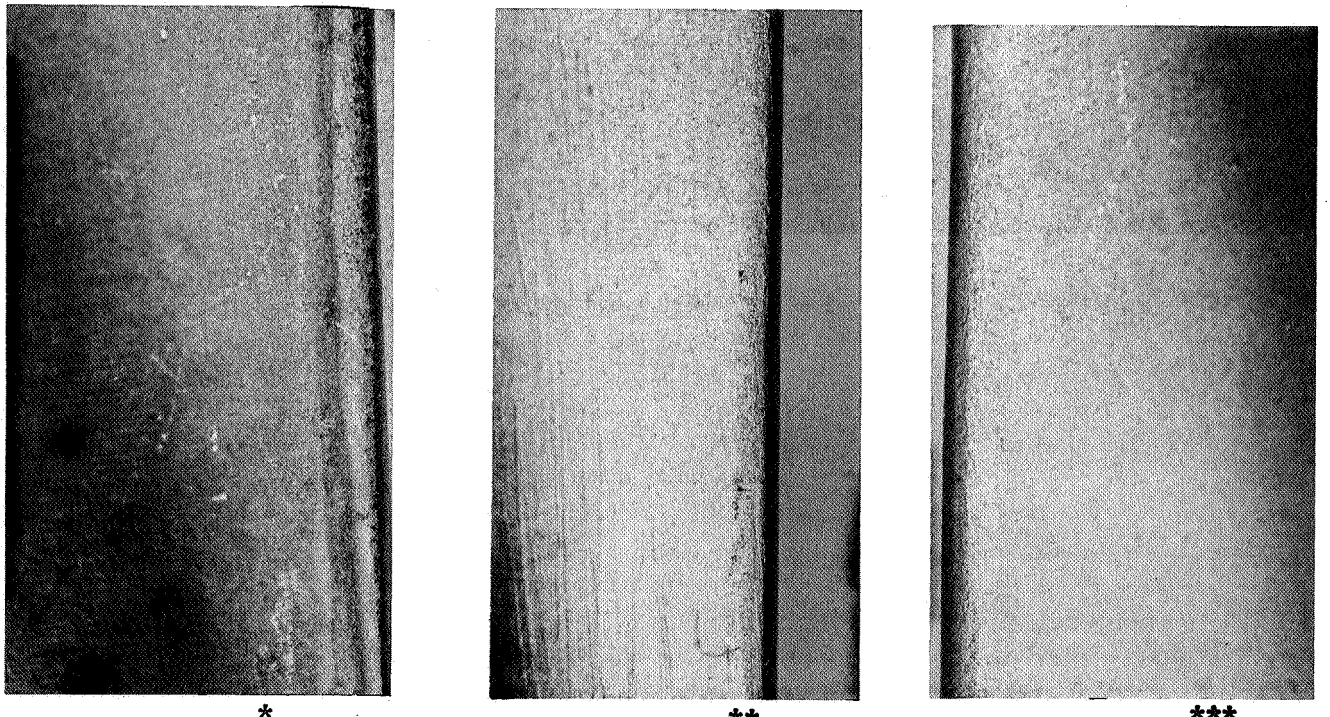
*Pits were Produced During Prior Steam Testing of Turbine

Figure 71. Convex Mid-Chord Airfoil Surfaces of U-700 Turbine Blades.
Mag: 10X

FIRST STAGE:



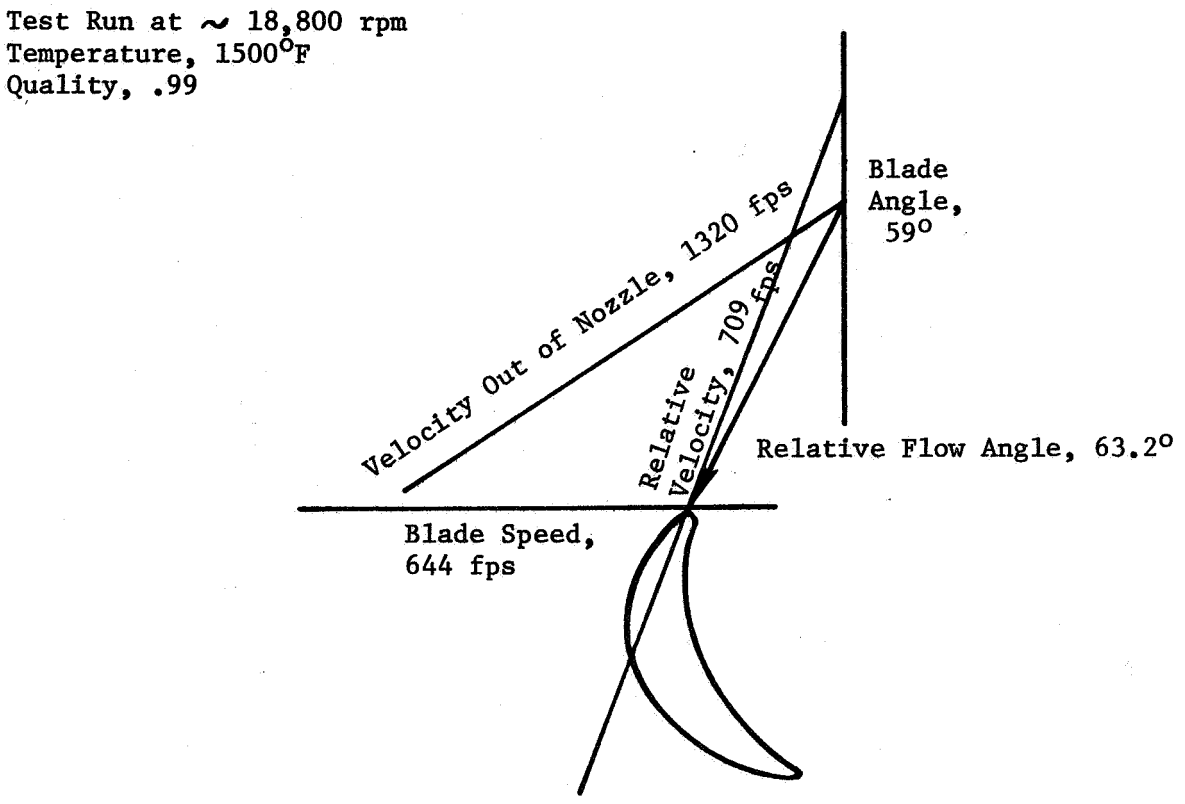
SECOND STAGE:



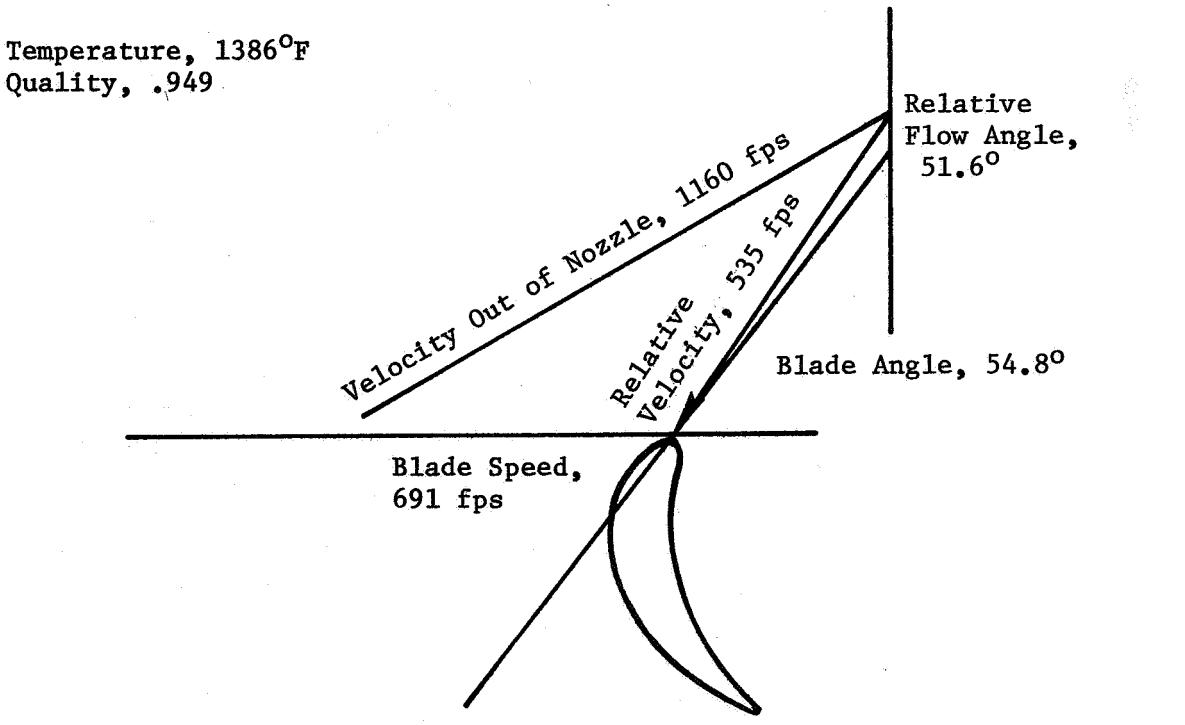
*Relatively Minor Corrosion
**No Evidence of Corrosion
***Apparent Removal of 2000-Hour Corrosion Evidence

T5433-72

Figure 72. Concave Leading Edge Airfoil Surfaces of U-700 Turbine Blades. Mag: 10X



(a) First Stage



(b) Second Stage

T5433-73

Figure 73. Rotor Blade Inlet Velocity Diagrams.

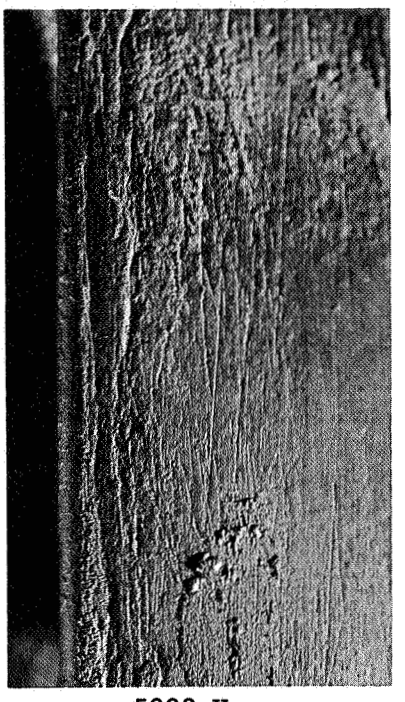
FIRST STAGE:

Tip

Trailing Edge

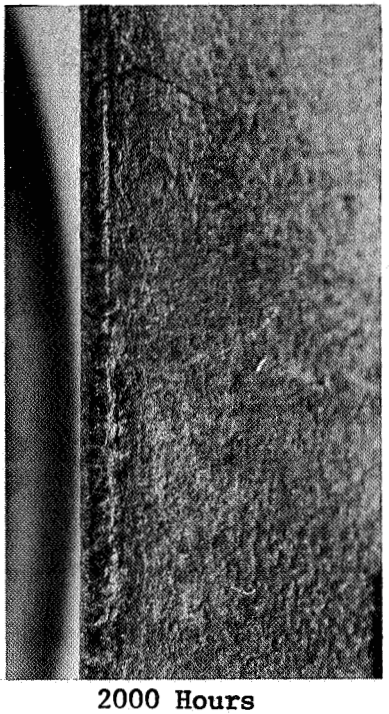


3000 Hours

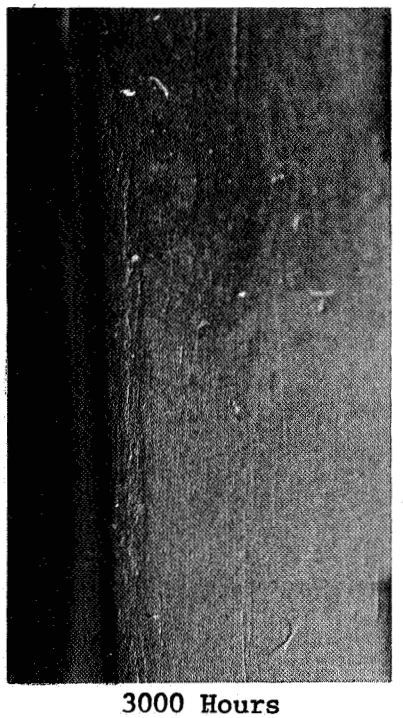


5000 Hours

SECOND STAGE:



2000 Hours



3000 Hours

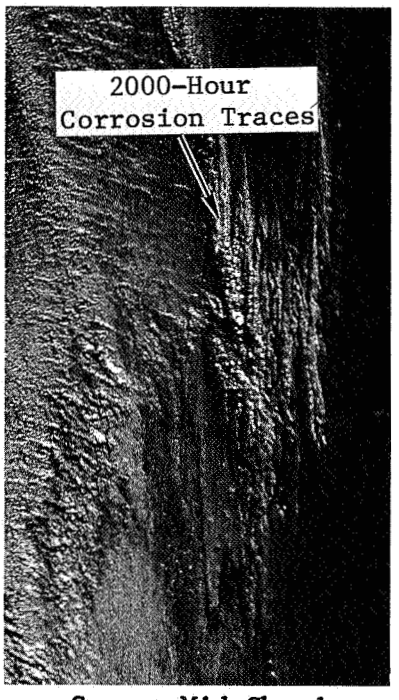


5000 Hours

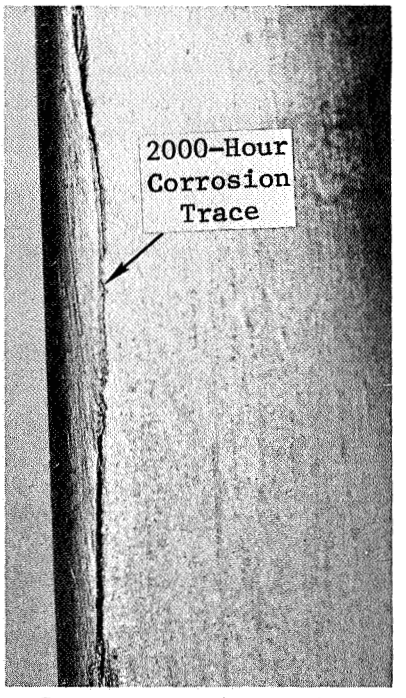
T5433-74

Figure 74. Convex Trailing Edge Airfoil Surfaces of U-700 Turbine Blades.
Mag: 10X

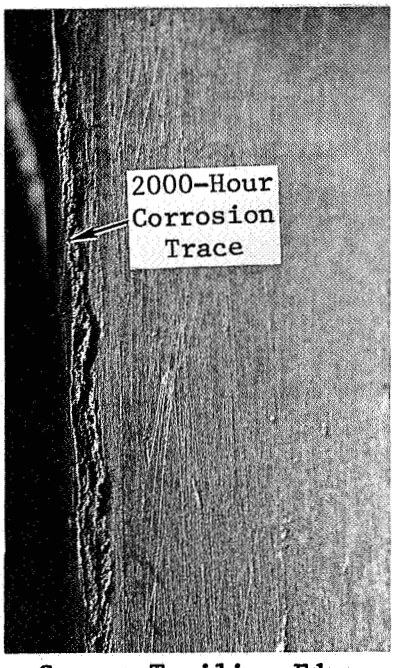
TZC:



Convex Mid-Chord

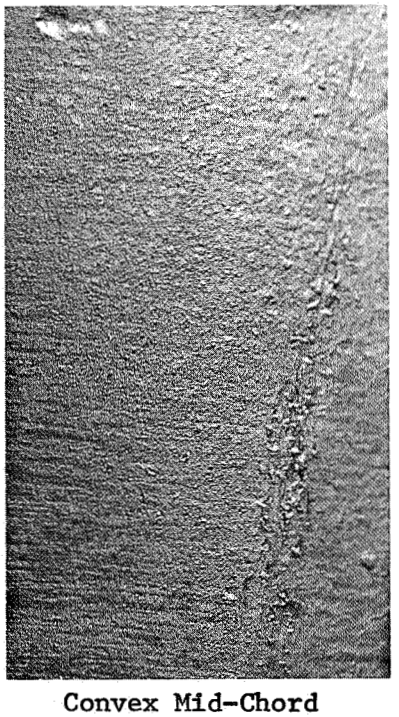


Concave Leading Edge

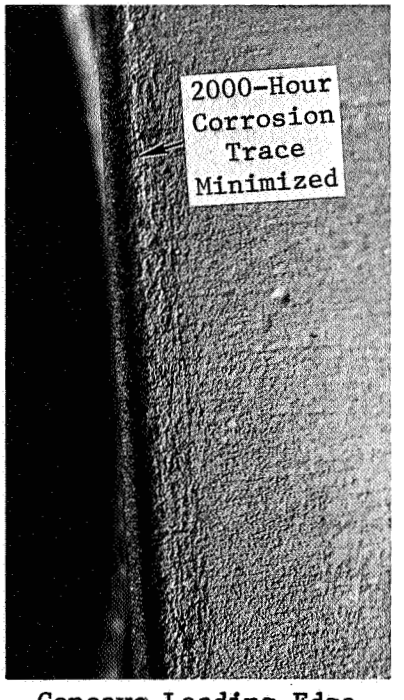


Convex Trailing Edge

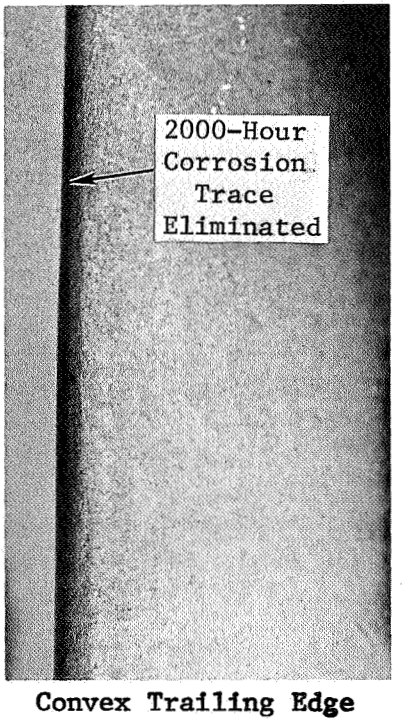
U-700:



Convex Mid-Chord



Concave Leading Edge



Convex Trailing Edge

T5433-75

Figure 75. Comparison of Airfoil Surfaces of Second Stage U-700 and TZC Blades After 5000 Hours Testing. Mag: 10X

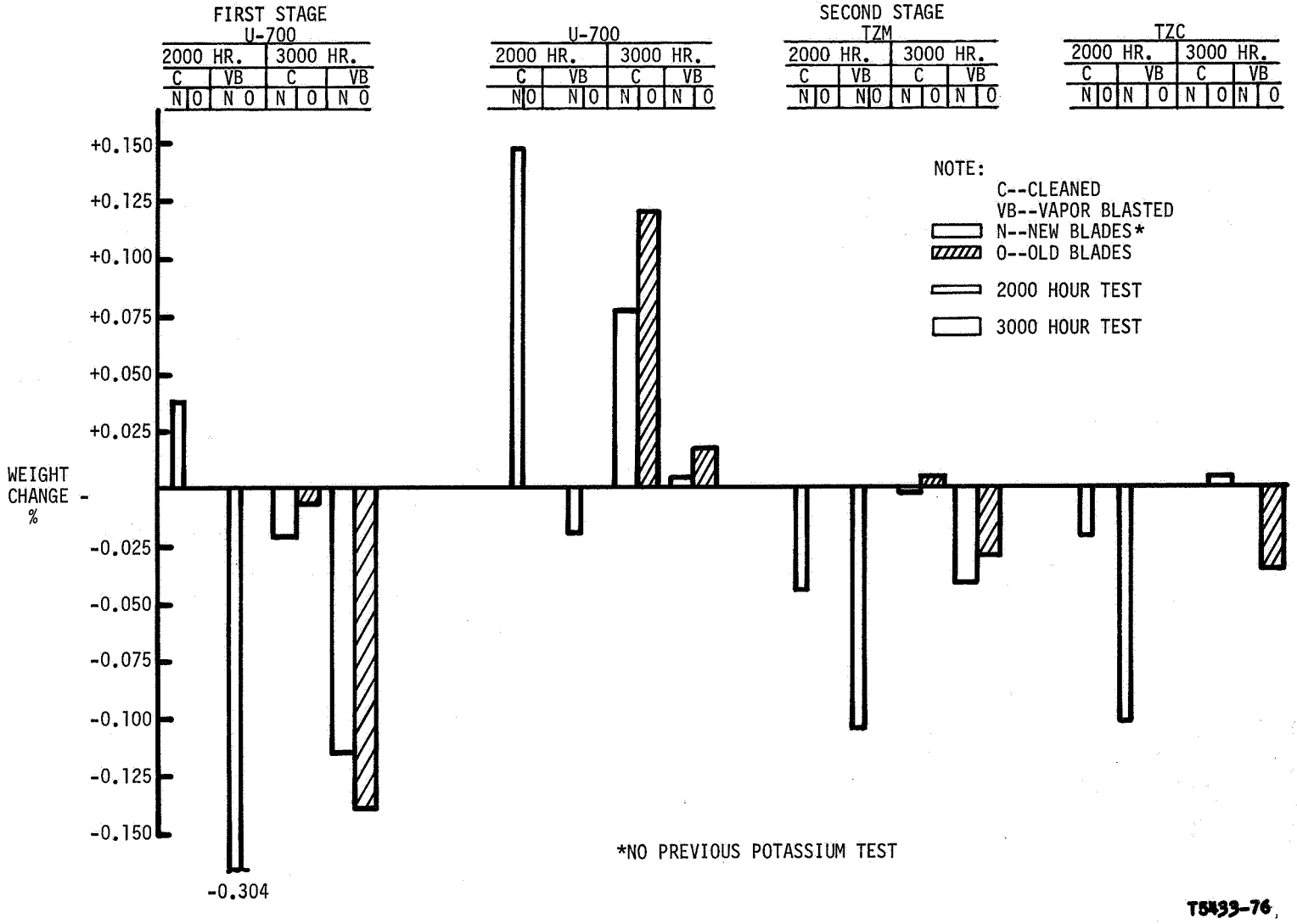
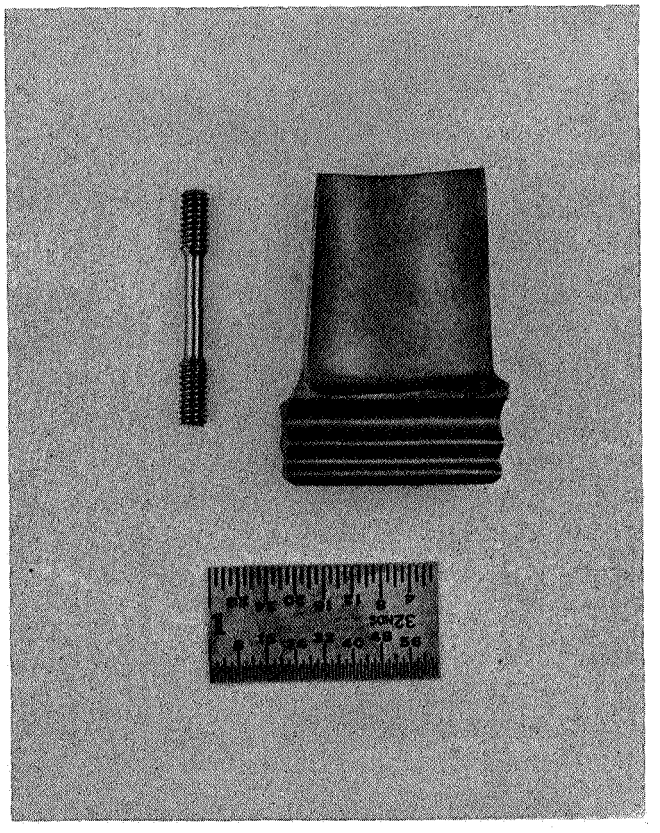


Figure 76. Blade Weight Changes After 2000-Hour and 3000-Hour Tests.



T5433-77

Figure 77. Miniature Tensile Bar Taken From a Second Stage U-700 Blade After 2000 Hours Test at 1260°F. A Second Stage U-700 Blade is Shown for Comparison. (MCRA 3043)

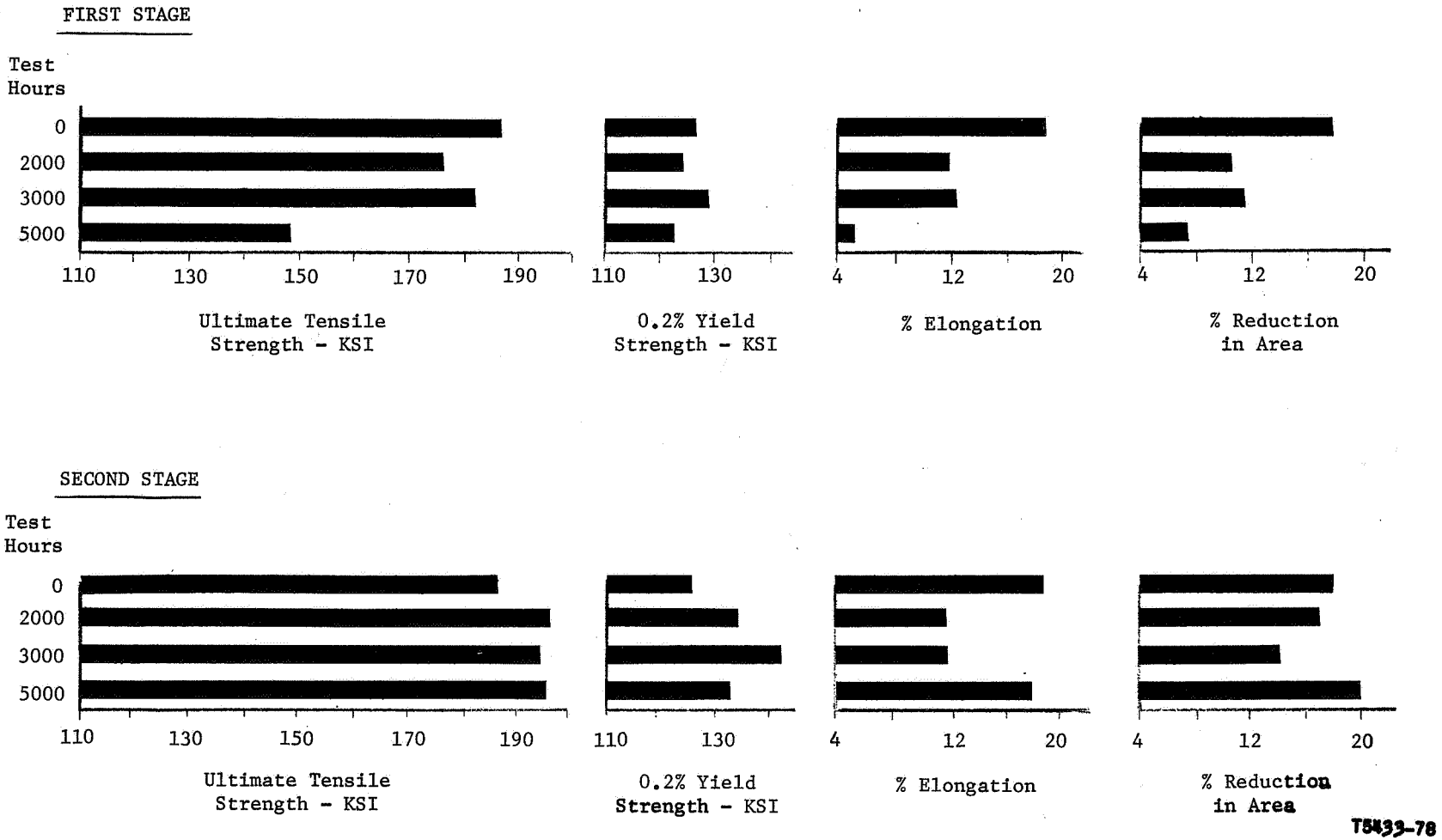
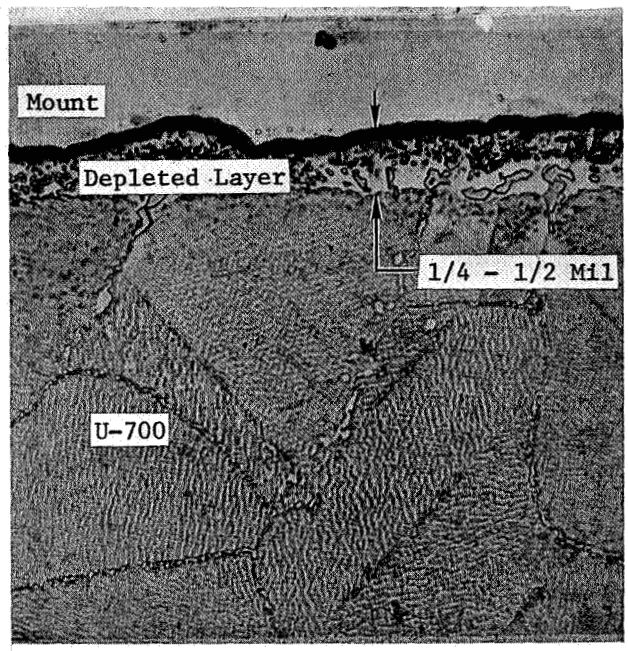


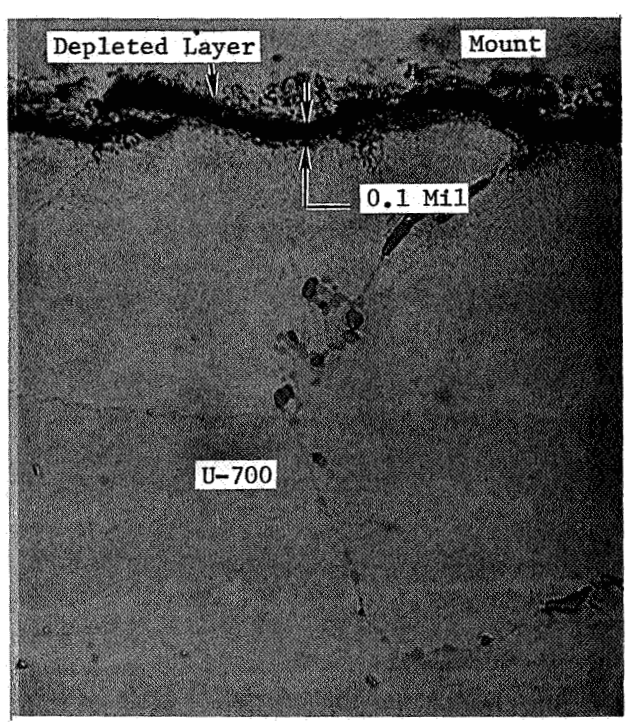
Figure 78. Room Temperature Tensile Properties of U-700 Turbine Blade Materials Before and After Endurance Testing.



T5433-79

Figure 79. **Deep Alloy Depletion** on Convex Surface of **First-Stage** 5000 Hour **Turbine Blade Near** Trailing Edge.

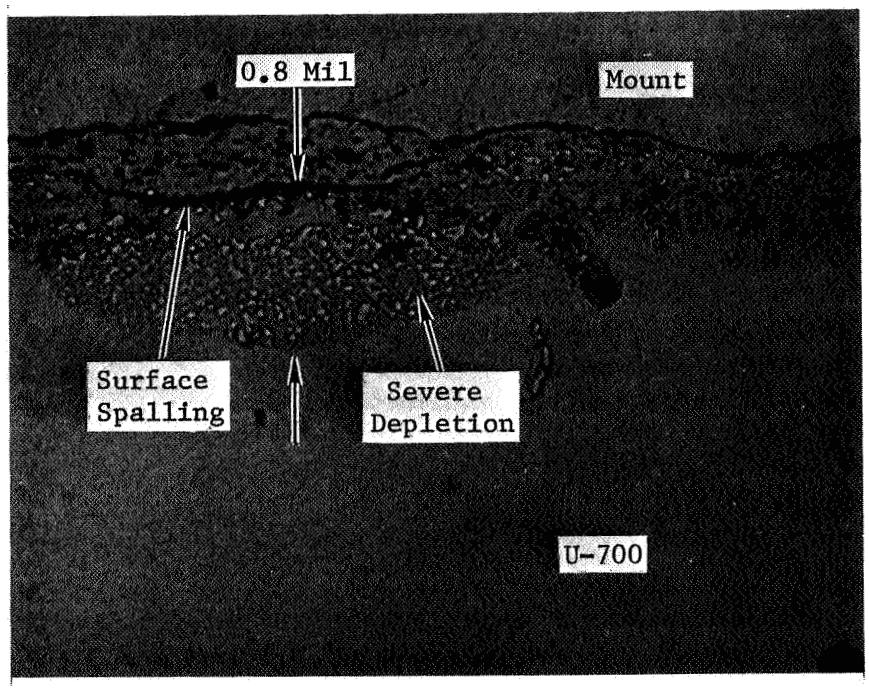
Etchant: $HCl + HNO_3$ + Acetic **Mag:** 1000X



T5433-80

Figure 80. **Thin** Alloy Depletion Layer on Convex Surface **of Second-Stage** 5000 Hour Test Blade.

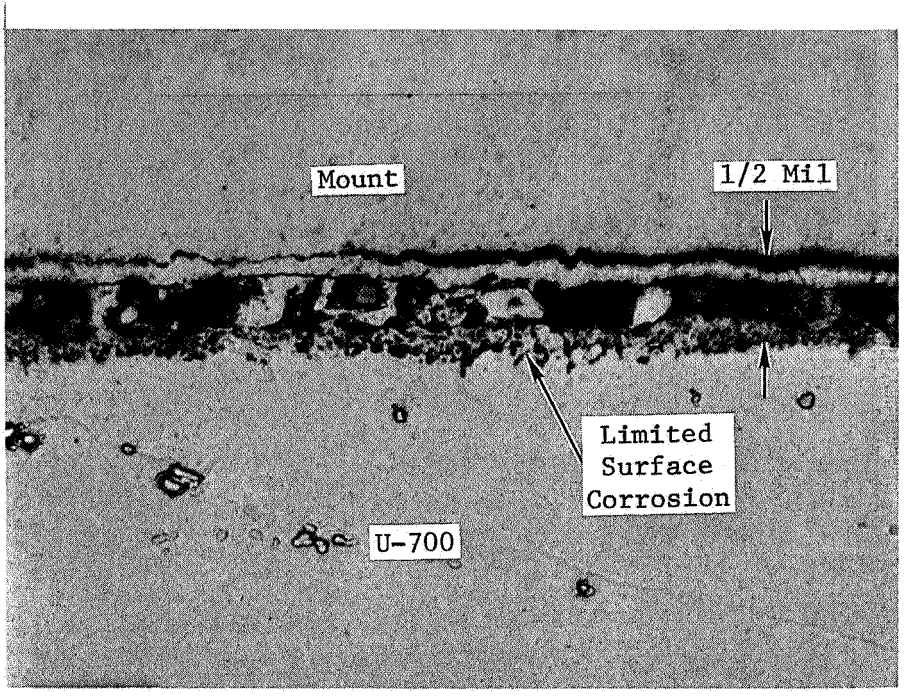
Etchant: Unetched. **Mag:** 1000X



T5433-81

Figure 81. Alloy Depletion on Convex Surface Near Leading Edge of Second Stage Turbine Blade After 5000 Hour Test.

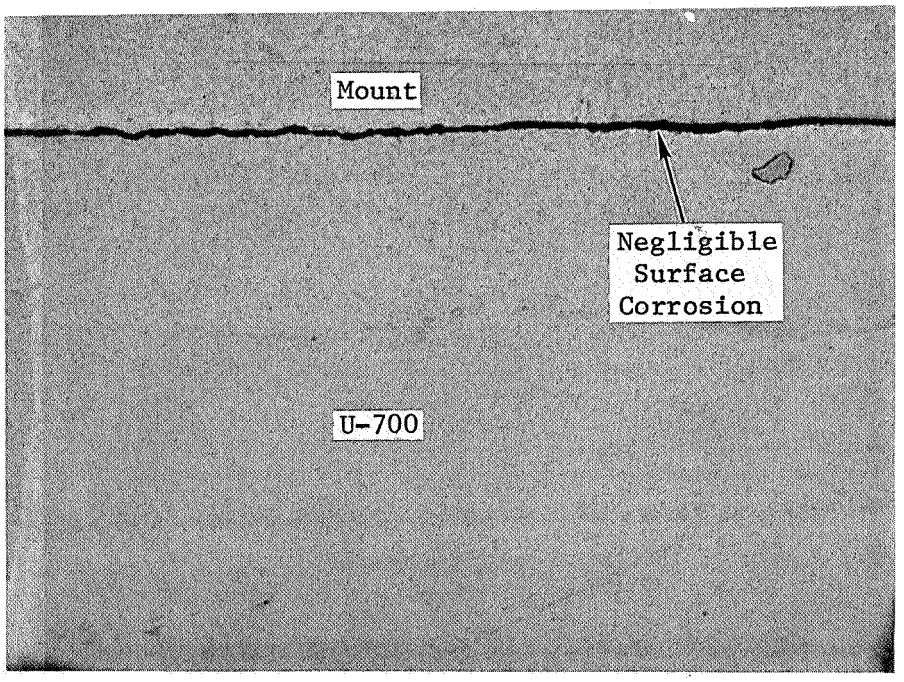
Etchant: Unetched. Mag: 1000X



T5433-82

Figure 82. Convex Airfoil Surface Near Mid-Chord of a 2000-Hour Test First-Stage Blade.

Etchant: Unetched. Mag: 1000X



T5433-83

Figure 83. Convex Airfoil Surface Near Mid-Chord of a 3000-Hour Test First-Stage Blade.

Etchant: Unetched. Mag: 1000X

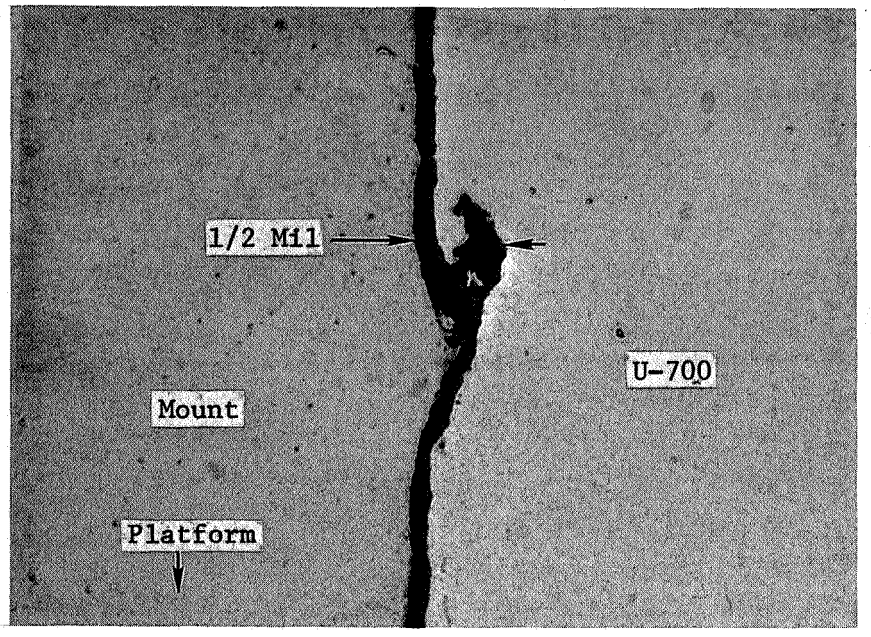


Figure 84. Corrosion Groove in Convex Surface Near Mid-Chord of a First-Stage U-700 Alloy, 3000-Hour Test Blade.

Etchant: Unetched Mag: 1000X

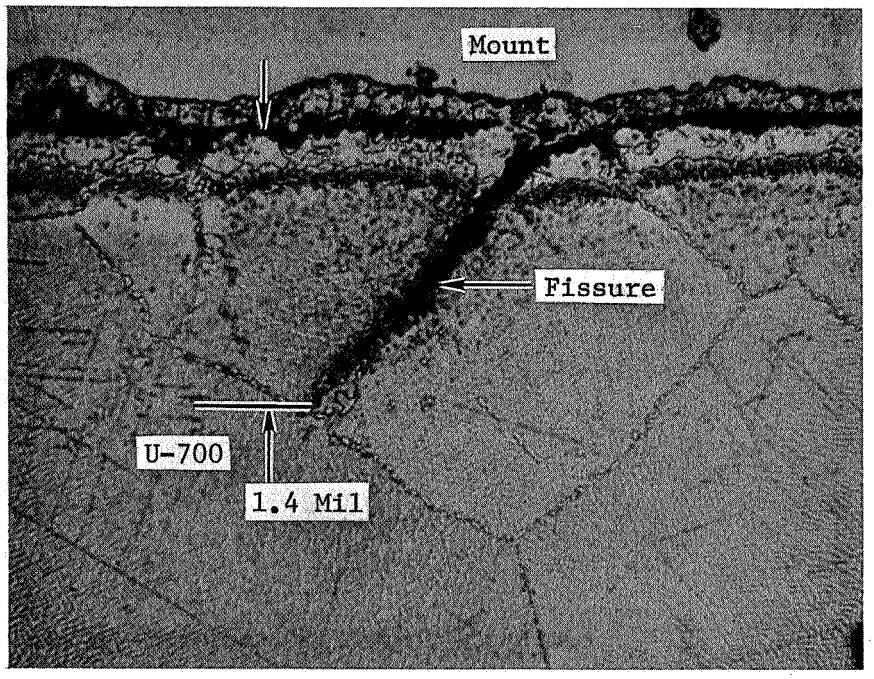


Figure 85. Concave Surface Near Trailing Edge of First-Stage, 5000 Hour Test Blade.

Etchant: HCl + HNO_3 + Acetic Mag: 1000X

PRECEDING PAGE BLANK NOT FILMED.



T5433-86

Figure 86. Mass Transfer Deposit on Aft Side of Second Stage Nozzle.

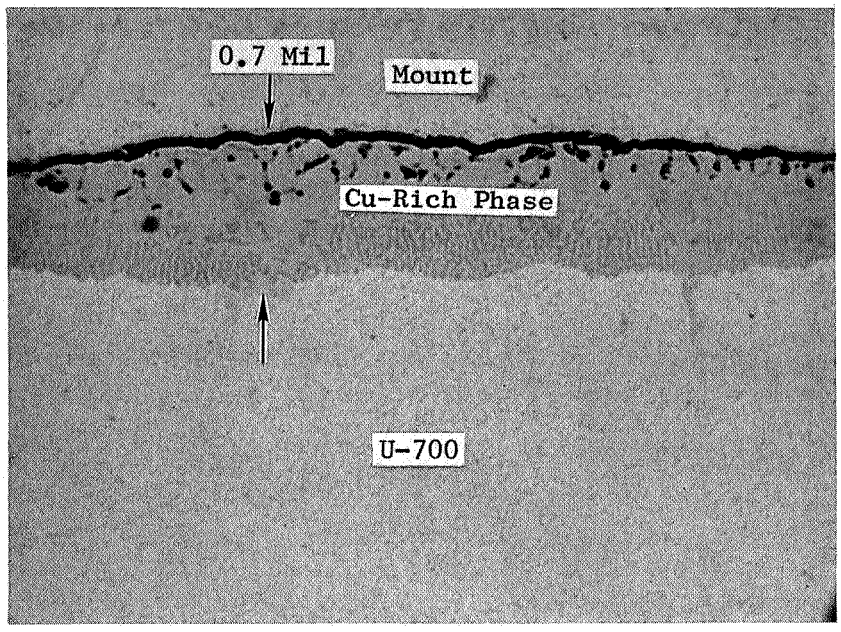
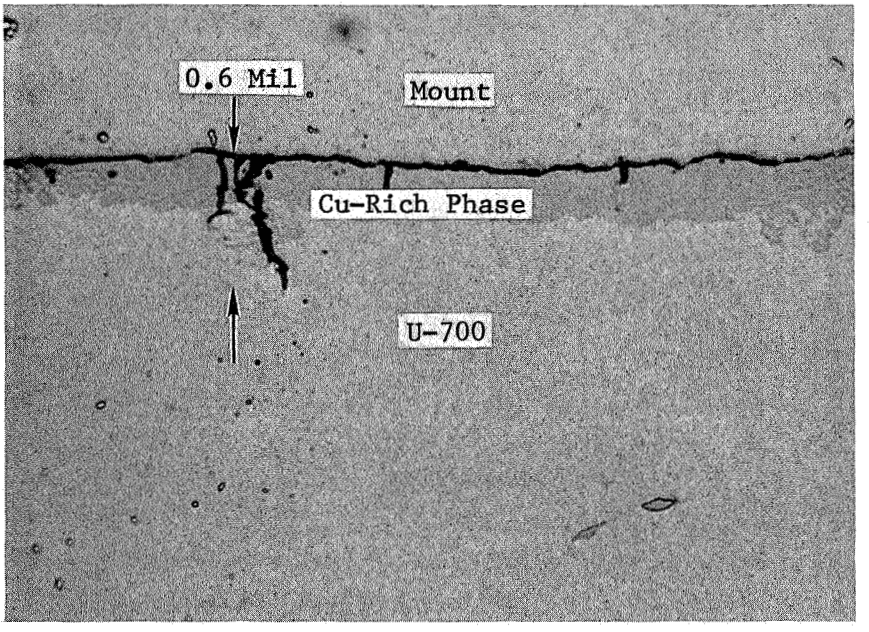


Figure 87. Copper-Rich Phase in Convex Surface Near Trailing Edge of First-Stage U-700 Alloy, 5000 Hour Test Blade.

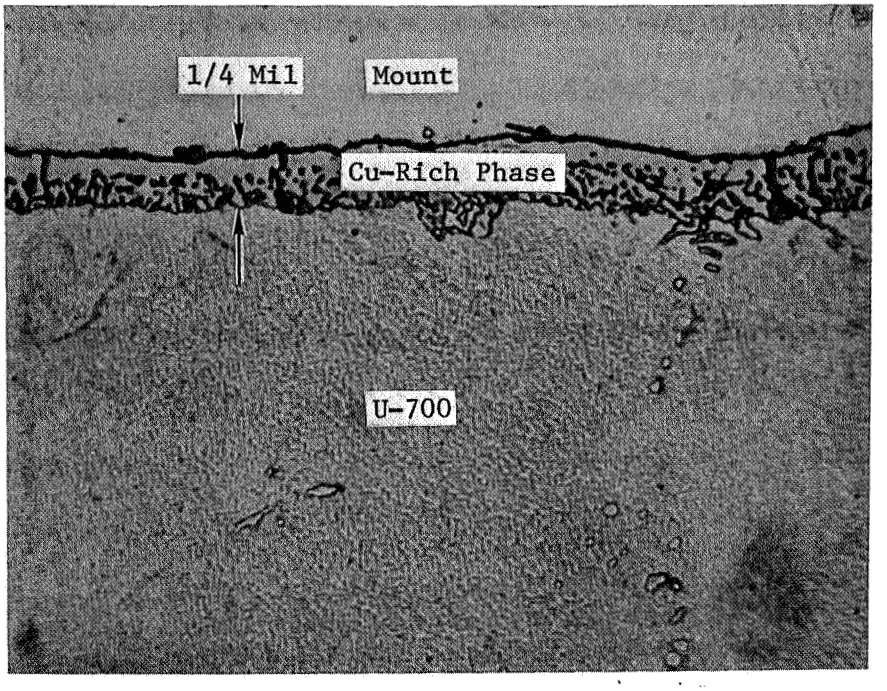
Etchant: Unetched Mag: 1000X



T5433-88

Figure 88. Copper-Rich Phase in Convex Surface Near Trailing Edge of First-Stage U-700 Alloy, 3000-Hour Test Blade.

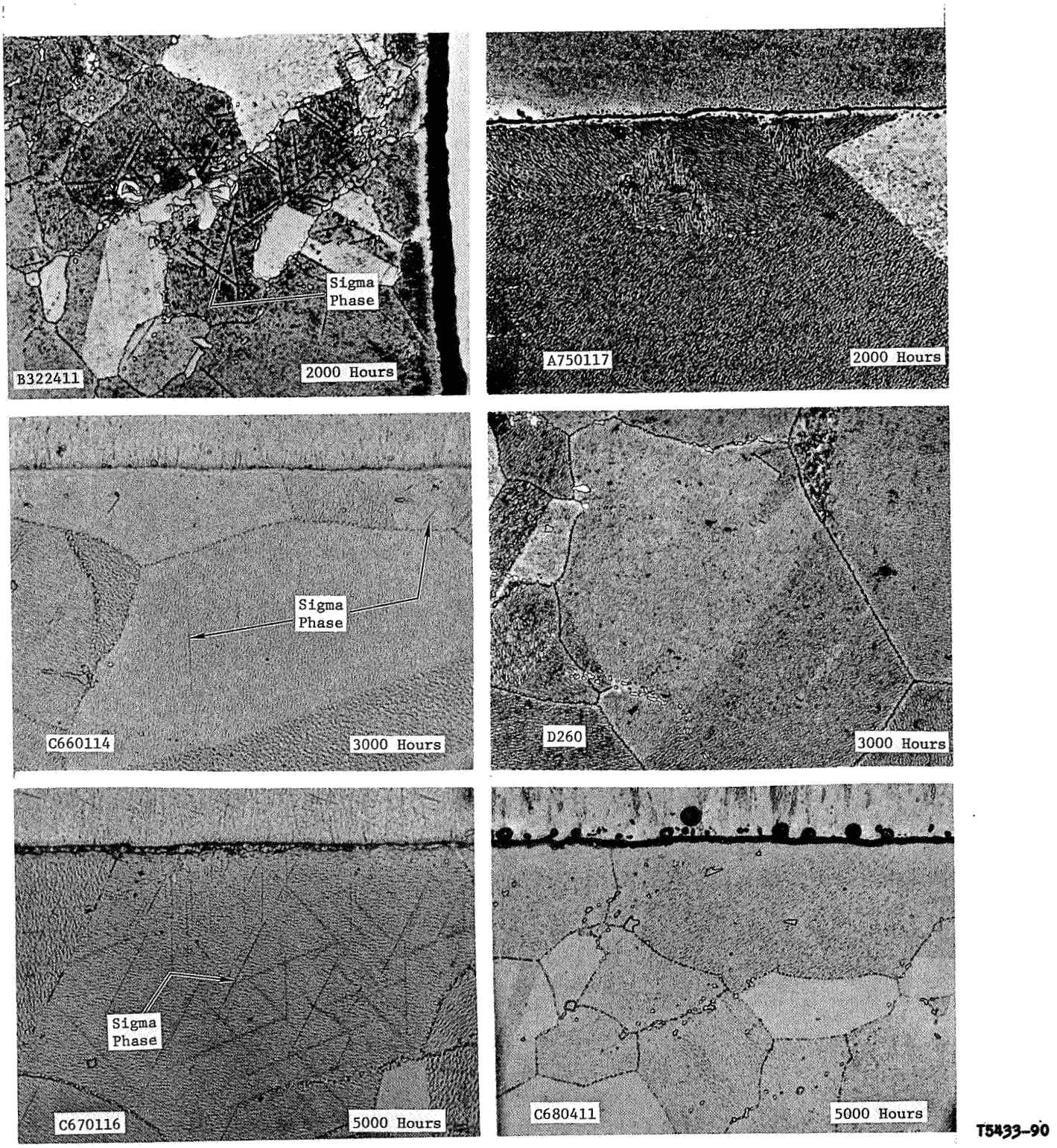
Etchant: Unetched Mag: 1000X



T5433-89

Figure 89. Copper-Rich Phase in Convex Surface Near Trailing Edge of First-Stage U-700 Alloy, 3000-Hour Test Blade.

Etchant: HCl + HNO_3 + Acetic Mag: 1000X



First Stage: Operating Temperature 1407°F Second Stage: Operating Temperature 1314°F

Note the absence of sigma phase in the second stage blades and the more extensive general sigma phase distribution in the longer test duration U-700 blades in the first stage. The 2000 hour, first stage micrograph was selected to show localized sigma phase in areas of high dovetail stresses.

Figure 90. Photomicrographs Showing Relative Quantities of Sigma Formation in Turbine Blades with Respect to Operating Conditions.
Oxalic Acid Etch.
Mag: 500X

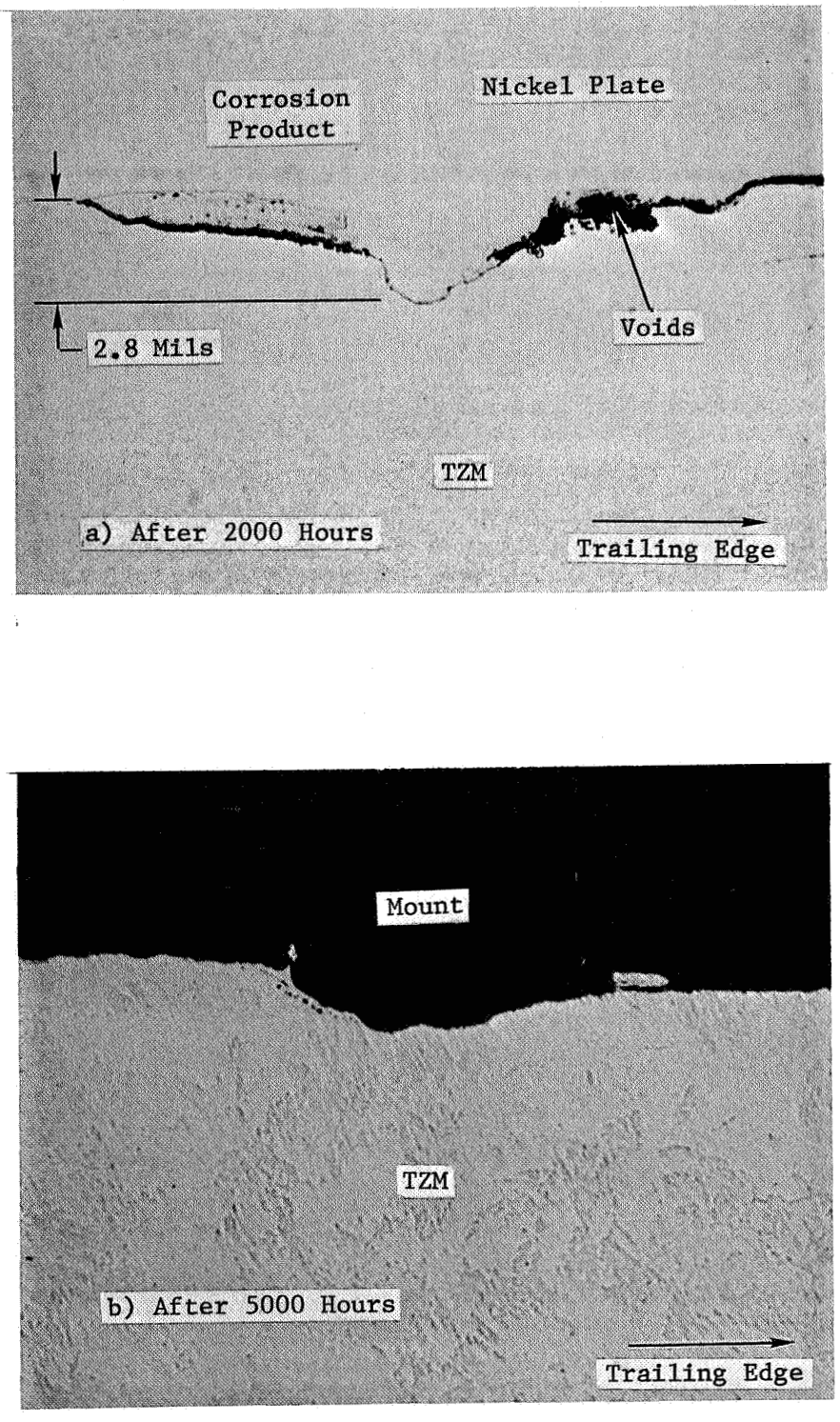
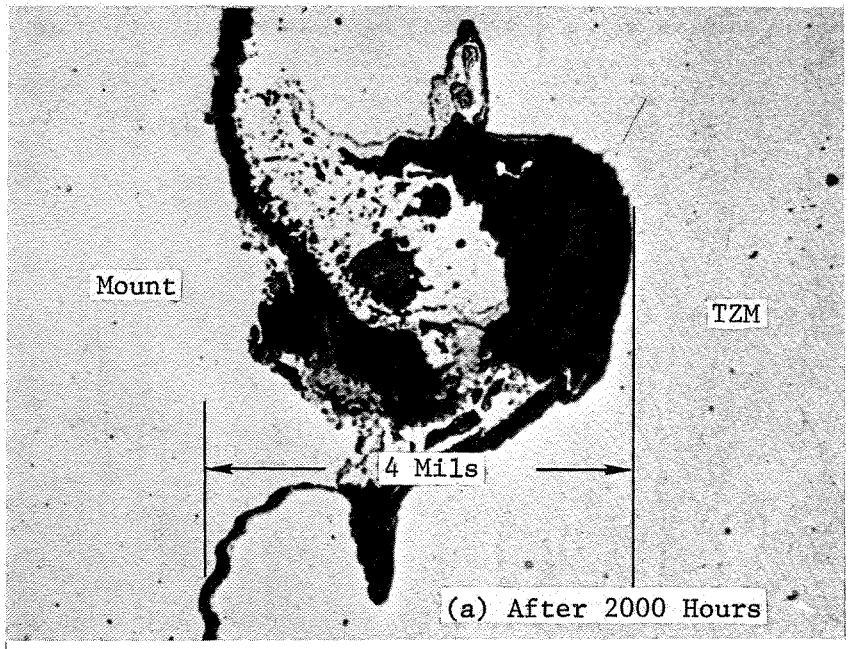
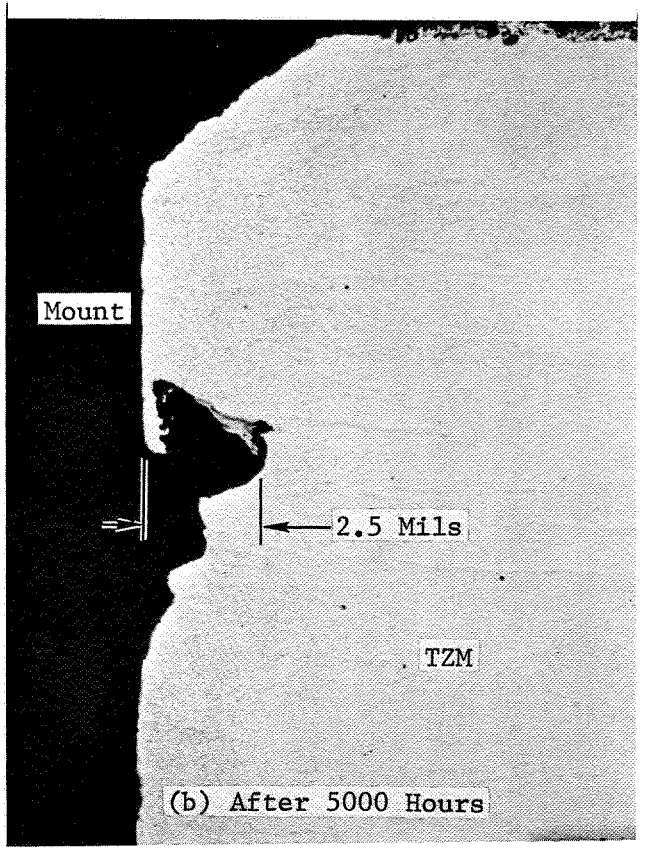


Figure 91. Photomicrograph of Trailing Edge, Convex Surface of Second-Stage, TZM Turbine Blade.

Etchant: Unetched Mag: 250X





T5433-92

Figure 92. Photomicrograph of Convex Surface at Tip of Second-Stage TZM Turbine Blade.

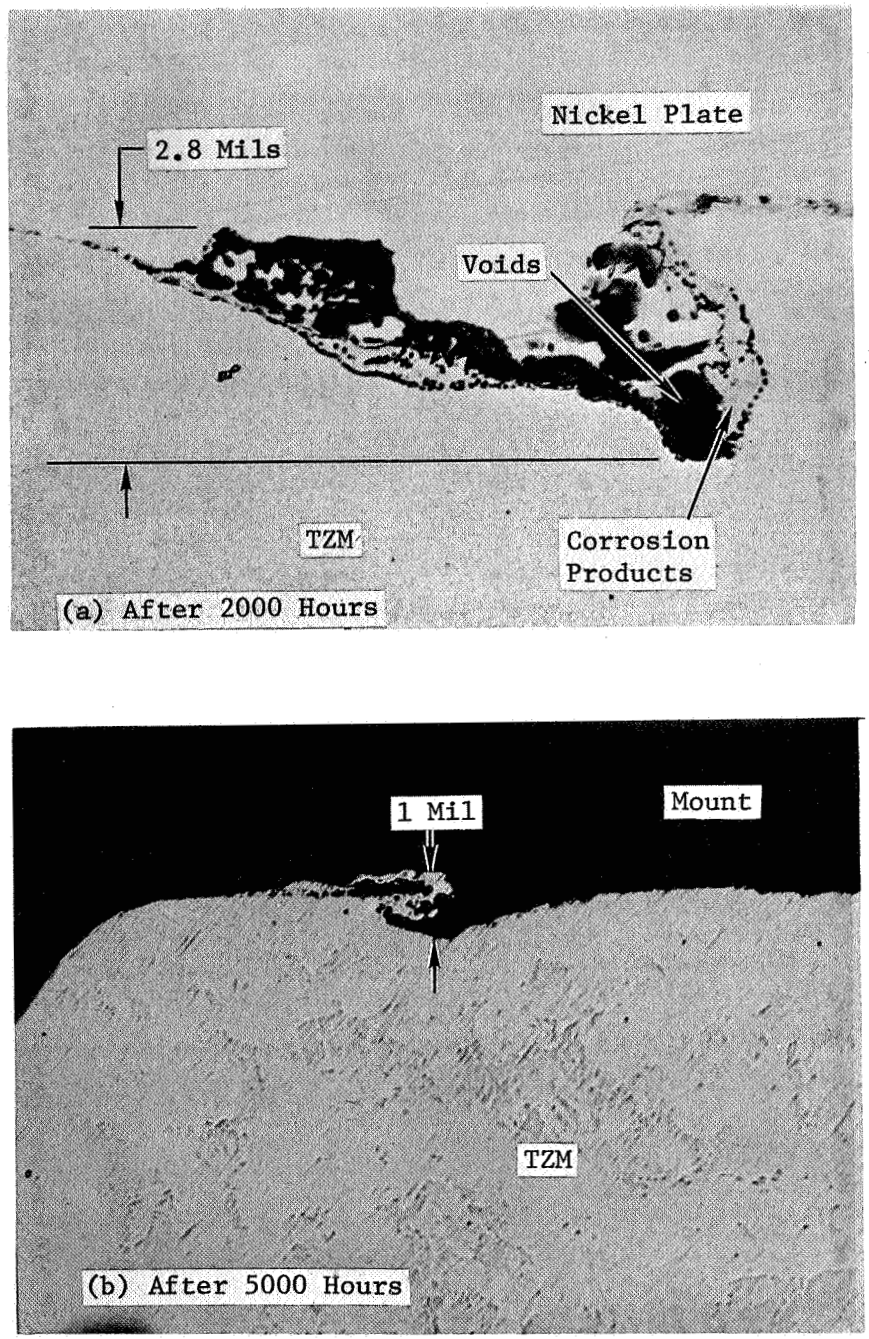


Figure 93. Concave Surface Aft of Leading Edge of Second-Stage, TZM Turbine Blade.

Etchant: Unetched Mag: 1000X

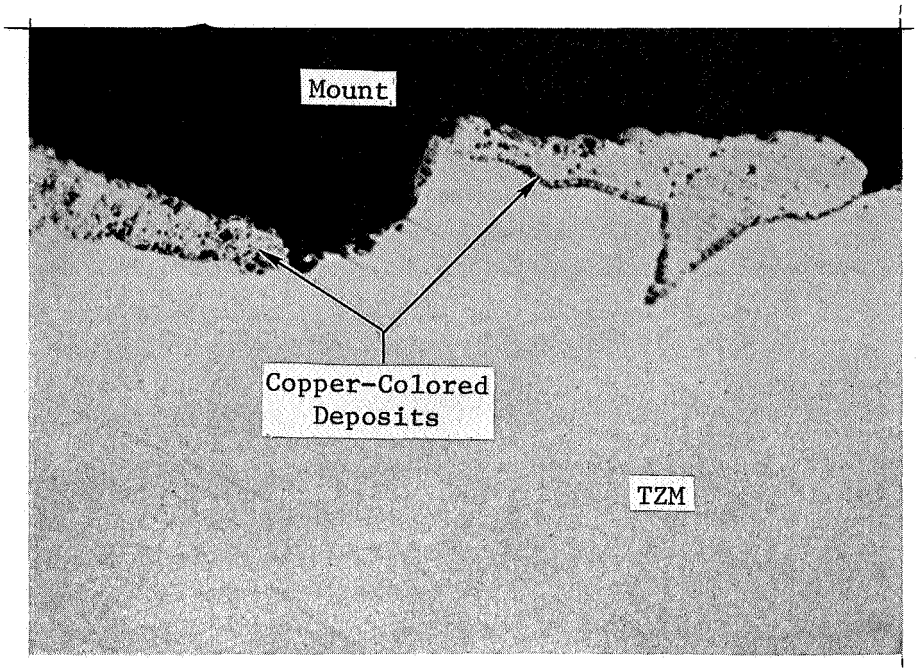


Figure 94. Copper-Colored Deposit on Platform of Second-Stage, 5000 Hour, TZM Turbine Blade.

Etchant: Unetched Mag: 1000X

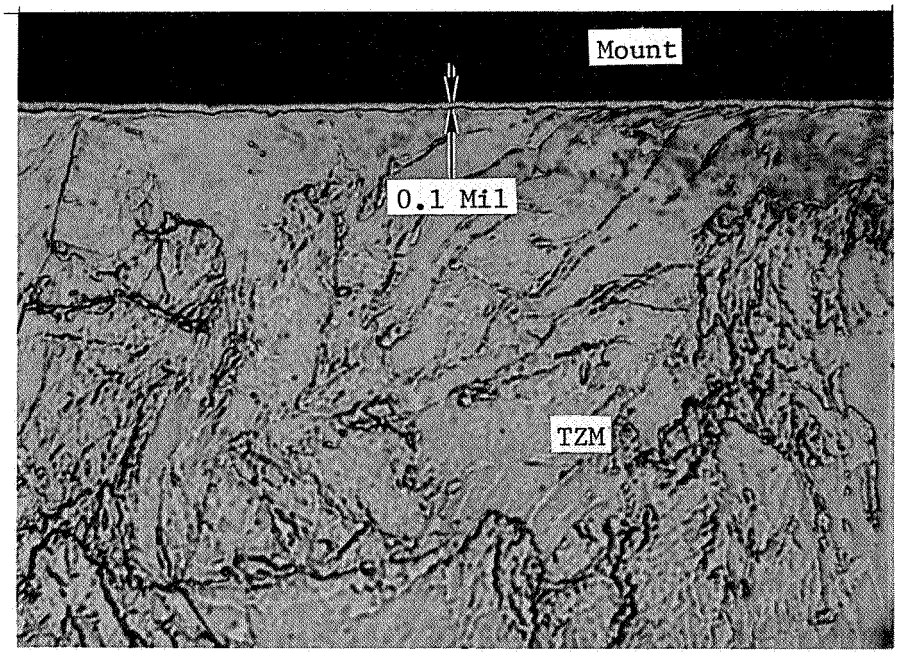
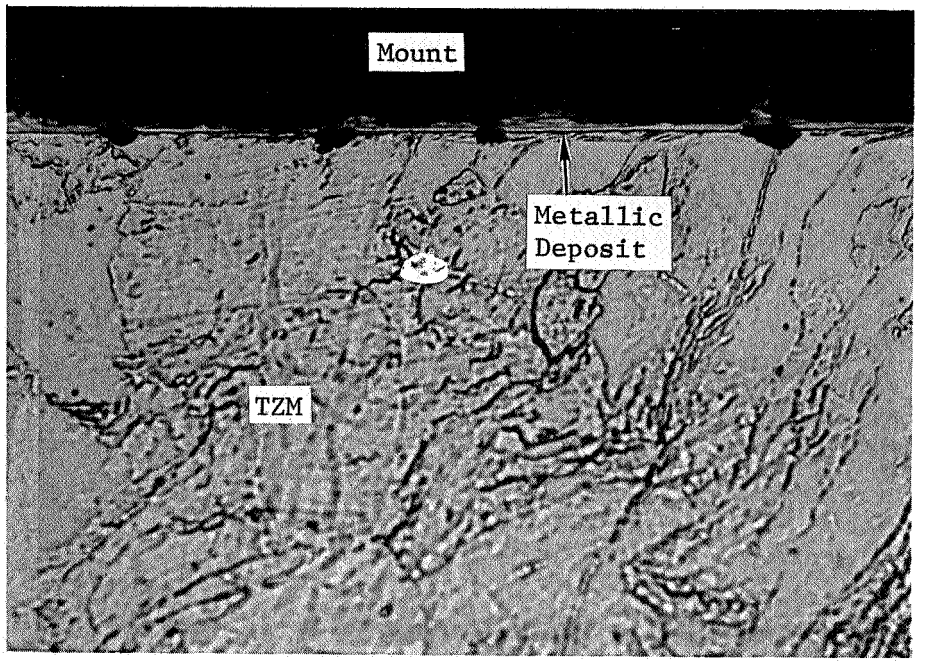


Figure 95. Thin, Metallic Deposit on Concave Surface of TZM 5000-Hour Turbine Blade. Layed Extended From Approximately Mid-Chord to Trailing Edge.

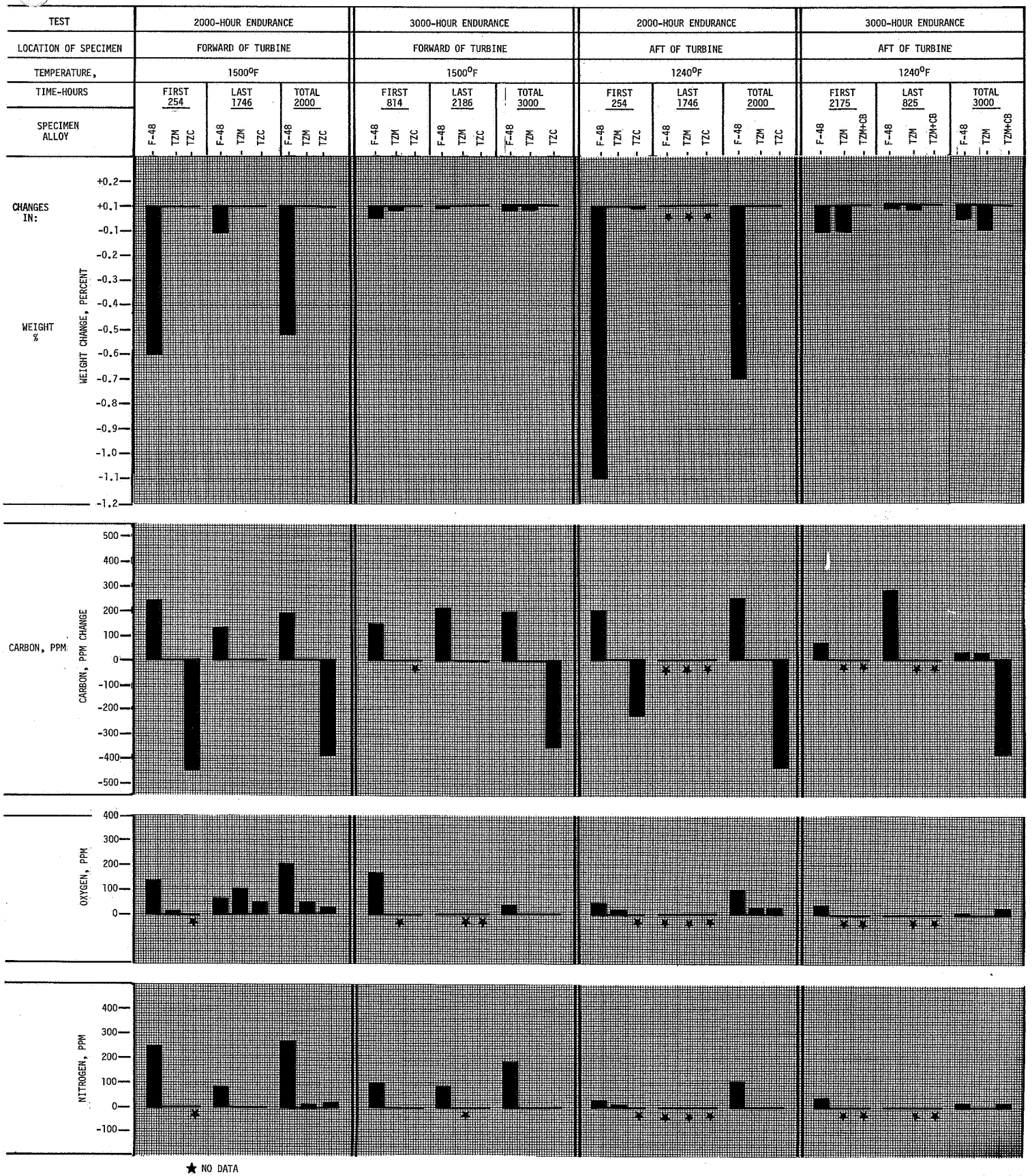
Etchant: Murikami's Mag: 1000X



T5433-96

Figure 96. Photomicrograph of Convex Surface Near Leading Edge of 3000 Hour TZM Turbine Blade Showing Thin Metallic Surface Deposit.

Etchant: Murikami's Mag: 1000X



T5433-97

Figure 97. Changes in Weight and in Carbon, Oxygen, and Nitrogen Content of Refractory Alloys During Turbine Testing.

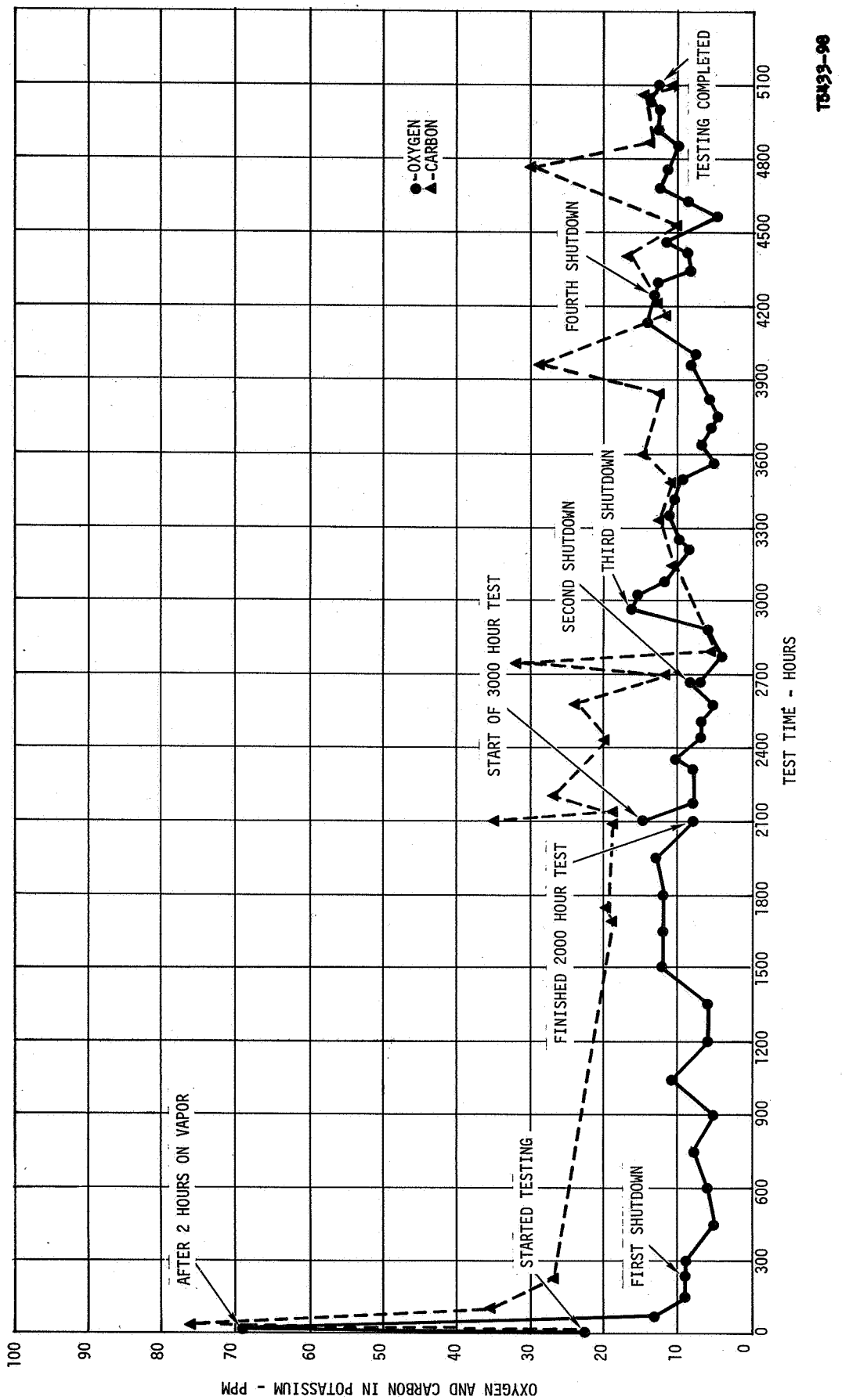
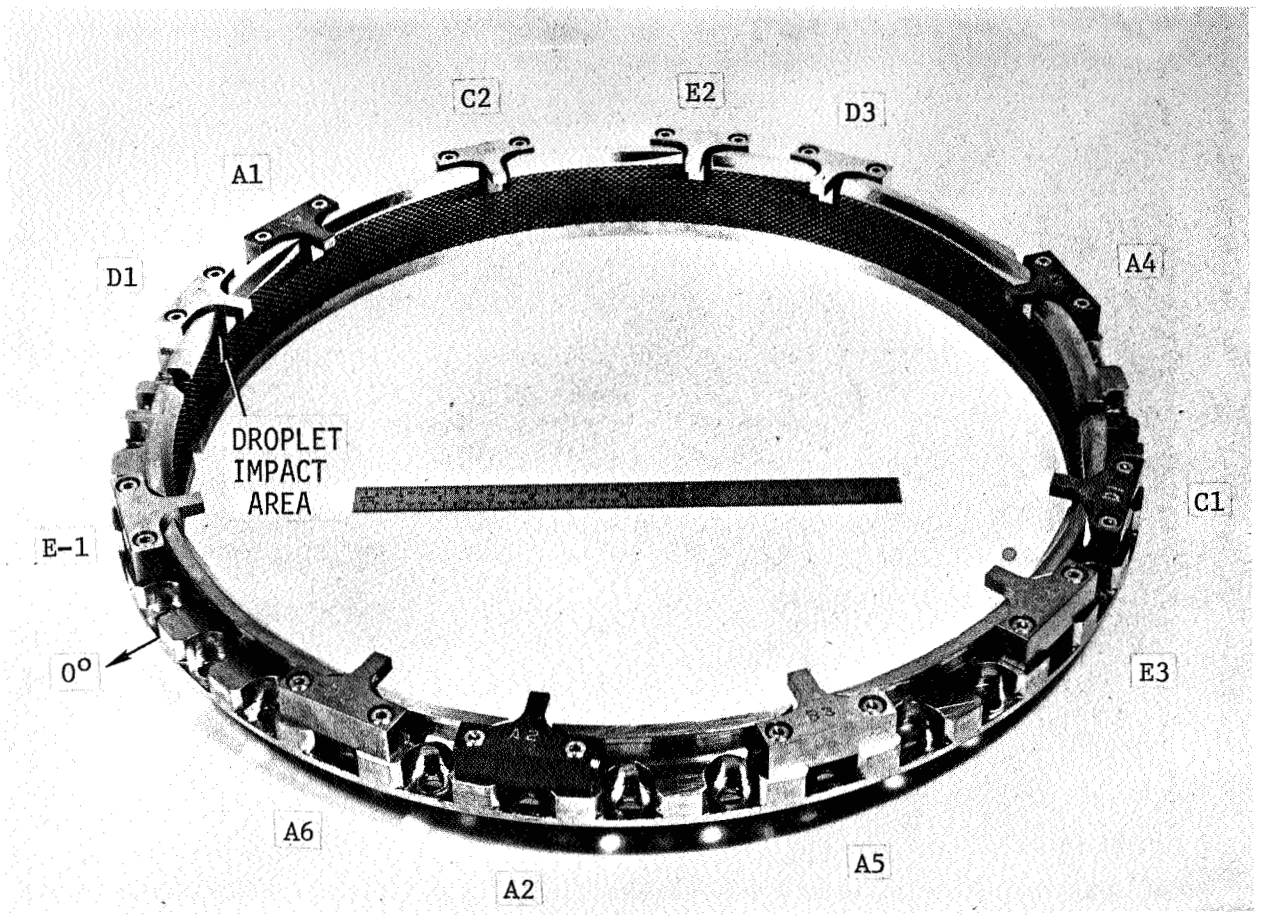
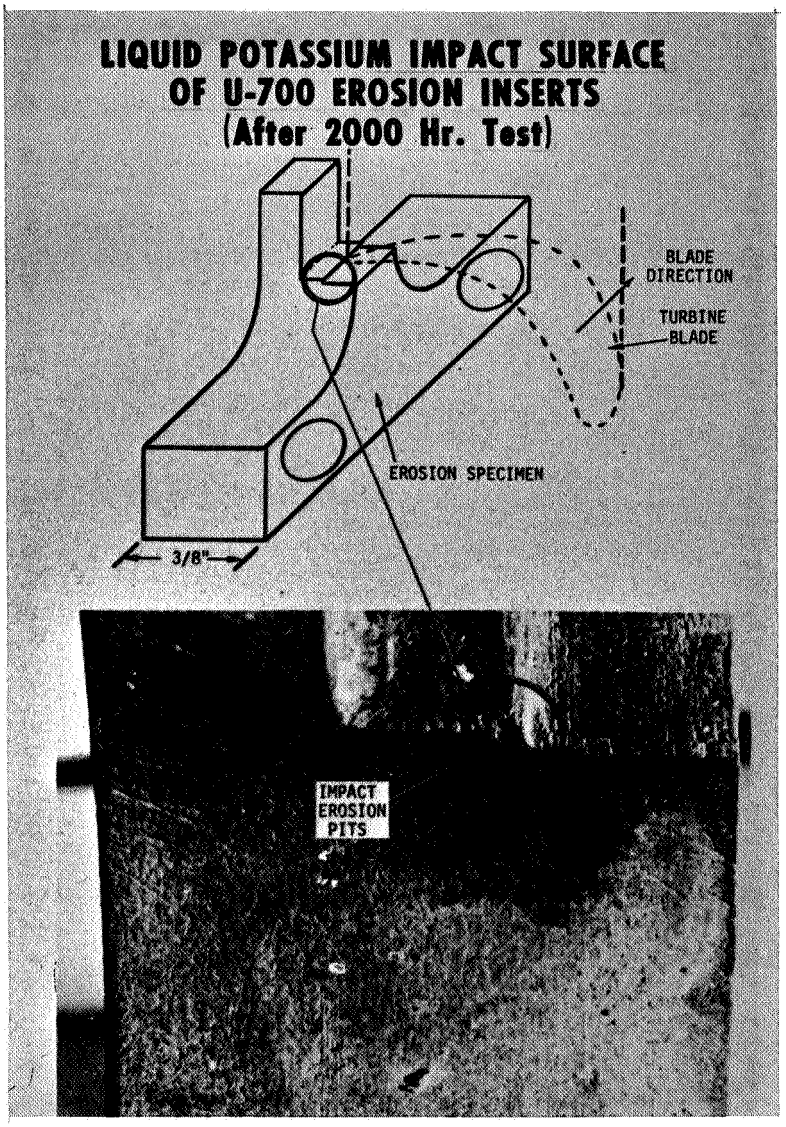


Figure 98. Oxygen and Carbon Concentrations in Potassium During Turbine Endurance Testing.



T5433-99

Figure 99. Installation of Erosion Inserts in Second Stage Shroud For the 3000 Hour Endurance Test.



T5433-100

Figure 100. Liquid Potassium Impact Surface of U-700 Erosion Inserts (After 2000 Hour Test).

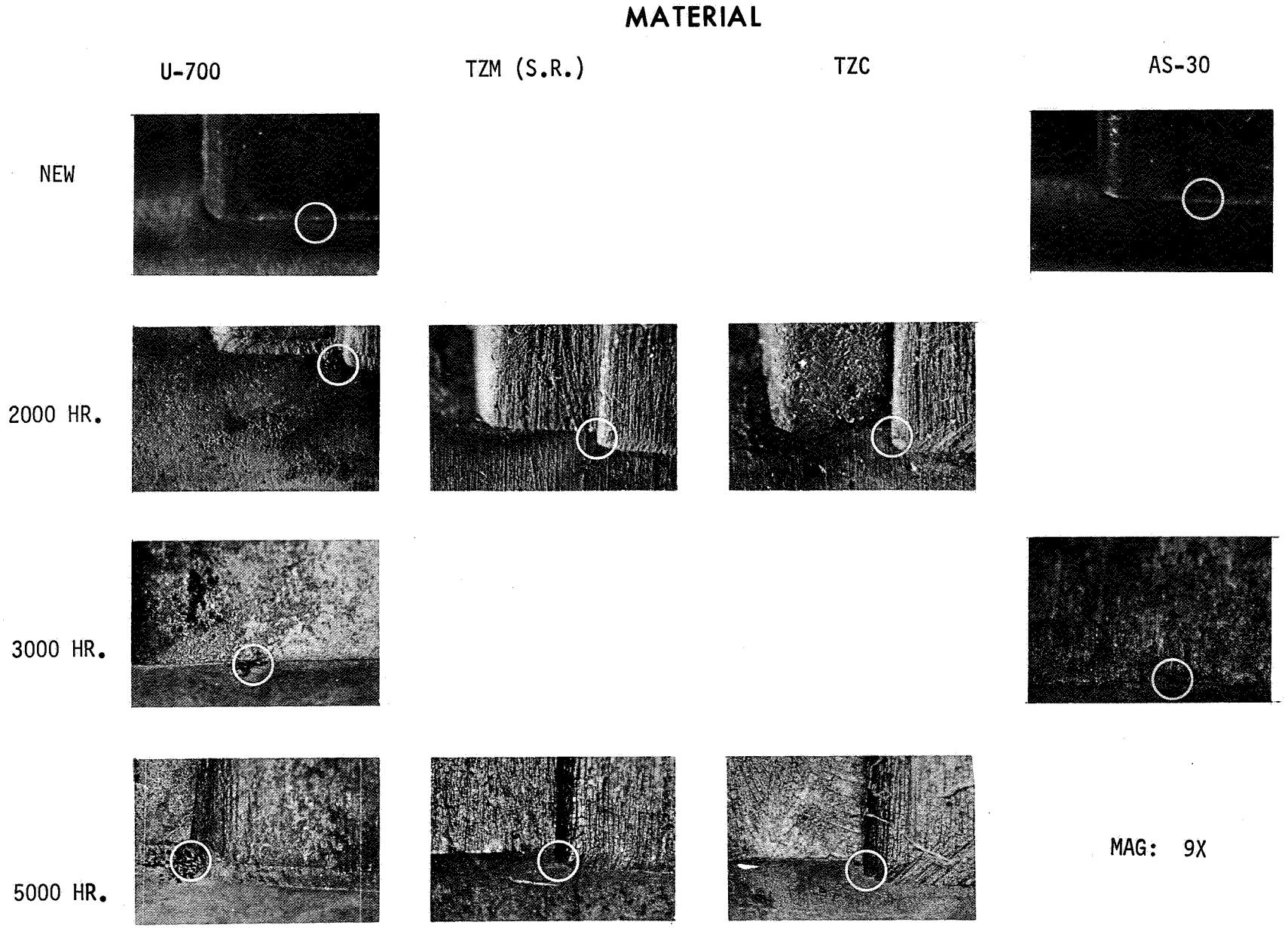
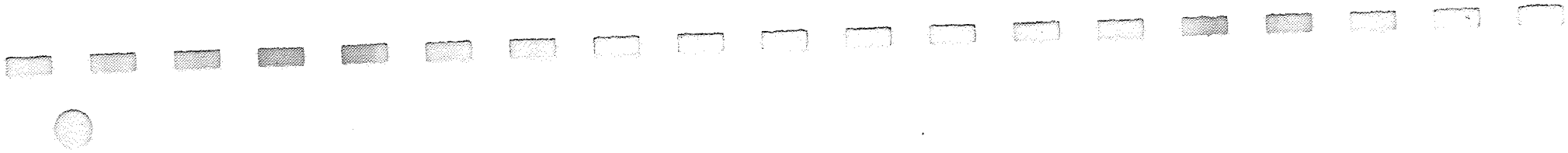
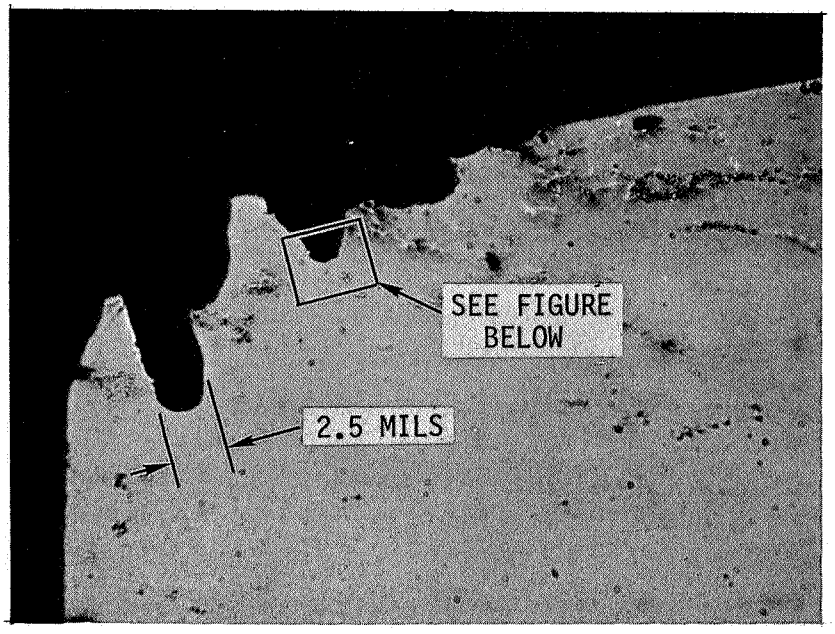


Figure 101. Comparison of Impact Erosion on Various Materials After Turbine Test For 2000-, 3000-, and 5000-Hours.



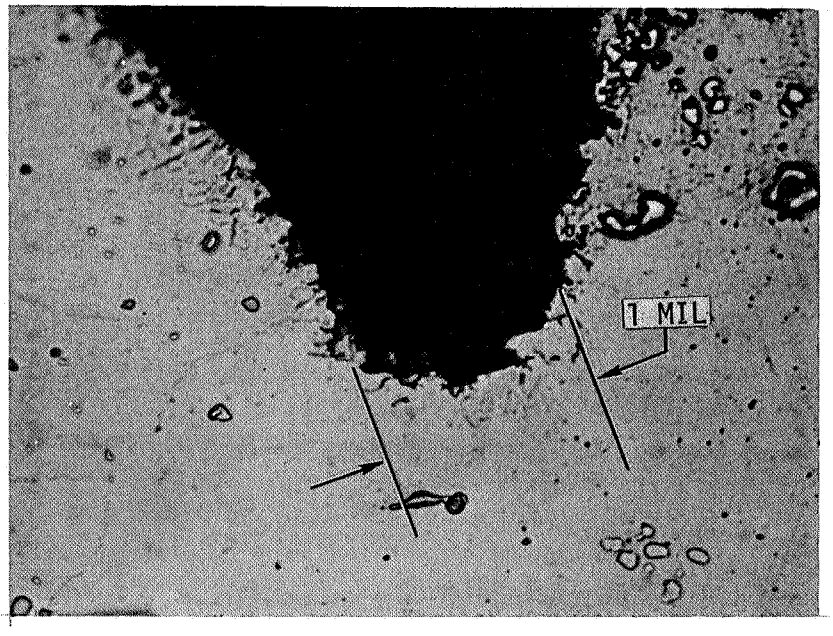
PRECEDING PAGE BLANK NOT FILMED.



T5433-102

Figure 102. Impact Erosion Pits in U-700 Erosion Insert A-3 After 2000-Hour Test.

Etchant: Unetched Mag: 100X



T5433-103

Figure 103. Impact Erosion Pits in U-700 Erosion Insert A-3 After 2000-Hour Test.

Etchant: Unetched Mag: 1000X

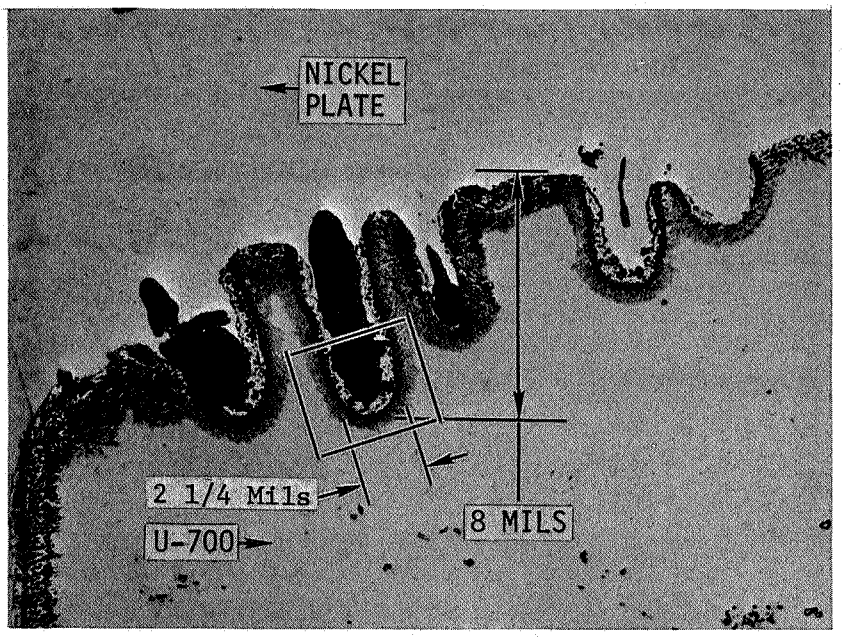


Figure 104. U-700 Erosion Insert A-1 After 5000 Hours Total Test Time. These Pits were Present After 2000 Hours Test.

Etchant: Unetched Mag: 150X

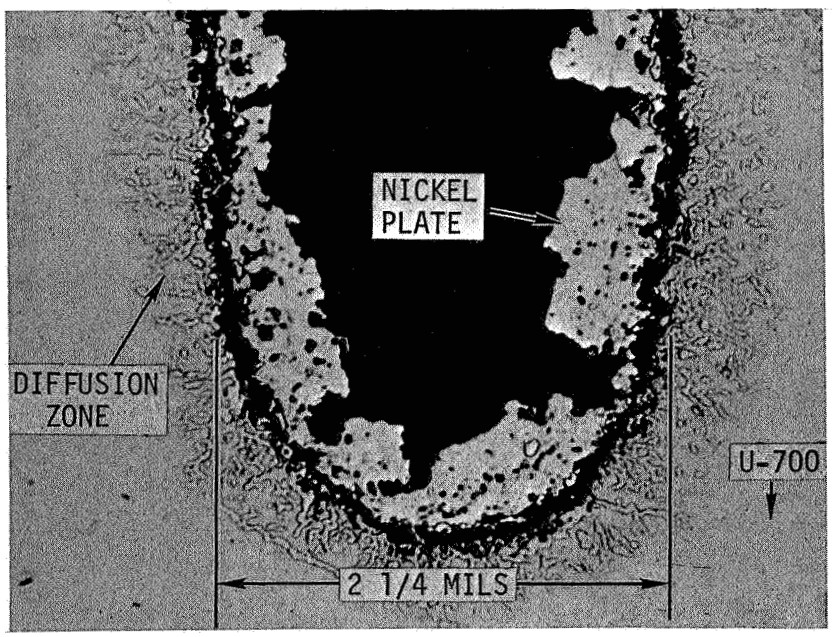


Figure 105. U-700 Erosion Insert A-1 After 5000 Hours Total Test Time. These Pits were Present After 2000 Hours Test.

Etchant: Unetched Mag: 1000X

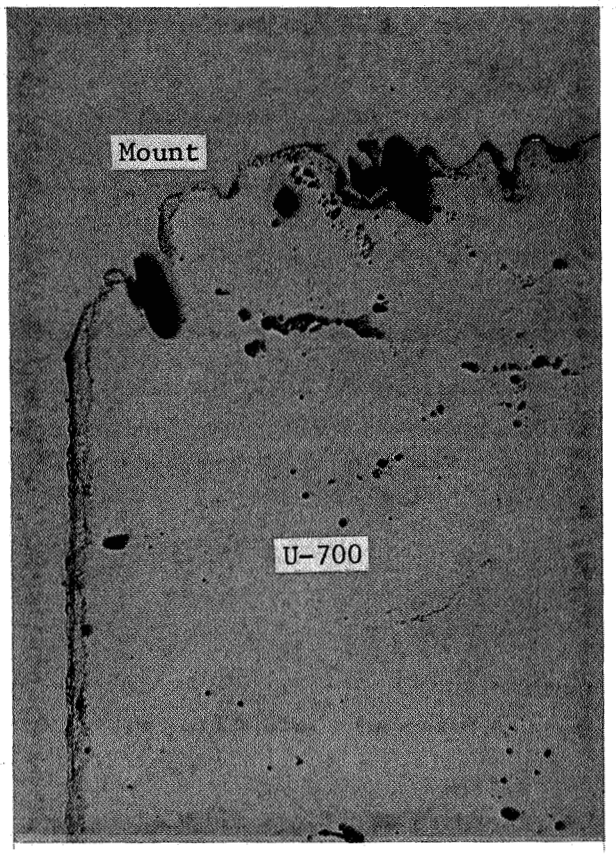
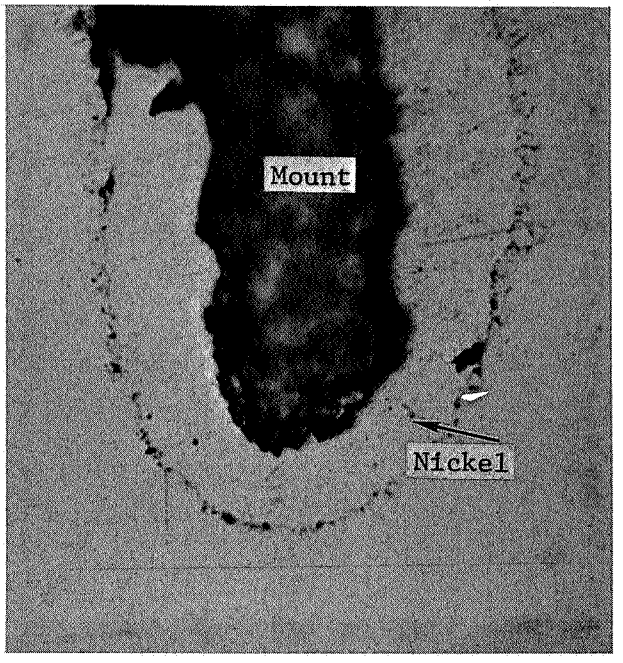


Figure 106. U-700 Erosion Insert A-1 After 3000-Hour Test. These New Pits were Located Slightly Aft of the Pits Formed Initially During the 2000-Hour Test.

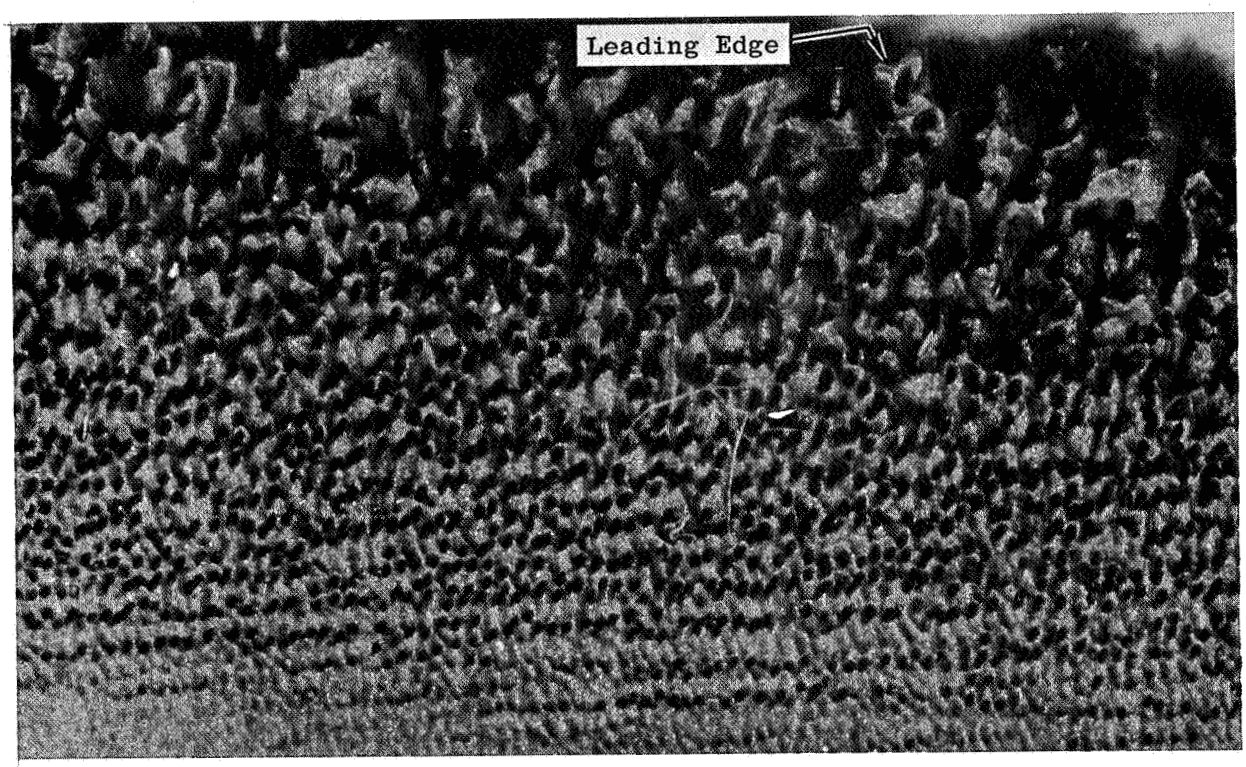
Etchant: Unetched Mag: 100X



T5433-107

Figure 107. U-700 Erosion Insert A-1 After 3000-Hour Test. These New Pits were Located Slightly Aft of the Pits Formed Initially During the 2000-Hour Test. This Section Represents Deepest Pit in Figure 106 After a Light Repolish.

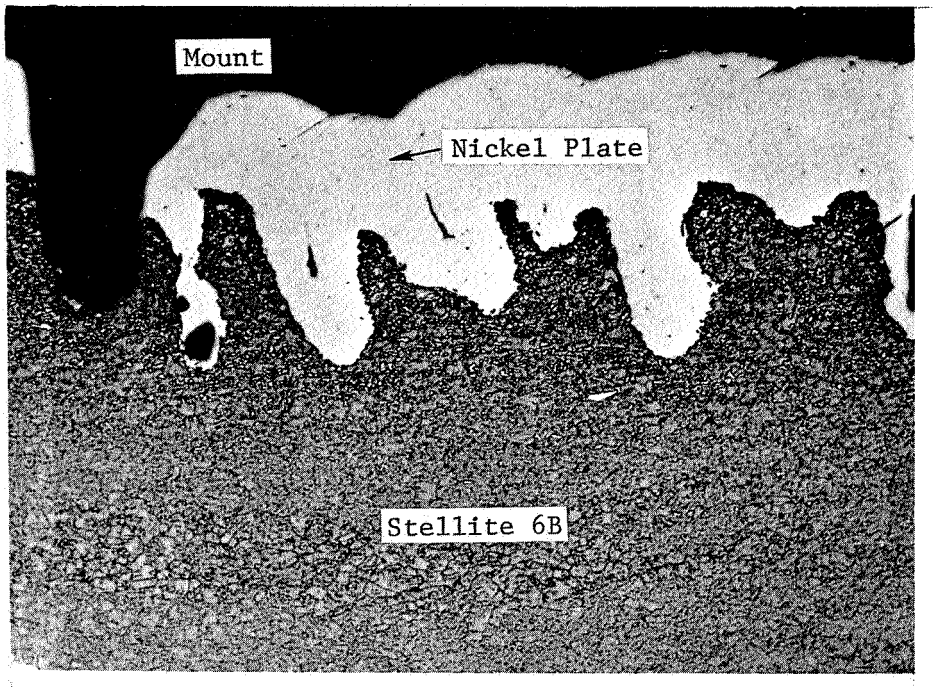
Etchant: Unetched Mag: 1000X



T5433-108

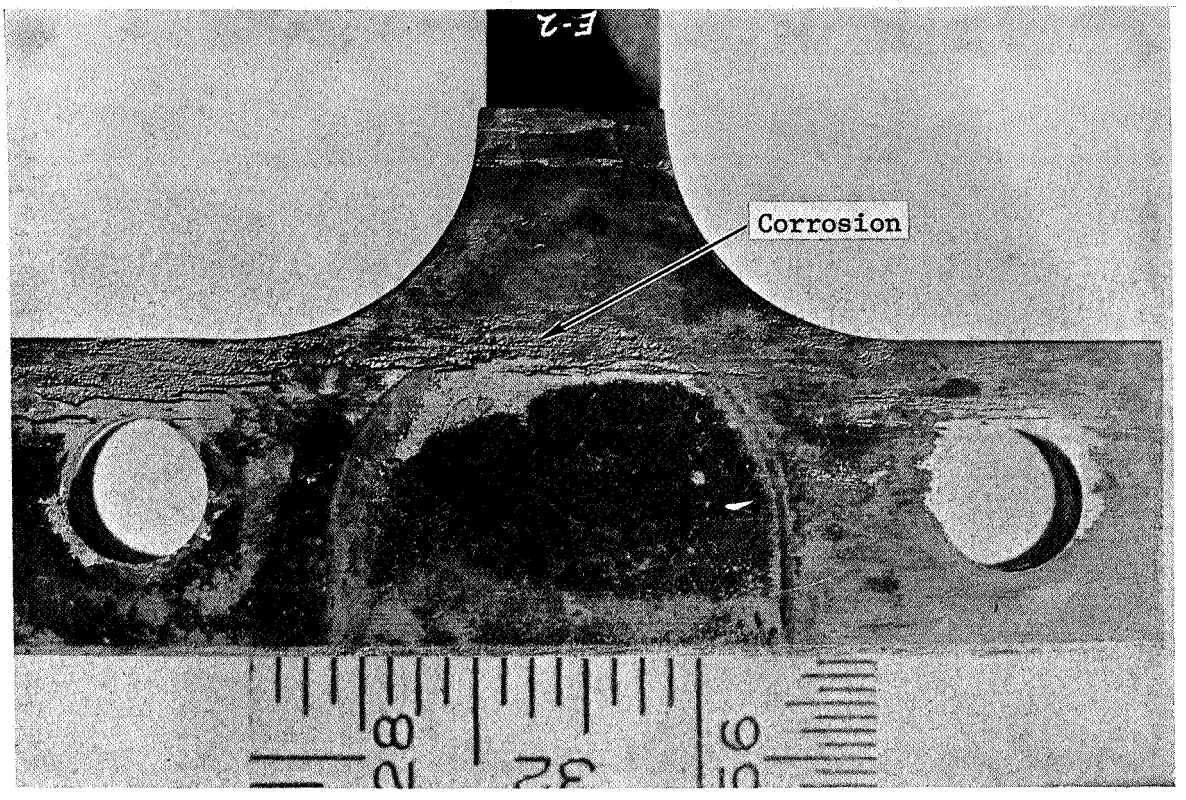
Figure 108. Characteristic Liquid Droplet Impact Erosion on Stellite 6B Steam Turbine Blade Insert. (C65061410)

Mag: 13X



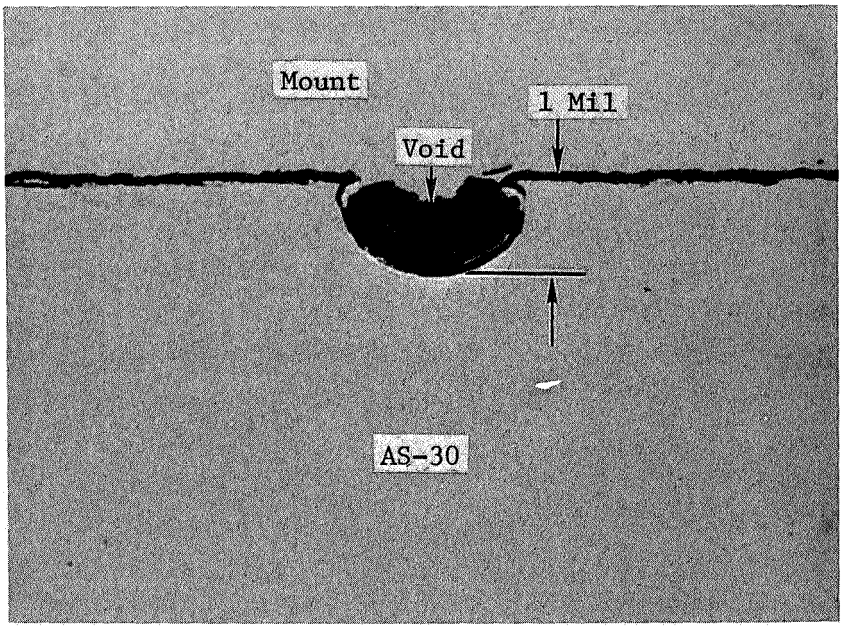
T5433-109

Figure 109. **Erosion Pits in Stellite 6B Steam Turbine Blade Shield.**
Etchant: Chromic Acid Mag: 100X



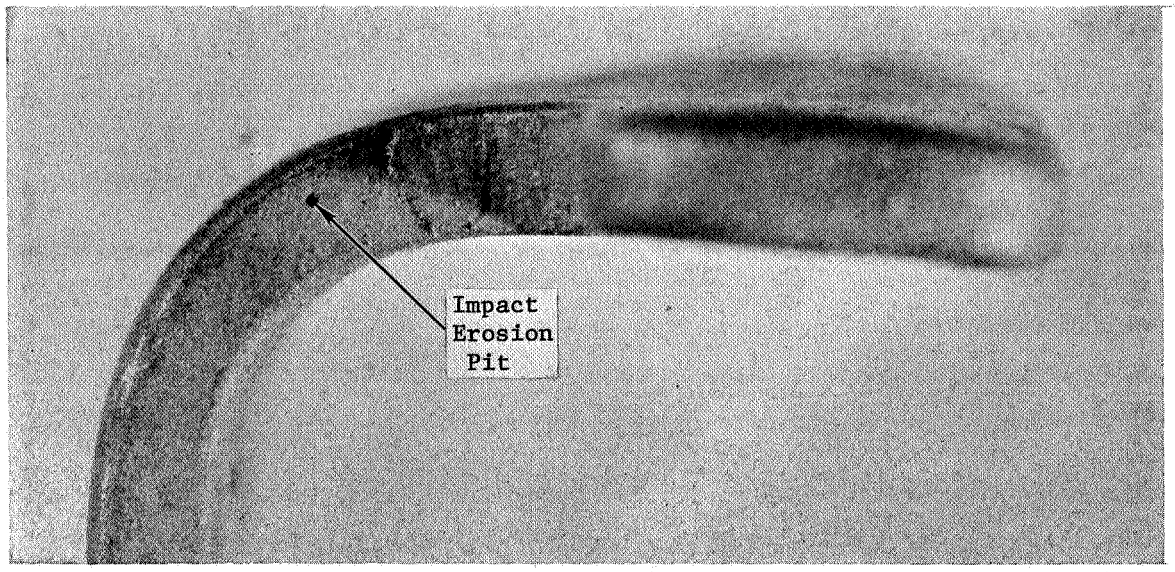
T5433-110

Figure 110. Forward Face of AS 30 Insert, Showing Corrosion. Similar Condition Exists on Aft Surface.



T5433-111

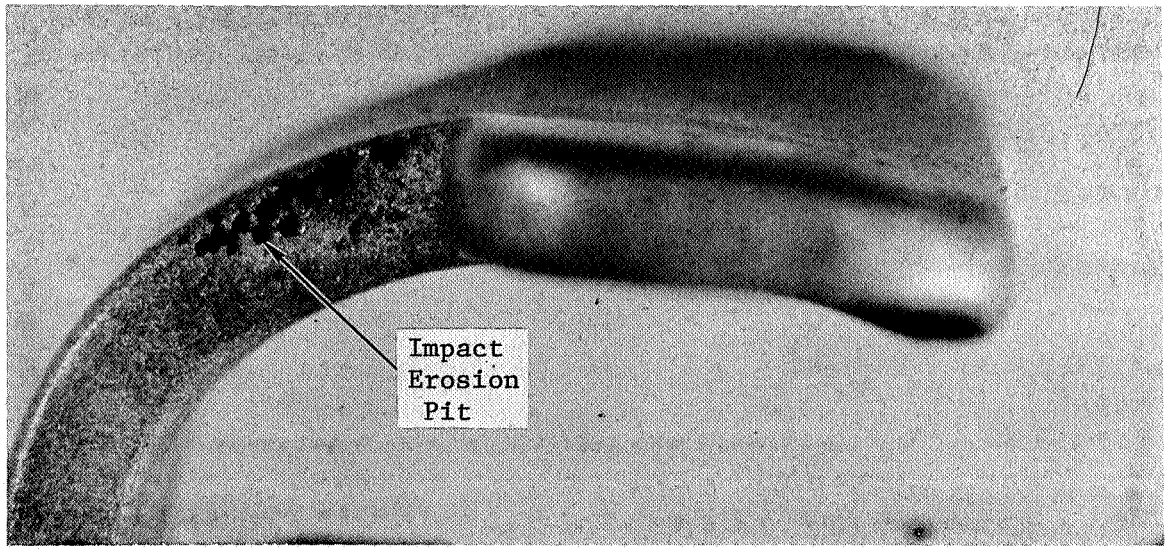
Figure 111. Corrosion Pit of AS-30 Erosion Insert E-2.
Etchant: Unetched Mag: 500X



T5433-112

Figure 112. **Aft End** of Second-Stage Blade Clips Showing Erosion **Experienced** During 3000 Hour Endurance Test.

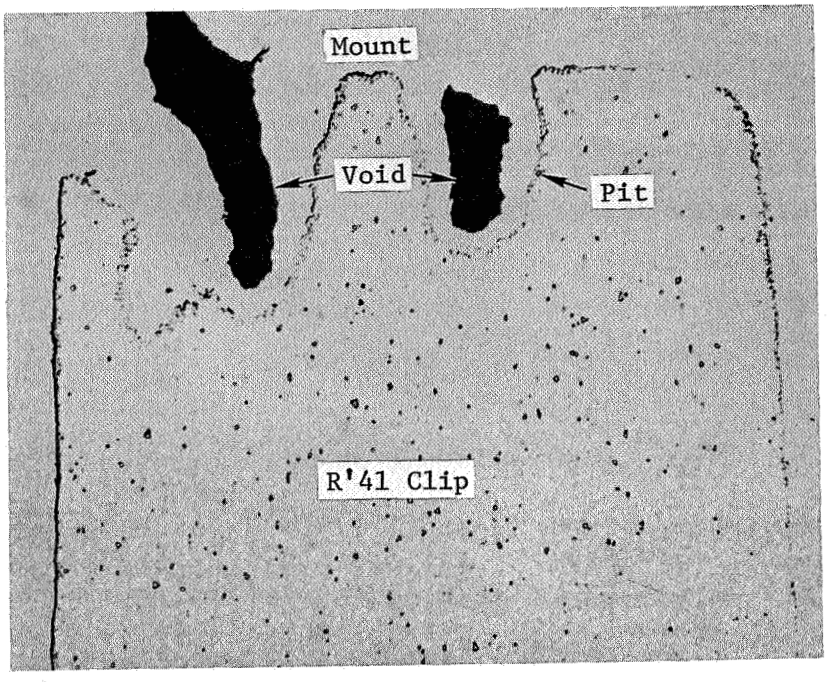
Mag: 23X



T5433-113

Figure 113. **Aft End of First**-Stage Blade Clips Showing Erosion **Experienced** During 3000 Hour Endurance Test.

Mag: 23X



T5433-114

Figure 114. Second Stage Blade Clip Erosion Pits.
Etchant: Unetched Mag: 100X

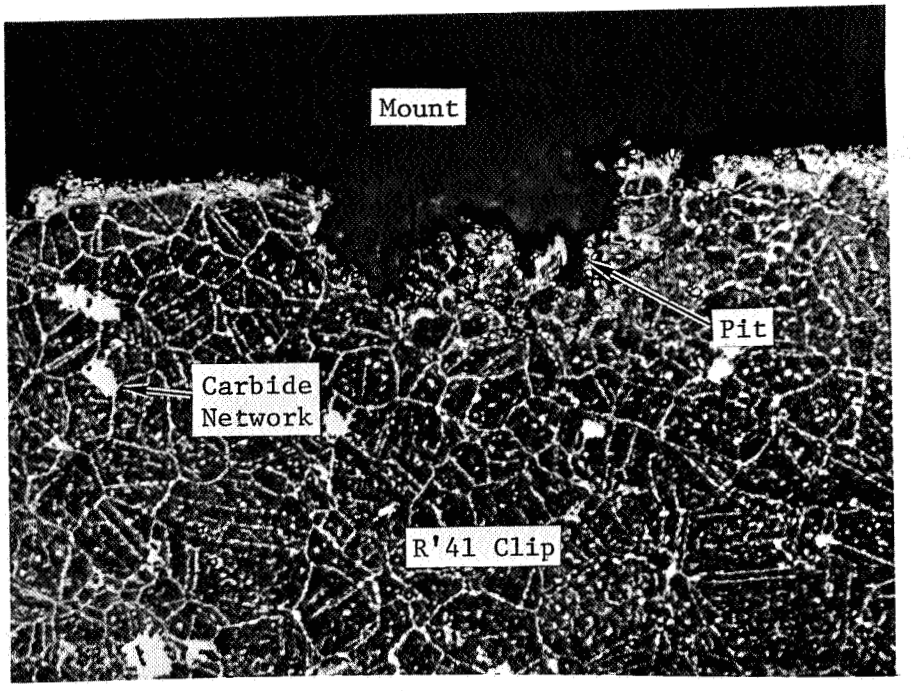
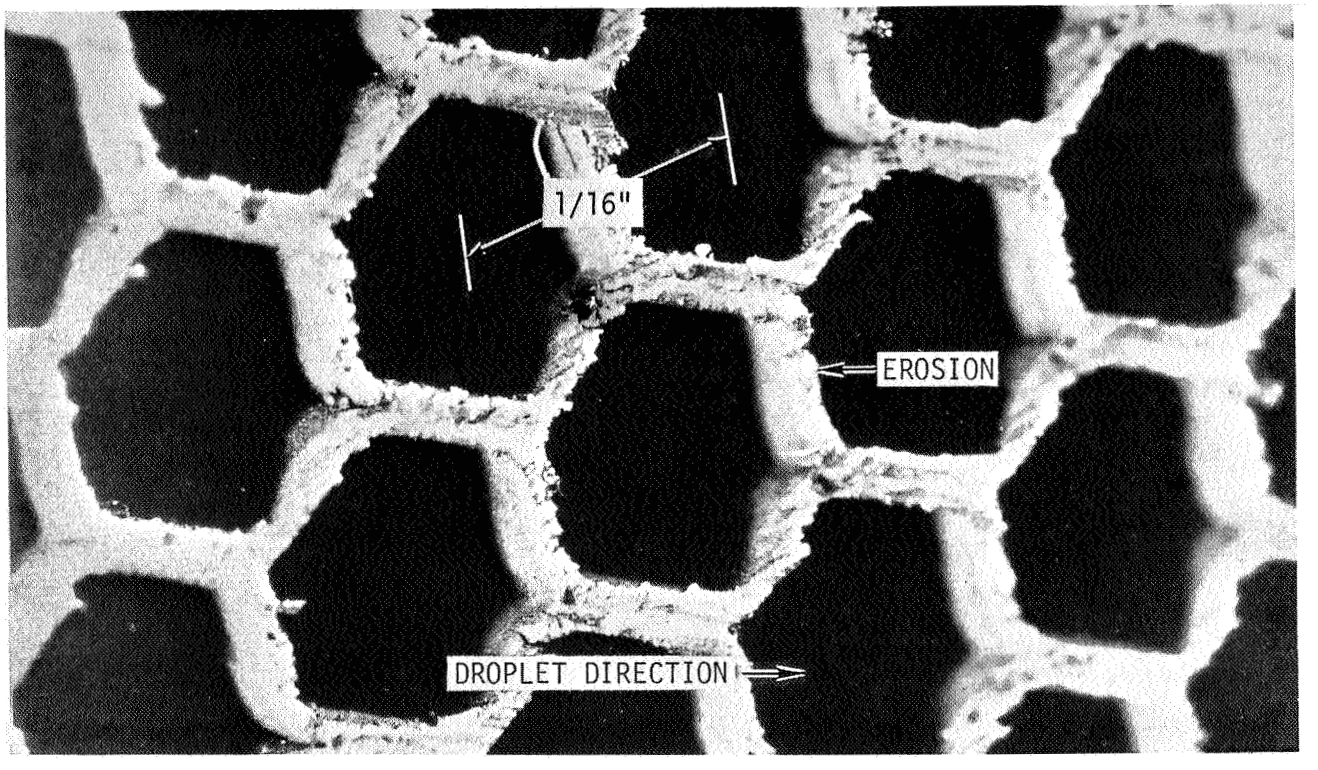


Figure 115. First Stage Blade Clip Erosion Pits.
Etchant: Oxalic Mag: 500X

T5433-115



T5433-116

Figure 116. **Erosion** of Second Stage Honeycomb Tip Shroud.

Mag: 34X

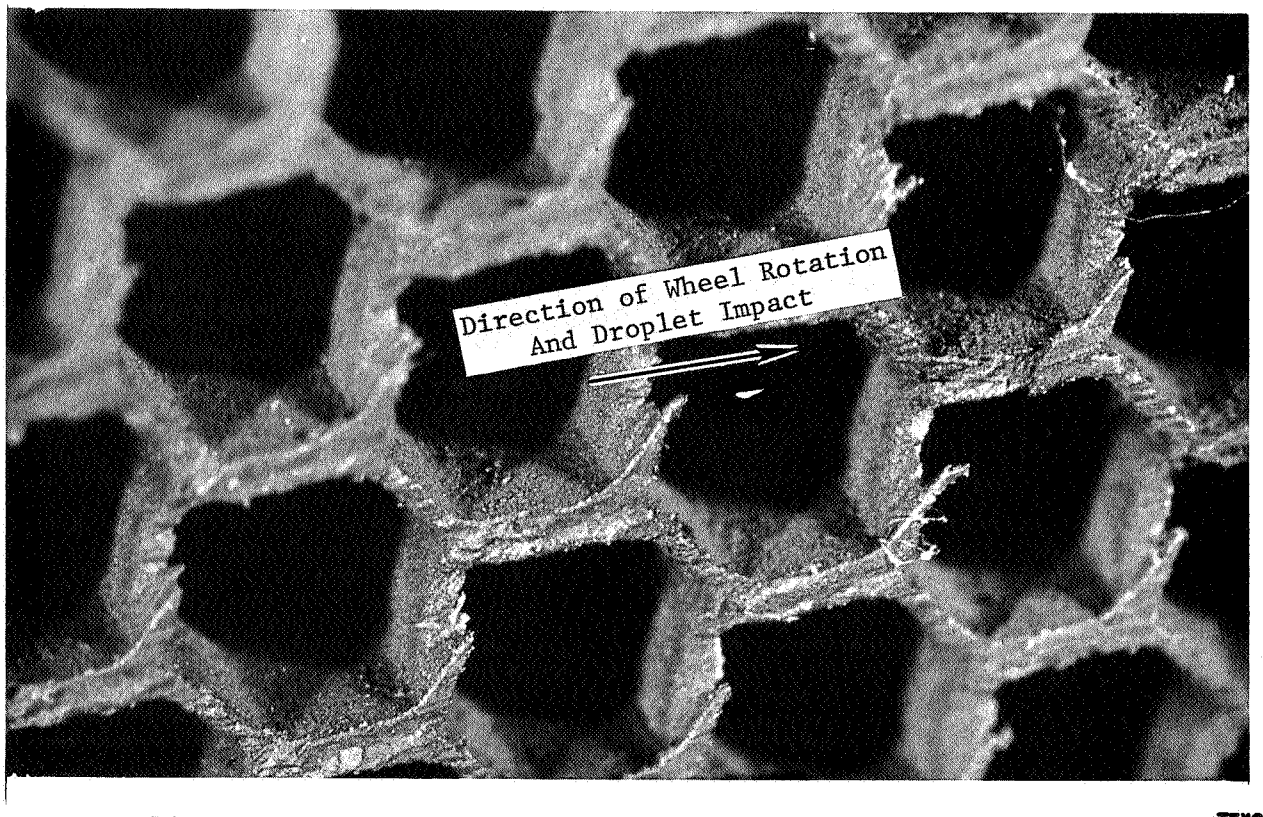


Figure 117. Section of Second Stage Honeycomb Tip Seal Showing Impact Erosion. T5439-117

Mag: 26X

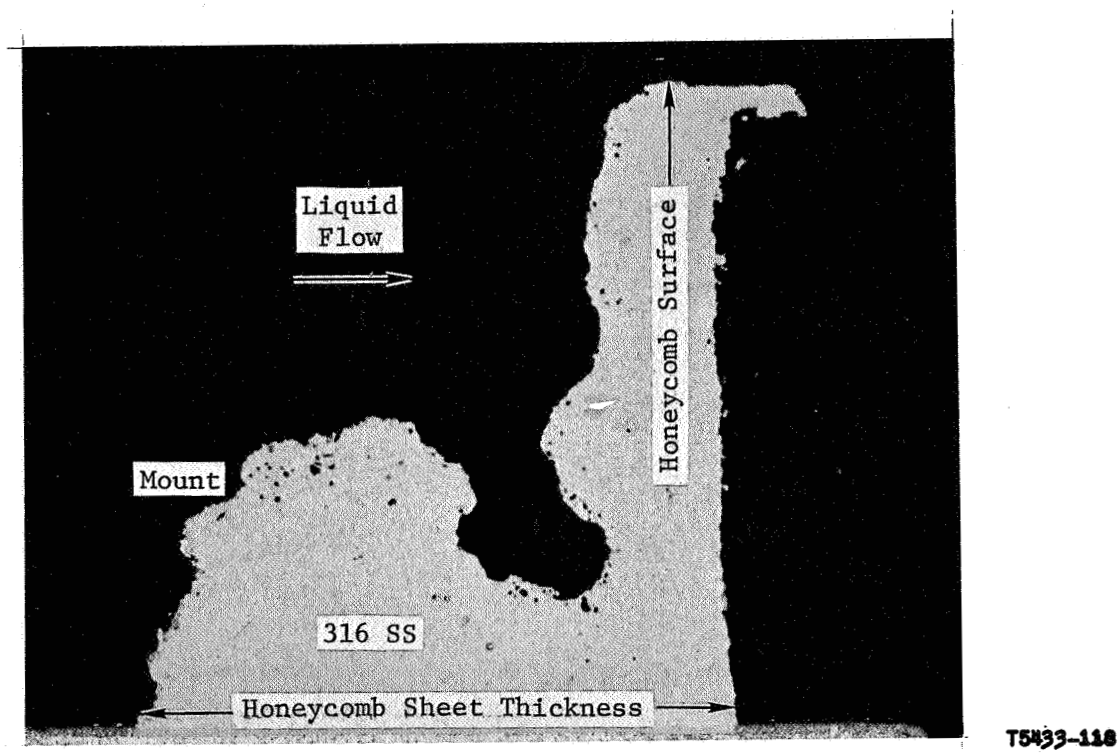


Figure 118. Photomicrograph of Eroded Section of Honeycomb Cell Wall.
Etchant: Unetched Mag: 250X

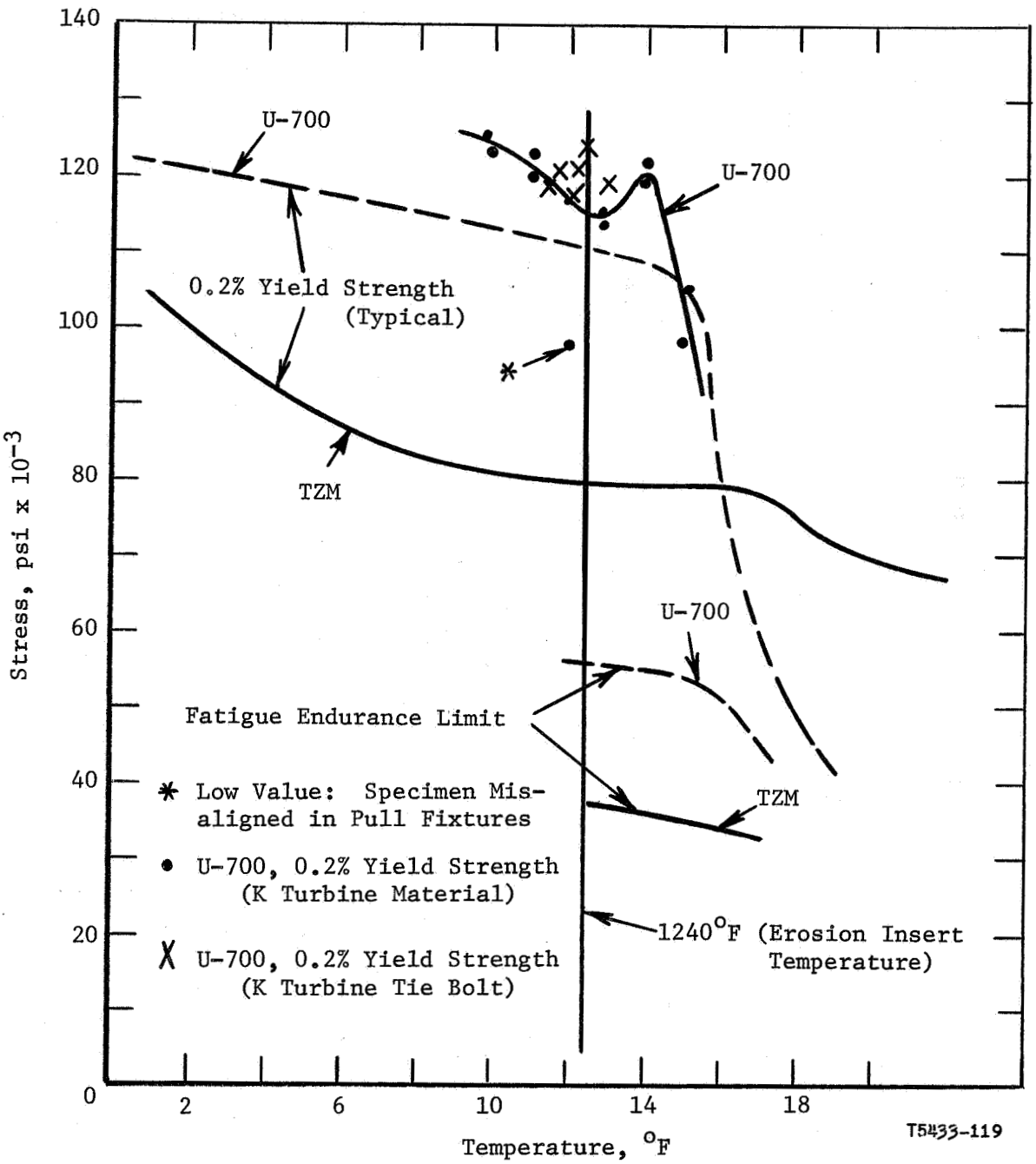


Figure 119. Comparison of Yield and Fatigue Strength of TZM and U-700 Near the Erosion Insert Temperature.

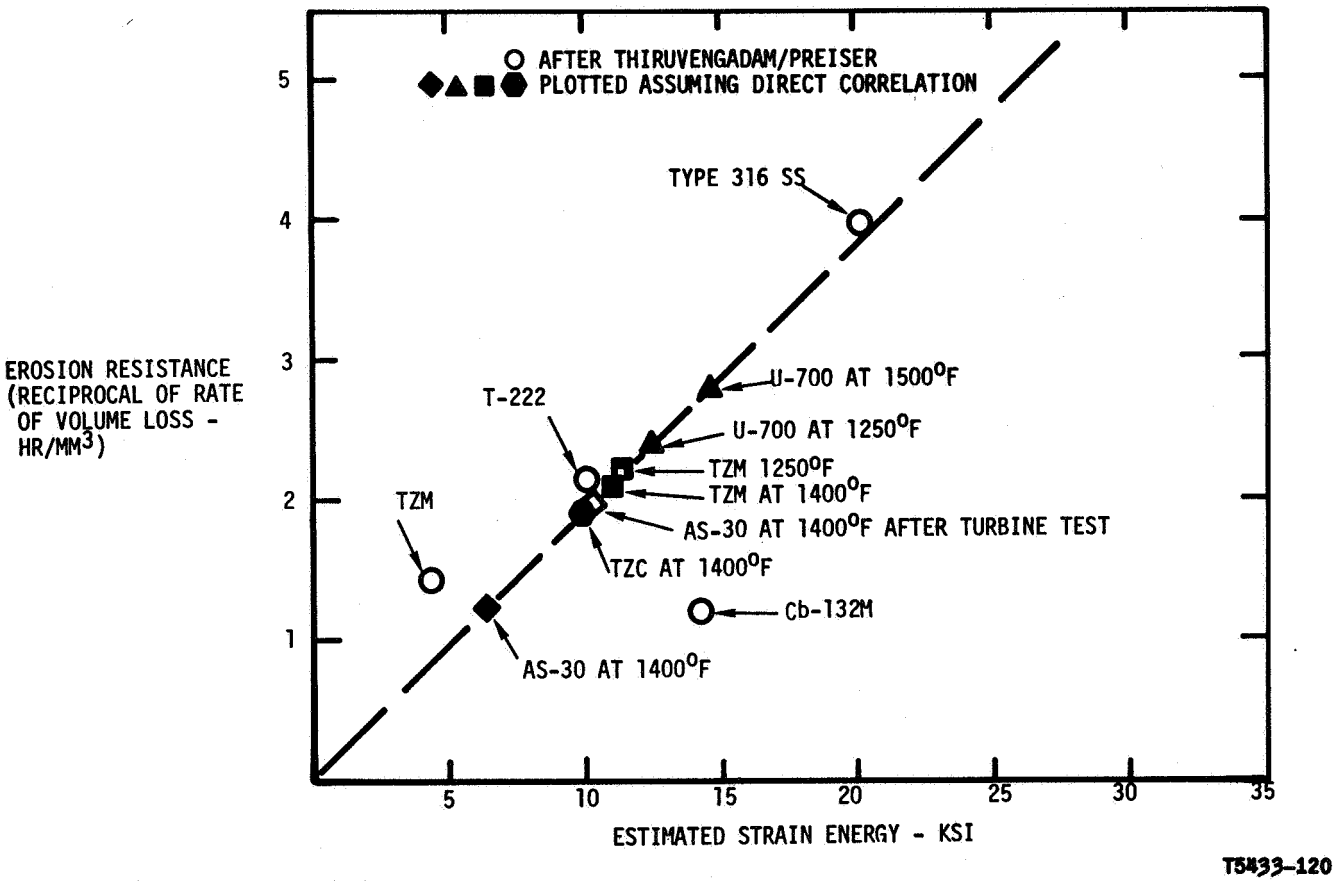


Figure 120. Relationship Between Cavitation Damage Resistance and Estimated Strain Energy in 1000°F Liquid Sodium (After Thiruvengadam and Preiser, NASA CR-72035).

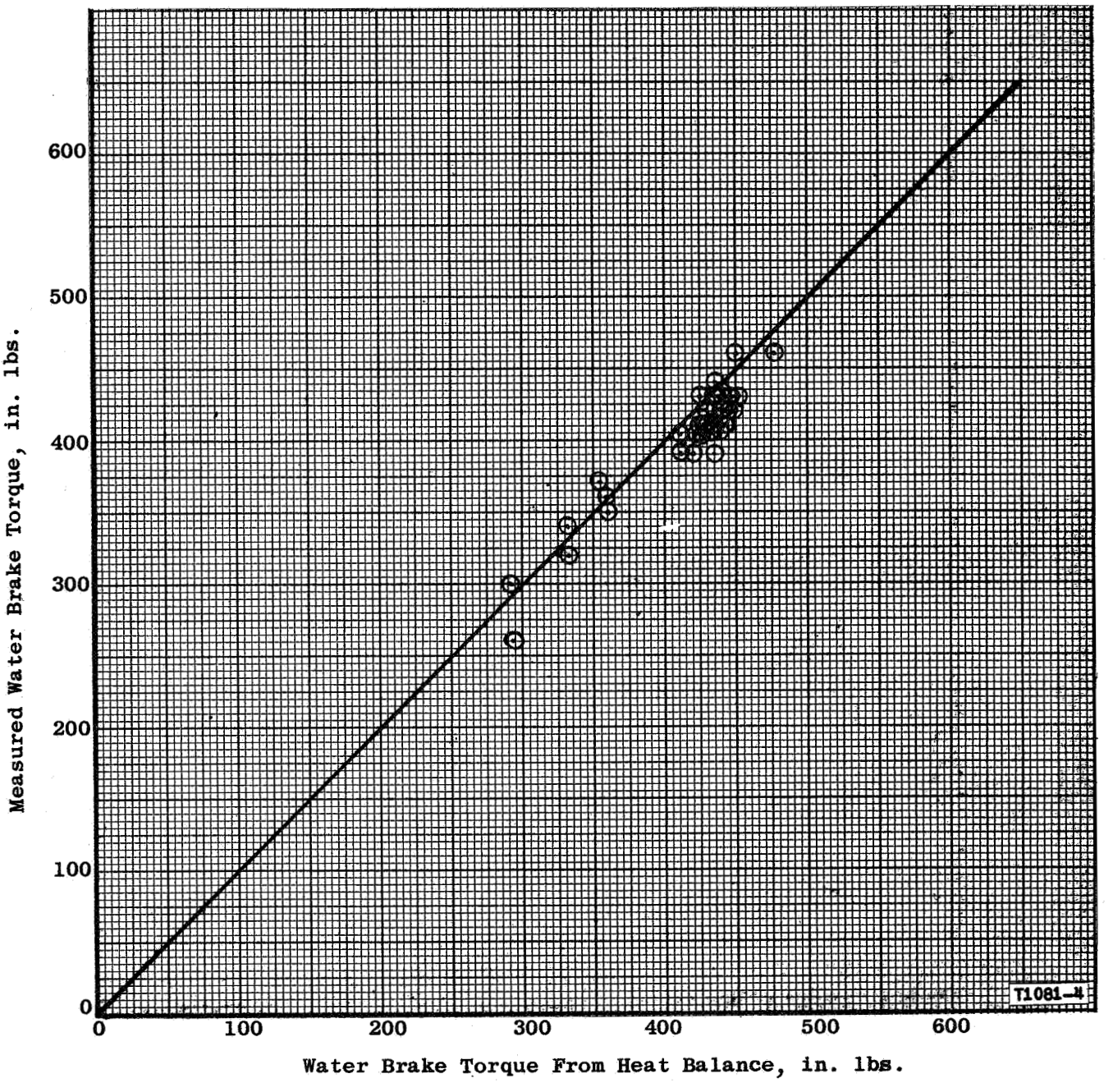


Figure 121. Comparison of Heat Balance Torque and Torque Meter Readings Obtained During 2000 Hour Test.

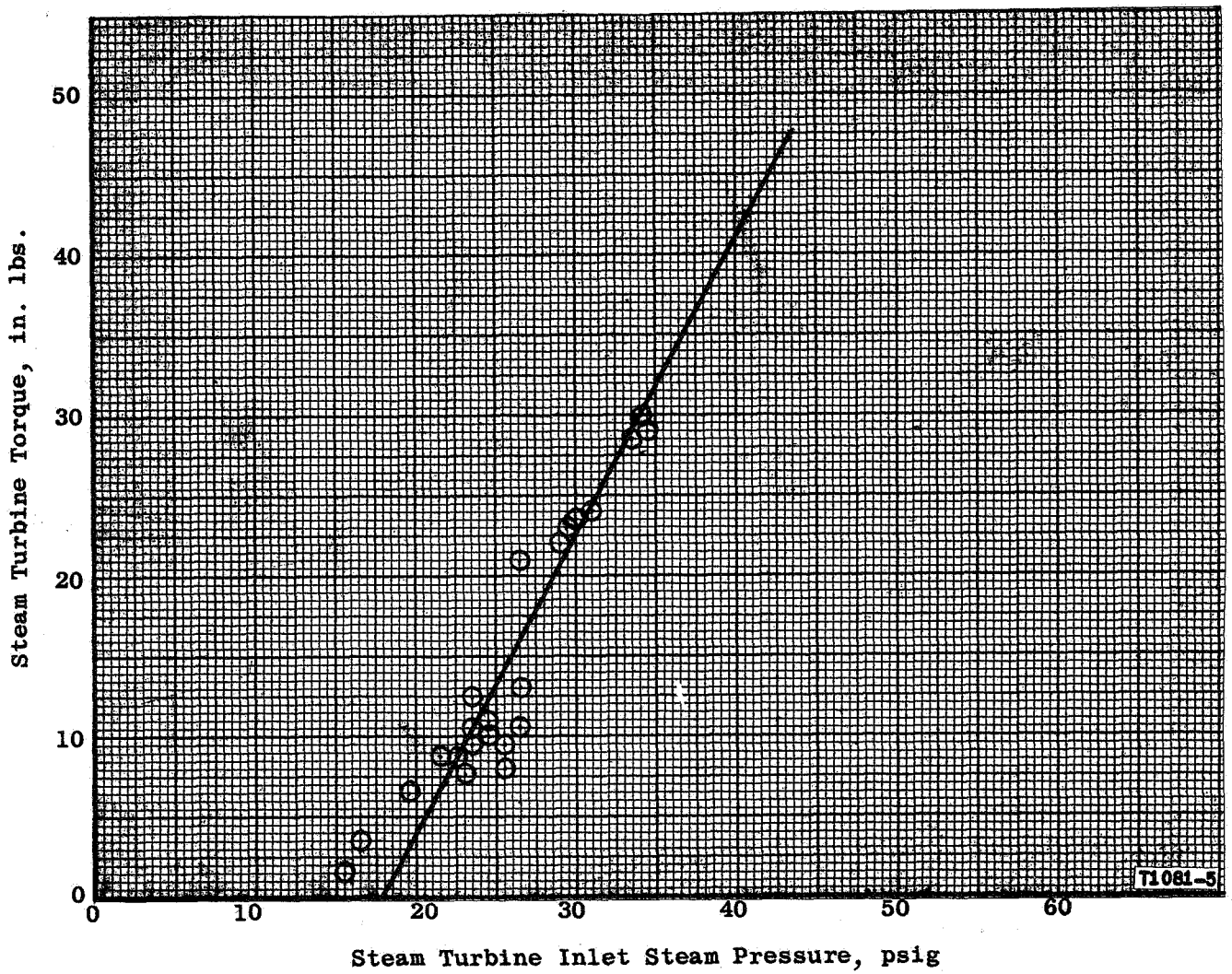


Figure 122. Variation of Steam Turbine Torque With Steam Inlet Pressure Obtained During 2000 Hour Test.

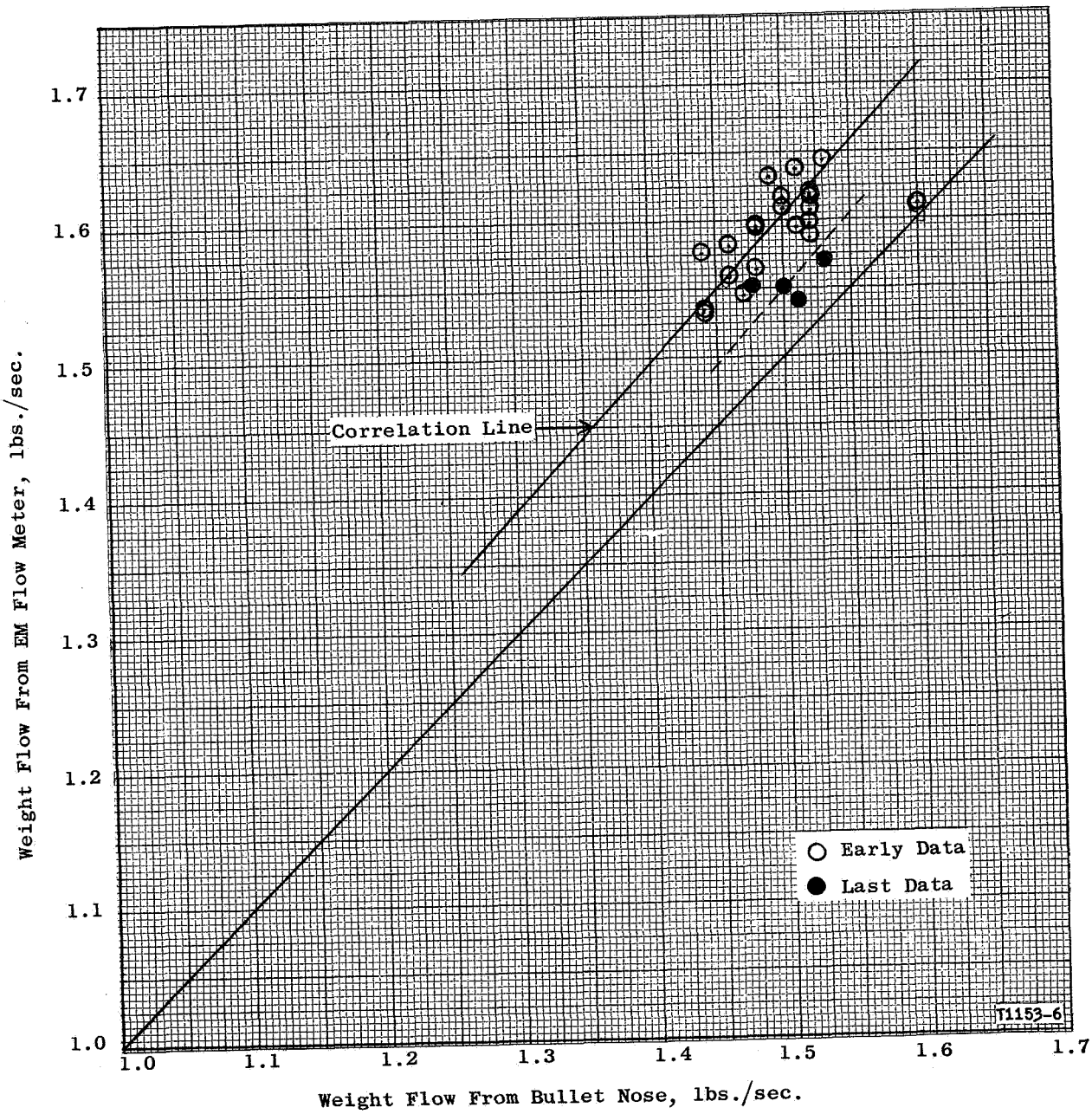


Figure 123. Comparison of Weight Flow Obtained From EM Flow Meter and Bullet Nose.

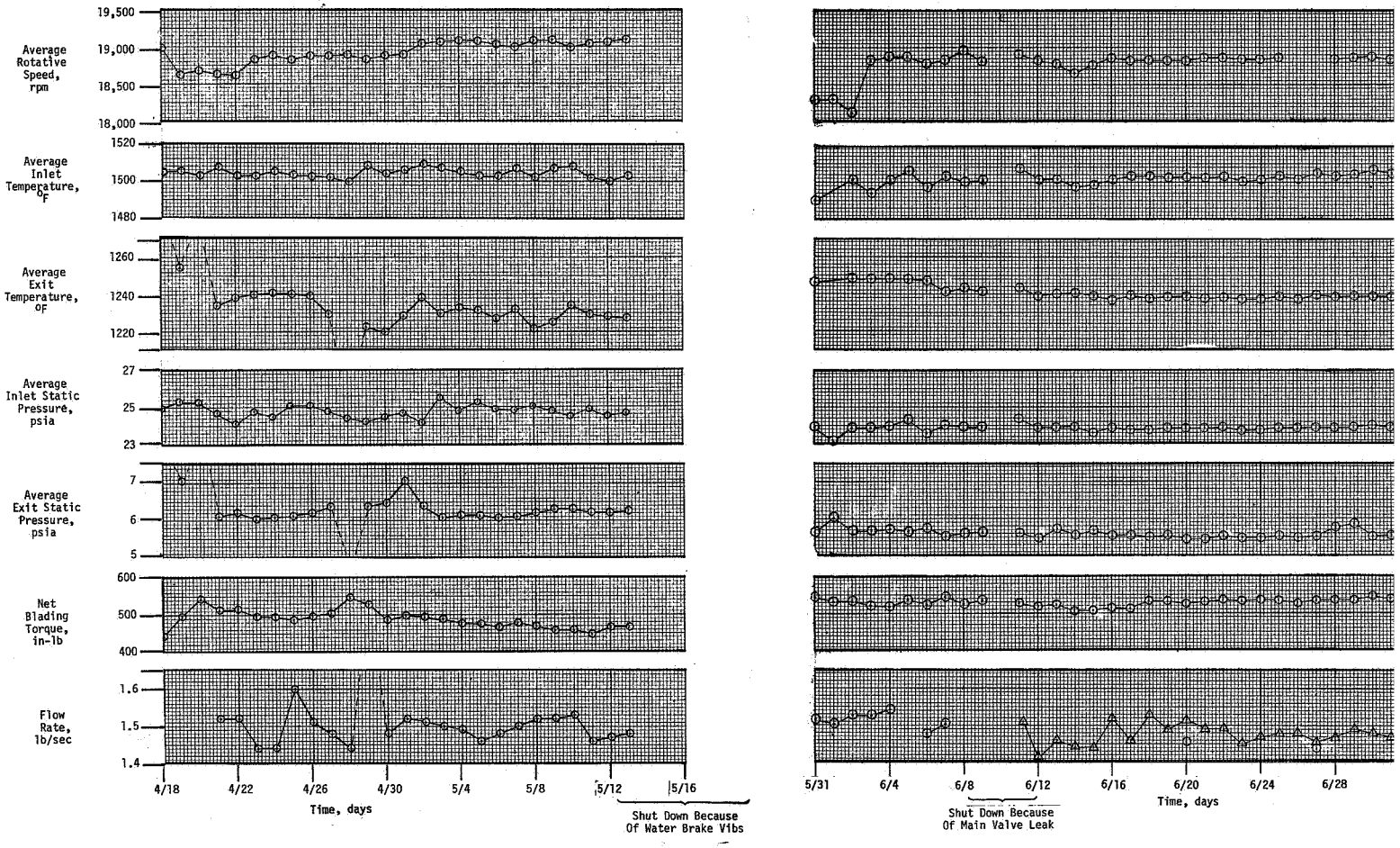
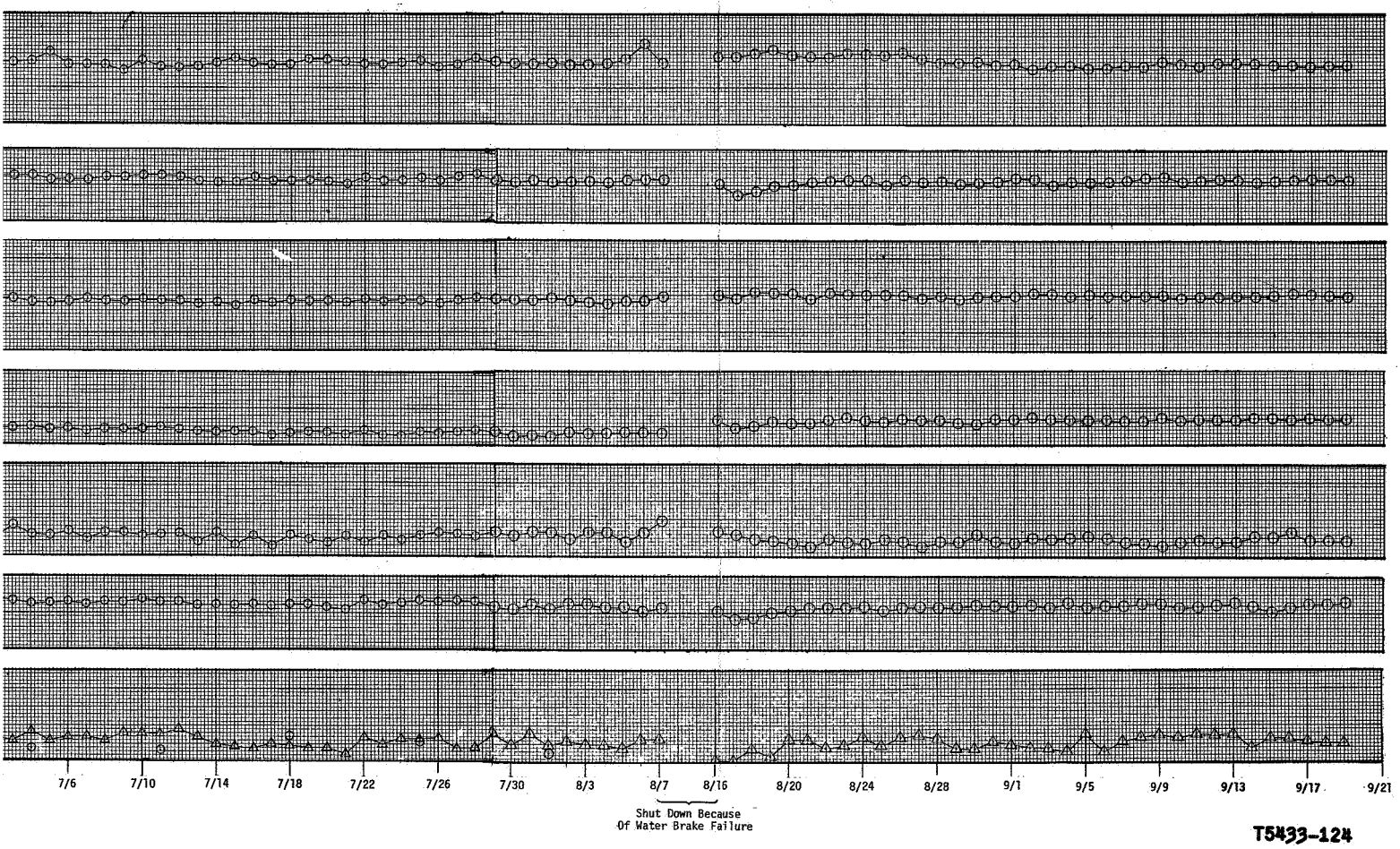


Figure 124. Var

FOLDOUT FRAME



ıtion of Turbine Parameters During Endurance Testing.

FOLDOUT FRAME

REPORT DISTRIBUTION LIST - CONTRACT NAS 5-1143
QUARTERLY AND FINAL

NASA-Lewis Research Center
21000 Brookpark Road
Cleveland, Ohio 44135
ATTN: Norman Musial M.S. 77-1
Patent Counsel Office

NASA-Lewis Research Center
Space Electric Power Procurement Office
21000 Brookpark Road
Cleveland, Ohio 44135
ATTN: J.E. Dilley M.S. 500-309

NASA-Lewis Research Center
21000 Brookpark Road
Cleveland, Ohio 44135
ATTN: Roger F. Mather M.S. 500-309

NASA-Lewis Research Center
21000 Brookpark Road
Cleveland, Ohio 44135
ATTN: Henry O. Slone M.S. 500-201

NASA-Lewis Research Center
21000 Brookpark Road
Cleveland, Ohio 44135
ATTN: I.I. Pinkel M.S. 5-3

NASA-Lewis Research Center
21000 Brookpark Road
Cleveland, Ohio 44135
ATTN: Dr. Bernard Lubarsky (SPSD)
M.S. 500-201

NASA-Lewis Research Center
21000 Brookpark Road
Cleveland, Ohio 44135
ATTN: Warner L. Steward M.S. 5-9

NASA-Lewis Research Center
21000 Brookpark Road
Cleveland, Ohio 44135
ATTN: James H. Dunn M.S. 500-201

NASA-Lewis Research Center
21000 Brookpark Road
Cleveland, Ohio 44135
ATTN: P.P. Moffitt M.S. 5-9

NASA-Lewis Research Center
21000 Brookpark Road
Cleveland, Ohio 44135
ATTN: Robert E. English M.S. 500-201

NASA-Lewis Research Center
21000 Brookpark Road
Cleveland, Ohio 44135
ATTN: Dr. Louis Rosenblum M.S. 106-1

NASA-Lewis Research Center
21000 Brookpark Road
Cleveland, Ohio 44135
ATTN: Mr. George Mandel
Library M.S. 5-5

NASA-Lewis Research Center
21000 Brookpark Road
Cleveland, Ohio 44135
ATTN: Joseph P. Joyce (2)
M.S. 500-201

NASA
Washington, D. C. 20546
ATTN: J. J. Lynch (RNP)

NASA
Washington, D. C. 20546
ATTN: George Deutsch (RR)

NASA
Washington, D. C. 20546
ATTN: W.H. Woodward

NASA-Western Operations Office
15 Pico Boulevard
Santa Monica, California 90406
ATTN: John Keeler

NASA-Jet Propulsion Labs
4800 Oak Grove Drive
Pasadena, California 99103
ATTN: J.W. Stearns

NASA-Goddard Space Flight Center
Greenbelt, Maryland 20771
ATTN: Office of Technical
Information, Code 250

National Aeronautics & Space Administration
Scientific & Technical Information Agency
Box 5700
Bethesda, Maryland 20014
ATTN: NASA Representative (2 plus one reproducible)

Aerojet-General Corporation
Department 4801, Bldg. 160
Von Karman Center
Azusa, California
ATTN: Mr. Charles Boone

AiResearch Mfg. Co. of Arizona
Division of Garrett Corporation
402 South 36th Street
Phoenix, Arizona 85000
ATTN: Mr. J. Dennan

U.S. Atomic Energy Commission
Germantown, Maryland
ATTN: Col. E.L. Douthett
AEC Deputy, SNAP 50/SPUR Office

U.S. Atomic Energy Commission
Germantown, Maryland
ATTN: Lt. Col. G.M. Anderson

NASA
Washington, D. C. 20546
ATTN: Mr. Herbert Rochen

U.S. Atomic Energy Commission
Division of Technical Information Extension
P.O. Box 62
Oak Ridge, Tennessee 37831

Battelle Memorial Institute
505 King Avenue
Columbus, Ohio
ATTN: Alexis Lemmon

Brookhaven National Laboratory
Upton, Long Island, New York
ATTN: Dr. O.E. Dwyer

Mr. Lance Hays
Jet Propulsion Laboratory
California Institute of Technology
3800 Oak Grove Drive
Pasadena, California

Ford Motor Company
Aeronutronic Division
Ford Road
Newport Beach, California 92660
ATTN: Mr. George P. Carver

Aeronutronic Division
Ford Motor Company
Ford Road
Newport Beach, California 92660
ATTN: Hans D. Linhardt

Dr. James Hadley
Head, Reactor Division
Lawrence Radiation Laboratory
Livermore, California

Prof. George A. Brown
Engineering Projects Laboratory
Massachusetts Instute of Technology
Research Laboratory of Electronics
Cambridge, Massachusetts 02139

Mechanical Technology, Incorporated
968 Albany - Shaker Road
Latham, New York
ATTN: Mr. R.J. Hocker
Mechanical Systems Engineer

Curtiss-Wright Corporation
Wright-Aeronautical Division
Wood-Ridge, New Jersey 07075
ATTN: S. Lombardo

Mechanical Technology, Inc.
968 Albany - Shaker Road
Latham, New York
ATTN: Dr. Beno Sternlicht

National Bureau of Standards
Washington, D. C. 20225
ATTN: Mr. C.W. Beckett

Oak Ridge National Laboratory
P.O. Box Y
Oak Ridge, Tennessee 37831
ATTN: A.G. Grindell

Oak Ridge National Laboratory
P.O. Box X
Oak Ridge, Tennessee 37831
ATTN: William O. Harms
Metals and Ceramics Division

Oak Ridge National Laboratory
Oak Ridge, Tennessee 37831
ATTN: W.D. Manly

Oak Ridge National Laboratory
Post Office Box Y
Oak Ridge, Tennessee 37831
ATTN: Mr. H.W. Savage

Pratt & Whitney Aircraft
400 Main Street
East Hart, Connecticut 66108
ATTN: William H. Podelny

Rocketdyne
Canoga Park, California 91303
ATTN: R.B. Dillaway

Sundstrand Denver
2480 West 70th Avenue
Denver 21, Colorado
ATTN: Robert Boyer

Thompson Ramo-Wooldridge, Inc.
New Devices Labs
7209 Platt Avenue
Cleveland, Ohio 44104
ATTN: J.E. Taylor

Westinghouse Electric Corporation
Astronuclear Laboratory
Box 10864
Pittsburgh, Pennsylvania 15236
ATTN: R.T. Begley, Manager,
Materials Service Group
Materials Department

Aeronautical Systems Division
Aeromechanical Branch
Wright-Patterson AFB, Ohio 45433
ATTN: Mr. Charles Armbruster
ASRMFP-1

Dr. G. Gyarmathy, ARN
Aerospace Research Laboratory
Building 450
Wright-Patterson AFB, Ohio 45433

Aeronautical Systems Division
Wright-Patterson Air Force Base, Ohio
ATTN: Mr. George Sherman - API

Aeronautical Systems Division
Wright-Patterson Air Force Base, Ohio
ATTN: Mr. George E. Thompson
APIP-1

Atomics International
P.O. Box 309
Canoga Park, California 91304
ATTN: Mr. R.W. Dickinson